**United States Department of Energy**

**Savannah River Site**

# Baseline Groundwater Model Update for P-Area Groundwater Operable Unit, NBN

**P-Area Reactor Groundwater Operable Unit**

**SRNS-RP-2015-00768**

**September 2015**

**Prepared by:**
**Savannah River Nuclear Solutions LLC**
**Savannah River Site**
**Aiken, SC 29808**

**Prepared for U.S. Department of Energy under Contract No. DE-AC09-96SR18500**

## DISCLAIMER



**Printed in the United States of America**
**Prepared for**
**U. S. Department of Energy**
**and**
**Savannah River Nuclear Solutions, LLC**
**Aiken, South Carolina**

## EXECUTIVE SUMMARY

This report documents the development of a numerical groundwater flow and transport model of the hydrogeologic system of the P-Area Reactor Groundwater Operable Unit at the Savannah River Site (Figure ES-1). The P-Area flow and transport model provides a tool to aid in understanding the hydrologic and geochemical processes that control the development and migration of the current tritium; tetrachloroethene (PCE); and trichloroethene (TCE) plumes in this region. The current model is a revision of an earlier model developed in 2011 (SRNS 2011).

The Hydrogeological Conceptual Model (HCM) used for this analysis is based largely on an earlier HCM (WSRC 2004), as documented in the 2011 modeling study (SRNS 2011), along with environmental data collected from 2011 through 2014.

The groundwater flow and contaminant transport model described in this report is based on data and knowledge that were acquired from previous studies of the groundwater system underlying the regional P Area. The flow model was calibrated and provides a reasonable representation of the long-term average groundwater flow field. The model was calibrated to various targets, including hydraulic heads at wells for matching groundwater flow conditions and historical plume trajectories for matching contaminant transport. A sensitivity analysis was performed for hydraulic conductivity and boundary conditions of the flow model to identify uncertainties in model inputs.

*Tritium*

Transport of tritium was simulated under steady state flow conditions for a model period of 100 years. The modeling shows that migration of tritium through groundwater is primarily towards Steel Creek but that the tritium plume does not exit into Steel Creek past stream gage location SC-04 at concentrations exceeding the maximum contaminant limit (MCL) (20 pCi/mL). However, the predicted concentration of tritium in groundwater discharging upgradient of SC-04 to stream gage location SC-03 is greater than the MCL and is predicted to remain above concentration the MCL for approximately 30 years from calendar year (CY) 2015. Table ES-1 provides concentration over time data at four target monitoring wells in the plume and at Steel Creek. Although tritium concentrations remain above MCLs in the Lower Lower Aquifer Zone

(LLAZ) for 100 years, no breakthrough of tritium to the Gordon Aquifer Unit (GAU) occurs over the modeled time period. The model predicts that tritium will not impact any other surface water bodies in the vicinity of P Area within the modeled duration, including PAR Pond and the canals and tributaries of PAR Pond. The plume does move past SC-04 in the Upper Lower Aquifer Zone (ULAZ) layer towards L-Lake, but the plume degrades due to a relatively fast radioactive decay (half life = 12.3 years) and disperses before reaching L-Lake for the entire 100-year simulation.

To approximate the observed retardation of tritium plumes in general at SRS a sensitivity of $K_d$ was completed with tritium assuming a $K_d$ equal to 0.1 and 1 (versus base case of 0). Increasing the $K_d$ results in the plume taking longer to reach concentrations below the MCL at downgradient monitoring well locations by up to 35 years.

*Chlorinated Volatile Organic Compounds*

Transport of chlorinated volatile organic compounds (CVOCs) was simulated for a period of 300 years under steady-state flow. The predicted PCE plumes change little over the first 100 years of simulation and do not migrate to any water bodies. Based on the location of the treated source area and its relative location on the water table groundwater divide, this is limiting the migration of the groundwater plume to the west to SC and the east towards PAR Pond. However, increased PCE concentrations are observed in the ULAZ and are predicted to increase because of the vertical migration pathway.

For TCE, the model predictions indicate the peak TCE concentration in groundwater occurs at Model Year 0 at the starting concentration for wells PGW014DU and PGW026DL (Table ES-1). Concentrations are predicted to exceed the MCL at PGW026DL for over 300 years. The transport model predicts TCE entering Steel Creek at a peak rate of 19 kg/yr in Model Year 8 with an average rate of 7.7 kg/yr over the first 100 years. The maximum concentration in groundwater discharging into Steel Creek and the canal is 351 µg/L in Model Year 10. The calculated TCE concentration in surface water (at SC-04) suggests that the TCE concentration would not fall below the MCL within 100 years and that the concentration would peak at 79 µg/L in Model Year 8. However, the maximum TCE concentration observed in surface water at SC-04, to date, has been 0.78 µg/L in March 2015 and 28 µg/L in March 2015 for SC-03.

The fact the model predicts current and future TCE concentrations in surface water much higher than observed TCE concentrations suggests that there may be wetland or surface water TCE attenuation processes that are not accounted for in the groundwater model. In particular, the model does not take into consideration volatilization in the stream or increased biodegradation in wetland sediments. While TCE and PCE do migrate eastward towards PAR Pond, they do not reach PAR Pond within the period of simulation (300 years).

For the sensitivity of CVOC sorption coefficient, the $K_d$ for all layers and CVOC constituents were reduced (divided by 10). This resulted in faster plume movement, and consequently increased discharge into Steel Creek in the near term. In the long term, plume extent is expanded but the time to reach MCLs is significantly reduced.

**Table ES-1 Predicted Future Tritium and TCE Concentration in Groundwater**

| Location | Maximum Tritium Concen-tration (pCi/mL) | Time of Maximum Tritium Concen-tration (yr) | Time to Reach Tritium MCL (yr) | Maximum TCE Concen-tration (µg/L) | Time of Maximum TCE Concen-tration (yr) | Time to Reach TCE MCL (yr) |
|---|---|---|---|---|---|---|
| **Groundwater at Well PGW014DU** | 546 | 3 | 32 | 130 | 0 | 47 |
| **Groundwater at PGW026DL** | 151 | 10 | 29 | 4,500 | 0 | >300 |
| **Groundwater at PGW027DU** | 2,757 | 2 | 22 | N/A | N/A | N/A |
| **Groundwater at PSB002AA** | 5,630 | 0 | 77 | N/A | N/A | N/A |
| **Groundwater Discharge into Steel Creek[a]** | 2,139 | 0 | 27 | 351 | 10 | >100 |
| **Surface Water at SC-04** | 430 | 3 | 17 | 79 | 8 | >100 |

[a]Groundwater discharge to Steel Creek represents the maximum concentration for the entire reach of Steel Creek and P-Area Discharge Canal.

**MCL = Maximum contaminant level.**

This model, like all models, is subject to limitations that arise from uncertainties and assumptions that are made in simplifying a complex natural system. However, the calibration of the model provides some confidence that the model is a reasonable representation of the natural system (especially for groundwater flow). Despite the uncertainties with the model, it is an effective tool for evaluation of the relative merits of various remedial alternatives. Prediction of absolute responses (e.g., attain MCL within a certain number of years) is less certain than relative results (e.g., Scenario X is more effective than Scenario Y) because the latter analysis is a comparison of the results of changes within the same framework.

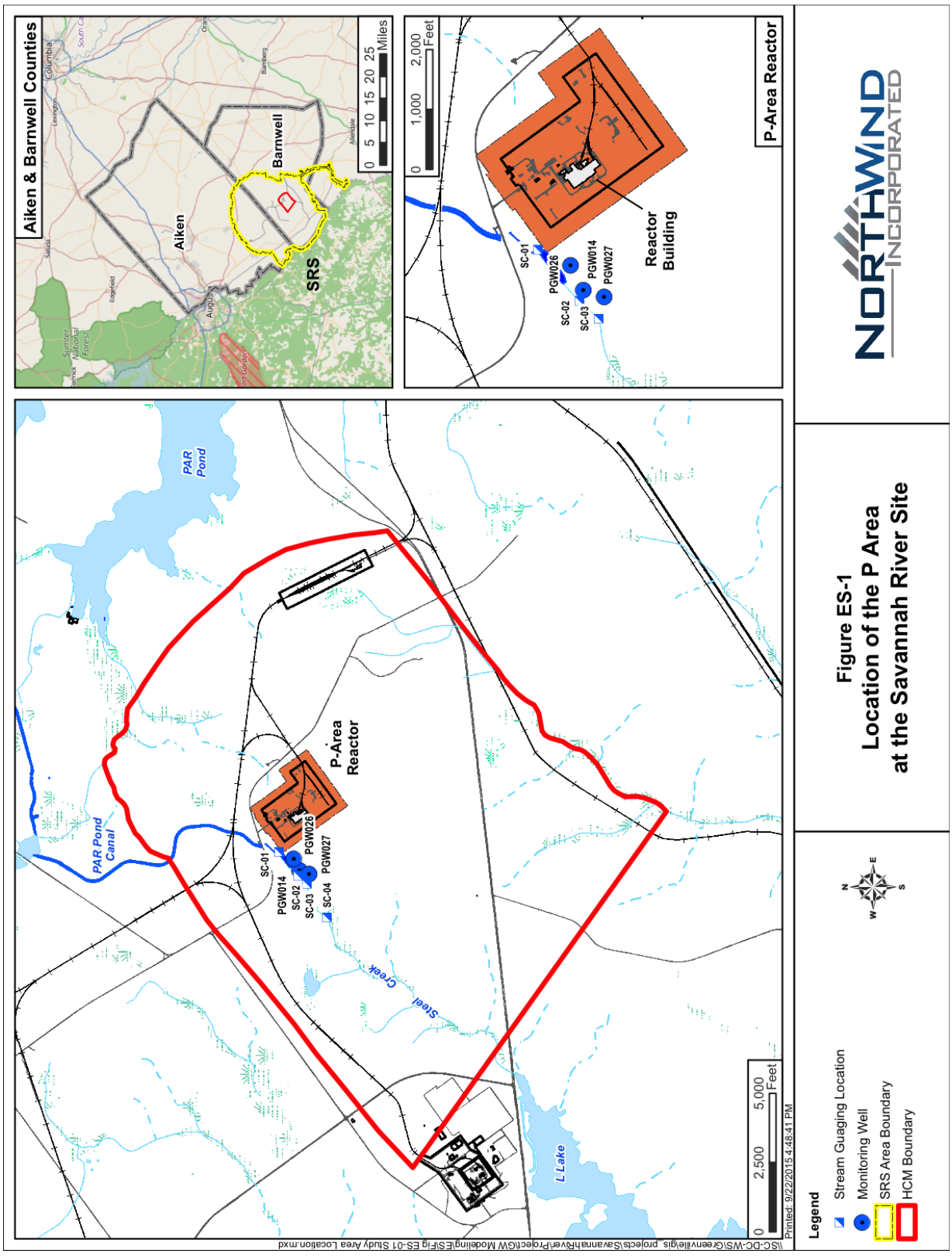


**Figure ES-1 Location of the P Area at the Savannah River Site**

**(This page intentionally left blank)**

## TABLE OF CONTENTS

## LIST OF APPENDICES

## LIST OF FIGURES

## LIST OF TABLES

**(This page intentionally left blank)**

## LIST OF ACRONYMS AND ABBREVIATIONS

| | |
|---|---|
| A/AA | ‘A’ and ‘AA’ horizons |
| amsl | above mean seal level |
| CBAU | Crouch Branch Aquifer Unit |
| CBCU | Crouch Branch Confining Unit |
| cfs | cubic feet per second |
| Ci/yr | curies per year |
| COC | contaminant of concern |
| CPT | cone penetrometer technology |
| CVOC | chlorinated volatile organic compound |
| CY | calendar year |
| DCE | dichloroethene |
| DPT | direct push technology |
| ft | feet |
| GAU | Gordon Aquifer Unit |
| GCU | Gordon Confining Unit |
| GIS | Geographical Information System |
| GMS | Groundwater Modeling System |
| HCM | hydrogeological conceptual model |
| in. | inch |
| kg | kilogram |
| kg/yr | kilogram per year |
| L | liter |
| LAZ | Lower Aquifer Zone |

| | |
|---|---|
| lb | pound |
| LGA | Lower Gordon Aquifer |
| LLAZ | Lower Lower Aquifer Zone |
| LTH | long-term head |
| MAE | mean absolute error |
| MC-LAZ | Middle Clay of the Lower Aquifer Zone |
| MCL | maximum contaminant level |
| MGA | Middle Silt of the Gordon Aquifer |
| µg/L | micrograms per liter |
| % | percent |
| PCE | tetrachloroethene |
| pCi/mL | picocuries per milliliter |
| PRSB | P-Reactor Seepage Basins |
| R | Retardation |
| RMSE | root-mean-square error |
| SRS | Savannah River Site |
| TCCZ | Tan Clay Confining Zone |
| TCE | trichloroethene |
| TZ | Transmissive Zone |
| UGA | Upper Gordon Aquifer |
| ULAZ | Upper Lower Aquifer Zone |
| UTRA | Upper Three Runs Aquifer |
| VC | vinyl chloride |
| yr | year |

# 1.0 MODELING OVERVIEW AND PURPOSE

This report documents the development of a numerical groundwater flow and transport model of the hydrogeologic system of the P-Area Reactor Groundwater Operable Unit at the Savannah River Site (SRS) (Figure 1-1). The P-Area model provides a tool to aid in understanding the hydrologic and geochemical processes that control the development and migration of the current tritium, tetrachloroethene (PCE), and trichloroethene (TCE) plumes in this region.

## 1.1 Background

P Area is located in the central portion of SRS (Figure 1-1) west of PAR Pond and upstream of L-Lake along Steel Creek. It is an industrialized area that maintained a high level of activity from the 1950s until reactor shut down in 1991. Steel Creek received cooling water discharges from the P-Area Reactor between 1954 and 1961. During that time, cooling water was discharged to an effluent canal that was constructed along the natural drainage path in the upper reach of Steel Creek. No operational activity has occurred within P Area since the reactor shut down in 1991 (WSRC 2004).

Groundwater investigations at the P-Area Burning/Rubble Pit in 1998 and at the P-Reactor Seepage Basins (PRSB) in 2001 revealed a previously unknown tritium plume and two chlorinated volatile organic compound (CVOC) plumes upgradient of these waste units near P Area (Figure 1-2). The tritium plume was found to originate from the PRSB, as expected, and in the vicinity of the P-Reactor building. The CVOC plumes originate in locations near reactor-area facilities (WSRC 2004).

## 1.2 Methodology and Organization

To facilitate the analysis, a numerical model of groundwater flow and transport was developed in 2011. This report is an update of the 2011 numerical model based on data obtained from 2011 through 2015. The numerical model is based on an understanding of the site and environmental processes as presented in Chapter 2.0. The design of the P-Area model is described in detail in Chapter 3.0. Initial parameter values for the flow and transport models were derived from field data and prior model calibration. The model was calibrated to various targets, including

hydraulic heads at wells for flow and historical plume trajectories for transport. A sensitivity analysis was performed for hydraulic conductivity and boundary conditions of the flow model to identify uncertainties in model inputs. Calibration and flow sensitivity analyses are described in Chapters 4.0. Chapter 5.0 documents the transport model and transport sensitivity analysis. These results are presented in the form of maps showing predicted future plume development, and discharge to model boundaries with time. Model uncertainties are presented in Chapter 6.0. Finally, conclusions and recommendations are presented in Chapter 7.0.

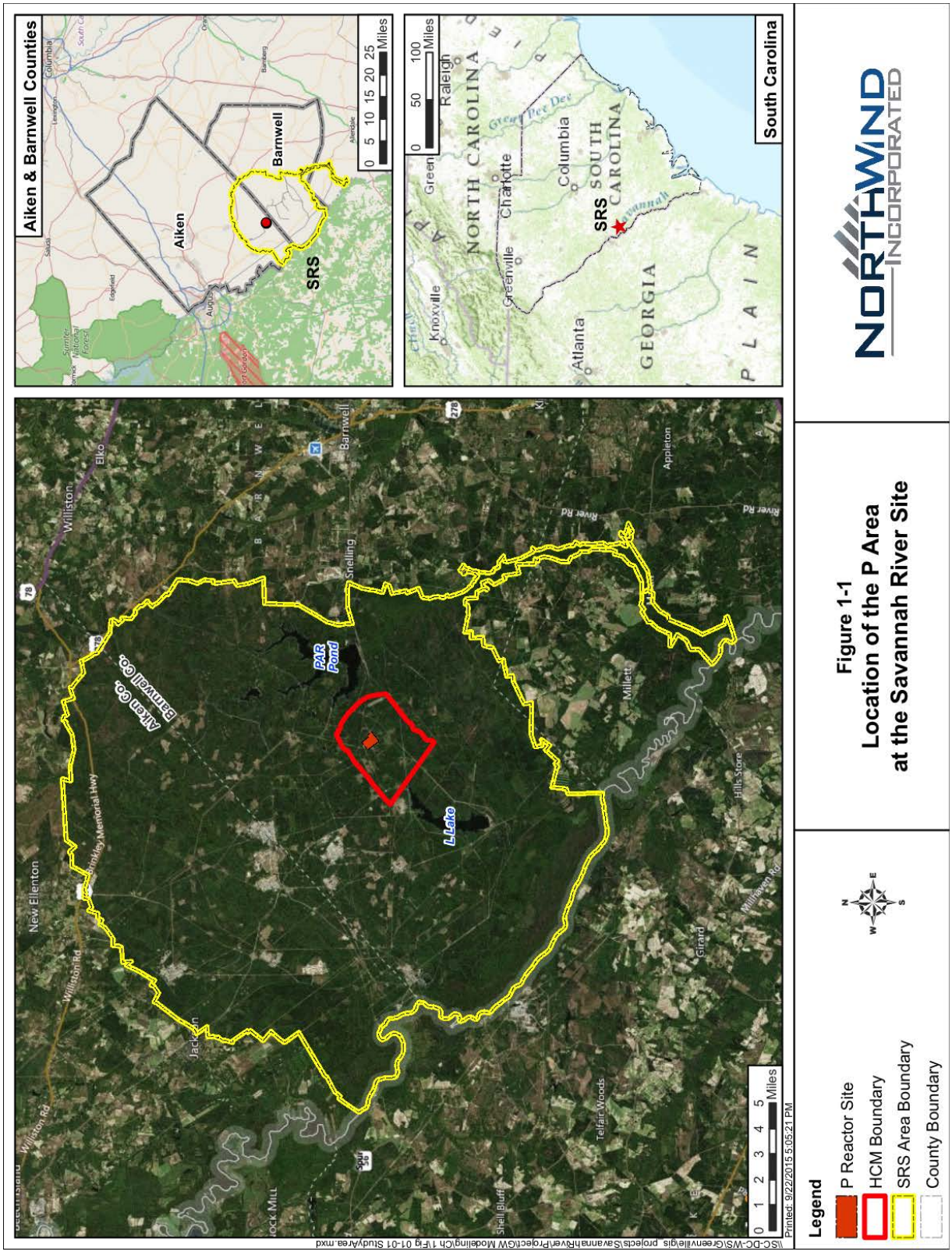


**Figure 1-1 Location of P Area at the Savannah River Site.**

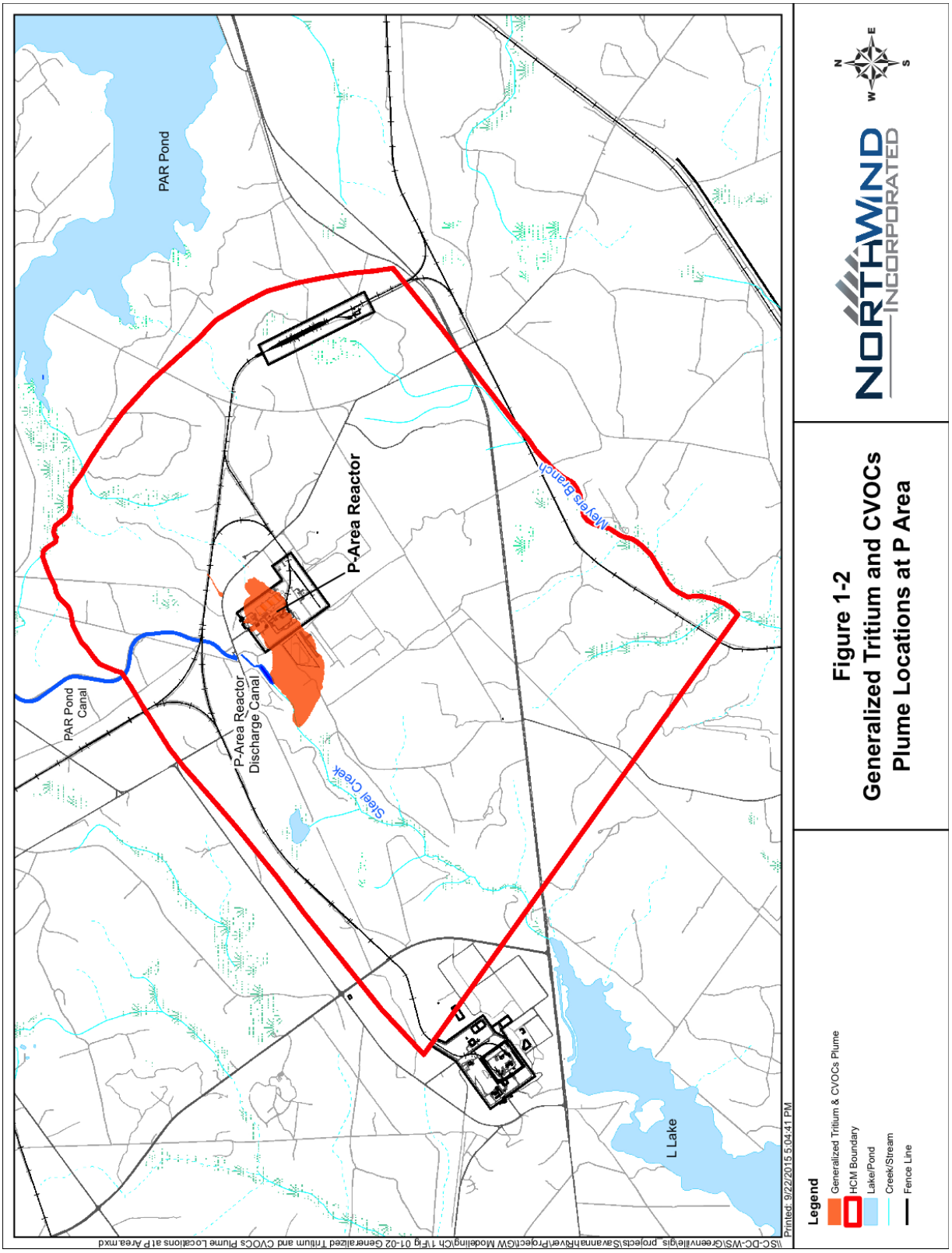


**Figure 1-2 Generalized Plume Locations at P Area.**

## 2.0 HYDROGEOLOGICAL CONCEPTUAL MODEL

A hydrogeological conceptual model[1] (HCM) describes the basis for model construction determined from review and analysis of the available data. Developing an HCM is a critical step in constructing a numerical flow and transport model. The P-Area HCM used for this analysis is based largely on an earlier HCM (WSRC 2004), as documented in the 2011 modeling study (SRNS 2011a), along with updates from 2011 (SRNS 2011b) and 2014 (SRNS 2014) studies, and describes:

- Hydrostratigraphic zones used to establish model layers,
- Regional groundwater flow boundaries,
- Lateral and vertical groundwater flow directions, and
- Contaminant transport pathways and possible source areas.

The following subsections present the various aspects of the conceptual models used in developing the numerical model presented in subsequent chapters.

### 2.1 Study Area

The study area includes the P-Reactor area and the observed PCE, TCE, dichloroethene (DCE) and tritium plumes (Figure 2-1). The study area includes all potential source areas, historic and current plume locations, and future possible plume extents.

Much of the study area is bounded by natural hydrogeologic boundaries (streams, groundwater divides, etc.) that should not change locations with time. The study area areal extent was chosen to be consistent with the P-Area HCM boundary (WSRC 2004) as it encompasses the potential source areas and plume extents. The study area external boundaries include, starting to the southeast and going clockwise, Meyers Branch, potentiometric head contours upgradient of L Lake, a groundwater divide between L Lake and PAR Pond, PAR Pond tributaries, and potentiometric head contours upgradient of PAR Pond.

[1] In this report, conceptual model refers to a general description of the pertinent physical controls on ground-water and contaminant movement. A conceptual model is often illustrated with a simple diagram. A HCM describes the general site features. The conceptual model(s) form the basis of the numerical model (sometimes just called the model), which is a detailed mathematical model used to solve for groundwater head and concentration at discretized points in space and time.

## 2.2 Hydrostratigraphy

The Savannah River Site (SRS) lies on the Aiken Plateau of the Atlantic Coastal Plain at an average elevation of 300 ft above mean sea level (amsl). Within the study area, the topography ranges from 330 ft amsl in the P-Reactor fence area to 190 ft amsl at the downstream end of Meyers Branch and Steel Creek (Figure 2-2). The topography used in model construction was derived from LIDAR data to ensure the elevation of Steel Creek was accurately measured.

The unconsolidated marine and fluvial sediment of the Atlantic Coastal Plain underlies SRS (Aadland and Bledsoe 1990). The sediment varies in age from Late Cretaceous to recent. It is a variably stratified, heterogeneous sequence of sand, clay, limestone, and gravel. The uppermost sediment makes up the Floridan Aquifer System. In P Area, the Floridan Aquifer System consists of, in descending order, the Upper Three Runs Aquifer (UTRA), the Gordon Confining Unit (GCU), and the Gordon Aquifer Unit (GAU). Below the Floridan Aquifer System are the Meyers Branch Confining System [Crouch Branch Confining Unit (CBCU)] and the Dublin-Midville Aquifer System [Crouch Branch Aquifer Unit (CBAU)].

The aquifers at P Area are further divided into hydrostratigraphic units based on observed lithology and head changes with depth. The generalized hydrostratigraphy in P Area (Figure 2-3) consists of (from the surface):

- Combined ’A‘ and ’AA‘ horizons (A/AA),
- Transmissive Zone (TZ),
- Tan Clay Confining Zone (TCCZ),
- Upper Lower Aquifer Zone (ULAZ),
- Middle Clay of the Lower Aquifer Zone (MC-LAZ),
- Lower Lower Aquifer Zone (LLAZ),
- Gordon Confining Unit (GCU),
- Upper Gordon Aquifer (UGA),

- Middle Silt of the Gordon Aquifer (MGA),
- Lower Gordon Aquifer (LGA),
- Crouch Branch Aquifer Unit (CBAU), and
- Crouch Branch Confining Unit (CBCU).

### *2.2.1 Development of the Physical Site Model*

The physical subsurface model depicts the site stratigraphic layer and includes the bounding surfaces for aquifers and aquitards. Data supplied by SRNS included tables of well or test hole locations (205 locations), geophysical logs for 44 borings, "picks" or tops and bottoms for the units listed above (A/AA to CBAU), tables of analytical data and water level data, and reports related to the study area.

#### 2.2.1.1 Hydrostratigraphic Picks

Boring locations, depths, logs, and picks were loaded into the subsurface mapping program PETRA. Cross-sections were developed using those 41 borings with logs and picks were refined (or assigned where none were supplied by SRNS). SURFER (Golden Software, ver 9) was used to develop isopach maps of the units to review unit tops and thicknesses. The current hydrostratigraphic picks for input into the solid hydrogeologic model are in Appendix A, Table A-1. The hydrostratigraphic picks that were excluded from the models are listed in Appendix A, Table A-2. Hydrostratigraphic picks that were modified per this effort are provided in Appendix A, Table A-3.

#### 2.2.1.2 Evaluation of Hydrostratigraphic Data

Table A-1 is a table of elevations (ft msl) for the tops of hydrostratigraphic units used for the model described in this document.

Initial values for most of the unit tops were provided by SRNS as two tables, "Rockworks Data" and "Hydrostratigraphic Picks". Additional data provided included geophysical logs for 44 borings, as well as other sources such a models near L Area.

During the course of development of the current model, unit tops and extents were reviewed, and some were modified from the initially furnished SRNS data. Refer to Appendix A, Tables A-2 and A-3 for updates to the picks.

### *2.2.2 Aquifer and Aquitard Properties*

In this study, the UTRA consists of the three aquifer zones: A/AA unit, TZ, and the Lower Aquifer Zone (LAZ). The A/AA unit consists of all material deposited above the Dry Branch Formation, including the Tobacco Road Formation and the "upland unit." The sediment of the A/AA unit is generally very dense and clayey and often contains gravely sand (WSRC 2004). The ground surface bounds the top of the A/AA unit, thus causing variable thickness from 0 ft in the incised streams to 125 ft. The TZ corresponds to the upper portion of the Dry Branch Formation and averages 15 ft thick. The sediment of the TZ is moderately to poorly sorted, coarse- to medium-grained silty sands, with sandy and silty clay layers and some pebble zones.

The TCCZ separates the TZ from the LAZ. It is composed of sediment from the Dry Branch Formation that is tan to orange clay and sandy clay interbedded with clayey sand and sand. The TCCZ is, on average, 20 ft thick. The LAZ is made up of the Santee Formation to the base of the Dry Branch Formation and has an average thickness of 80 ft. There is a significant zone of low-conductivity clayey silt (MC-LAZ), or where the formation undergoes a facies change to a micritic calcareous sandy clay, that divides the LAZ into two transmissive layers, thus causing a marked head difference between the ULAZ and LLAZ portions of the LAZ.

The next aquifer is the GAU. It is separated from the UTRA by the GCU. The GCU is sometimes referred to as the "green clay" and is composed of fine-grained sand, glauconitic clayey sand, clay of the Warley Hill Formation, and clayey limestone of the Santee Formation. The GCU is ill defined in P Area with distinct "green clay" layers missing in some areas. The GCU varies in thickness between 4 ft and 20 ft in the vicinity of the reactor areas, averaging 12 ft in thickness and thickens to the south in P Area. The GAU at P Area can be subdivided into three distinct layers based on its lithological makeup and head change with depth. In this study, the GAU consists of three hydrostratigraphic sub-units in the P Area: UGA, MGA, and LGA. The UGA consists of poorly sorted, loose, medium- to fine-grained sand with approximately 25% clay. The MGA consists of poorly sorted fine-grained sand with interbeds of silt and clay.

The LGA consists of loose, medium- to coarse-grained sand with less than 10% clay matrix. The MGA provides a definitive separation between the upper and lower thirds of the aquifer due to its lithological makeup and thickness. Unlike other parts of SRS, observed heads in portions of P Area are markedly different in the UGA and LGA. Overall, the GAU is 130 ft thick and thickens to the west in P Area.

The CBCU consists of dark gray to black, moderately to poorly sorted, fine- to coarse-grained, micaceous, lignitic, silt and clayey sand of the Snapp and Lang Syne/Sawdust Landing Formations and the uppermost clay portions of the Steel Creek Formation (Aadland et al. 1995). The CBCU is approximately 150 thick in P Area and is not subdivided in this numerical model.

The Steel Creek and Black Creek Formations form the CBAU, which is part of the Dublin Aquifer System. The Steel Creek Formation consists of medium- to coarse-grained, poorly to well-sorted sand and silty sand and thin beds of micaceous and carbonaceous clay. The Black Creek Formation consists of fine- to medium-grained upward-fining sand that is moderately well sorted, micaceous, carbonaceous, and locally glauconitic (Aadland et al. 1995). The CBAU generally thickens to the southeast.

## 2.3 Recharge

Annual precipitation is approximately 49 in. at P Area based on the meteorological data found at meteorological Station 100P (WSRC 2004). The majority of the precipitation flows overland to area water bodies (L Lake and PAR Pond), evaporates at the surface, or is transpired by vegetation. The remainder percolates through the soil and reaches the water table as recharge. Previous SRS modeling studies (WSRC 2004) have used recharge rates to the water table aquifer that range from 0.0 ft/day (0.0 in./yr) (a value typically used in groundwater discharge zones or capped areas) to 0.00388 ft/day (17 in./yr). The recharge rate is estimated to be 17 in./yr over most of the study area. The industrialized area of P Area is assumed to have a reduced average recharge rate (0.001939 ft/day or 8.5 in./yr) because of the high percentage of non-permeable surfaces (i.e., buildings and parking lots). Wetlands and other groundwater discharge zones were assumed to have zero recharge (Figure 2-4).

## 2.4 Source Description

The principal contaminants of concern (COCs) for this study area are tritium, and CVOCs PCE, TCE, and DCE, which have measured concentrations above their maximum contaminant levels (MCLs) in the vicinity of P Area. There are several contaminant source areas in P Area (Figure 2-5).

*Tritium*

The main source area for tritium is associated with the P-Reactor Seepage Basins (PRSB) waste unit located to the southwest of the P Area. This unit received waste water discharges from the P-Area Reactor Building disassembly basin that contained tritium, other radionuclides, and metals. Previous characterization of the PRSB indicated that a majority of the radionuclides, except tritium, and metals were contained within the basin bottoms due to the presence of naturally occurring clays, which tend to bind up these materials and prevent further migration. Other source(s) of tritium are related to operational and maintenance activities associated with process sewer line work on the west side of the P-Area Reactor Building, which resulted in releases of tritium-contaminated water to the subsurface. In addition, operational activities that resulted in minor releases of tritium to the subsurface also occurred on the east side of the building.

Actions completed to prevent the future impact to groundwater from tritium-contaminated soils and structures include in-situ stabilization and covering of the PRSB, evaporation of water from the disassembly basin and related structures, and in situ decommissioning of the reactor building complex (including grouting the entire subsurface).

*CVOCs*

Characterization of the P-Area Operable Unit determined two source areas of CVOC contamination. One was principally a PCE source area while the other was a TCE source area. The principal PCE source is located at the southwest corner of the P-Area Administration Building (704-P) and is designated as Source Area 3B. Source Area 3A contains TCE that originates north of the P-Area Reactor Building. DCE (combined *cis*- and *trans*-), which is a degradation product of TCE and PCE, has also been determined to be present. However, this CVOC is not considered a waste by-product of previous operations (WSRC 2004).

Actions completed to prevent the future impact to groundwater from PCE and TCE in these two source areas included soil vapor extraction and in-situ oxidation.

## 2.5 Plume Characterization

Figures 2-6 through 2-10 show the inferred PCE, TCE, and tritium plume extents, respectively, for the TZ, TCCZ, and LAZ hydrostratigraphic units based on the 2002 cone penetrometer technology (CPT) sampling event and updated with 2010-2011 direct push technology (DPT) data, and 2014-2015 DPT and groundwater monitoring well data. At each boring or well and for each contaminant, the measured concentration from the 2014 DPT sampling events and routine 2014-2015 groundwater sampling was used to modify 2011 concentration maps provided by Savannah River Nuclear Solutions as Geographical Information System (GIS) shapefiles. If concentration data existed in 2014 and 2015 at the same location, then the 2014 data was used to correspond to available DPT collected data.

The PCE plume is centered at Source Area 3B (Figure 2-6) near the P-Area Administration Building with concentrations up to 2,490 µg/L in the A/AA and TZ units reported in 2003, but the maximum detected in 2015 at monitoring well PGW025C was 260 µg/L. The PCE plume extends down to the LAZ with a maximum concentration of 71 µg/l detected during DPT sampling at PRGW063 and 58 µg/L at PRGW087 in 2014.

The TCE plume is centered on Source Area 3A (Figure 2-7) near the P-Area Reactor Building with concentrations over 15,000 µg/L in the A/AA and TZ units reported in 2002/2003. The plume extends in a narrow band to the west towards Steel Creek, then spreads following the creek to the southwest at concentrations over 100 µg/L. By the 2014/2015 sampling the maximum in the A/AA and TZ units is at PGW026DL near Steel Creek, at 4500 µg/L in 2014 and 4900 µg/L in 2015. The TCE plume extends down to the LAZ where the maximum concentration observed in 2010-2011 DPT sampling was 12,000 µg/L at PRGW066. The northeastern extent of the TCE plume may be between PRGW088 and PRGW090, where concentrations between 3.5 and 8 µg/L were measured in 2014. The LAZ plume originates at Source Area 3A and extends east towards Source Area 3B. The DCE plume is centered on Source Area 3A and extends in a narrow band to the west towards Steel Creek following the path of TCE but at much lower concentrations.

The main source area for tritium is associated with the PRSB waste unit located to the southwest of P Area (Figure 2-9). However, releases of tritium contaminated process water had occurred at the P-Reactor Building which also is contributing to the tritium plume. The plume extends to the west towards Steel Creek, then spreads following the creek to the southwest at concentrations over 500 pCi/mL. The tritium plume extends down into the LAZ just southeast of the Emergency Cooling Water Retention Basin at a maximum concentration of 10,000 pCi/mL with its vertical extent into the GCU at one well location (Figure 2-10). Tritium concentrations are still the highest at the PRSB. Monitoring well cluster PSB002 depicts maximum tritium concentrations well above the MCL (except PSB002AL) throughout the UTRA (16,400 pCi/mL in 2014 at PSB002C) and into the GCU (5,630 pCi/mL in 2014 at PSB002AA).

Groundwater data in tabular form from groundwater sampling and analysis events were provided to aid in further review of contaminant trends. Figure 2-11 shows tritium concentrations in well PSB 1A at the PRSB since 1999. Initially, concentrations were about 200,000 pCi/mL. Radioactive decay would have reduced this to about 50,000 pCi/mL by 2015. However, the observed concentrations of under 1,000 pCi/mL indicate dilution and downgradient transport of tritium in groundwater. Similar declines in contaminant levels are observed for all wells examined.

The vertical extents of the plumes are limited by the GCU. There are no measured concentrations above MCLs for PCE (MCL = 5 µg/L), DCE (MCL = 70 µg/L), or tritium (MCL = 20 pCi/mL) below the GCU. There is one TCE detection in 2002 [21.7 µg/L, flagged as estimated (J)] in the LGA above the MCL (5 µg/L); this is believed to be an aberration because (1) all TCE measurements in the GAU above this sample are below the MCL, (2) there were no detections anywhere at the same elevation, (3) the location is far from any known source, and (4) it is not supported by recent fieldwork. Detection of tritium in the LAZ occurred in the 2011, 2014, and 2015 sampling events. The maximum detections were 0.16 pCi/mL, 14 pCi/mL, and 12 pCi/mL respectively for years 2011, 2014, and 2015. The number of detects were 3, 11, and 11 for the three years.

Vinyl chloride (VC) was not detected in enough locations to define plumes. Additionally, the lack of detection of VC is most likely attributed to incomplete degradation of TCE and PCE in aerobic groundwater as noted by the buildup of DCE. Only 6 of 887 samples for VC had concentrations greater than the MCL (2 µg/L), with a maximum measured concentration of 5 µg/L.

Concentrations of CVOCs and tritium vary along the length of Steel Creek. The maximum concentration of TCE in Steel Creek occurred at SC-03 at 21.65 µg/L in June 2008 (Figure 2-12). The concentrations of PCE, DCE and VC have not been measured at concentrations above the MCL in Steel Creek. PCE only had detections in August 2003 (at SC-01 at 1.83 µg/L, at SC-02 at 0.85 µg/L, and at SC-03 at 0.6 µg/L), and there have not been detections of VC. By the time the water reaches SC-04, the concentrations of all CVOCs drop below the MCLs. The maximum concentration of tritium in Steel Creek occurred at SC-03 at 2,920 pCi/mL in September 2005 (Figure 2-13). At SC-04, farther downgradient, the trend is decreasing over time. The tritium remains above the MCL (20 pCI/mL) downstream to SC-07, near L Lake.

## 2.6 Groundwater Flow

Groundwater flow directions in the study area were determined from interpreted potentiometric surfaces based on the Long-term Heads (LTH, described below) and confirmed by the shape of the plumes. Reliable LTH can provide dependable calibration targets for the purpose of modeling groundwater flow. Newfields and GeoTrans (2004) documented a methodology of statistically adjusting measured head data to take into account lack of long term historical data and climatically-biased data at monitoring wells. Afterwards, Andersen and Grogin (2008) documented a method of extending the data set from 2003 to the present.

Since the last P-Area model (SRNS 2011a) the methods outlined in Andersen and Grogin (2008) were applied to water level data from fourth quarter 2003 through second quarter 2015 for the "representative" site-wide wells (Newfields and GeoTrans 2004) and local P-Area wells to update the LTH for each well. These calculations were the basis of the targets used in model calibration (Appendix B, Table B-1) and in the production of potentiometric surfaces shown in Figures 2-14 through 2-19. As part of the LTH process, wells with standard error measurements greater than 5 feet or total number of measurements under 11 were excluded (pre- and post-2003

combined) (Appendix B, Table B-2). Thirty-eight new monitoring wells installed since 2011 were excluded because they had fewer than 11 measurements (Table B-2). Appendix B, Table B-1 contains the LTHs used in the model. For reference purposes, Table 2-2 is included that contains all wells in the P Area.

In the development of the potentiometric surfaces each LTH was analyzed for appropriateness of inclusion based on: (1) if the well appears to be screened across or within in a low hydraulic conductivity unit (e.g., TCCZ), which means that there could be a large head variation vertically along the length of the well screen (calling into question the point at which the head is equal to the measured water level) (i.e. P 24C); (2) if the target head for the well does not match those of nearby wells with the same aquifer designation and there is some reason to question the aquifer designation (e.g., the screen midpoint location unit does not match the aquifer designation); or (3) if the well was removed from consideration in the development of the solids model.

For instance, recently installed monitoring wells PGW033A and PSB002AA were removed from consideration as they were screened at the very top of the GAU, with additional clay layers below the screen, and had heads about 8 feet higher than the surrounding UGA wells. Appendix B, Table B-2 lists wells removed from potentiometric surface development, as well as the reason for their removal. Additionally, well PSB002AL and other CBAU wells were included, even with fewer than 11 measurements, to increase the number of targets in this under-represented aquifer.

The LTH range in head is from 172.22 to 282.00 ft. The number of valid targets per hydrostratigraphic unit is shown in Table 2-3, for a total of 133. There are no wells present in the following units: TCCZ, MC-LAZ, GCU, MGA, and CBCU, because these layers represent low permeability or confining units. Wells were placed in hydrostratigraphic units based on the mid-screen elevations and the model layers as described in Chapter 3.

Groundwater flow directions in the A/AA and TZ appear to generally follow topography, with a groundwater mound under the P-Area Reactor (Figures 2-14 and 2-15). Groundwater flow at Source Area 3B is stagnant due to slow groundwater movement in the shallow aquifer and a fluctuating groundwater divide; seasonal changes in head in the area result in a minimally dispersed PCE plume. However, this lack of dispersion could result in further vertical migration

into deeper units. Near the other source areas, flow is directed towards Steel Creek on the west side of the P-Area Reactor and to PAR Pond tributaries on the east side. The groundwater mound also exists in the ULAZ and LLAZ (Figures 2-16 and 2-17). There is a downward component of groundwater flow across the GCU into the GAU. The potentiometric surface of the UGA is relatively flat on the west side with a dip across the P-Area Reactor to the east. The horizontal gradient and southward direction of groundwater flow in the LGA is similar to that of the GAU found in the L Lake area (GeoTrans 2004) and the gradient shown in the *Hydrogeologic Framework of West-Central South Carolina* (Aadland et al. 1995) (Figure 2-18). There is a significant downward gradient between the UGA and the LGA. There is also a downward component of groundwater flow across the CBCU into the CBAU. Groundwater flow in the CBAU is south-southwesterly in much of the study area (Aadland et al. 1995).

## 2.7 Solute Transport Processes

All dissolved constituents are affected by the processes of advection, diffusion, and hydrodynamic dispersion. Advection is the process that describes the movement of dissolved constituents along the groundwater flow path and is often conceptualized as a particle trace. Diffusion is the process of random molecular motion that effectively results in mass flux from areas of high concentration to areas of lower concentration at the pore scale. A more important process for most solute transport problems is hydrodynamic dispersion, in which a heterogeneous velocity field causes plume-scale mass flux from areas of high concentration to areas of low concentration. Greater velocities result in greater plume spreading. In the current analysis, as in most groundwater transport problems, diffusion is ignored but hydrodynamic dispersion is considered.

As a radioactive element, tritium ($H^3$), an isotope of hydrogen, spontaneously decays with a half-life of 12.3 yr. It is readily soluble in water and generally does not adsorb to the soil. Therefore, the adsorption coefficient tritium is generally assumed to be zero. The assumption of no adsorption is challenged by the observation that the groundwater flow velocities exceed the observed tritium plume velocity. The observed “retardation” may result from a fraction of the plume being affected by stringers of low hydraulic conductivity material that significantly

reduces velocities of that part of the plume. This type of retardation can be approximated with a dual porosity model or its effect represented using standard adsorption / desorption exchange.

PCE, TCE, and DCE are CVOCs. CVOCs are readily volatilized to air in the unsaturated zone and at the surface of water bodies. Dissolved CVOCs in the groundwater also may be affected by sorption and biodegradation (Figure 2-20). Sorption is the process by which PCE, TCE, and DCE mass is adsorbed to and desorbed from soil particles, thus effectively retarding the movement of the plume. An equilibrium sorption process is assumed; whereby, the concentration of the CVOC in groundwater is proportional to the CVOC concentration in the soil. The proportionality constant is called the sorption coefficient, or $K_d$, and is dependent on the organic-carbon content of the soil.

## 2.8 Contaminant Pathways

In general, contaminants originate from a source in the vadose zone and move, essentially, vertically downward until they reach the water table. In most source areas, the vertical hydraulic gradient within the saturated zone is downward and, hence, the contaminants move downward and laterally as they follow the horizontal gradients within a particular aquifer, usually towards surface water bodies that represent discharge points. In the study area, the primary surface water bodies are Steel Creek and tributaries of PAR Pond. Pathways within aquitards are assumed to be essentially vertical; although, heterogeneity within units classified as aquitards may result in some horizontal movement. Contaminant pathways are complex due to the interaction between horizontal and vertical components of flow as well as differences in flow directions from aquifer to aquifer.

## 2.9 Composite Hydrogeologic Conceptual Model

The HCM is shown schematically in Figure 2-21, which is a cross section along a typical flow line from P Area towards Steel Creek. The depth to water varies in the study area from zero near water bodies to a maximum of 80 ft near L-Area. The average depth to water is 45 ft.

Contamination migrates from the various source areas downward through the vadose zone and enters the groundwater system at the water table. Tritium in the water naturally decays. CVOCs, such as PCE and TCE, dissolve into the resident water and generally flow with the groundwater, both horizontally and vertically, into deeper aquifers. The CVOC concentrations are reduced due to mixing and dispersion. Retardation may further attenuate the CVOC concentrations. The plumes discharge to surface water bodies.

The groundwater flow system that drives the plume migration is controlled by boundary conditions, including recharge and discharge locations within the model domain and some that are more regional and outside the model domain. The plume velocity is controlled by the head differences imparted by these boundary conditions and hydraulic parameters such as hydraulic conductivity and porosity. Hydraulic conductivity is highly variable from aquifer to aquifer and especially between aquifers and aquitards. Therefore, the groundwater flow velocities also vary from aquifer to aquifer by orders of magnitude with the highest being in the ULAZ.

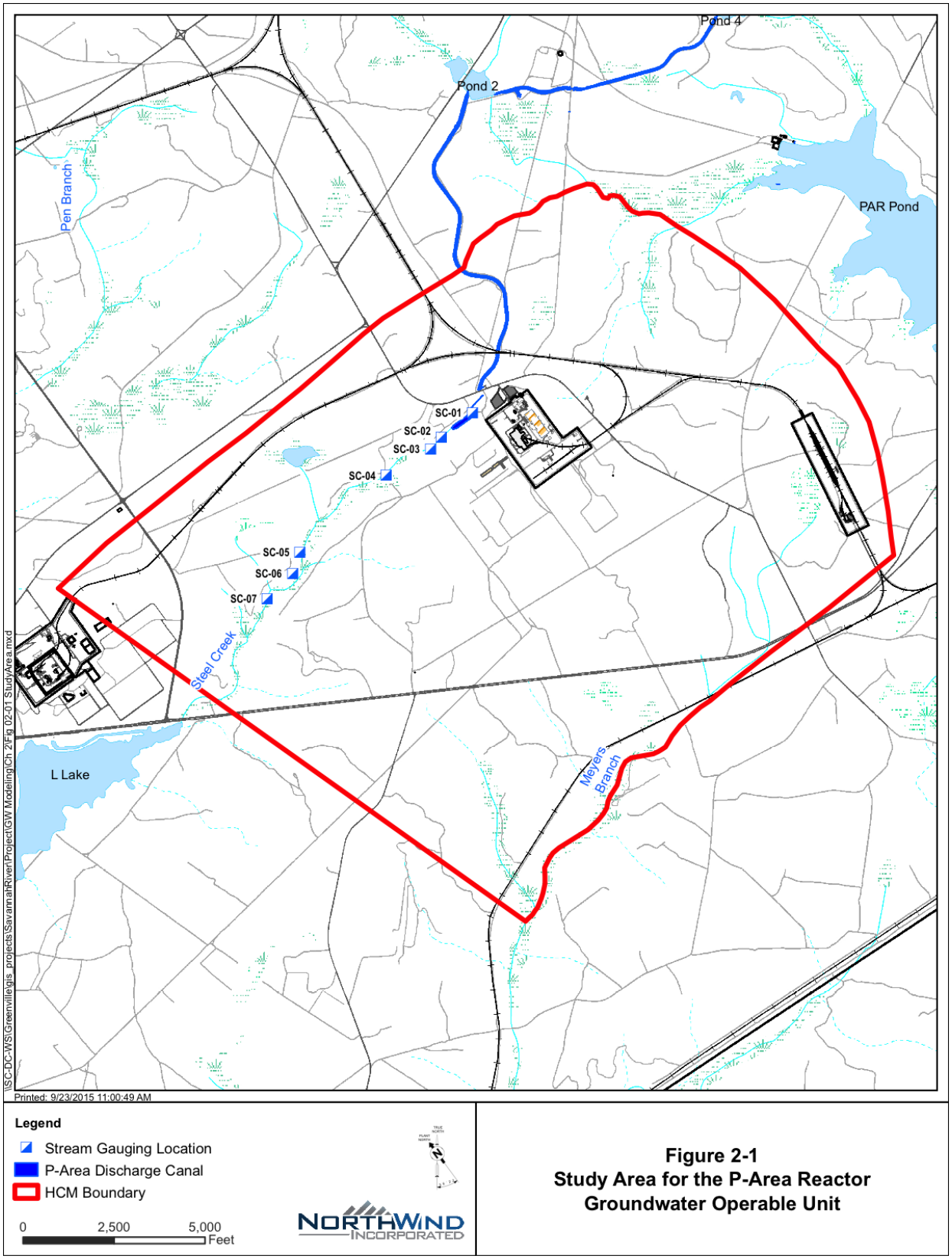


**Figure 2-1 Study Area for the P-Area Reactor Groundwater Operable Unit**

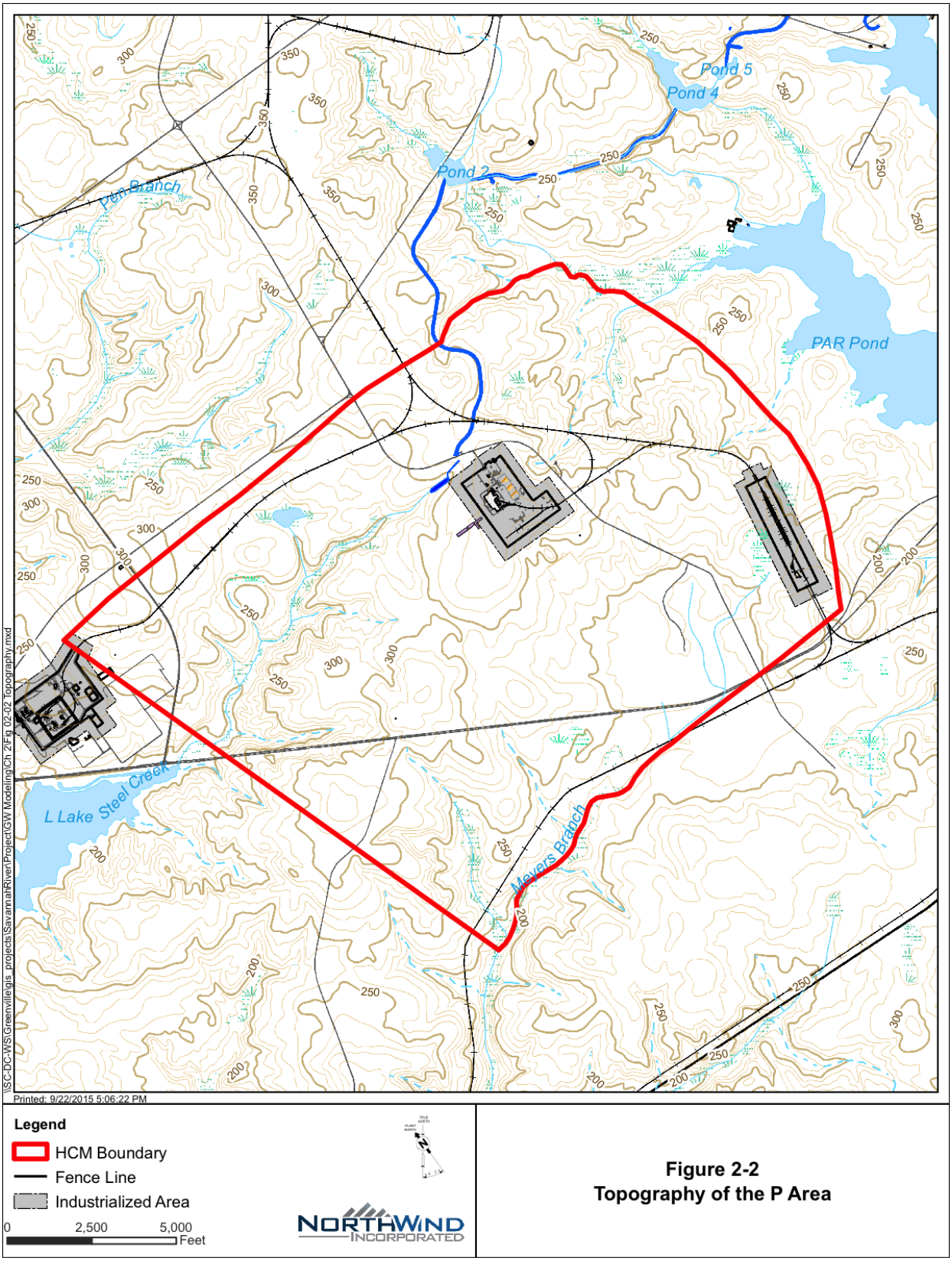


**Figure 2-2 Topography of the P Area**

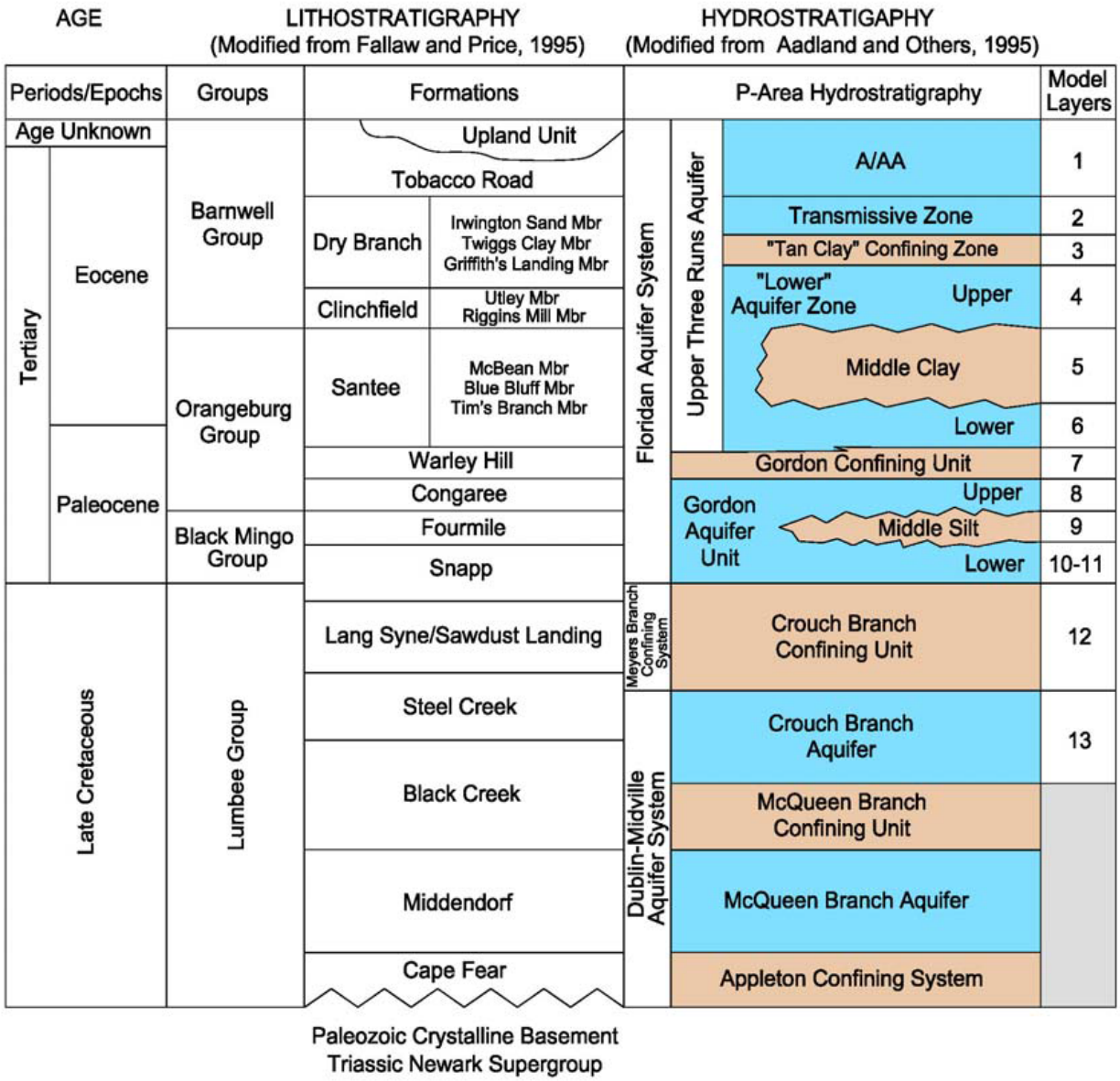


**Figure 2-3 Hydrostratigraphy of P Area**

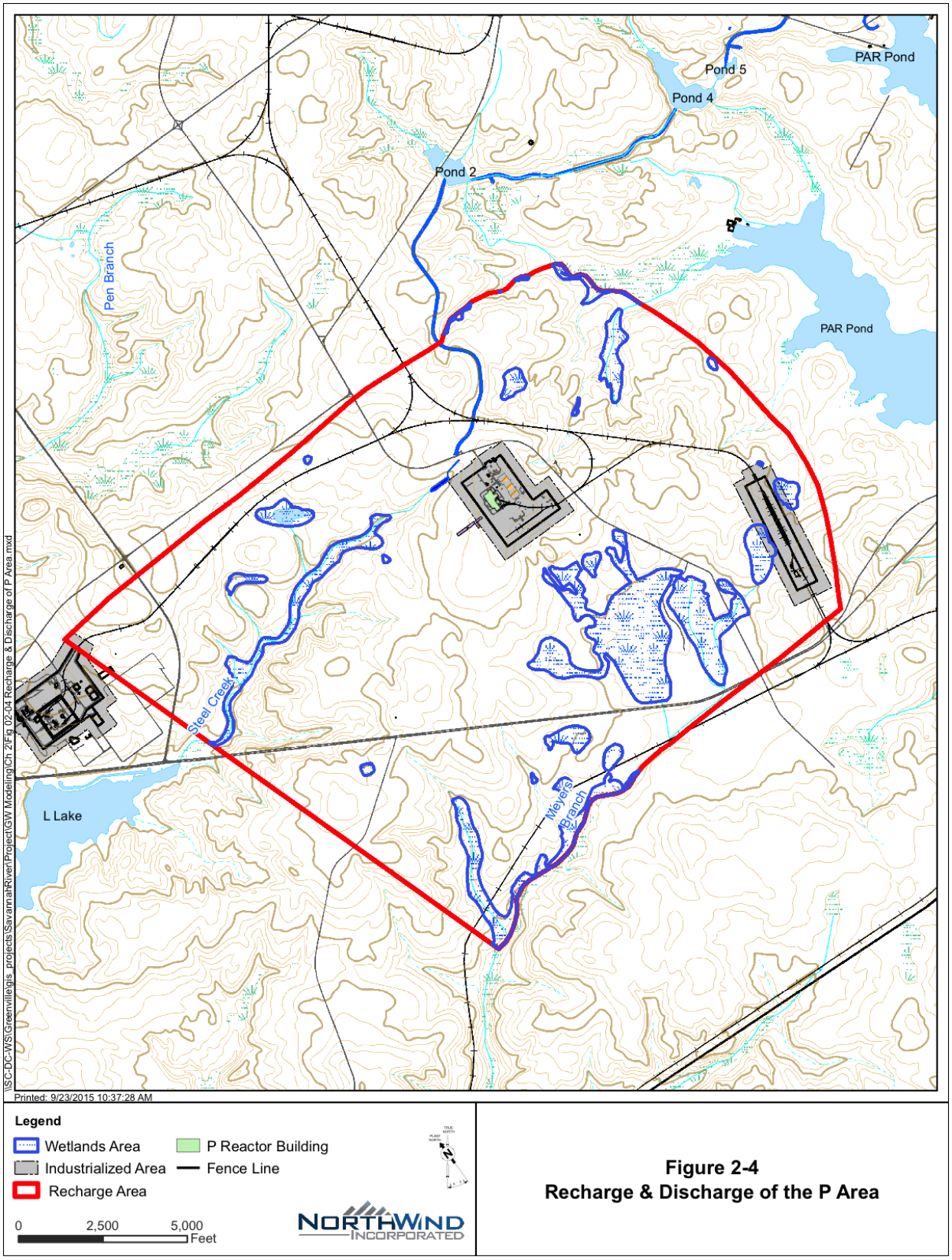


**Figure 2-4 Groundwater Recharge and Discharge Located in the P Area**

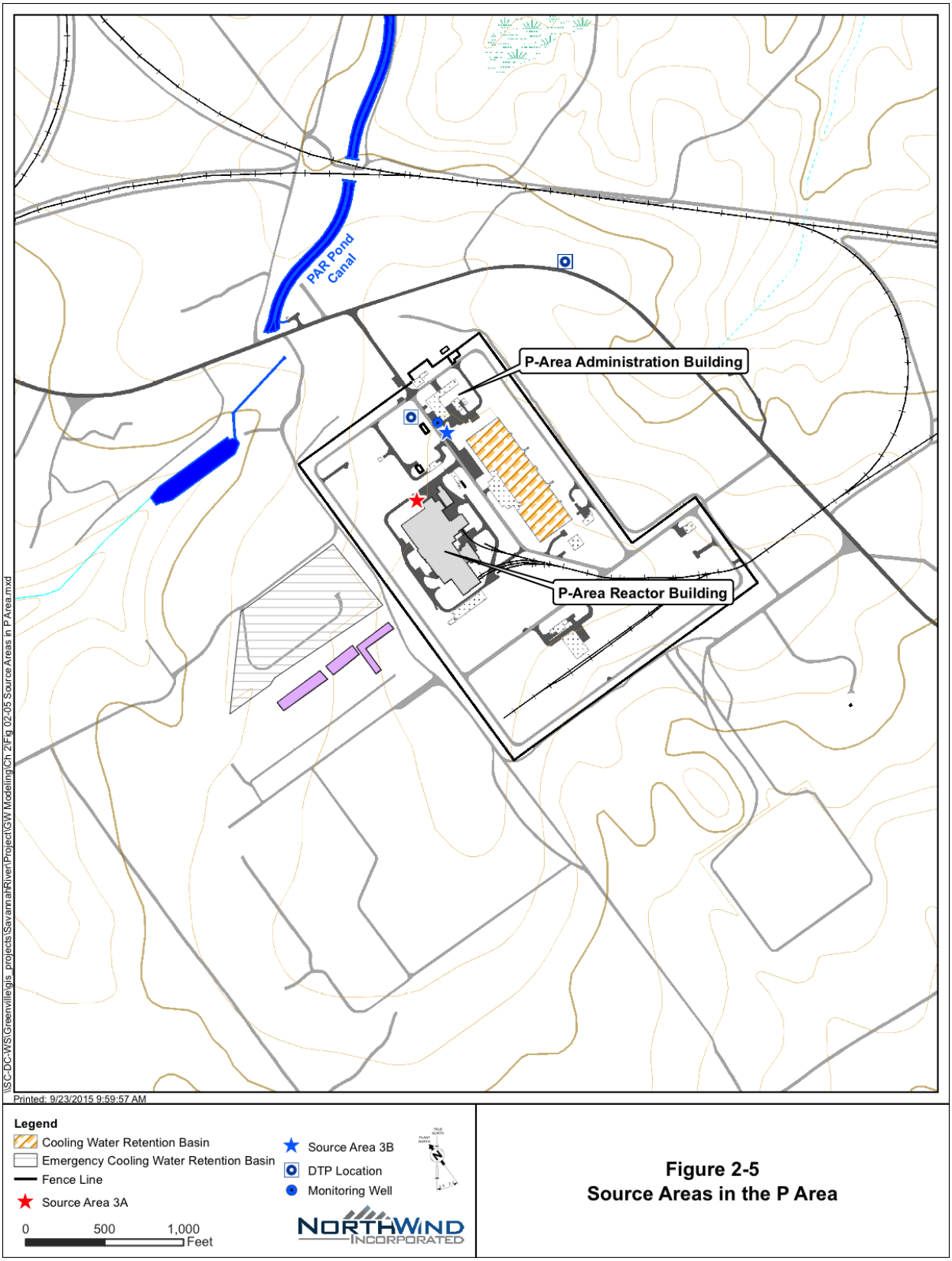


**Figure 2-5 Source Areas in the P Area**


**Figure 2-6 PCE Plumes in the TZ, TCCZ, & LAZ**

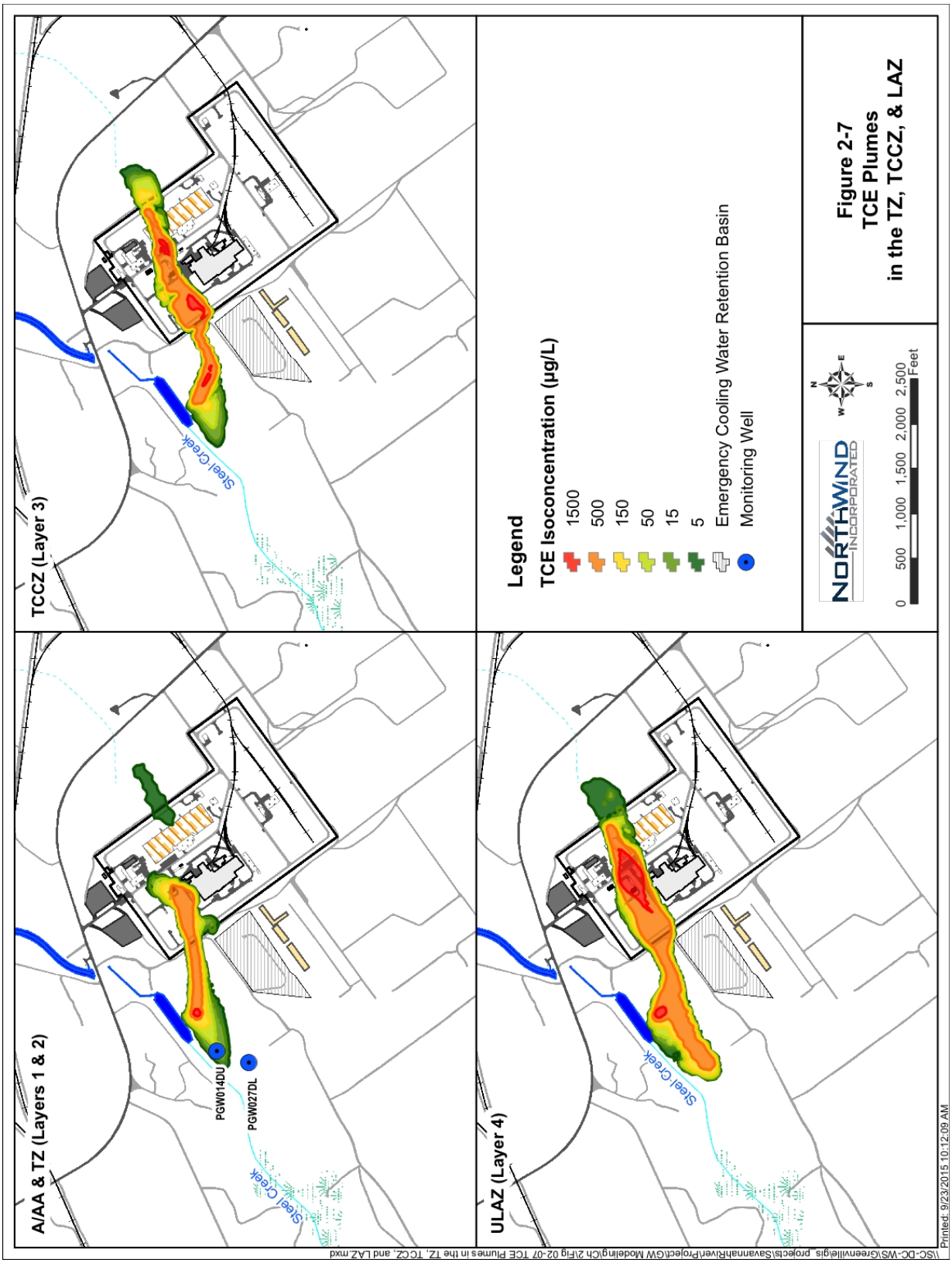


**Figure 2-7 TCE Plumes in the TZ, TCCZ, & LAZ**

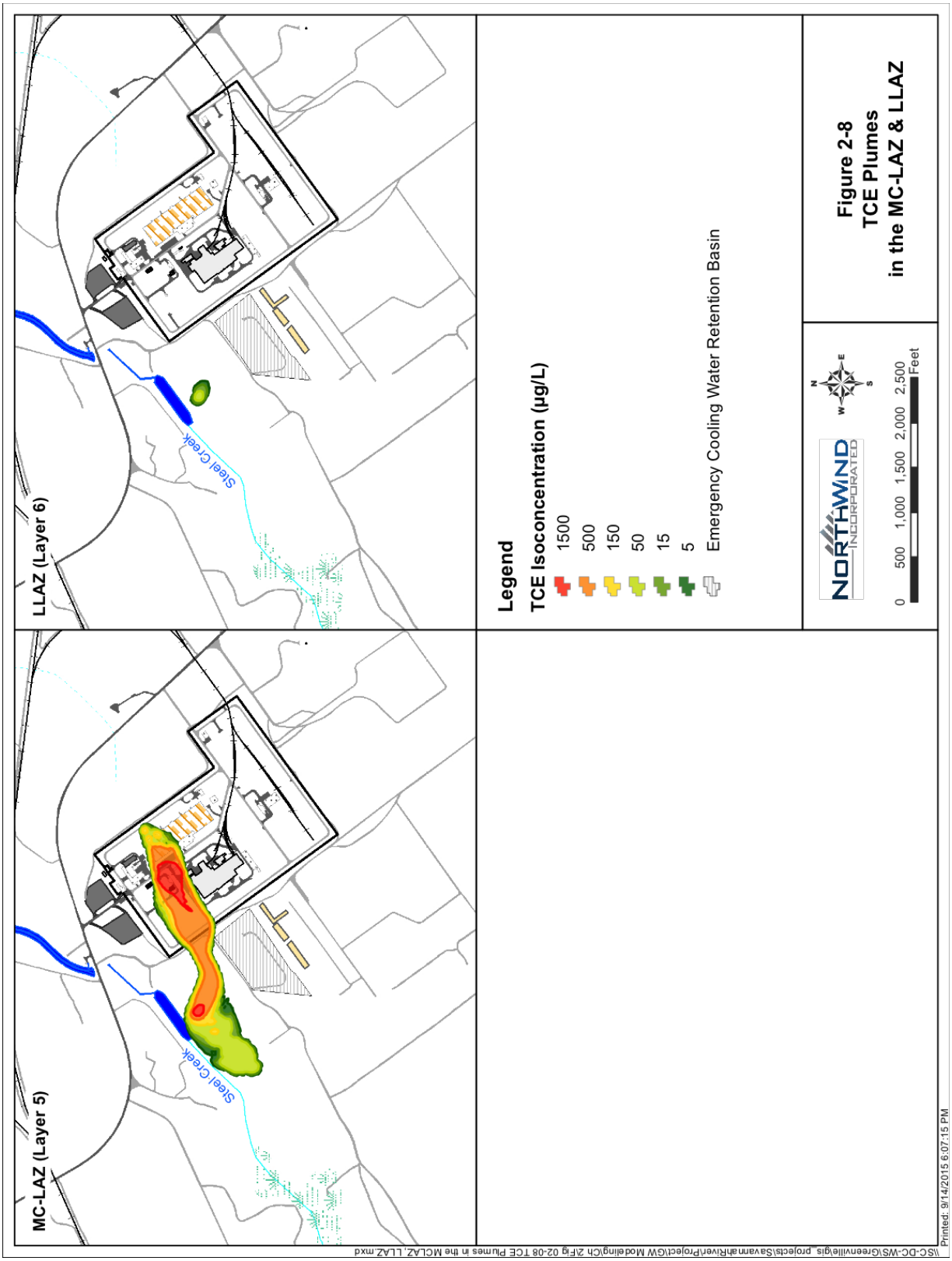


**Figure 2-8 TCE Plumes in the MC-LAZ & LLAZ**

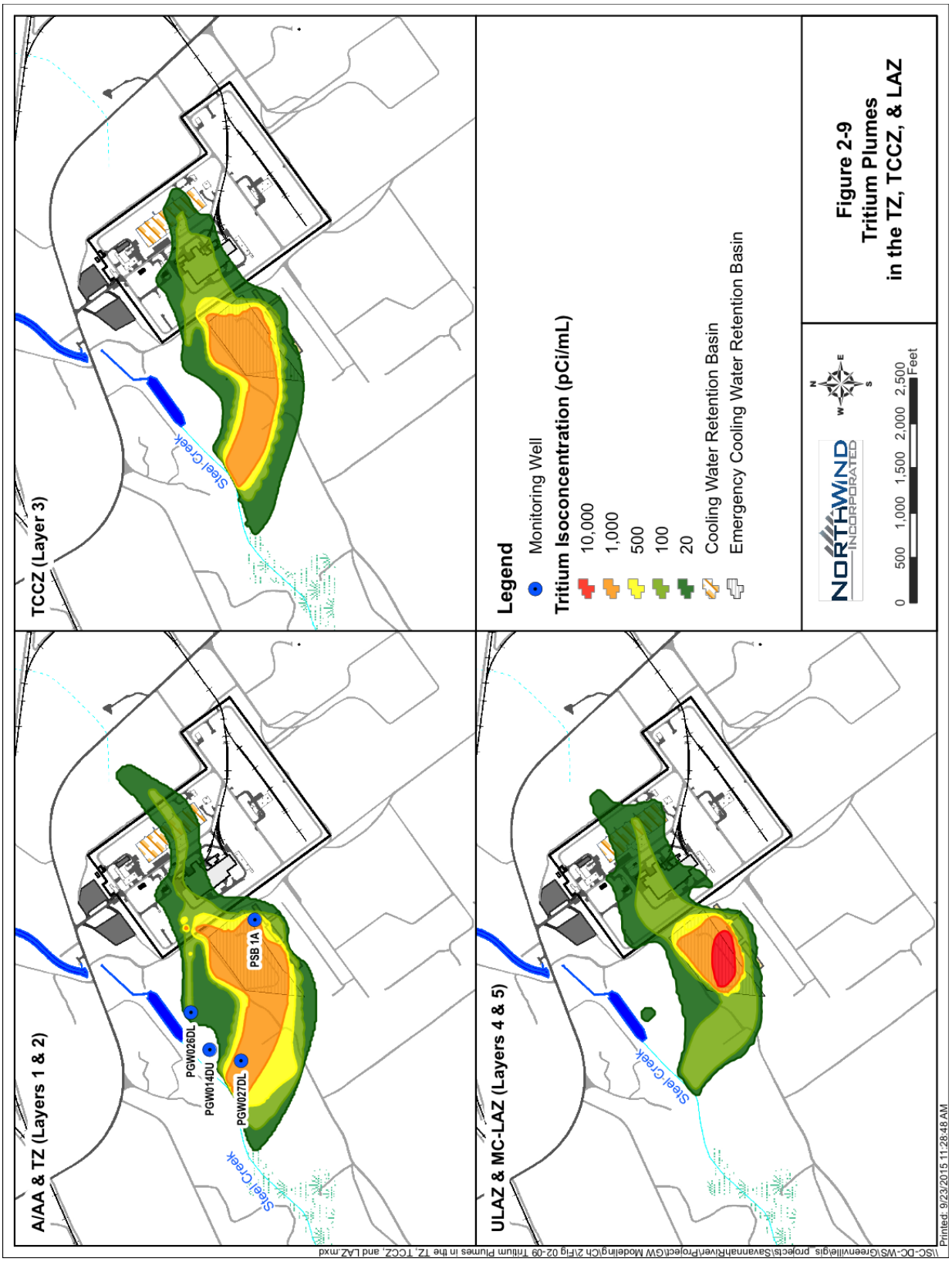


**Figure 2-9 Tritium Plumes in the TZ, TCCZ, & LAZ**

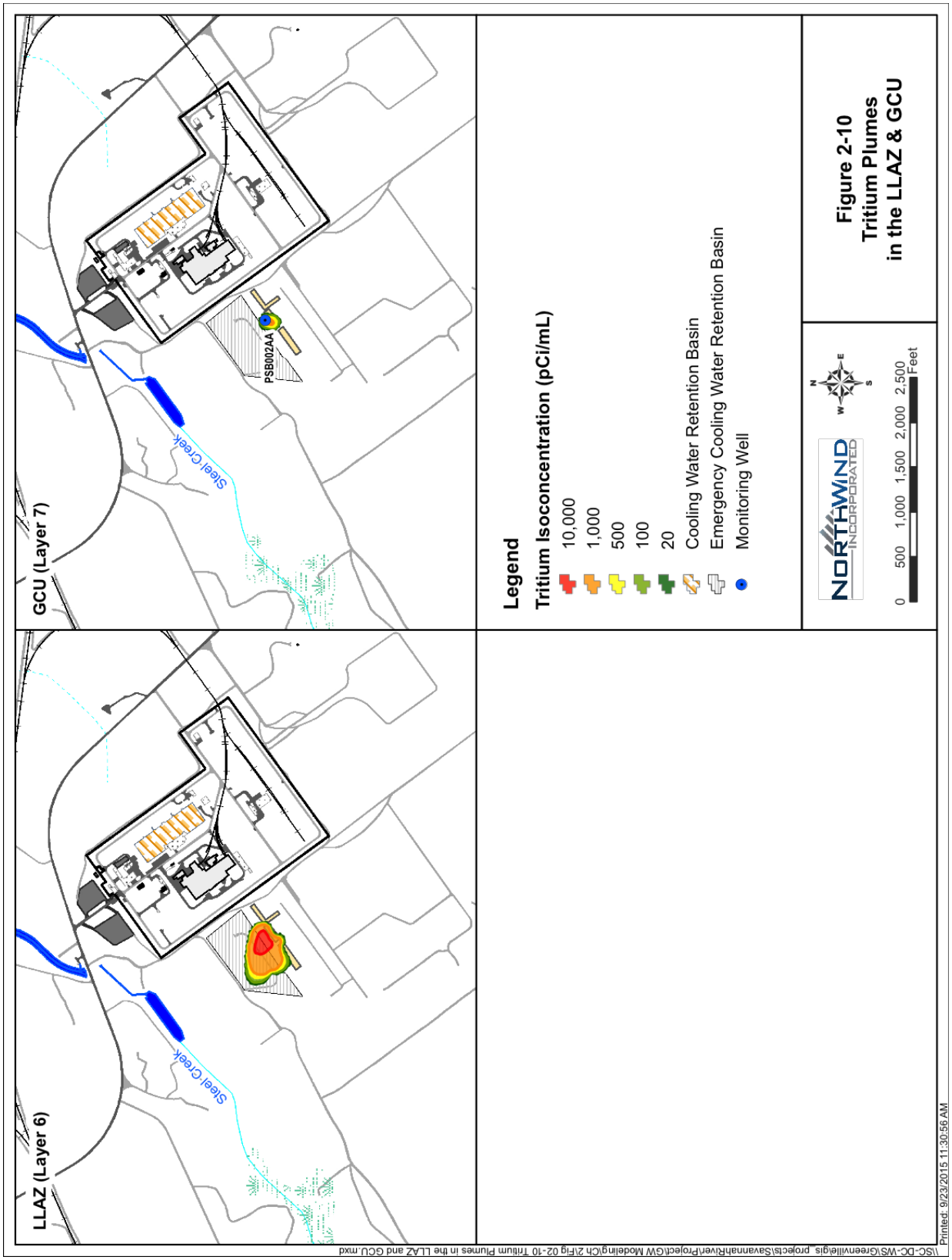


**Figure 2-10 Tritium Plumes in the LLAZ & GCU**

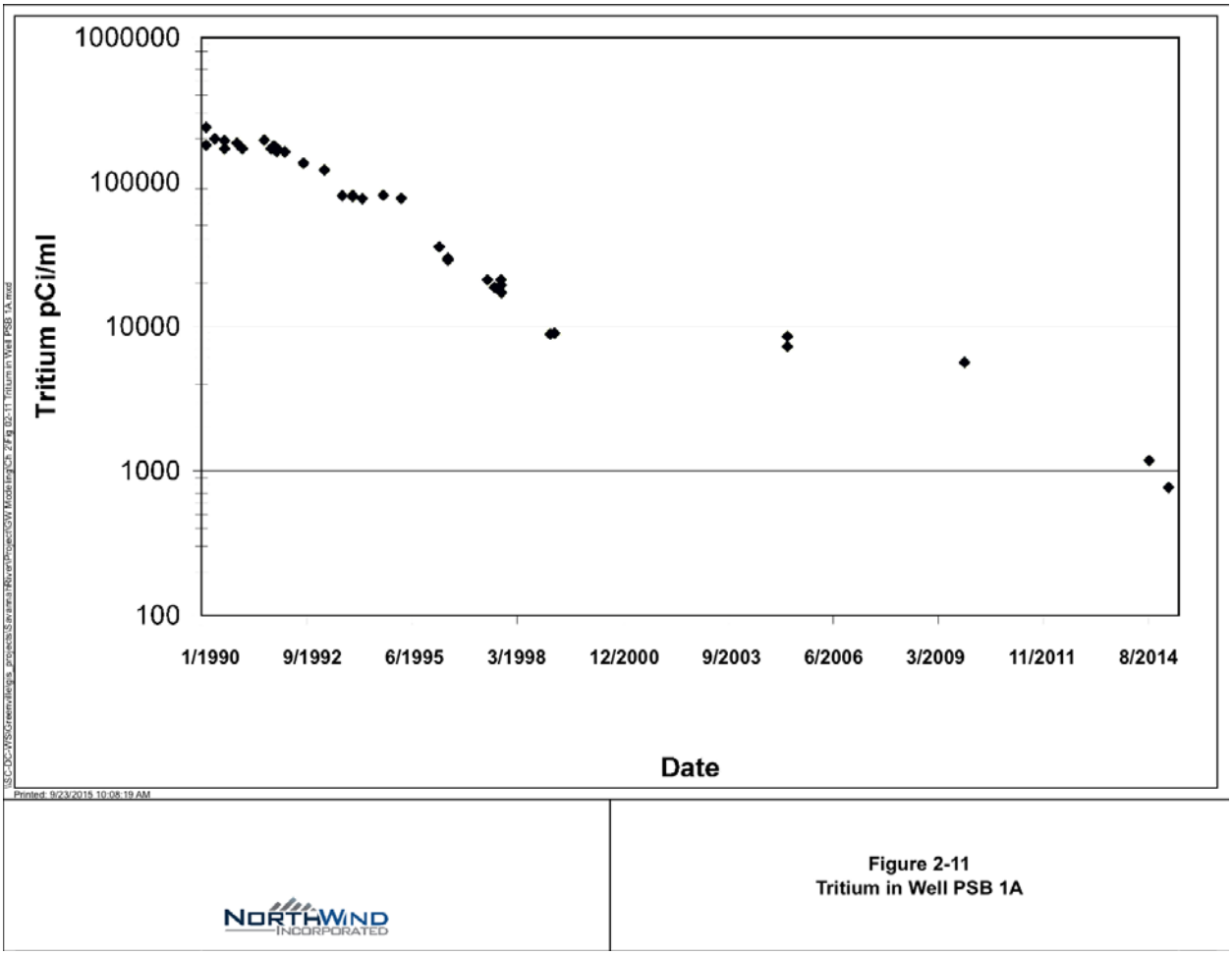


**Figure 2-11 Tritium in Well PSB 1A**

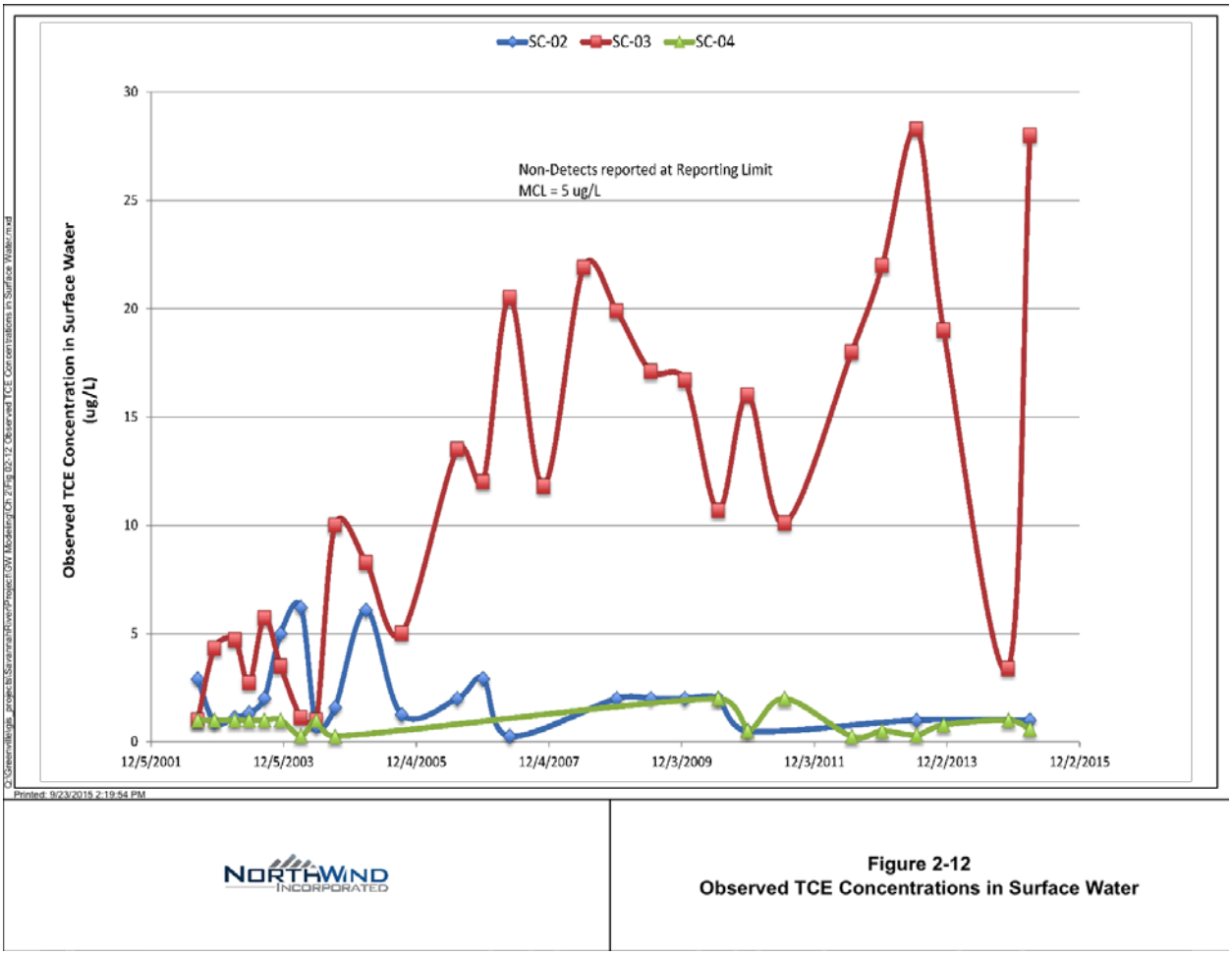


**Figure 2-12 Observed TCE Concentrations in Surface Water**

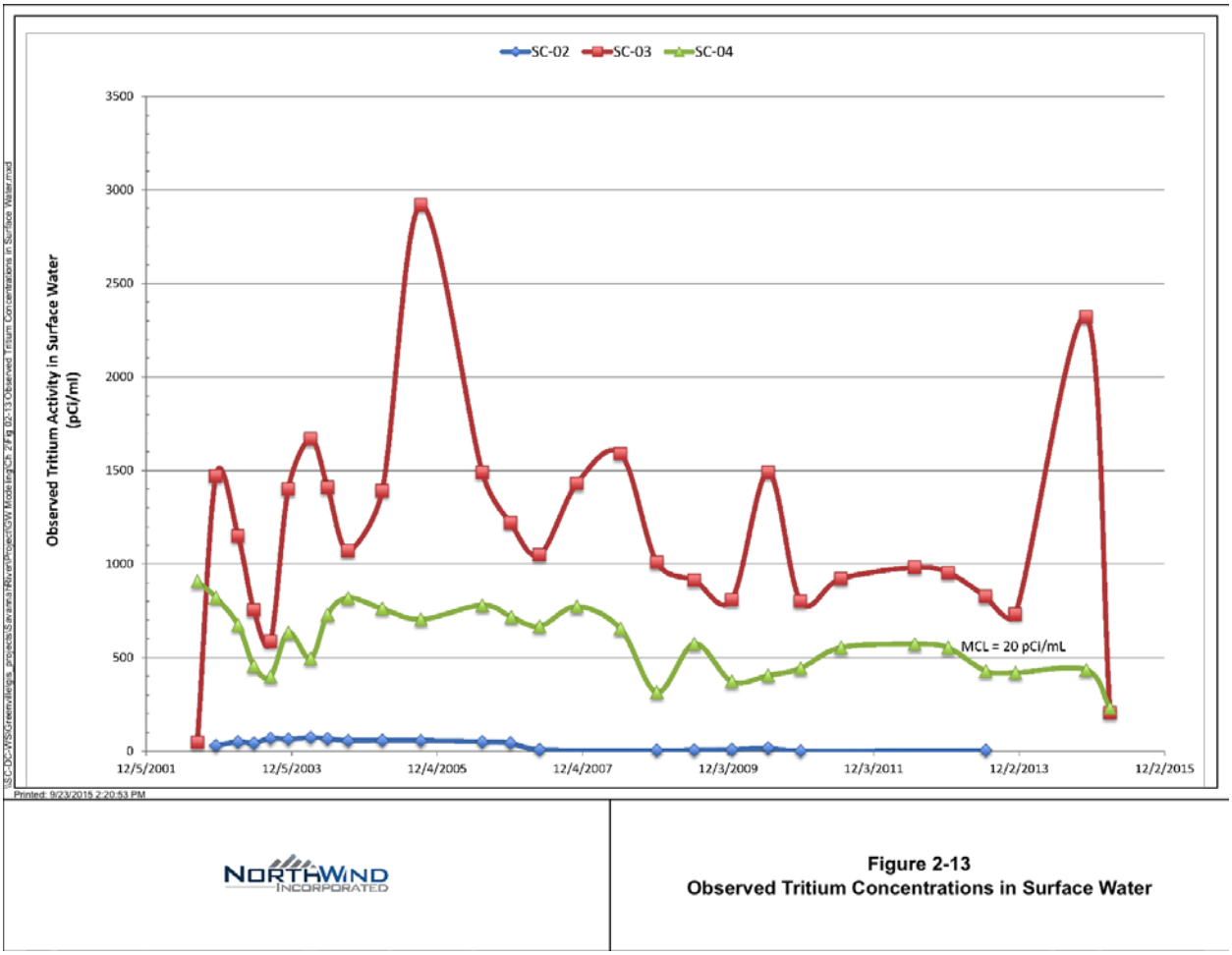


**Figure 2-13 Observed Tritium Concentrations in Surface Water**

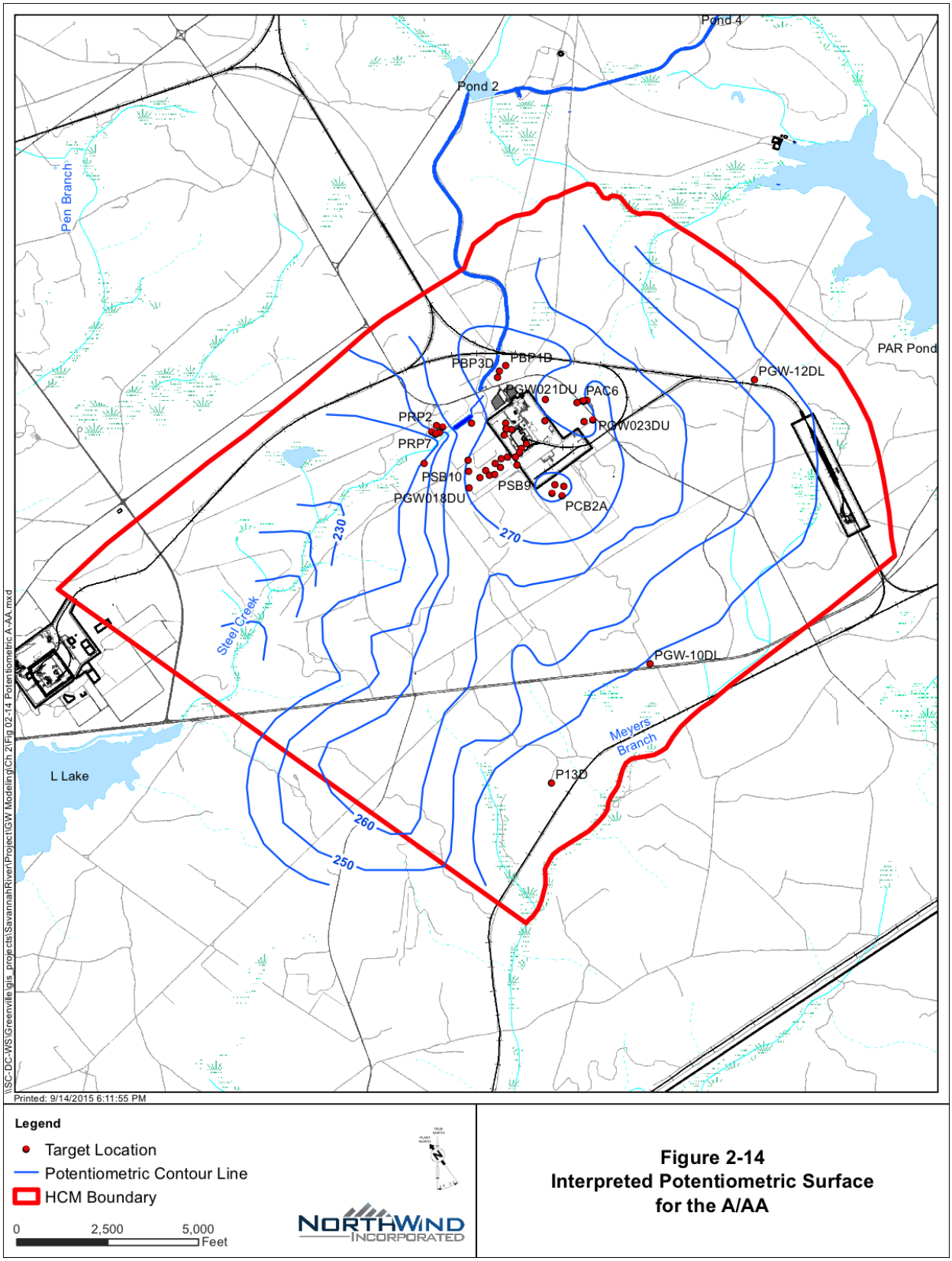


**Figure 2-14 Interpreted Potentiometric Surface for the A/AA**

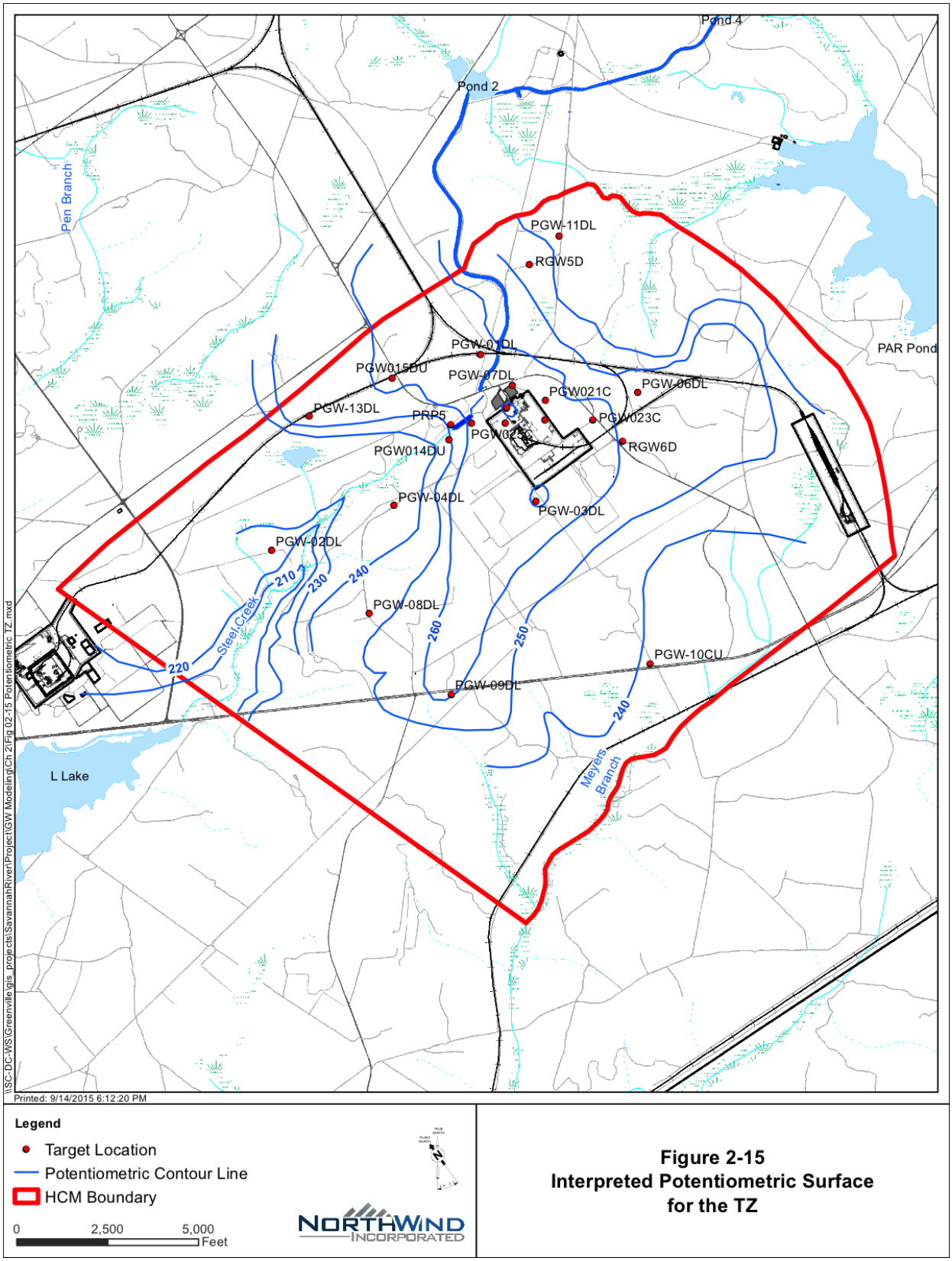


**Figure 2-15 Interpreted Potentiometric Surface for the TZ**

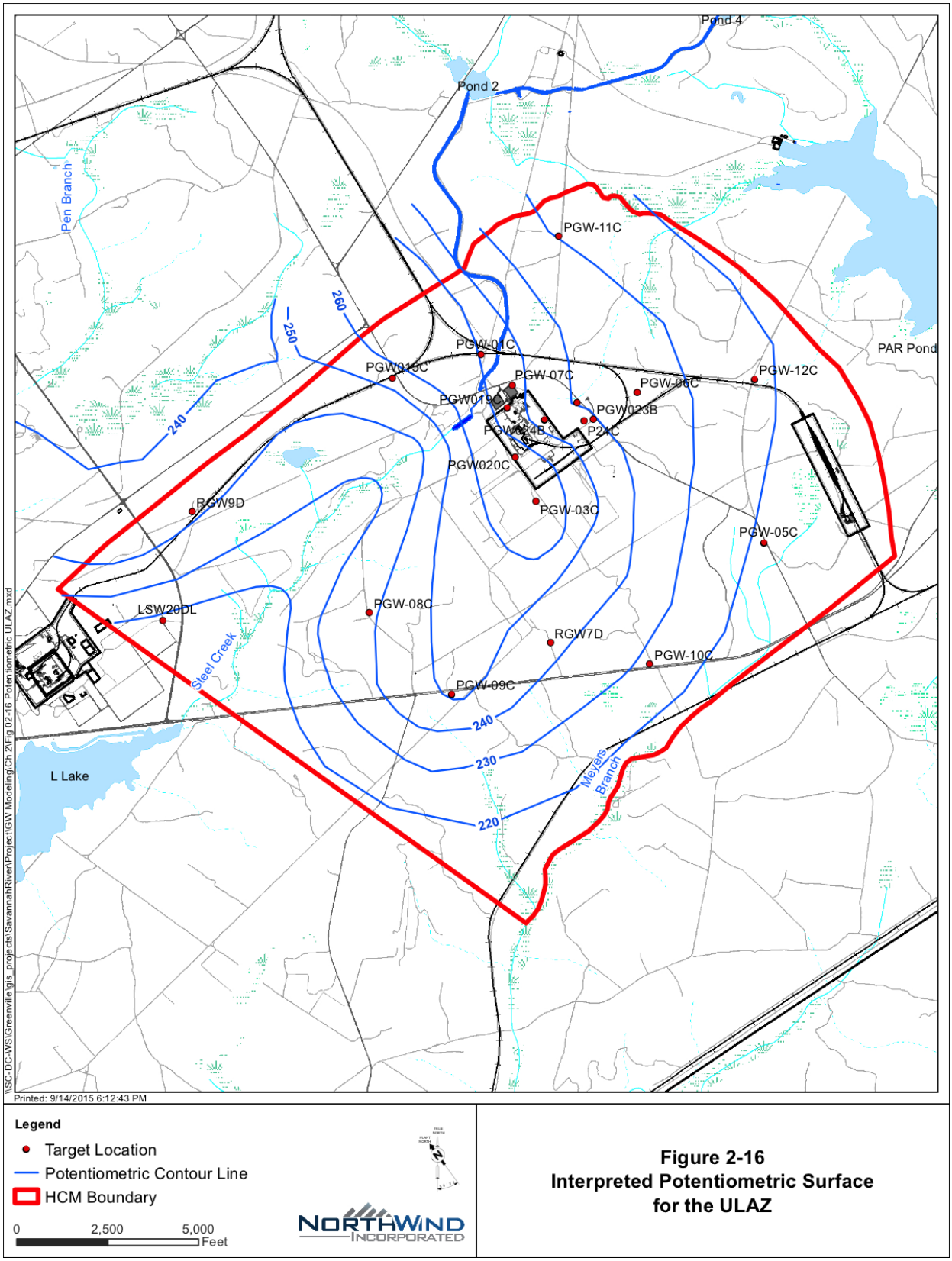


**Figure 2-16 Interpreted Potentiometric Surface for the ULAZ**

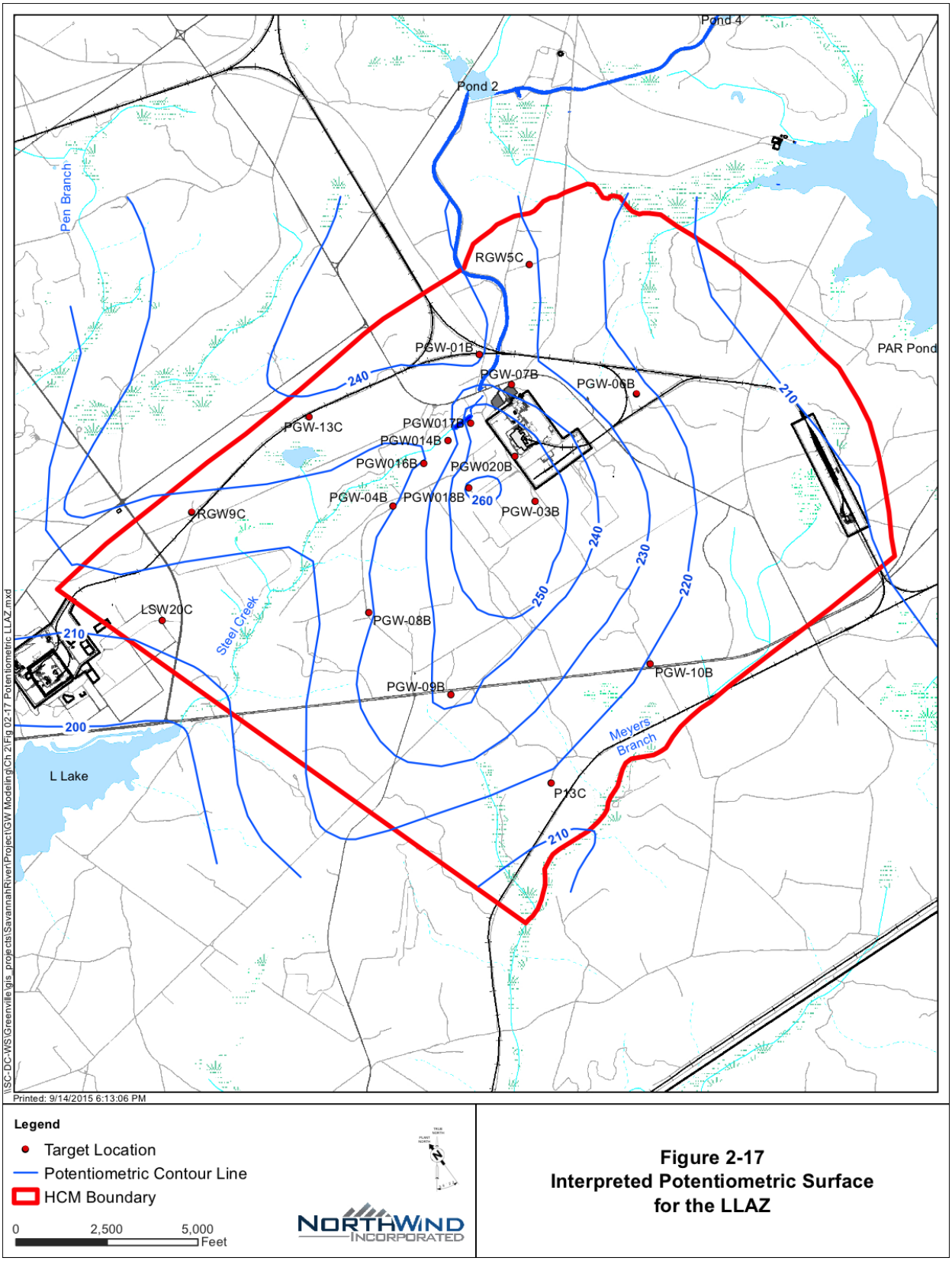


**Figure 2-17 Interpreted Potentiometric Surface for the LLAZ**

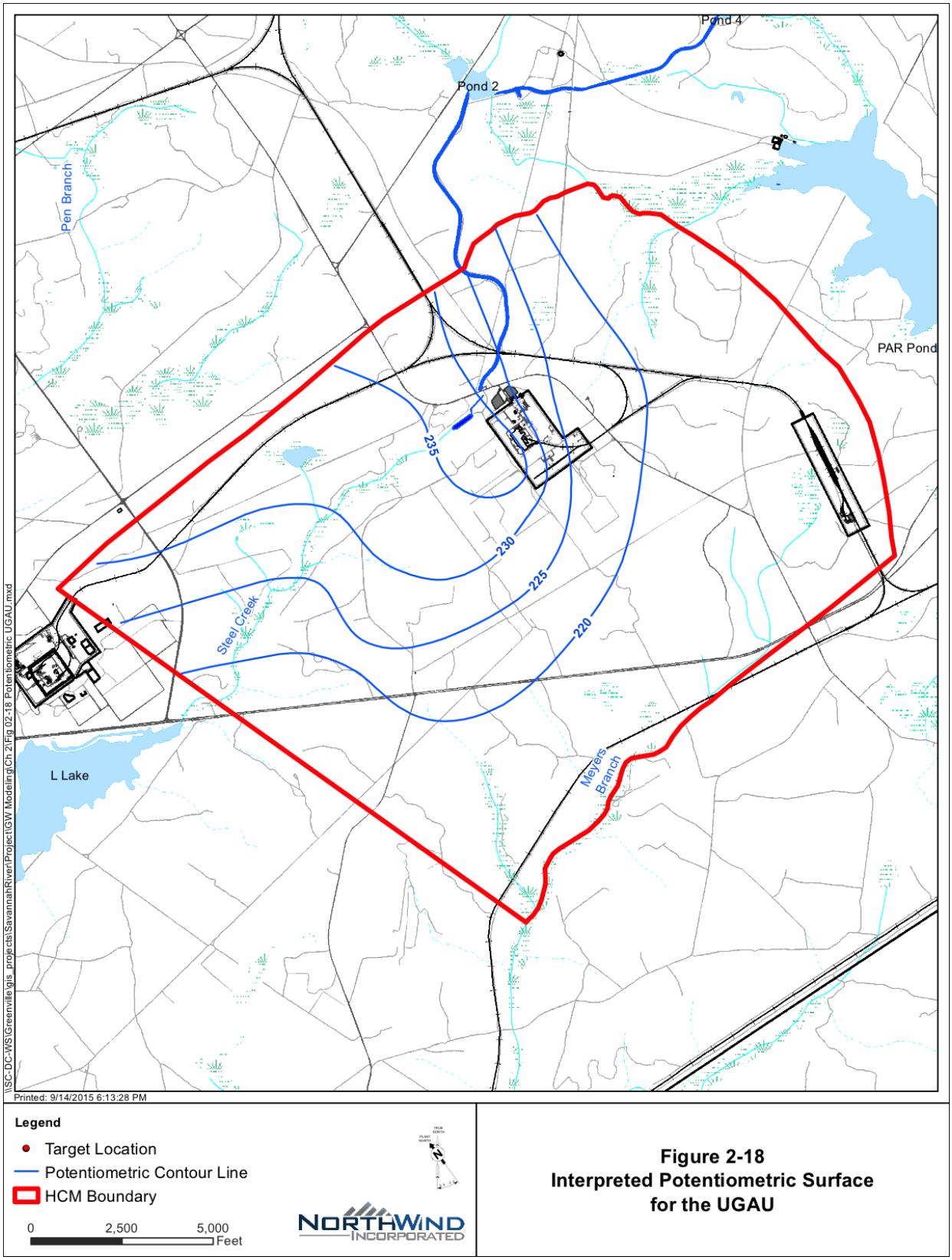


**Figure 2-18 Interpreted Potentiometric Surface for the UGA**

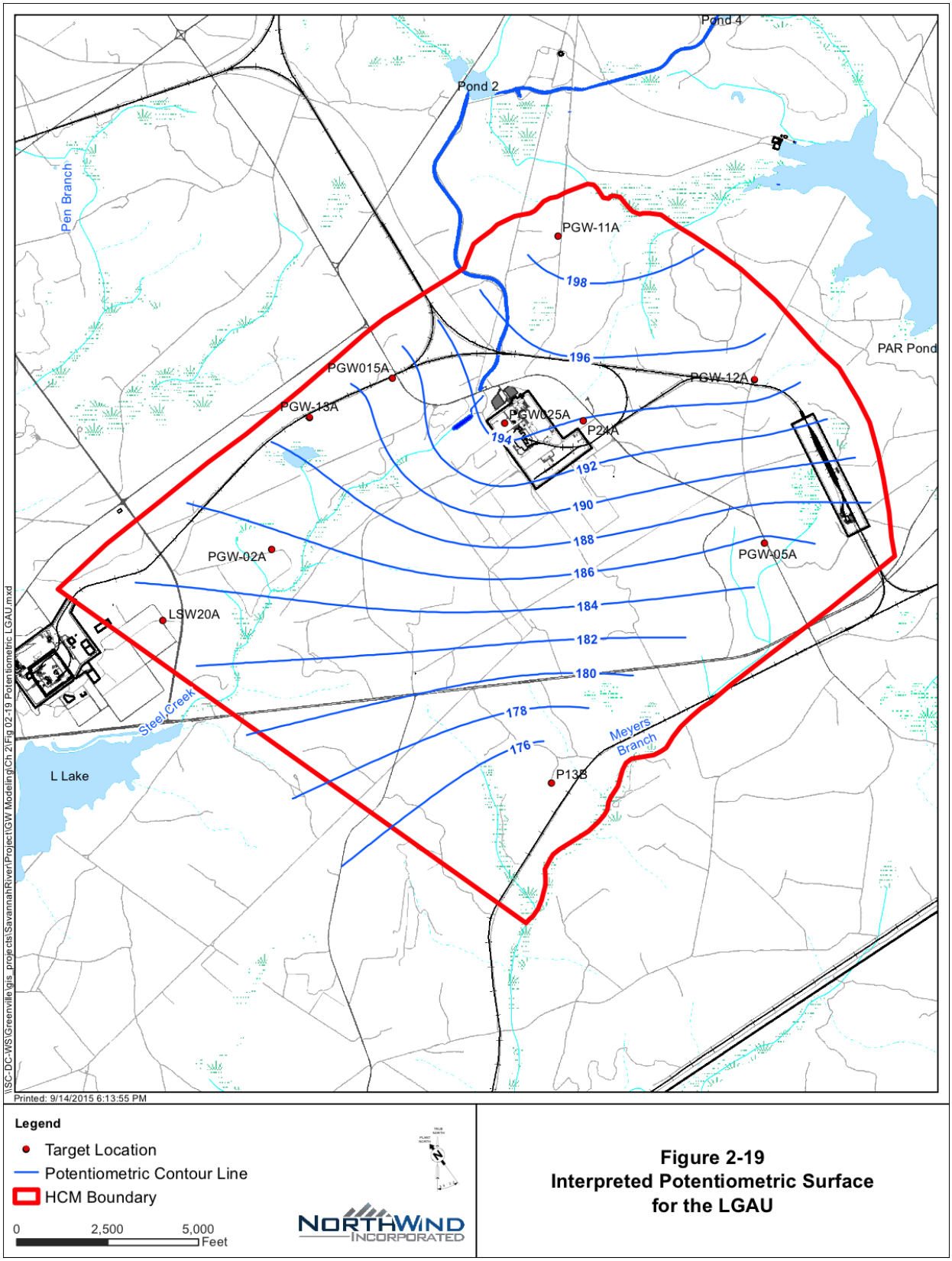


**Figure 2-19 Interpreted Potentiometric Surface for the LGA**

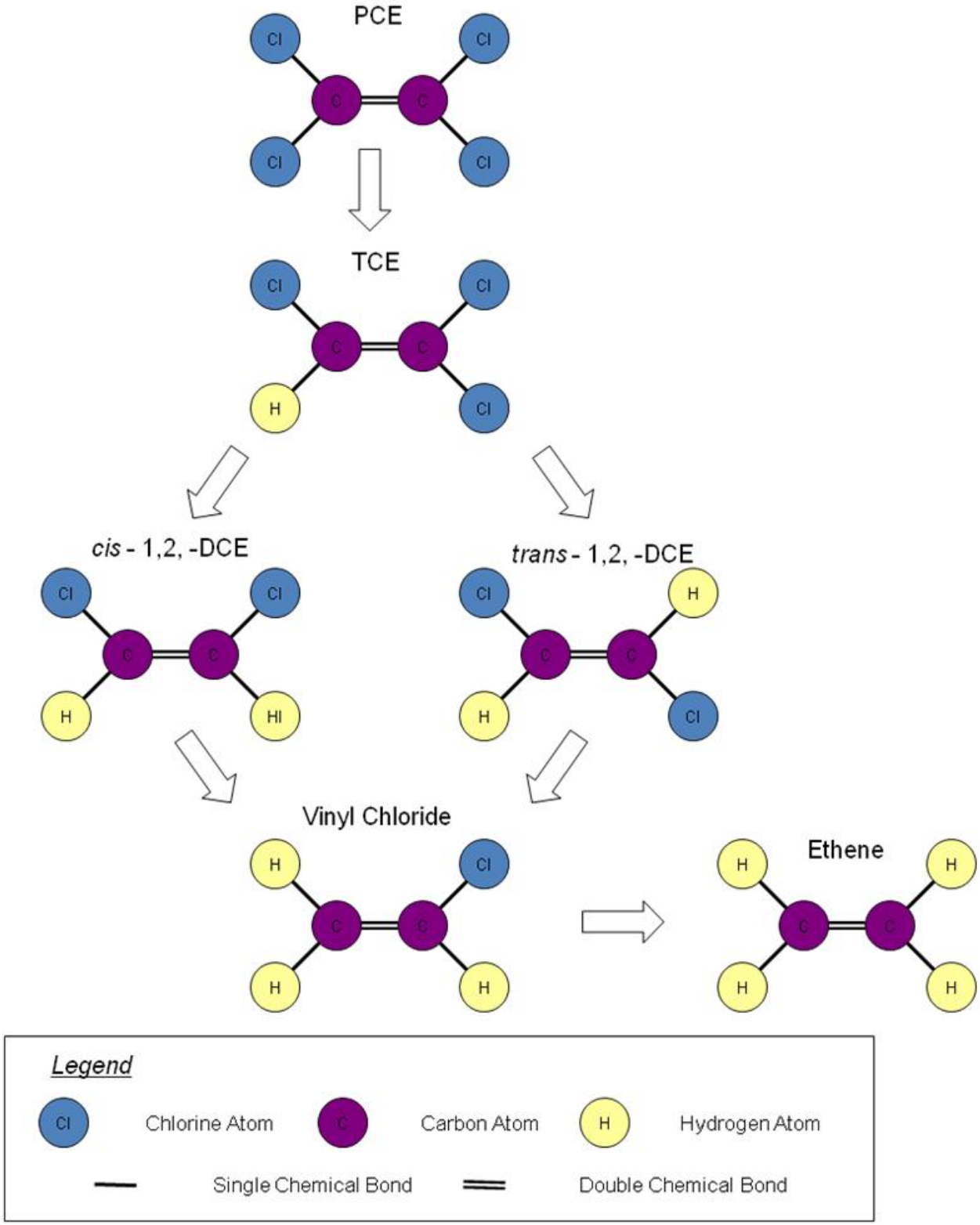


**Figure 2-20 Biodegradation Steps for PCE/TCE**

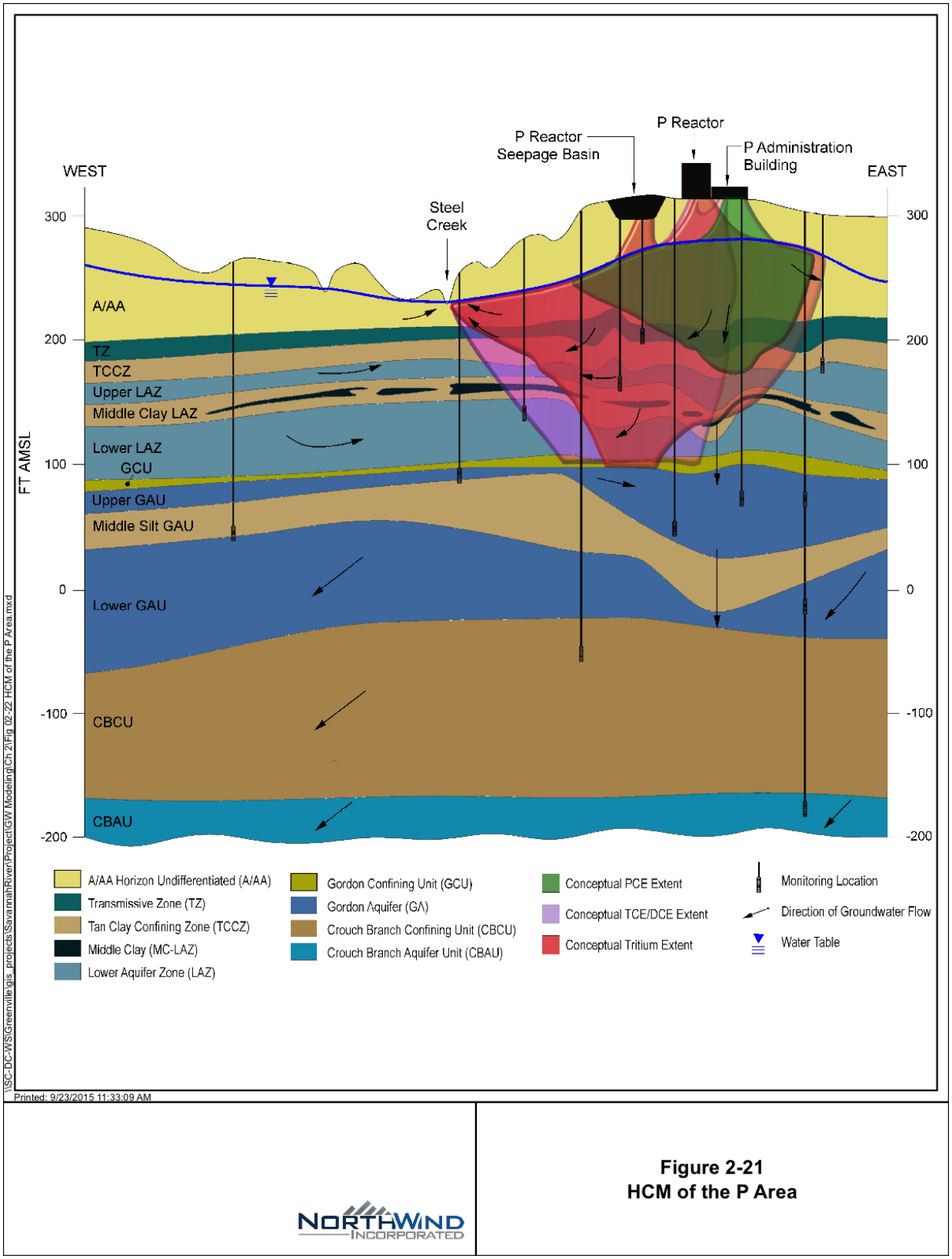


**Figure 2-21 HCM for P Area**

**Table 2-1 Monitoring Wells Completed between 1/1/2011 and 9/26/2014**

| STATION_ID | COMPLETION DATE | WELL SERIES | UTM_E (1927) | UTM_N | SZ TOP FT_MSL | SZ BOT FT_MSL | GROUND ELEVATION | REFERENCE ELEVATION | TOTAL DEPTH | DIA | Hydrostratigraphic_Unit | ABBREV HYDRO UNIT | GENERALIZED HYDRO UNIT | ABBREV HYDRO SUBUNIT |
|---|---|---|---|---|---|---|---|---|---|---|---|---|---|---|
| PAS001C | 06/13/2011 | PAS | 446660.688 | 3675629.447 | 167.29 | | 263.29 | 265.78 | 117 | 2 | Lower Aquifer Zone of the Upper Three Runs Aquifer Unit | LAZ_UTRA | UTRAU | LAZ |
| PAS001D | 06/13/2011 | PAS | 446658.442 | 3675626.681 | 203.32 | | 263.32 | 265.65 | 72.25 | 2 | Upper Aquifer Zone of the Upper Three Runs Aquifer Unit | UAZ_UTRA | UTRAU | UAZ |
| PAS002D | 06/14/2011 | PAS | 447527.305 | 3675404.201 | 195.64 | | 242.64 | 244.96 | 60 | 2 | Upper Aquifer Zone of the Upper Three Runs Aquifer Unit | UAZ_UTRA | UTRAU | UAZ |
| PAS003D | 06/15/2011 | PAS | 447590.835 | 3674744.524 | 182.35 | | 240.35 | 242.84 | 70.17 | 2 | Upper Aquifer Zone of the Upper Three Runs Aquifer Unit | UAZ_UTRA | UTRAU | UAZ |
| PDB003C | 06/03/2014 | PDB | 445938.943 | 3676546.01 | 186.71 | 176.71 | 316.16 | 319.17 | 141.7 | 2 | upper Lower Aquifer Zone of the Upper Three Runs Aquifer Unit | uLAZ_UTRA | UTRA | LAZ |
| PGW026B | 04/20/2011 | PGW | 445388.407 | 3676612.467 | 129.66 | 119.66 | 289.47 | 291.8 | 175 | 2 | lower Lower Aquifer Zone of the Upper Three Runs Aquifer Unit | lLAZ_UTRA | UTRAU | LAZ |
| PGW026C | 04/21/2011 | PGW | 445390.389 | 3676614.664 | 159.63 | 149.63 | 289.43 | 291.77 | 145 | 2 | Lower Aquifer Zone of the Upper Three Runs Aquifer Unit | LAZ_UTRA | UTRAU | LAZ |
| PGW026DL | 04/21/2011 | PGW | 445391.493 | 3676615.995 | 204.54 | 194.54 | 289.35 | 291.62 | 100 | 2 | lower Upper Aquifer Zone of the Upper Three Runs Aquifer Unit | lUAZ_UTRA | UTRAU | |
| PGW027C | 04/26/2011 | PGW | 445227.206 | 3676441.826 | 155.01 | 145.01 | 279.8 | 282.08 | 140 | 2 | upper Lower Aquifer Zone of the Upper Three Runs Aquifer Unit | uLAZ_UTRA | UTRAU | LAZ |
| PGW027DL | 04/29/2011 | PGW | 445227.073 | 3676444.442 | 177.96 | 167.96 | 279.58 | 281.88 | 117 | 2 | lower Upper Aquifer Zone of the Upper Three Runs Aquifer Unit | lUAZ_UTRA | UTRAU | |
| PGW027DU | 04/29/2011 | PGW | 445226.969 | 3676447.381 | 212.75 | 202.75 | 279.42 | 281.76 | 82 | 2 | Upper Aquifer Zone of the Upper Three Runs Aquifer Unit | UAZ_UTRA | UTRAU | UAZ |
| PGW028C | 05/04/2011 | PGW | 445193.279 | 3676265.804 | 184.64 | 174.64 | 296.27 | 298.7 | 127 | 2 | upper Lower Aquifer Zone of the Upper Three Runs Aquifer Unit | uLAZ_UTRA | UTRAU | LAZ |
| PGW028DU | 05/04/2011 | PGW | 445196.587 | 3676268.25 | 226.72 | 216.72 | 296.42 | 298.91 | 85 | 2 | Upper Aquifer Zone of the Upper Three Runs Aquifer Unit | UAZ_UTRA | UTRAU | UAZ |
| PGW029C | 05/19/2011 | PGW | 445800.553 | 3676754.312 | 187.87 | 177.87 | 314.5 | 316.82 | 142 | 2 | upper Lower Aquifer Zone of the Upper Three Runs Aquifer Unit | uLAZ_UTRA | UTRAU | LAZ |
| PGW029DL | 05/23/2011 | PGW | 445802.651 | 3676755.727 | 229.71 | 219.71 | 314.37 | 316.69 | 100 | 2 | lower Upper Aquifer Zone of the Upper Three Runs Aquifer Unit | lUAZ_UTRA | UTRAU | |
| PGW030B | 05/24/2011 | PGW | 445844.45 | 3676750.651 | 188.36 | 178.36 | 315.02 | 317.27 | 142 | 2 | Lower Aquifer Zone of the Upper Three Runs Aquifer Unit | LAZ_UTRA | UTRAU | LAZ |
| PGW030BL | 05/24/2011 | PGW | 445843.28 | 3676752.362 | 163.39 | 153.39 | 315.06 | 317.49 | 167 | 2 | lower Lower Aquifer Zone of the Upper Three Runs Aquifer Unit | lLAZ_UTRA | UTRAU | LAZ |
| PGW031B | 05/18/2011 | PGW | 446038.977 | 3676793.401 | 165.77 | 155.77 | 315.63 | 318.01 | 165.2 | 2 | Lower Aquifer Zone of the Upper Three Runs Aquifer Unit | LAZ_UTRA | UTRAU | LAZ |
| PGW031C | 05/18/2011 | PGW | 446037.742 | 3676795.253 | 188.97 | 178.97 | 315.64 | 317.89 | 142 | 2 | upper Lower Aquifer Zone of the Upper Three Runs Aquifer Unit | uLAZ_UTRA | UTRAU | LAZ |
| PGW033A | 09/25/2014 | PGW | 445831.993 | 3676320.489 | 105.47 | 95.37 | 328.67 | 332.14 | 236 | 2 | upper Gordon Aquifer Unit | uGAU | GAU | |

**Table 2-1 (continued)**

| STATION_ID | COMPLETION DATE | WELL SERIES | UTM_E (1927) | UTM_N | SZ TOP FT_MSL | SZ BOT FT_MSL | GROUND ELEVATION | REFERENCE ELEVATION | TOTAL DEPTH | DIA | Hydrostratigraphic_Unit | ABBREV HYDRO UNIT | GENERALIZED HYDRO UNIT | ABBREV HYDRO SUBUNIT |
|---|---|---|---|---|---|---|---|---|---|---|---|---|---|---|
| PGW034DL | 09/26/2014 | PGW | 446092.356 | 3677110.743 | 212.23 | 202.23 | 310.73 | 313.02 | 112 | 2 | lower Upper Aquifer Zone of the Upper Three Runs Aquifer Unit | lUAZ_UTRA | UTRA | UAZ |
| PRB001DU | 08/23/2011 | PRB | 445835.042 | 3676499.995 | 266.96 | 246.96 | 316.61 | 319.52 | 75 | 2 | Upper Aquifer Zone of the Upper Three Runs Aquifer Unit | UAZ_UTRA | UTRAU | UAZ |
| PRB002DU | 08/24/2011 | PRB | 445793.365 | 3676545.546 | 267.44 | 247.44 | 317.1 | 319.64 | 75 | 2 | Upper Aquifer Zone of the Upper Three Runs Aquifer Unit | UAZ_UTRA | UTRAU | UAZ |
| PRB003C | 05/28/2014 | PRB | 445962.694 | 3676408.479 | 187.91 | 177.91 | 317.42 | 319.97 | 142 | 2 | upper Lower Aquifer Zone of the Upper Three Runs Aquifer Unit | uLAZ_UTRA | UTRA | LAZ |
| PRB003DU | 08/25/2011 | PRB | 445964.477 | 3676412.526 | 267.47 | 247.47 | 317.11 | 319.89 | 75 | 2 | Upper Aquifer Zone of the Upper Three Runs Aquifer Unit | UAZ_UTRA | UTRAU | UAZ |
| PRB004DU | 08/24/2011 | PRB | 445905.852 | 3676613.904 | 266.32 | 246.32 | 315.97 | 319.12 | 75 | 2 | Upper Aquifer Zone of the Upper Three Runs Aquifer Unit | UAZ_UTRA | UTRAU | UAZ |
| PRB005C | 05/21/2014 | PRB | 445866.257 | 3676675.05 | 176.61 | 166.61 | 316.17 | 318.8 | 152 | 2 | upper Lower Aquifer Zone of the Upper Three Runs Aquifer Unit | uLAZ_UTRA | UTRA | LAZ |
| PRB005DU | 08/25/2011 | PRB | 445861.479 | 3676675.761 | 266.11 | 246.11 | 315.77 | 318.57 | 75 | 2 | Upper Aquifer Zone of the Upper Three Runs Aquifer Unit | UAZ_UTRA | UTRAU | UAZ |
| PSB002AA | 05/11/2011 | PSB | 445656.558 | 3676357.961 | 112.91 | 102.91 | 322.57 | 324.93 | 225 | 2 | upper Gordon Aquifer Unit | uGAU | GAU | |
| PSB002AL | 05/13/2014 | PSB | 445655.832 | 3676361.384 | 7.57 | -2.45 | 322.98 | 325.34 | 328.5 | 2 | lower Gordon Aquifer Unit | lGAU | GAU | |
| PSB002B | 05/12/2011 | PSB | 445658.726 | 3676359.539 | 142.99 | 132.99 | 322.64 | 325.04 | 195 | 2 | lower Lower Aquifer Zone of the Upper Three Runs Aquifer Unit | lLAZ_UTRA | UTRAU | LAZ |
| PSB002C | 05/13/2011 | PSB | 445648.524 | 3676354.035 | 187.57 | 177.57 | 322.18 | 324.54 | 150 | 2 | upper Lower Aquifer Zone of the Upper Three Runs Aquifer Unit | uLAZ_UTRA | UTRAU | LAZ |
| PSB002DL | 05/13/2011 | PSB | 445646.276 | 3676352.36 | 254.37 | 244.37 | 322.03 | 324.38 | 83 | 2 | lower Upper Aquifer Zone of the Upper Three Runs Aquifer Unit | lUAZ_UTRA | UTRAU | |
| PSB003DL | 05/14/2014 | PSB | 445571.726 | 3676296.968 | 247.78 | 237.76 | 317.78 | 320.22 | 82.2 | 2 | lower Upper Aquifer Zone of the Upper Three Runs Aquifer Unit | lUAZ_UTRA | UTRA | UAZ |
| PSB011A | 05/20/2014 | PSB | 445423.978 | 3676395.988 | 97.89 | 87.87 | 307.61 | 310.07 | 222 | 2 | upper Gordon Aquifer Unit | uGAU | GAU | |
| PSB011B | 05/06/2011 | PSB | 445423.72 | 3676390.931 | 171.48 | 161.48 | 307.2 | 309.57 | 151 | 2 | lower Lower Aquifer Zone of the Upper Three Runs Aquifer Unit | lLAZ_UTRA | UTRAU | LAZ |
| PSB011C | 05/09/2011 | PSB | 445423.415 | 3676387.467 | 202.37 | 192.37 | 307.05 | 309.44 | 120 | 2 | upper Lower Aquifer Zone of the Upper Three Runs Aquifer Unit | uLAZ_UTRA | UTRAU | LAZ |
| PSB011DL | 05/09/2011 | PSB | 445423.078 | 3676384.772 | 224.2 | 214.2 | 307 | 309.29 | 98 | 2 | lower Upper Aquifer Zone of the Upper Three Runs Aquifer Unit | lUAZ_UTRA | UTRAU | |

**Table 2-2 Construction of Monitoring Wells and Piezometers**

| STATION ID | WELL SERIES | STATION TYPE | WELL USE | UTM_E | UTM_N | SZ TOP ft MSL | SZ BOT ft MSL | GE | REFERENCE ELEVATION CODE | REFERENCE ELEVATION | TOTAL DEPTH | CONSTRU OBJ DIAMETER | CONSTR OBJ MATERIAL | COMPLETION DATE | DATE SEALED | Hydrostratigraphic_Unit |
|---|---|---|---|---|---|---|---|---|---|---|---|---|---|---|---|---|
| LAW 3A | LAW | MONITORING WELL | ACTIVE | 442428.25 | 3674752.87 | -159 | -164 | 246 | C | 248.5 | 412.5 | 4 | CS | 12-Feb-85 | | Crouch Branch Aquifer Unit |
| LAW 3B | LAW | MONITORING WELL | ACTIVE | 442426.39 | 3674757.13 | 4 | -1 | 246 | C | 248.4 | 249.4 | 4 | PVC | 18-Feb-85 | | Gordon Aquifer Unit |
| LAW 3C | LAW | MONITORING WELL | INACTIVE | 442424.47 | 3674761.54 | 214.9 | 194.9 | 245.9 | C | 248 | 53.1 | 4 | PVC | 27-Feb-85 | | AA Horizon of the Upper Aquifer Zone of the Upper Three Runs Aquifer Unit |
| LBP 1D | LBP | MONITORING WELL | ACTIVE | 442172.768 | 3675746.8 | 256.29 | 246.29 | 304.3 | C | 306.79 | 65 | 2 | PVC | 21-May-97 | | AA Horizon of the Upper Aquifer Zone of the Upper Three Runs Aquifer Unit |
| LBP 2D | LBP | MONITORING WELL | ACTIVE | 442127.596 | 3675792.5 | 251.88 | 241.88 | 296.9 | C | 299.38 | 62 | 2 | PVC | 22-May-97 | | AA Horizon of the Upper Aquifer Zone of the Upper Three Runs Aquifer Unit |
| LBP 3D | LBP | MONITORING WELL | ACTIVE | 442014.291 | 3675705.41 | 252.84 | 242.84 | 292.8 | C | 295.34 | 59 | 2 | PVC | 22-May-97 | | AA Horizon of the Upper Aquifer Zone of the Upper Three Runs Aquifer Unit |
| LSP 1DU | LSP | MONITORING WELL | ACTIVE | 442292.149 | 3674932.79 | 232.35 | 212.39 | 249 | C | 251.59 | 52 | 2 | PVC | 13-Sep-00 | | |
| LSP 3DU | LSP | MONITORING WELL | ACTIVE | 442103.456 | 3675365.71 | 240.69 | 225.69 | 278.3 | C | 280.92 | 55 | 2 | PVC | 14-Sep-00 | | |
| LSW 4C | LSW | ML MONITOR WELL | ACTIVE | 442299.453 | 3674933 | 119.24 | 113.58 | 249.1 | S | 250.76 | 177.5 | 4 | PVC | 27-Sep-01 | | Lower Aquifer Zone of the Upper Three Runs Aquifer Unit |
| LSW 4DL | LSW | ML MONITOR WELL | ACTIVE | 442299.453 | 3674933 | 139.85 | 134.19 | 249.1 | S | 250.76 | 177.5 | 4 | PVC | 27-Sep-01 | | Transmissive Zone of the Upper Aquifer Zone of the Upper Three Runs Aquifer Unit |
| LSW 16C | LSW | ML MONITOR WELL | ACTIVE | 442511.26 | 3673342.44 | 87.16 | 81.48 | 239.1 | S | 240.81 | 160.13 | 4 | PVC | 26-Feb-03 | | Lower Aquifer Zone of the Upper Three Runs Aquifer Unit |
| LSW 16DL | LSW | ML MONITOR WELL | ACTIVE | 442511.26 | 3673342.44 | 127.89 | 122.24 | 239.1 | S | 240.81 | 119.37 | 4 | PVC | 29-May-02 | | Transmissive Zone of the Upper Aquifer Zone of the Upper Three Runs Aquifer Unit |
| LSW 17A | LSW | ML MONITOR WELL | ACTIVE | 442245.62 | 3673072.31 | 16.44 | 10.74 | 240.2 | S | 242.02 | 232.61 | 4 | PVC | 26-Feb-03 | | Gordon Aquifer Unit |
| LSW 17C | LSW | ML MONITOR WELL | ACTIVE | 442245.62 | 3673072.31 | 112.31 | 106.61 | 240.2 | S | 242.02 | 136.74 | 4 | PVC | 26-Feb-03 | | Lower Aquifer Zone of the Upper Three Runs Aquifer Unit |
| LSW 17DL | LSW | ML MONITOR WELL | ACTIVE | 442245.62 | 3673072.31 | 173.18 | 167.48 | 240.2 | S | 242.02 | 75.87 | 4 | PVC | 26-Feb-03 | | Transmissive Zone of the Upper Aquifer Zone of the Upper Three Runs Aquifer Unit |
| LSW 18C | LSW | ML MONITOR WELL | ACTIVE | 442124.35 | 3672704.25 | 117.62 | 111.92 | 243.5 | S | 245.63 | 134.33 | 4 | PVC | 27-Feb-03 | | Lower Aquifer Zone of the Upper Three Runs Aquifer Unit |
| LSW 18DL | LSW | ML MONITOR WELL | ACTIVE | 442124.35 | 3672704.25 | 178.52 | 172.82 | 243.5 | S | 245.63 | 73.43 | 4 | PVC | 27-Feb-03 | | Transmissive Zone of the Upper Aquifer Zone of the Upper Three Runs Aquifer Unit |
| LSW 19C | LSW | ML MONITOR WELL | ACTIVE | 442536.36 | 3672814.8 | 119.55 | 113.85 | 273.4 | S | 275.18 | 161.99 | 4 | PVC | 27-Feb-03 | | Lower Aquifer Zone of the Upper Three Runs Aquifer Unit |
| LSW 19DL | LSW | ML MONITOR WELL | ACTIVE | 442536.36 | 3672814.8 | 165.39 | 159.69 | 273.4 | S | 275.18 | 116.15 | 4 | PVC | 27-Feb-03 | | Transmissive Zone of the Upper Aquifer Zone of the Upper Three Runs Aquifer Unit |
| LSW 20A | LSW | ML MONITOR WELL | ACTIVE | 442872.74 | 3675041.01 | 58.52 | 52.81 | 268.8 | S | 270.9 | 222.82 | 4 | PVC | 26-Jun-02 | | Gordon Aquifer Unit |
| LSW 20C | LSW | ML MONITOR WELL | ACTIVE | 442872.74 | 3675041.01 | 119.36 | 113.66 | 268.8 | S | 270.9 | 161.97 | 4 | PVC | 05-Jun-03 | | Lower Aquifer Zone of the Upper Three Runs Aquifer Unit |
| LSW 20DL | LSW | ML MONITOR WELL | ACTIVE | 442872.74 | 3675041.01 | 152.77 | 147.06 | 268.8 | S | 270.9 | 128.57 | 4 | PVC | 05-Jun-03 | | Transmissive Zone of the Upper Aquifer Zone of the Upper Three Runs Aquifer Unit |

**Table 2-2 (continued)**

| STATION ID | WELL SERIES | STATION TYPE | WELL USE | UTM_E | UTM_N | SZ TOP ft MSL | SZ BOT ft MSL | GE | REFERENCE ELEVATION CODE | REFERENCE ELEVATION | TOTAL DEPTH | CONSTRU OBJ DIAMETER | CONSTR OBJ MATERIAL | COMPLETION DATE | DATE SEALED | Hydrostratigraphic_Unit |
|---|---|---|---|---|---|---|---|---|---|---|---|---|---|---|---|---|
| P 13A | P | MONITORING WELL | ACTIVE | 446124.24 | 3673679.82 | -57.4 | -67.3 | 252.7 | S | 255.2 | 325 | 4 | PVC | 01-Jan-84 | | lower Gordon Aquifer Unit |
| P 13B | P | MONITORING WELL | ACTIVE | 446124.24 | 3673679.82 | 3 | -7.2 | 252.8 | S | 255.4 | 265.6 | 4 | PVC | 01-Jan-84 | | upper Gordon Aquifer Unit |
| P 13C | P | MONITORING WELL | ACTIVE | 446124.24 | 3673679.82 | 43.1 | 33.1 | 253.1 | S | 255.6 | 227.8 | 4 | PVC | 01-Jan-84 | | Lower Aquifer Zone of the Upper Three Runs Aquifer Unit |
| P 13D | P | MONITORING WELL | ACTIVE | 446124.24 | 3673679.82 | 228.3 | 206.6 | 253.3 | C | 255.7 | 53 | 4 | PVC | 01-Jan-84 | | Upper Aquifer Zone of the Upper Three Runs Aquifer Unit |
| P 24A | P | MONITORING WELL | ACTIVE | 446390.1 | 3676715.98 | 8.9 | -1.9 | 313.1 | S | 315.3 | 325 | 4 | CS | 04-Aug-86 | | middle Gordon Aquifer Unit |
| P 24B | P | MONITORING WELL | ACTIVE | 446393.5 | 3676713.02 | 93.8 | 83.8 | 313.3 | S | 315.4 | 240 | 4 | PVC | 19-Aug-86 | | Lower Aquifer Zone of the Upper Three Runs Aquifer Unit |
| P 24C | P | MONITORING WELL | ACTIVE | 446397 | 3676709.92 | 183.5 | 163.4 | 313.4 | S | 315.6 | 155 | 4 | PVC | 04-Aug-86 | | Middle Aquifer Zone of the TCCZ of the Upper Three Runs Aquifer Unit |
| P 24D | P | MONITORING WELL | ACTIVE | 446400.35 | 3676706.97 | 268.3 | 248.3 | 313.3 | S | 315.4 | 71 | 4 | PVC | 18-Aug-86 | | Upper Aquifer Zone of the Upper Three Runs Aquifer Unit |
| P001L | P00 | PIEZOMETER WELL | ACTIVE | 445569.085 | 3676646.2 | 194.51 | 189.51 | 309.3 | C | 311.31 | 119.9 | 0.75 | PVC | 28-Sep-06 | | TZ/TCCZ of the Upper Aquifer Zone of the Upper Three Runs Aquifer Unit |
| P001U | P00 | PIEZOMETER WELL | ACTIVE | 445569.794 | 3676646.41 | 218.94 | 213.94 | 309.1 | C | 311.32 | 95.3 | 0.75 | PVC | 28-Sep-06 | | AA Horizon of the Upper Aquifer Zone of the Upper Three Runs Aquifer Unit |
| P002L | P00 | PIEZOMETER WELL | ACTIVE | 445589.684 | 3676614.34 | 197.2 | 192.2 | 311.5 | C | 313.52 | 119.4 | 0.75 | PVC | 27-Sep-06 | | TZ/TCCZ of the Upper Aquifer Zone of the Upper Three Runs Aquifer Unit |
| P002U | P00 | PIEZOMETER WELL | ACTIVE | 445590.302 | 3676613.83 | 223.98 | 218.98 | 311.5 | C | 313.51 | 92.6 | 0.75 | PVC | 03-Oct-06 | | AA Horizon of the Upper Aquifer Zone of the Upper Three Runs Aquifer Unit |
| P003L | P00 | PIEZOMETER WELL | ACTIVE | 445619.078 | 3676627.09 | 197.14 | 192.14 | 310.7 | C | 312.7 | 118.7 | 0.75 | PVC | 28-Sep-06 | | TZ/TCCZ of the Upper Aquifer Zone of the Upper Three Runs Aquifer Unit |
| P003U | P00 | PIEZOMETER WELL | ACTIVE | 445619.682 | 3676625.94 | 226.42 | 221.42 | 310.7 | C | 312.74 | 89.4 | 0.75 | PVC | 28-Sep-06 | | AA Horizon of the Upper Aquifer Zone of the Upper Three Runs Aquifer Unit |
| P004L | P00 | PIEZOMETER WELL | ACTIVE | 445641.273 | 3676595.5 | 211.08 | 206.08 | 314.4 | C | 315.88 | 108.4 | 0.75 | PVC | 17-Jan-07 | | TZ/TCCZ of the Upper Aquifer Zone of the Upper Three Runs Aquifer Unit |
| P004U | P00 | PIEZOMETER WELL | ACTIVE | 445640.71 | 3676596.45 | 236.03 | 231.03 | 314.3 | C | 315.87 | 83.4 | 0.75 | PVC | 17-Jan-07 | | AA Horizon of the Upper Aquifer Zone of the Upper Three Runs Aquifer Unit |
| PAC 1 | PAC | MONITORING WELL | ABANDONED | 446363.43 | 3676847.73 | 283.9 | 253.9 | 293.9 | S | 296.2 | 42 | 4 | PVC | 03-Nov-83 | 6/6/2006 | |
| PAC 2 | PAC | MONITORING WELL | ABANDONED | 446422.27 | 3676884.68 | 277.9 | 247.9 | 282.9 | S | 285.1 | 36.9 | 4 | PVC | 04-Nov-83 | 4/4/1996 | |
| PAC 3 | PAC | MONITORING WELL | ABANDONED | 446382.45 | 3676877.52 | 282.9 | 252.9 | 287.9 | S | 290.2 | 37 | 4 | PVC | 03-Nov-83 | 4/4/1996 | |
| PAC 4 | PAC | MONITORING WELL | ABANDONED | 446399.07 | 3676855.62 | 280.6 | 250.6 | 289.6 | S | 291.8 | 41 | 4 | PVC | 06-Jul-84 | 4/4/1996 | |
| PAC 5 | PAC | MONITORING WELL | ABANDONED | 446397.99 | 3676879.83 | 275.1 | 255.1 | 287.1 | S | 289.6 | 34.2 | 4 | PVC | 22-Sep-88 | 6/6/2006 | |
| PAC 6 | PAC | MONITORING WELL | ABANDONED | 446391.64 | 3676882.14 | 275.2 | 255.2 | 287.2 | S | 289.6 | 34.2 | 4 | PVC | 23-Sep-88 | 4/4/1996 | |
| PAO001DU | PAO | MONITORING WELL | ACTIVE | 445790.253 | 3676639.29 | 271.96 | 251.96 | 316.3 | S | 318.74 | 69.6 | 2 | SS | 18-Mar-10 | | Upper Aquifer Zone of the Upper Three Runs Aquifer Unit |
| PAO002DL | PAO | MONITORING WELL | ACTIVE | 445769.478 | 3676651.41 | 228.89 | 213.89 | 314.9 | S | 317.48 | 106.3 | 2 | PVC | 26-Mar-10 | | lower Upper Aquifer Zone of the Upper Three Runs Aquifer Unit |
| PAO002DU | PAO | MONITORING WELL | ACTIVE | 445766.47 | 3676649.07 | 270.24 | 250.24 | 315 | S | 317.65 | 70.1 | 2 | PVC | 29-Mar-10 | | Upper Aquifer Zone of the Upper Three Runs Aquifer Unit |

**Table 2-2 (continued)**

| STATION ID | WELL SERIES | STATION TYPE | WELL USE | UTM_E | UTM_N | SZ TOP ft MSL | SZ BOT ft MSL | GE | REFERENCE ELEVATION CODE | REFERENCE ELEVATION | TOTAL DEPTH | CONSTRU OBJ DIAMETER | CONSTR OBJ MATERIAL | COMPLETION DATE | DATE SEALED | Hydrostratigraphic_Unit |
|---|---|---|---|---|---|---|---|---|---|---|---|---|---|---|---|---|
| PAO003DU | PAO | MONITORING WELL | ACTIVE | 445846.528 | 3676792.53 | 272.22 | 252.22 | 315.8 | S | 318.5 | 68.9 | 2 | PVC | 19-Mar-10 | | Upper Aquifer Zone of the Upper Three Runs Aquifer Unit |
| PAS001C | PAS | MONITORING WELL | ACTIVE | 446660.688 | 3675629.45 | 167.29 | | 263.3 | C | 265.78 | 117 | 2 | PVC | 13-Jun-11 | | Lower Aquifer Zone of the Upper Three Runs Aquifer Unit |
| PAS001D | PAS | MONITORING WELL | ACTIVE | 446658.442 | 3675626.68 | 203.32 | | 263.3 | C | 265.65 | 72.25 | 2 | PVC | 13-Jun-11 | | Upper Aquifer Zone of the Upper Three Runs Aquifer Unit |
| PAS002D | PAS | MONITORING WELL | ACTIVE | 447527.305 | 3675404.2 | 195.64 | | 242.6 | C | 244.96 | 60 | 2 | PVC | 14-Jun-11 | | Upper Aquifer Zone of the Upper Three Runs Aquifer Unit |
| PAS003D | PAS | MONITORING WELL | ACTIVE | 447590.835 | 3674744.52 | 182.35 | | 240.4 | C | 242.84 | 70.17 | 2 | PVC | 15-Jun-11 | | Upper Aquifer Zone of the Upper Three Runs Aquifer Unit |
| PBP 1D | PBP | MONITORING WELL | ACTIVE | 445739.865 | 3677173.22 | 279.08 | 269.08 | 315.1 | C | 317.58 | 58 | 2 | PVC | 21-May-97 | | A Horizon of the Upper Aquifer Zone of the Upper Three Runs Aquifer Unit |
| PBP 2D | PBP | MONITORING WELL | ACTIVE | 445672.563 | 3677075.29 | 272.8 | 262.8 | 313.8 | C | 316.3 | 58 | 2 | PVC | 21-May-97 | | A Horizon of the Upper Aquifer Zone of the Upper Three Runs Aquifer Unit |
| PBP 3D | PBP | MONITORING WELL | ACTIVE | 445687.704 | 3677132.31 | 278.89 | 268.89 | 316.9 | C | 319.39 | 55 | 2 | PVC | 21-May-97 | | A Horizon of the Upper Aquifer Zone of the Upper Three Runs Aquifer Unit |
| PCB 1 | PCB | MONITORING WELL | ABANDONED | 446224.88 | 3676164.68 | 276.1 | 256.1 | 303.6 | C | 305.6 | 49.5 | 4 | STEEL | 31-Mar-80 | 1/1/1984 | |
| PCB 1A | PCB | MONITORING WELL | ABANDONED | 446227.75 | 3676162.86 | 293.5 | 263.5 | 303.5 | S | 305.7 | 42 | 4 | PVC | 16-Feb-84 | 6/6/2006 | |
| PCB 2 | PCB | MONITORING WELL | ABANDONED | 446208.47 | 3676086.63 | 290.5 | 270.5 | 302.8 | C | 304.8 | 34.3 | 4 | STEEL | 01-Apr-80 | 1/1/1984 | |
| PCB 2A | PCB | MONITORING WELL | ACTIVE | 446213.52 | 3676089.63 | 287.8 | 257.8 | 302.8 | S | 305 | 47.1 | 4 | PVC | 17-Dec-83 | | A Horizon of the Upper Aquifer Zone of the Upper Three Runs Aquifer Unit |
| PCB 3 | PCB | MONITORING WELL | ABANDONED | 446131.97 | 3676105.61 | 293.4 | 273.4 | 301.7 | C | 303.7 | 30.3 | 4 | STEEL | 03-Apr-80 | 1/1/1984 | |
| PCB 3A | PCB | MONITORING WELL | ABANDONED | 446129.44 | 3676109.3 | 292.7 | 262.7 | 302.7 | S | 304.8 | 41.9 | 4 | PVC | 05-Mar-84 | 6/6/2006 | |
| PCB 4 | PCB | MONITORING WELL | ABANDONED | 446148.32 | 3676175.62 | 294.8 | 274.8 | 307.1 | C | 309.1 | 34.3 | 4 | STEEL | 02-Apr-80 | 1/1/1984 | |
| PCB 4A | PCB | MONITORING WELL | ABANDONED | 446153.29 | 3676177.55 | 292.9 | 262.9 | 307.9 | S | 309.7 | 46.7 | 4 | PVC | 15-Feb-84 | 6/6/2006 | |
| PDB 2 | PDB | MONITORING WELL | ACTIVE | 445873.61 | 3676479.78 | 268.7 | 247.7 | 316.9 | S | 319.76 | 71.8 | 4 | PVC | 25-Aug-86 | | A Horizon of the Upper Aquifer Zone of the Upper Three Runs Aquifer Unit |
| PDB 3 | PDB | MONITORING WELL | ACTIVE | 445916.45 | 3676521.94 | 269.1 | 248.1 | 317.1 | S | 319.74 | 71.4 | 4 | PVC | 28-Aug-86 | | A Horizon of the Upper Aquifer Zone of the Upper Three Runs Aquifer Unit |
| PDB 4 | PDB | MONITORING WELL | ACTIVE | 445854.62 | 3676444.1 | 286.2 | 266.2 | 317.1 | S | 319.54 | 62 | 4 | PVC | 25-Jan-95 | | A Horizon of the Upper Aquifer Zone of the Upper Three Runs Aquifer Unit |
| PDB 5 | PDB | MONITORING WELL | ACTIVE | 445728.08 | 3676597.53 | 284.2 | 264.2 | 317.2 | S | 319.59 | 62 | 4 | PVC | 20-Jan-95 | | A Horizon of the Upper Aquifer Zone of the Upper Three Runs Aquifer Unit |
| PDB003C | PDB | MONITORING WELL | ACTIVE | 445938.943 | 3676546.01 | 186.71 | 176.71 | 316.2 | C | 319.17 | 141.7 | 2 | PVC | 03-Jun-14 | | upper Lower Aquifer Zone of the Upper Three Runs Aquifer Unit |
| PGW014 A | PGW | MONITORING WELL | ACTIVE | 445261.245 | 3676546.09 | 4.17 | -5.83 | 275.2 | S | 277.77 | 283.6 | 2 | PVC | 27-Feb-04 | | lower Gordon Aquifer Unit |
| PGW014 B | PGW | MONITORING WELL | ACTIVE | 445262.514 | 3676547.92 | 130.09 | 120.09 | 275.1 | S | 277.72 | 157.63 | 2 | PVC | 27-Feb-04 | | lower Lower Aquifer Zone of the Upper Three Runs Aquifer Unit |
| PGW014 C | PGW | MONITORING WELL | ACTIVE | 445263.779 | 3676549.86 | 185.25 | 175.25 | 275.3 | S | 277.8 | 102.55 | 2 | PVC | 27-Feb-04 | | upper Lower Aquifer Zone of the Upper Three Runs Aquifer Unit |
| PGW014DU | PGW | MONITORING WELL | ACTIVE | 445264.871 | 3676551.67 | 210.24 | 200.24 | 275.2 | S | 277.79 | 77.55 | 2 | PVC | 27-Feb-04 | | Transmissive Zone of the Upper Aquifer Zone of the Upper Three Runs Aquifer Unit |

**Table 2-2 (continued)**

| STATION ID | WELL SERIES | STATION TYPE | WELL USE | UTM_E | UTM_N | SZ TOP ft MSL | SZ BOT ft MSL | GE | REFERENCE ELEVATION CODE | REFERENCE ELEVATION | TOTAL DEPTH | CONSTRU OBJ DIAMETER | CONSTR OBJ MATERIAL | COMPLETION DATE | DATE SEALED | Hydrostratigraphic_Unit |
|---|---|---|---|---|---|---|---|---|---|---|---|---|---|---|---|---|
| PGW015 A | PGW | PIEZOMETER WELL | ACTIVE | 444792.999 | 3677071.9 | 31.7 | 21.7 | 302.2 | C | 304.64 | 282.94 | 2 | PVC | 07-Oct-03 | | upper Gordon Aquifer Unit |
| PGW015 B | PGW | PIEZOMETER WELL | ACTIVE | 444790.539 | 3677070.82 | 159.37 | 149.37 | 302.4 | C | 304.61 | 155.24 | 2 | PVC | 07-Oct-03 | | upper Lower Aquifer Zone of the Upper Three Runs Aquifer Unit |
| PGW015 C | PGW | PIEZOMETER WELL | ACTIVE | 444793.797 | 3677069.35 | 184.75 | 174.75 | 301.8 | C | 304.06 | 129.31 | 2 | PVC | 08-Oct-03 | | upper Lower Aquifer Zone of the Upper Three Runs Aquifer Unit |
| PGW015DU | PGW | PIEZOMETER WELL | ACTIVE | 444791.522 | 3677068.33 | 216.85 | 206.85 | 301.9 | C | 303.95 | 97.1 | 2 | PVC | 09-Oct-03 | | Transmissive Zone of the Upper Aquifer Zone of the Upper Three Runs Aquifer Unit |
| PGW016 B | PGW | MONITORING WELL | ACTIVE | 445057.644 | 3676357.17 | 136.72 | 126.72 | 281.7 | S | 284.31 | 157.59 | 2 | PVC | 23-Feb-04 | | middle Lower Aquifer Zone of the Upper Three Runs Aquifer Unit |
| PGW016 C | PGW | MONITORING WELL | ACTIVE | 445058.987 | 3676354.34 | 205.05 | 195.05 | 282.1 | S | 284.71 | 89.66 | 2 | PVC | 23-Feb-04 | | Transmissive Zone of the Upper Aquifer Zone of the Upper Three Runs Aquifer Unit |
| PGW016DU | PGW | MONITORING WELL | ACTIVE | 445060.164 | 3676352.26 | 239.34 | 229.34 | 282.3 | S | 284.91 | 55.57 | 2 | PVC | 23-Feb-04 | | A Horizon of the Upper Aquifer Zone of the Upper Three Runs Aquifer Unit |
| PGW017 B | PGW | MONITORING WELL | ACTIVE | 445452.052 | 3676693.51 | 160.36 | 150.36 | 305.4 | S | 308.03 | 157.67 | 2 | PVC | 25-Feb-04 | | upper Lower Aquifer Zone of the Upper Three Runs Aquifer Unit |
| PGW017 C | PGW | MONITORING WELL | ACTIVE | 445453.828 | 3676694.95 | 195.45 | 185.45 | 305.5 | S | 308.01 | 122.56 | 2 | PVC | 25-Feb-04 | | Transmissive Zone of the Upper Aquifer Zone of the Upper Three Runs Aquifer Unit |
| PGW017DU | PGW | MONITORING WELL | ACTIVE | 445455.75 | 3676696.35 | 255.68 | 245.68 | 305.7 | S | 308.14 | 62.46 | 2 | PVC | 25-Feb-04 | | A Horizon of the Upper Aquifer Zone of the Upper Three Runs Aquifer Unit |
| PGW018 B | PGW | MONITORING WELL | ACTIVE | 445435.756 | 3676151.77 | 148.85 | 138.85 | 304.9 | S | 307.19 | 168.34 | 2 | PVC | 24-Feb-04 | | middle Lower Aquifer Zone of the Upper Three Runs Aquifer Unit |
| PGW018 C | PGW | MONITORING WELL | ACTIVE | 445437.287 | 3676149.72 | 194.81 | 184.81 | 304.8 | S | 307.34 | 122.53 | 2 | PVC | 24-Feb-04 | | Transmissive Zone of the Upper Aquifer Zone of the Upper Three Runs Aquifer Unit |
| PGW018DU | PGW | MONITORING WELL | ACTIVE | 445434.252 | 3676153.99 | 254.91 | 244.91 | 304.9 | S | 307.51 | 62.6 | 2 | PVC | 24-Feb-04 | | A Horizon of the Upper Aquifer Zone of the Upper Three Runs Aquifer Unit |
| PGW019 B | PGW | MONITORING WELL | ACTIVE | 445751.189 | 3676822.17 | 167.89 | 157.89 | 312.9 | S | 315.85 | 157.96 | 2 | PVC | 18-Feb-04 | | upper Lower Aquifer Zone of the Upper Three Runs Aquifer Unit |
| PGW019 C | PGW | MONITORING WELL | ACTIVE | 445753.154 | 3676823.57 | 187.92 | 177.92 | 312.9 | S | 315.65 | 137.73 | 2 | PVC | 18-Feb-04 | | upper Lower Aquifer Zone of the Upper Three Runs Aquifer Unit |
| PGW019DU | PGW | MONITORING WELL | ACTIVE | 445749.261 | 3676820.73 | 222.77 | 212.77 | 312.8 | S | 315.37 | 102.6 | 2 | PVC | 18-Feb-04 | | Transmissive Zone of the Upper Aquifer Zone of the Upper Three Runs Aquifer Unit |
| PGW-01A | PGW | PIEZOMETER WELL | ACTIVE | 445526.926 | 3677263.87 | 92.75 | 82.74 | 310.7 | C | 312.99 | 230.47 | 2 | PVC | 12-Dec-02 | | upper Gordon Aquifer Unit |
| PGW-01B | PGW | PIEZOMETER WELL | ACTIVE | 445523.413 | 3677263.73 | 160.45 | 150.45 | 310.8 | C | 313.03 | 162.8 | 2 | PVC | 12-Dec-02 | | middle Lower Aquifer Zone of the Upper Three Runs Aquifer Unit |
| PGW-01C | PGW | PIEZOMETER WELL | ACTIVE | 445534.086 | 3677264.18 | 186.61 | 176.61 | 310.7 | C | 312.92 | 136.55 | 2 | PVC | 10-Dec-02 | | upper Lower Aquifer Zone of the Upper Three Runs Aquifer Unit |
| PGW-01DL | PGW | PIEZOMETER WELL | ACTIVE | 445530.817 | 3677264.07 | 227.75 | 217.75 | 310.6 | C | 312.74 | 95.3 | 2 | PVC | 22-Nov-02 | | Transmissive Zone of the Upper Aquifer Zone of the Upper Three Runs Aquifer Unit |
| PGW020 B | PGW | MONITORING WELL | ACTIVE | 445820.753 | 3676412.81 | 160.36 | 150.36 | 320.4 | S | 323.17 | 172.81 | 2 | PVC | 03-Mar-04 | | middle Lower Aquifer Zone of the Upper Three Runs Aquifer Unit |
| PGW020 C | PGW | MONITORING WELL | ACTIVE | 445822.201 | 3676410.93 | 190.22 | 180.22 | 320.2 | S | 323.07 | 142.85 | 2 | PVC | 03-Mar-04 | | upper Lower Aquifer Zone of the Upper Three Runs Aquifer Unit |

**Table 2-2 (continued)**

| STATION ID | WELL SERIES | STATION TYPE | WELL USE | UTM_E | UTM_N | SZ TOP ft MSL | SZ BOT ft MSL | GE | REFERENCE ELEVATION CODE | REFERENCE ELEVATION | TOTAL DEPTH | CONSTRU OBJ DIAMETER | CONSTR OBJ MATERIAL | COMPLETION DATE | DATE SEALED | Hydrostratigraphic_Unit |
|---|---|---|---|---|---|---|---|---|---|---|---|---|---|---|---|---|
| PGW020DU | PGW | MONITORING WELL | ACTIVE | 445823.614 | 3676409.09 | 235.23 | 225.23 | 320.2 | S | 323.04 | 97.81 | 2 | PVC | 03-Mar-04 | | AA Horizon of the Upper Aquifer Zone of the Upper Three Runs Aquifer Unit |
| PGW021 B | PGW | MONITORING WELL | ACTIVE | 446075.325 | 3676883.52 | 166.87 | 156.87 | 311.9 | S | 314.51 | 157.64 | 2 | PVC | 24-Feb-04 | | upper Lower Aquifer Zone of the Upper Three Runs Aquifer Unit |
| PGW021 C | PGW | MONITORING WELL | ACTIVE | 446073.879 | 3676885.56 | 206.91 | 196.91 | 311.9 | S | 314.51 | 117.6 | 2 | PVC | 24-Feb-04 | | Transmissive Zone of the Upper Aquifer Zone of the Upper Three Runs Aquifer Unit |
| PGW021DU | PGW | MONITORING WELL | ACTIVE | 446072.401 | 3676887.53 | 222.9 | 212.9 | 311.9 | S | 314.51 | 101.6 | 2 | PVC | 24-Feb-04 | | AA Horizon of the Upper Aquifer Zone of the Upper Three Runs Aquifer Unit |
| PGW022 B | PGW | MONITORING WELL | ACTIVE | 446335.496 | 3676864.15 | 155.77 | 145.77 | 290.8 | S | 293.32 | 147.55 | 2 | PVC | 17-Feb-04 | | middle Lower Aquifer Zone of the Upper Three Runs Aquifer Unit |
| PGW022 C | PGW | MONITORING WELL | ACTIVE | 446337.73 | 3676863.93 | 191.07 | 181.07 | 291.1 | S | 293.46 | 112.39 | 2 | PVC | 17-Feb-04 | | tan clay confining zone of the Upper Three Runs Aquifer Unit |
| PGW022DU | PGW | MONITORING WELL | ACTIVE | 446339.988 | 3676863.73 | 221.24 | 211.24 | 291.2 | S | 293.73 | 82.49 | 2 | PVC | 17-Feb-04 | | AA Horizon of the Upper Aquifer Zone of the Upper Three Runs Aquifer Unit |
| PGW023 B | PGW | MONITORING WELL | ACTIVE | 446472.472 | 3676725.74 | 176.67 | 166.67 | 306.7 | S | 309.16 | 142.49 | 2 | PVC | 18-Feb-04 | | upper Lower Aquifer Zone of the Upper Three Runs Aquifer Unit |
| PGW023 C | PGW | MONITORING WELL | ACTIVE | 446470.618 | 3676724.36 | 216.58 | 206.58 | 306.6 | S | 308.92 | 102.34 | 2 | PVC | 18-Feb-04 | | Transmissive Zone of the Upper Aquifer Zone of the Upper Three Runs Aquifer Unit |
| PGW023DU | PGW | MONITORING WELL | ACTIVE | 446468.717 | 3676723.09 | 261.15 | 251.15 | 306.7 | S | 309.04 | 57.89 | 2 | PVC | 18-Feb-04 | | A Horizon of the Upper Aquifer Zone of the Upper Three Runs Aquifer Unit |
| PGW024 A | PGW | MONITORING WELL | ACTIVE | 446065.244 | 3676722.78 | 69.81 | 59.81 | 316.8 | S | 319.34 | 259.53 | 2 | PVC | 05-Mar-04 | | middle Gordon Aquifer Unit |
| PGW024 B | PGW | MONITORING WELL | ACTIVE | 446066.558 | 3676720.88 | 179.88 | 169.88 | 316.9 | S | 319.49 | 149.61 | 2 | PVC | 04-Mar-04 | | upper Lower Aquifer Zone of the Upper Three Runs Aquifer Unit |
| PGW024 C | PGW | MONITORING WELL | ACTIVE | 446068.636 | 3676717.87 | 219.89 | 209.89 | 316.9 | S | 319.44 | 109.55 | 2 | PVC | 04-Mar-04 | | Transmissive Zone of the Upper Aquifer Zone of the Upper Three Runs Aquifer Unit |
| PGW024DU | PGW | MONITORING WELL | ACTIVE | 446069.939 | 3676716.03 | 259.9 | 249.9 | 316.9 | S | 319.51 | 69.61 | 2 | PVC | 04-Mar-04 | | A Horizon of the Upper Aquifer Zone of the Upper Three Runs Aquifer Unit |
| PGW025 A | PGW | MONITORING WELL | ACTIVE | 445734.067 | 3676689.86 | 43.11 | 33.11 | 313.1 | S | 315.83 | 282.72 | 2 | PVC | 08-Mar-04 | | middle Gordon Aquifer Unit |
| PGW025 B | PGW | MONITORING WELL | ACTIVE | 445735.867 | 3676691.32 | 168.16 | 158.16 | 313.2 | S | 315.74 | 157.58 | 2 | PVC | 19-Feb-04 | | upper Lower Aquifer Zone of the Upper Three Runs Aquifer Unit |
| PGW025 C | PGW | MONITORING WELL | ACTIVE | 445737.766 | 3676692.85 | 203.17 | 193.17 | 313.2 | S | 316.01 | 122.84 | 2 | PVC | 19-Feb-04 | | TZ/TCCZ of the Upper Aquifer Zone of the Upper Three Runs Aquifer Unit |
| PGW025DU | PGW | MONITORING WELL | ACTIVE | 445739.676 | 3676694.32 | 223.37 | 213.37 | 313.4 | S | 316.09 | 102.72 | 2 | PVC | 19-Feb-04 | | AA/TZ Horizon of the Upper Aquifer Zone of the Upper Three Runs Aquifer Unit |
| PGW026B | PGW | MONITORING WELL | ACTIVE | 445388.407 | 3676612.47 | 129.66 | 119.66 | 289.5 | C | 291.8 | 175 | 2 | PVC | 20-Apr-11 | | lower Lower Aquifer Zone of the Upper Three Runs Aquifer Unit |
| PGW026C | PGW | MONITORING WELL | ACTIVE | 445390.389 | 3676614.66 | 159.63 | 149.63 | 289.4 | C | 291.77 | 145 | 2 | PVC | 21-Apr-11 | | Lower Aquifer Zone of the Upper Three Runs Aquifer Unit |
| PGW026DL | PGW | MONITORING WELL | ACTIVE | 445391.493 | 3676616 | 204.54 | 194.54 | 289.4 | C | 291.62 | 100 | 2 | PVC | 21-Apr-11 | | lower Upper Aquifer Zone of the Upper Three Runs Aquifer Unit |
| PGW027C | PGW | MONITORING WELL | ACTIVE | 445227.206 | 3676441.83 | 155.01 | 145.01 | 279.8 | C | 282.08 | 140 | 2 | PVC | 26-Apr-11 | | upper Lower Aquifer Zone of the Upper Three Runs Aquifer Unit |
| PGW027DL | PGW | MONITORING WELL | ACTIVE | 445227.073 | 3676444.44 | 177.96 | 167.96 | 279.6 | C | 281.88 | 117 | 2 | PVC | 29-Apr-11 | | lower Upper Aquifer Zone of the Upper Three Runs Aquifer Unit |

**Table 2-2 (continued)**

| STATION ID | WELL SERIES | STATION TYPE | WELL USE | UTM_E | UTM_N | SZ TOP ft MSL | SZ BOT ft MSL | GE | REFERENCE ELEVATION CODE | REFERENCE ELEVATION | TOTAL DEPTH | CONSTRU OBJ DIAMETER | CONSTR OBJ MATERIAL | COMPLETION DATE | DATE SEALED | Hydrostratigraphic_Unit |
|---|---|---|---|---|---|---|---|---|---|---|---|---|---|---|---|---|
| PGW027DU | PGW | MONITORING WELL | ACTIVE | 445226.969 | 3676447.38 | 212.75 | 202.75 | 279.4 | C | 281.76 | 82 | 2 | PVC | 29-Apr-11 | | Upper Aquifer Zone of the Upper Three Runs Aquifer Unit |
| PGW028C | PGW | MONITORING WELL | ACTIVE | 445193.279 | 3676265.8 | 184.64 | 174.64 | 296.3 | C | 298.7 | 127 | 2 | PVC | 04-May-11 | | upper Lower Aquifer Zone of the Upper Three Runs Aquifer Unit |
| PGW028DU | PGW | MONITORING WELL | ACTIVE | 445196.587 | 3676268.25 | 226.72 | 216.72 | 296.4 | C | 298.91 | 85 | 2 | PVC | 04-May-11 | | Upper Aquifer Zone of the Upper Three Runs Aquifer Unit |
| PGW029C | PGW | MONITORING WELL | ACTIVE | 445800.553 | 3676754.31 | 187.87 | 177.87 | 314.5 | C | 316.82 | 142 | 2 | PVC | 19-May-11 | | upper Lower Aquifer Zone of the Upper Three Runs Aquifer Unit |
| PGW029DL | PGW | MONITORING WELL | ACTIVE | 445802.651 | 3676755.73 | 229.71 | 219.71 | 314.4 | C | 316.69 | 100 | 2 | PVC | 23-May-11 | | lower Upper Aquifer Zone of the Upper Three Runs Aquifer Unit |
| PGW-02A | PGW | PIEZOMETER WELL | ACTIVE | 443783.152 | 3675635.89 | 40.09 | 30.08 | 251.8 | C | 253.84 | 224.19 | 2 | PVC | 17-Apr-03 | | upper Gordon Aquifer Unit |
| PGW-02C | PGW | PIEZOMETER WELL | ACTIVE | 443783.406 | 3675633.21 | 165.68 | 155.65 | 251.7 | C | 253.77 | 98.59 | 2 | PVC | 17-Apr-03 | | upper Lower Aquifer Zone of the Upper Three Runs Aquifer Unit |
| PGW-02CU | PGW | PIEZOMETER WELL | ACTIVE | 443779.705 | 3675632.7 | 186.95 | 176.95 | 252 | C | 253.88 | 76.93 | 2 | PVC | 01-Oct-03 | | tan clay confining zone of the Upper Three Runs Aquifer Unit |
| PGW-02DL | PGW | PIEZOMETER WELL | ACTIVE | 443783.481 | 3675630.36 | 204.22 | 194.21 | 251.8 | C | 253.83 | 60.5 | 2 | PVC | 17-Apr-03 | | Transmissive Zone of the Upper Aquifer Zone of the Upper Three Runs Aquifer Unit |
| PGW030B | PGW | MONITORING WELL | ACTIVE | 445844.45 | 3676750.65 | 188.36 | 178.36 | 315 | C | 317.27 | 142 | 2 | PVC | 24-May-11 | | Lower Aquifer Zone of the Upper Three Runs Aquifer Unit |
| PGW030BL | PGW | MONITORING WELL | ACTIVE | 445843.28 | 3676752.36 | 163.39 | 153.39 | 315.1 | C | 317.49 | 167 | 2 | PVC | 24-May-11 | | lower Lower Aquifer Zone of the Upper Three Runs Aquifer Unit |
| PGW031B | PGW | MONITORING WELL | ACTIVE | 446038.977 | 3676793.4 | 165.77 | 155.77 | 315.6 | C | 318.01 | 165.2 | 2 | PVC | 18-May-11 | | Lower Aquifer Zone of the Upper Three Runs Aquifer Unit |
| PGW031C | PGW | MONITORING WELL | ACTIVE | 446037.742 | 3676795.25 | 188.97 | 178.97 | 315.6 | C | 317.89 | 142 | 2 | PVC | 18-May-11 | | upper Lower Aquifer Zone of the Upper Three Runs Aquifer Unit |
| PGW033A | PGW | MONITORING WELL | ACTIVE | 445831.993 | 3676320.49 | 105.47 | 95.37 | 328.7 | C | 332.14 | 236 | 2 | PVC | 25-Sep-14 | | upper Gordon Aquifer Unit |
| PGW034DL | PGW | MONITORING WELL | ACTIVE | 446092.356 | 3677110.74 | 212.23 | 202.23 | 310.7 | C | 313.02 | 112 | 2 | PVC | 26-Sep-14 | | lower Upper Aquifer Zone of the Upper Three Runs Aquifer Unit |
| PGW-03A | PGW | PIEZOMETER WELL | ACTIVE | 445988.766 | 3676038.45 | 95.58 | 85.57 | 324.1 | C | 326.36 | 241.01 | 2 | PVC | 14-Jan-03 | | upper Gordon Aquifer Unit |
| PGW-03B | PGW | PIEZOMETER WELL | ACTIVE | 445990.873 | 3676040.06 | 141.73 | 131.71 | 323.7 | C | 325.87 | 194.52 | 2 | PVC | 14-Jan-03 | | lower Lower Aquifer Zone of the Upper Three Runs Aquifer Unit |
| PGW-03C | PGW | PIEZOMETER WELL | ACTIVE | 445992.96 | 3676041.54 | 175.55 | 165.55 | 323.6 | C | 325.73 | 160.5 | 2 | PVC | 14-Jan-03 | | upper Lower Aquifer Zone of the Upper Three Runs Aquifer Unit |
| PGW-03DL | PGW | PIEZOMETER WELL | ACTIVE | 445995.213 | 3676043.11 | 223.33 | 213.33 | 323.3 | C | 325.3 | 112.5 | 2 | PVC | 14-Jan-03 | | Transmissive Zone of the Upper Aquifer Zone of the Upper Three Runs Aquifer Unit |
| PGW-04A | PGW | PIEZOMETER WELL | ACTIVE | 444800.626 | 3675999.23 | 92 | 81.96 | 278 | C | 280.27 | 198.54 | 2 | PVC | 10-Mar-03 | | upper Gordon Aquifer Unit |
| PGW-04B | PGW | PIEZOMETER WELL | ACTIVE | 444802.971 | 3676000.82 | 126.51 | 116.31 | 278.1 | C | 280.24 | 164.1 | 2 | PVC | 10-Mar-03 | | lower Lower Aquifer Zone of the Upper Three Runs Aquifer Unit |
| PGW-04C | PGW | PIEZOMETER WELL | ACTIVE | 444805.21 | 3676002.71 | 174.99 | 164.98 | 278 | C | 280.25 | 115.51 | 2 | PVC | 10-Mar-03 | | upper Lower Aquifer Zone of the Upper Three Runs Aquifer Unit |
| PGW-04DL | PGW | PIEZOMETER WELL | ACTIVE | 444807.539 | 3676004.49 | 213.35 | 203.34 | 278 | C | 280.04 | 77.2 | 2 | PVC | 10-Mar-03 | | Transmissive Zone of the Upper Aquifer Zone of the Upper Three Runs Aquifer Unit |
| PGW-05A | PGW | PIEZOMETER WELL | ACTIVE | 447908.324 | 3675686.81 | 9.79 | -0.23 | 243.5 | C | 245.63 | 246.21 | 2 | PVC | 06-May-03 | | upper Gordon Aquifer Unit |

**Table 2-2 (continued)**

| STATION ID | WELL SERIES | STATION TYPE | WELL USE | UTM_E | UTM_N | SZ TOP ft MSL | SZ BOT ft MSL | GE | REFERENCE ELEVATION CODE | REFERENCE ELEVATION | TOTAL DEPTH | CONSTRU OBJ DIAMETER | CONSTR OBJ MATERIAL | COMPLETION DATE | DATE SEALED | Hydrostratigraphic_Unit |
|---|---|---|---|---|---|---|---|---|---|---|---|---|---|---|---|---|
| PGW-05B | PGW | PIEZOMETER WELL | ACTIVE | 447906.432 | 3675688.79 | 60.78 | 50.75 | 243.5 | C | 245.59 | 195.2 | 2 | PVC | 06-May-03 | | lower Lower Aquifer Zone of the Upper Three Runs Aquifer Unit |
| PGW-05C | PGW | PIEZOMETER WELL | ACTIVE | 447904.612 | 3675690.67 | 147.42 | 137.35 | 243.4 | C | 245.56 | 108.57 | 2 | PVC | 07-May-03 | | upper Lower Aquifer Zone of the Upper Three Runs Aquifer Unit |
| PGW-06A | PGW | PIEZOMETER WELL | ACTIVE | 446841.329 | 3676941.76 | 68 | 58 | 295 | C | 297.13 | 239.5 | 2 | PVC | 18-Feb-03 | | middle Gordon Aquifer Unit |
| PGW-06B | PGW | PIEZOMETER WELL | ACTIVE | 446840.001 | 3676938.87 | 109.42 | 99.39 | 295.4 | C | 297.61 | 198.53 | 2 | PVC | 09-May-03 | | upper Gordon Aquifer Unit |
| PGW-06C | PGW | PIEZOMETER WELL | ACTIVE | 446843.701 | 3676947.4 | 154.65 | 144.64 | 294.6 | C | 296.87 | 152.5 | 2 | PVC | 18-Feb-03 | | middle Lower Aquifer Zone of the Upper Three Runs Aquifer Unit |
| PGW-06DL | PGW | PIEZOMETER WELL | ACTIVE | 446844.911 | 3676950.25 | 207.35 | 197.33 | 294.3 | C | 296.7 | 99.5 | 2 | PVC | 18-Feb-03 | | Transmissive Zone of the Upper Aquifer Zone of the Upper Three Runs Aquifer Unit |
| PGW-07A | PGW | PIEZOMETER WELL | ACTIVE | 445792.687 | 3677017.05 | 116.51 | 106.51 | 321.6 | C | 323.8 | 217.6 | 2 | PVC | 18-Dec-02 | | upper Gordon Aquifer Unit |
| PGW-07B | PGW | PIEZOMETER WELL | ACTIVE | 445793.988 | 3677014.64 | 166.47 | 156.47 | 321.8 | C | 324.09 | 167.8 | 2 | PVC | 18-Dec-02 | | middle Lower Aquifer Zone of the Upper Three Runs Aquifer Unit |
| PGW-07C | PGW | PIEZOMETER WELL | ACTIVE | 445795.512 | 3677012.13 | 191.14 | 181.14 | 321.8 | C | 323.99 | 143.2 | 2 | PVC | 18-Dec-02 | | upper Lower Aquifer Zone of the Upper Three Runs Aquifer Unit |
| PGW-07DL | PGW | PIEZOMETER WELL | ACTIVE | 445796.931 | 3677009.51 | 231.64 | 221.64 | 321.7 | C | 323.99 | 102.6 | 2 | PVC | 18-Dec-02 | | Transmissive Zone of the Upper Aquifer Zone of the Upper Three Runs Aquifer Unit |
| PGW-08A | PGW | PIEZOMETER WELL | ACTIVE | 444599.681 | 3675111.85 | 70.02 | 60 | 298.7 | C | 300.9 | 241.15 | 2 | PVC | 19-Mar-03 | | lower Lower Aquifer Zone of the Upper Three Runs Aquifer Unit |
| PGW-08B | PGW | PIEZOMETER WELL | ACTIVE | 444599.373 | 3675109.07 | 128.9 | 118.87 | 298.9 | C | 301.2 | 182.53 | 2 | PVC | 19-Mar-03 | | middle Lower Aquifer Zone of the Upper Three Runs Aquifer Unit |
| PGW-08C | PGW | PIEZOMETER WELL | ACTIVE | 444599.168 | 3675106.24 | 188.32 | 178.3 | 299.5 | C | 301.7 | 123.65 | 2 | PVC | 19-Mar-03 | | upper Lower Aquifer Zone of the Upper Three Runs Aquifer Unit |
| PGW-08DL | PGW | PIEZOMETER WELL | ACTIVE | 444599.01 | 3675103.3 | 224.27 | 214.24 | 299.4 | C | 301.52 | 87.65 | 2 | PVC | 12-Mar-03 | | Transmissive Zone of the Upper Aquifer Zone of the Upper Three Runs Aquifer Unit |
| PGW-09A | PGW | PIEZOMETER WELL | ACTIVE | 445284.403 | 3674419.21 | 33.9 | 23.88 | 309.7 | C | 311.78 | 288.32 | 2 | PVC | 04-Apr-03 | | upper Gordon Aquifer Unit |
| PGW-09B | PGW | PIEZOMETER WELL | ACTIVE | 445284.592 | 3674421.79 | 121.93 | 111.91 | 309.7 | C | 311.73 | 200.32 | 2 | PVC | 04-Apr-03 | | middle Lower Aquifer Zone of the Upper Three Runs Aquifer Unit |
| PGW-09C | PGW | PIEZOMETER WELL | ACTIVE | 445288.056 | 3674424.54 | 159.79 | 149.79 | 309.8 | C | 311.81 | 162.02 | 2 | PVC | 19-Sep-03 | | upper Lower Aquifer Zone of the Upper Three Runs Aquifer Unit |
| PGW-09DL | PGW | PIEZOMETER WELL | ACTIVE | 445284.631 | 3674424.54 | 220.11 | 210.1 | 309.8 | C | 311.7 | 97.2 | 2 | PVC | 25-Mar-03 | | TZ/TCCZ of the Upper Aquifer Zone of the Upper Three Runs Aquifer Unit |
| PGW-10B | PGW | PIEZOMETER WELL | ACTIVE | 446953.143 | 3674679.32 | 77.51 | 67.49 | 253.5 | C | 255.86 | 188.52 | 2 | PVC | 08-May-03 | | lower Lower Aquifer Zone of the Upper Three Runs Aquifer Unit |
| PGW-10C | PGW | PIEZOMETER WELL | ACTIVE | 446947.157 | 3674678.43 | 152.75 | 142.74 | 253.8 | C | 256.08 | 113.51 | 2 | PVC | 28-Jan-03 | | upper Lower Aquifer Zone of the Upper Three Runs Aquifer Unit |
| PGW-10CU | PGW | PIEZOMETER WELL | ACTIVE | 446949.425 | 3674681.48 | 198.64 | 188.64 | 253.6 | C | 255.91 | 67.27 | 2 | PVC | 30-Sep-03 | | Transmissive Zone of the Upper Aquifer Zone of the Upper Three Runs Aquifer Unit |
| PGW-10DL | PGW | PIEZOMETER WELL | ACTIVE | 446949.919 | 3674678.94 | 207.6 | 197.6 | 253.6 | C | 255.9 | 58.5 | 2 | PVC | 28-Jan-03 | | AA/TZ Horizon of the Upper Aquifer Zone of the Upper Three Runs Aquifer Unit |
| PGW-11A | PGW | PIEZOMETER WELL | ACTIVE | 446180.975 | 3678260.22 | 24.34 | 14.33 | 273.8 | C | 276.06 | 162.01 | 2 | PVC | 04-Feb-03 | | middle Gordon Aquifer Unit |

**Table 2-2 (continued)**

| STATION ID | WELL SERIES | STATION TYPE | WELL USE | UTM_E | UTM_N | SZ TOP ft MSL | SZ BOT ft MSL | GE | REFERENCE ELEVATION CODE | REFERENCE ELEVATION | TOTAL DEPTH | CONSTRU OBJ DIAMETER | CONSTR OBJ MATERIAL | COMPLETION DATE | DATE SEALED | Hydrostratigraphic_Unit |
|---|---|---|---|---|---|---|---|---|---|---|---|---|---|---|---|---|
| PGW-11B | PGW | PIEZOMETER WELL | ACTIVE | 446183.525 | 3678259.93 | 75.43 | 65.4 | 273.6 | C | 275.83 | 210.7 | 2 | PVC | 03-Feb-03 | | upper Gordon Aquifer Unit |
| PGW-11C | PGW | PIEZOMETER WELL | ACTIVE | 446186.536 | 3678259.52 | 158.64 | 148.63 | 273.3 | C | 275.55 | 127.19 | 2 | PVC | 03-Feb-03 | | upper Lower Aquifer Zone of the Upper Three Runs Aquifer Unit |
| PGW-11DL | PGW | PIEZOMETER WELL | ACTIVE | 446189.547 | 3678259.11 | 207.32 | 197.31 | 273 | C | 275.26 | 78.19 | 2 | PVC | 04-Feb-03 | | Transmissive Zone of the Upper Aquifer Zone of the Upper Three Runs Aquifer Unit |
| PGW-12A | PGW | PIEZOMETER WELL | ACTIVE | 447825.99 | 3677061.37 | 41.2 | 31.19 | 273.2 | C | 275.48 | 244.51 | 2 | PVC | 22-Apr-03 | | upper Gordon Aquifer Unit |
| PGW-12C | PGW | PIEZOMETER WELL | ACTIVE | 447825.039 | 3677058.79 | 162.19 | 152.18 | 273.2 | C | 275.62 | 123.51 | 2 | PVC | 14-Apr-03 | | upper Lower Aquifer Zone of the Upper Three Runs Aquifer Unit |
| PGW-12DL | PGW | PIEZOMETER WELL | ACTIVE | 447824.142 | 3677056.14 | 215.93 | 205.94 | 273.3 | C | 275.54 | 69.88 | 2 | PVC | 14-Apr-03 | | Transmissive Zone of the Upper Aquifer Zone of the Upper Three Runs Aquifer Unit |
| PGW-13A | PGW | PIEZOMETER WELL | ACTIVE | 444101.502 | 3676743.92 | 67.93 | 57.9 | 287.9 | C | 290.2 | 232.53 | 2 | PVC | 29-Apr-03 | | upper Gordon Aquifer Unit |
| PGW-13C | PGW | PIEZOMETER WELL | ACTIVE | 444100.054 | 3676746.22 | 136.69 | 126.67 | 287.7 | C | 289.89 | 163.52 | 2 | PVC | 29-Apr-03 | | lower Lower Aquifer Zone of the Upper Three Runs Aquifer Unit |
| PGW-13CU | PGW | PIEZOMETER WELL | ACTIVE | 444102.963 | 3676748.07 | 157.78 | 147.78 | 287.8 | C | 289.87 | 142.09 | 2 | PVC | 18-Sep-03 | | upper Lower Aquifer Zone of the Upper Three Runs Aquifer Unit |
| PGW-13DL | PGW | PIEZOMETER WELL | ACTIVE | 444098.509 | 3676748.6 | 197.48 | 187.46 | 287.4 | C | 289.66 | 102.41 | 2 | PVC | 29-Apr-03 | | Transmissive Zone of the Upper Aquifer Zone of the Upper Three Runs Aquifer Unit |
| PMP001DL | PMP | PIEZOMETER WELL | ACTIVE | 445700.328 | 3676623.69 | 228.4 | 210.4 | 314.2 | C | 316.59 | 100.9 | 0.75 | PVC | 01-Oct-08 | | Upper Aquifer Zone of the Upper Three Runs Aquifer Unit |
| PMP002DL | PMP | PIEZOMETER WELL | ACTIVE | 445699.53 | 3676631.17 | 228 | 213 | 313.5 | C | 315.81 | 100.6 | 0.75 | PVC | 30-Sep-08 | | Upper Aquifer Zone of the Upper Three Runs Aquifer Unit |
| PMP003DL | PMP | PIEZOMETER WELL | ACTIVE | 445700.279 | 3676639.58 | 228.4 | | 313.4 | C | 315.7 | 100.1 | 0.75 | PVC | 30-Sep-08 | | Upper Aquifer Zone of the Upper Three Runs Aquifer Unit |
| PMP004DL | PMP | PIEZOMETER WELL | ACTIVE | 445677.978 | 3676618.63 | 229.6 | 214.6 | 313.7 | C | 315.89 | 99.2 | 0.75 | PVC | 30-Sep-08 | | Upper Aquifer Zone of the Upper Three Runs Aquifer Unit |
| PMP005DL | PMP | PIEZOMETER WELL | ACTIVE | 445678.742 | 3676629.74 | 227.5 | 212.5 | 313.1 | C | 315.07 | 100.7 | 0.75 | PVC | 02-Oct-08 | | Upper Aquifer Zone of the Upper Three Runs Aquifer Unit |
| PMP006DL | PMP | PIEZOMETER WELL | ACTIVE | 445679.019 | 3676639.93 | 226.9 | 212 | 312.2 | C | 314.59 | 101.3 | 0.75 | PVC | 06-Oct-08 | | Upper Aquifer Zone of the Upper Three Runs Aquifer Unit |
| PMP007DL | PMP | PIEZOMETER WELL | ACTIVE | 445679.756 | 3676650.81 | 225.6 | 210.7 | 311.8 | C | 313.97 | 101.2 | 0.75 | PVC | 13-Oct-08 | | Upper Aquifer Zone of the Upper Three Runs Aquifer Unit |
| PMP008DL | PMP | PIEZOMETER WELL | ACTIVE | 445667.277 | 3676635.93 | 225.9 | 210.9 | 312.3 | C | 314.61 | 101.4 | 0.75 | PVC | 14-Oct-08 | | Upper Aquifer Zone of the Upper Three Runs Aquifer Unit |
| PMW001DL | PMW | MONITORING WELL | ACTIVE | 445746.069 | 3676645.58 | 230.42 | 215.42 | 314.9 | C | 317.26 | 101.8 | 4 | PVC | 31-Mar-09 | | Upper Aquifer Zone of the Upper Three Runs Aquifer Unit |
| PMW002DL | PMW | MONITORING WELL | ACTIVE | 445706.334 | 3676619.66 | 229.55 | 214.55 | 314.3 | C | 316.68 | 102 | 4 | PVC | 27-Mar-09 | | Upper Aquifer Zone of the Upper Three Runs Aquifer Unit |
| PMW003DL | PMW | MONITORING WELL | ACTIVE | 445708.202 | 3676632.89 | 230.78 | 215.78 | 315.1 | C | 317.36 | 101.6 | 4 | PVC | 30-Mar-09 | | Upper Aquifer Zone of the Upper Three Runs Aquifer Unit |
| PMW004DL | PMW | MONITORING WELL | ACTIVE | 445693.526 | 3676622.07 | 229.65 | 214.65 | 314.4 | C | 316.72 | 102 | 4 | PVC | 24-Mar-09 | | Upper Aquifer Zone of the Upper Three Runs Aquifer Unit |
| PMW005DL | PMW | MONITORING WELL | ACTIVE | 445693.49 | 3676633.91 | 228.48 | 213.48 | 313.5 | C | 315.79 | 102.3 | 4 | PVC | 25-Mar-09 | | Upper Aquifer Zone of the Upper Three Runs Aquifer Unit |
| PMW006DL | PMW | MONITORING WELL | ACTIVE | 445694.09 | 3676644.46 | 228.57 | 213.57 | 312.8 | C | 315.12 | 101.5 | 4 | PVC | 26-Mar-09 | | Upper Aquifer Zone of the Upper Three Runs Aquifer Unit |

**Table 2-2 (continued)**

| STATION ID | WELL SERIES | STATION TYPE | WELL USE | UTM_E | UTM_N | SZ TOP ft MSL | SZ BOT ft MSL | GE | REFERENCE ELEVATION CODE | REFERENCE ELEVATION | TOTAL DEPTH | CONSTRU OBJ DIAMETER | CONSTR OBJ MATERIAL | COMPLETION DATE | DATE SEALED | Hydrostratigraphic_Unit |
|---|---|---|---|---|---|---|---|---|---|---|---|---|---|---|---|---|
| PPP 1 | PPP | PIEZOMETER WELL | ACTIVE | 448904.96 | 3677561.81 | | | | | | 40 | 2 | PVC | 11-Apr-95 | unknown | Upper Aquifer Zone of the Upper Three Runs Aquifer Unit |
| PRB001DU | PRB | MONITORING WELL | ACTIVE | 445835.042 | 3676500 | 266.96 | 246.96 | 316.6 | C | 319.52 | 75 | 2 | PVC | 23-Aug-11 | | Upper Aquifer Zone of the Upper Three Runs Aquifer Unit |
| PRB002DU | PRB | MONITORING WELL | ACTIVE | 445793.365 | 3676545.55 | 267.44 | 247.44 | 317.1 | C | 319.64 | 75 | 2 | PVC | 24-Aug-11 | | Upper Aquifer Zone of the Upper Three Runs Aquifer Unit |
| PRB003C | PRB | MONITORING WELL | ACTIVE | 445962.694 | 3676408.48 | 187.91 | 177.91 | 317.4 | C | 319.97 | 142 | 2 | PVC | 28-May-14 | | upper Lower Aquifer Zone of the Upper Three Runs Aquifer Unit |
| PRB003DU | PRB | MONITORING WELL | ACTIVE | 445964.477 | 3676412.53 | 267.47 | 247.47 | 317.1 | C | 319.89 | 75 | 2 | PVC | 25-Aug-11 | | Upper Aquifer Zone of the Upper Three Runs Aquifer Unit |
| PRB004DU | PRB | MONITORING WELL | ACTIVE | 445905.852 | 3676613.9 | 266.32 | 246.32 | 316 | C | 319.12 | 75 | 2 | PVC | 24-Aug-11 | | Upper Aquifer Zone of the Upper Three Runs Aquifer Unit |
| PRB005C | PRB | MONITORING WELL | ACTIVE | 445866.257 | 3676675.05 | 176.61 | 166.61 | 316.2 | C | 318.8 | 152 | 2 | PVC | 21-May-14 | | upper Lower Aquifer Zone of the Upper Three Runs Aquifer Unit |
| PRB005DU | PRB | MONITORING WELL | ACTIVE | 445861.479 | 3676675.76 | 266.11 | 246.11 | 315.8 | C | 318.57 | 75 | 2 | PVC | 25-Aug-11 | | Upper Aquifer Zone of the Upper Three Runs Aquifer Unit |
| PRP 1A | PRP | MONITORING WELL | ACTIVE | 445122.88 | 3676625.52 | 262.9 | 232.9 | 282.9 | S | 284.7 | 51.7 | 4 | PVC | 17-Oct-83 | | A/AA Horizon of the Upper Aquifer Zone of the Upper Three Runs Aquifer Unit |
| PRP 2 | PRP | MONITORING WELL | ACTIVE | 445164.12 | 3676670.5 | 264.1 | 234.1 | 284.1 | S | 286.6 | 52.3 | 4 | PVC | 18-Oct-83 | | AA Horizon of the Upper Aquifer Zone of the Upper Three Runs Aquifer Unit |
| PRP 3 | PRP | MONITORING WELL | ACTIVE | 445182.33 | 3676612.6 | 258.6 | 228.6 | 278.6 | S | 280.8 | 52.1 | 4 | PVC | 13-Oct-83 | | AA Horizon of the Upper Aquifer Zone of the Upper Three Runs Aquifer Unit |
| PRP 4 | PRP | MONITORING WELL | ABANDONED | 445214.54 | 3676661.75 | 262.9 | 232.9 | 282.9 | S | 284.8 | 51.8 | 4 | PVC | 05-Jul-84 | 9/4/2003 | |
| PRP 5 | PRP | MONITORING WELL | ACTIVE | 445281.37 | 3676683.92 | 210.29 | 200.31 | 285.3 | S | 287.76 | 90.15 | 2 | PVC | 31-Mar-98 | | Transmissive Zone of the Upper Aquifer Zone of the Upper Three Runs Aquifer Unit |
| PRP 6 | PRP | MONITORING WELL | ACTIVE | 445186.934 | 3676616.71 | 249.32 | 234.32 | 279.3 | S | 281.87 | 48 | 2 | CS | 10-Sep-99 | | A/AA Horizon of the Upper Aquifer Zone of the Upper Three Runs Aquifer Unit |
| PRP 7 | PRP | MONITORING WELL | ACTIVE | 445156.165 | 3676605.45 | 244.15 | 229.15 | 279.2 | S | 281.99 | 53.5 | 2 | PVC | 17-Sep-99 | | AA Horizon of the Upper Aquifer Zone of the Upper Three Runs Aquifer Unit |
| PSB 1 | PSB | MONITORING WELL | ABANDONED | 445709.47 | 3676400.77 | | | | | | | 4 | STEEL | 31-May-78 | 4/1/1984 | |
| PSB 1A | PSB | MONITORING WELL | ACTIVE | 445706.34 | 3676398.04 | 287.4 | 257.4 | 327.4 | S | 329.3 | 71.7 | 4 | PVC | 15-Mar-84 | | A Horizon of the Upper Aquifer Zone of the Upper Three Runs Aquifer Unit |
| PSB 2 | PSB | MONITORING WELL | ABANDONED | 445650.77 | 3676352.8 | | | | | | | 4 | STEEL | 01-Jun-78 | 4/1/1984 | |
| PSB 2A | PSB | MONITORING WELL | ACTIVE | 445652.17 | 3676356.01 | 287.2 | 257.2 | 322.2 | S | 323.9 | 66.5 | 4 | PVC | 16-Mar-84 | | A Horizon of the Upper Aquifer Zone of the Upper Three Runs Aquifer Unit |
| PSB 3 | PSB | MONITORING WELL | ABANDONED | 445577.8 | 3676297 | | | | | | | 4 | STEEL | 05-Jun-78 | 4/1/1984 | |
| PSB 3A | PSB | MONITORING WELL | ACTIVE | 445574.1 | 3676294.42 | 286.5 | 256.5 | 316.5 | S | 318.8 | 62.1 | 4 | PVC | 19-Mar-84 | | A Horizon of the Upper Aquifer Zone of the Upper Three Runs Aquifer Unit |
| PSB 4 | PSB | MONITORING WELL | ABANDONED | 445527.66 | 3676232.09 | | | | | | | 4 | STEEL | 05-Jun-78 | 4/1/1984 | |
| PSB 4A | PSB | MONITORING WELL | ACTIVE | 445525.9 | 3676234.61 | 285.5 | 255.5 | 310.5 | S | 312.7 | 57 | 4 | PVC | 20-Mar-84 | | A Horizon of the Upper Aquifer Zone of the Upper Three Runs Aquifer Unit |
| PSB 5 | PSB | MONITORING WELL | ABANDONED | 445610.19 | 3676259.86 | | | | | | | 4 | STEEL | 05-Jun-78 | 4/1/1984 | |

**Table 2-2 (continued)**

| STATION ID | WELL SERIES | STATION TYPE | WELL USE | UTM_E | UTM_N | SZ TOP ft MSL | SZ BOT ft MSL | GE | REFERENCE ELEVATION CODE | REFERENCE ELEVATION | TOTAL DEPTH | CONSTRU OBJ DIAMETER | CONSTR OBJ MATERIAL | COMPLETION DATE | DATE SEALED | Hydrostratigraphic_Unit |
|---|---|---|---|---|---|---|---|---|---|---|---|---|---|---|---|---|
| PSB 5A | PSB | MONITORING WELL | ACTIVE | 445606.63 | 3676258.07 | 292.3 | 262.3 | 317.3 | S | 319.5 | 57 | 4 | PVC | 20-Mar-84 | | A Horizon of the Upper Aquifer Zone of the Upper Three Runs Aquifer Unit |
| PSB 6 | PSB | MONITORING WELL | ABANDONED | 445694.68 | 3676326.76 | | | | | | | 4 | STEEL | 06-Jun-78 | 4/1/1984 | |
| PSB 6A | PSB | MONITORING WELL | ACTIVE | 445698.39 | 3676323.17 | 292.1 | 262.1 | 322.1 | S | 324.4 | 62.1 | 4 | PVC | 21-Mar-84 | | A Horizon of the Upper Aquifer Zone of the Upper Three Runs Aquifer Unit |
| PSB 7 | PSB | MONITORING WELL | ABANDONED | 445760.19 | 3676406.64 | | | | | | | 4 | STEEL | 06-Jun-78 | 4/1/1984 | |
| PSB 7A | PSB | MONITORING WELL | ACTIVE | 445757.49 | 3676410.4 | 289 | 259 | 329 | S | 330.9 | 71.7 | 4 | PVC | 14-Mar-84 | | A Horizon of the Upper Aquifer Zone of the Upper Three Runs Aquifer Unit |
| PSB 8 | PSB | MONITORING WELL | ACTIVE | 445837.418 | 3676342.55 | 270.75 | 260.75 | 321.8 | S | 324.96 | 63.84 | 2 | PVC | 24-Sep-01 | | A Horizon of the Upper Aquifer Zone of the Upper Three Runs Aquifer Unit |
| PSB 9 | PSB | MONITORING WELL | ACTIVE | 445651.075 | 3676263.43 | 267.29 | 257.29 | 317.3 | S | 321.55 | 62.5 | 2 | PVC | 17-Sep-01 | | A Horizon of the Upper Aquifer Zone of the Upper Three Runs Aquifer Unit |
| PSB 10 | PSB | MONITORING WELL | ACTIVE | 445429.971 | 3676290 | 265.54 | 255.54 | 306.5 | S | 309.57 | 53.84 | 2 | PVC | 13-Sep-01 | | A Horizon of the Upper Aquifer Zone of the Upper Three Runs Aquifer Unit |
| PSB 11 | PSB | MONITORING WELL | ACTIVE | 445426.521 | 3676383.42 | 260.02 | 250.02 | 306 | S | 309.56 | 58.5 | 2 | PVC | 11-Sep-01 | | A Horizon of the Upper Aquifer Zone of the Upper Three Runs Aquifer Unit |
| PSB 12 | PSB | MONITORING WELL | ACTIVE | 445486.887 | 3676453.7 | 274.92 | 264.92 | 308.9 | S | 311.92 | 46.5 | 2 | PVC | 14-Sep-01 | | A Horizon of the Upper Aquifer Zone of the Upper Three Runs Aquifer Unit |
| PSB002AA | PSB | MONITORING WELL | ACTIVE | 445656.558 | 3676357.96 | 112.91 | 102.91 | 322.6 | C | 324.93 | 225 | 2 | PVC | 11-May-11 | | upper Gordon Aquifer Unit |
| PSB002AL | PSB | MONITORING WELL | ACTIVE | 445655.832 | 3676361.38 | 7.57 | -2.45 | 323 | C | 325.34 | 328.5 | 2 | PVC | 13-May-14 | | lower Gordon Aquifer Unit |
| PSB002B | PSB | MONITORING WELL | ACTIVE | 445658.726 | 3676359.54 | 142.99 | 132.99 | 322.6 | C | 325.04 | 195 | 2 | PVC | 12-May-11 | | lower Lower Aquifer Zone of the Upper Three Runs Aquifer Unit |
| PSB002C | PSB | MONITORING WELL | ACTIVE | 445648.524 | 3676354.04 | 187.57 | 177.57 | 322.2 | C | 324.54 | 150 | 2 | PVC | 13-May-11 | | upper Lower Aquifer Zone of the Upper Three Runs Aquifer Unit |
| PSB002DL | PSB | MONITORING WELL | ACTIVE | 445646.276 | 3676352.36 | 254.37 | 244.37 | 322 | C | 324.38 | 83 | 2 | PVC | 13-May-11 | | lower Upper Aquifer Zone of the Upper Three Runs Aquifer Unit |
| PSB003DL | PSB | MONITORING WELL | ACTIVE | 445571.726 | 3676296.97 | 247.78 | 237.76 | 317.8 | C | 320.22 | 82.2 | 2 | PVC | 14-May-14 | | lower Upper Aquifer Zone of the Upper Three Runs Aquifer Unit |
| PSB011A | PSB | MONITORING WELL | ACTIVE | 445423.978 | 3676395.99 | 97.89 | 87.87 | 307.6 | C | 310.07 | 222 | 2 | PVC | 20-May-14 | | upper Gordon Aquifer Unit |
| PSB011B | PSB | MONITORING WELL | ACTIVE | 445423.72 | 3676390.93 | 171.48 | 161.48 | 307.2 | C | 309.57 | 151 | 2 | PVC | 06-May-11 | | lower Lower Aquifer Zone of the Upper Three Runs Aquifer Unit |
| PSB011C | PSB | MONITORING WELL | ACTIVE | 445423.415 | 3676387.47 | 202.37 | 192.37 | 307.1 | C | 309.44 | 120 | 2 | PVC | 09-May-11 | | upper Lower Aquifer Zone of the Upper Three Runs Aquifer Unit |
| PSB011DL | PSB | MONITORING WELL | ACTIVE | 445423.078 | 3676384.77 | 224.2 | 214.2 | 307 | C | 309.29 | 98 | 2 | PVC | 09-May-11 | | lower Upper Aquifer Zone of the Upper Three Runs Aquifer Unit |
| PSS 1D | PSS | MONITORING WELL | ACTIVE | 449705.35 | 3676926.88 | 202.1 | 182.1 | 217.5 | S | 219.9 | 37.5 | 4 | PVC | 14-Nov-88 | | |
| PSS 2D | PSS | MONITORING WELL | ACTIVE | 449965.1 | 3676640.89 | 197.1 | 177.1 | 226.6 | S | 229 | 51.6 | 4 | PVC | 14-Nov-88 | | |
| PSS 3D | PSS | MONITORING WELL | ACTIVE | 450032.86 | 3676666.17 | 198.5 | 178.5 | 231.8 | S | 234.2 | 55.5 | 4 | PVC | 14-Nov-88 | | |
| RGW 4C | RGW | PIEZOMETER WELL | ACTIVE | 444576.284 | 3677465.99 | 140.2 | 130.2 | 332.2 | C | 334.7 | 207 | 2 | PVC | 28-Sep-98 | | middle Lower Aquifer Zone of the Upper Three Runs Aquifer Unit |
| RGW 4D | RGW | PIEZOMETER WELL | ACTIVE | 444577.18 | 3677468.98 | 192.06 | 182.06 | 332.1 | C | 334.56 | 154 | 2 | PVC | 12-Oct-98 | | Transmissive Zone of the Upper Aquifer Zone of the Upper Three Runs Aquifer Unit |

**Table 2-2 (continued)**

| STATION ID | WELL SERIES | STATION TYPE | WELL USE | UTM_E | UTM_N | SZ TOP ft MSL | SZ BOT ft MSL | GE | REFERENCE ELEVATION CODE | REFERENCE ELEVATION | TOTAL DEPTH | CONSTRU OBJ DIAMETER | CONSTR OBJ MATERIAL | COMPLETION DATE | DATE SEALED | Hydrostratigraphic_Unit |
|---|---|---|---|---|---|---|---|---|---|---|---|---|---|---|---|---|
| RGW 5C | RGW | PIEZOMETER WELL | ACTIVE | 445941.943 | 3678018.32 | 116.83 | 106.83 | 283.8 | C | 286.33 | 182 | 2 | PVC | 16-Sep-98 | | lower Lower Aquifer Zone of the Upper Three Runs Aquifer Unit |
| RGW 5D | RGW | PIEZOMETER WELL | ACTIVE | 445938.6 | 3678017.73 | 194.17 | 184.17 | 284.2 | C | 286.62 | 104 | 2 | PVC | 16-Sep-98 | | Transmissive Zone of the Upper Aquifer Zone of the Upper Three Runs Aquifer Unit |
| RGW 6C | RGW | PIEZOMETER WELL | ACTIVE | 446723.719 | 3676545.11 | 113.12 | 103.12 | 315.1 | C | 317.72 | 218 | 2 | PVC | 11-Sep-98 | | lower Lower Aquifer Zone of the Upper Three Runs Aquifer Unit |
| RGW 6D | RGW | PIEZOMETER WELL | ACTIVE | 446720.512 | 3676546.02 | 210.14 | 200.14 | 315.1 | C | 317.54 | 119 | 2 | PVC | 14-Sep-98 | | Transmissive Zone of the Upper Aquifer Zone of the Upper Three Runs Aquifer Unit |
| RGW 7C | RGW | PIEZOMETER WELL | ACTIVE | 446116.243 | 3674853.5 | 93.85 | 83.85 | 295.9 | C | 298.35 | 222 | 2 | PVC | 29-Jul-98 | | Lower Aquifer Zone of the Upper Three Runs Aquifer Unit |
| RGW 7D | RGW | PIEZOMETER WELL | ACTIVE | 446115.51 | 3674856.43 | 175.45 | 165.45 | 295.5 | C | 297.95 | 138 | 2 | PVC | 29-Jul-98 | | Transmissive Zone of the Upper Aquifer Zone of the Upper Three Runs Aquifer Unit |
| RGW 9C | RGW | PIEZOMETER WELL | ACTIVE | 443118.529 | 3675949.37 | 112.28 | 102.28 | 288.3 | C | 290.78 | 189.5 | 2 | PVC | 12-Aug-98 | | lower Lower Aquifer Zone of the Upper Three Runs Aquifer Unit |
| RGW 9D | RGW | PIEZOMETER WELL | ACTIVE | 443116.012 | 3675952.87 | 161.69 | 151.69 | 288.7 | C | 291.19 | 141 | 2 | PVC | 23-Jul-98 | | upper Lower Aquifer Zone of the Upper Three Runs Aquifer Unit |
| RGW 10C | RGW | PIEZOMETER WELL | ABANDONED | 444273.426 | 3673336.91 | | | | | | | | | | 10/12/1998 | |
| RGW 10CR | RGW | PIEZOMETER WELL | ACTIVE | 444275.268 | 3673334.6 | 87.65 | 77.65 | 300.7 | C | 303.15 | 223.5 | 2 | PVC | 24-Sep-98 | | Lower Aquifer Zone of the Upper Three Runs Aquifer Unit |
| RGW 10D | RGW | PIEZOMETER WELL | ACTIVE | 444271.879 | 3673338.25 | 156.05 | 146.05 | 301.1 | C | 303.55 | 159 | 2 | PVC | 10-Jul-98 | | Transmissive Zone of the Upper Aquifer Zone of the Upper Three Runs Aquifer Unit |
| SSS 16 | SSS | MONITORING WELL | ABANDONED | 449965.13 | 3676640.95 | 226.4 | 226.4 | 226.4 | C | 228 | | 2 | PVC | 04-Nov-80 | 11/10/1988 | |
| SSS 17 | SSS | MONITORING WELL | ACTIVE | 450024.95 | 3676873.51 | 221 | 221 | 221 | S | 222.7 | 36.6 | 2 | PVC | 04-Nov-80 | | |
| SSS 18 | SSS | MONITORING WELL | ABANDONED | 449705.36 | 3676926.81 | 217.3 | 217.3 | 217.3 | C | 218.6 | | 2 | PVC | 04-Nov-80 | 11/9/1988 | |

**(This page intentionally left blank)**

**Table 2-3 Number of Calibration Targets per Unit**

| Hydrostratigraphic Unit | Number of Targets |
|---|---|
| 'A' and 'AA' Horizons (A/AA) | 47 |
| Transmissive Zone (TZ) | 24 |
| Tan Clay Confining Zone (TCCZ) | 0 |
| Upper Lower Aquifer Zone (ULAZ) | 21 |
| Middle Clay of the Lower Aquifer Zone (MC- LAZ) | 0 |
| Lower Lower Aquifer Zone (LLAZ) | 18 |
| Gordon Confining Unit (GCU) | 0 |
| Upper Gordon Aquifer (UGA) | 8 |
| Middle Silt of the Gordon Aquifer (MGA) | 0 |
| Lower Gordon Aquifer (LGA) | 13 |
| Crouch Branch Confining Unit (CBCU) | 0 |
| Crouch Branch Aquifer Unit (CBAU) | 2 |
| **Total** | **133** |

**(This page intentionally left blank)**

# 3.0 NUMERICAL MODEL CONSTRUCTION

In this chapter, the construction of a numerical groundwater flow and contaminant transport model for P Area is documented. The numerical model is based on the HCM of Chapter 2.0 and the previous model (SRNS 2011a).

## 3.1 Numerical Methods

In the saturated groundwater, a combination of continuity (mass conservation) and Darcy's Law leads to the following mathematical description of steady-state groundwater flow:

$$\frac{\partial}{\partial x}\left(K_x \frac{\partial h}{\partial x}\right)+\frac{\partial}{\partial y}\left(K_y \frac{\partial h}{\partial y}\right)+\frac{\partial}{\partial z}\left(K_z \frac{\partial h}{\partial z}\right)=0 \quad (1)$$

In this equation, the dependent variable is the hydraulic head, $h$, which is defined in the traditional Cartesian coordinate system ($x$, $y$, $z$). The horizontal and vertical hydraulic conductivities ($K_x$, $K_y$, and $K_z$) are known functions. Boundary conditions must be specified to solve Equation 1. The boundary conditions may be specified head (Dirichlet), specified flux (Neumann), or head-dependent flux (Cauchy). It is assumed that groundwater flow is unchanging in time (steady state).

The U.S. Geological Survey groundwater flow modeling software MODFLOW-2000 (Harbaugh et al. 2000) provides a means to solve Equation 1 for $h$ in a chosen domain, with specified values for hydraulic conductivity and boundary conditions. MODFLOW-2000 uses the finite difference method to approximate the groundwater flow equation as a set of algebraic equations in a discretized three-dimensional grid of rectangular cells. The contaminant transport model implemented in this study is MT3DMS (Zheng 1999), which simulates the transport of tritium, including radioactive decay, and the transport of TCE and PCE. The process of degradation of TCE and PCE is simulated using a first order decay term; dechlorination and the fate of degradation daughter products is not directly simulated.

The transport of contaminants in groundwater is governed by the advection-dispersion-reaction equation, which can be written as follows:

$$\left(n+\rho_b K_d\right)\frac{\partial c}{\partial t}+\frac{\partial}{\partial x_i}\left(nv_i\right)=\frac{\partial}{\partial x_i}\left(nD_{ij}\frac{\partial c}{\partial x_j}\right)-\lambda\left(n+\rho_b K_d\right)c+q_s c_s \quad (2)$$

In this equation, the Cartesian coordinates are represented by $x_i$ (i = 1, 2, 3), where i = rows and j = columns, and the dependent variable is the contaminant concentration in groundwater, c. The velocity field, $v_i$, is determined from the flow solution (Equation 1) and Darcy's Law. The effective porosity is n, and the porous medium bulk density is $\rho_b$. First-order (exponential) decay is assumed at a rate of $\lambda$. Equilibrium sorption is also assumed, with a sorption coefficient of $K_d$. The dispersion coefficient tensor, $D_{ij}$, is dependent on the groundwater velocity and specified length scales for dispersion, called dispersivities. Dispersivities are specified as longitudinal (along the direction of flow, $\alpha_L$), horizontal-transverse ($\alpha_T$), and vertical-transverse ($\alpha_V$). The initial value of c also must be specified to solve Equation 2.

Contaminant sources and sinks are represented in Equation 2 by the source/sink groundwater flow per unit volume ($q_s$) and the source/sink concentration ($c_s$). In the modeling presented here, a no-source assumption is made. Therefore, $q_s$ is set to zero.

MT3DMS (Zheng 1999) is a software program for solving Equation 2 that uses the same finite-difference framework as MODFLOW-2000. Once the steady-state values of h are determined from MODFLOW-2000, and the independent variables of Equation 2 are specified, MT3DMS can be used to solve for each contaminant concentration (c) as a function of space and time in the modeled domain. MT3DMS provides several methods for simulating advection, including the finite-difference method, the total-variation-diminishing method (TVD), and the method of characteristics (MOC). In this analysis, the TVD method is used to simulate advection in MT3DMS.

Both MODFLOW-2000 and MT3DMS are included in the Groundwater Modeling System (GMS) (Brigham Young University 2000) software package (version 6.5; February 2, 2009 build date). GMS is a standard suite of tools for modeling analyses at SRS and other USDOE sites.

## 3.2 Model Domain

The horizontal domain of the P-Area model (Figure 3-1) was chosen to be coincident with the HCM boundary documented in Chapter 2 and used for the previous model in SRNS 2011a. The model boundaries include, starting to the southeast and going clockwise, Meyers Branch, potentiometric head contours perpendicular to Steel Creek upgradient of L Lake, a groundwater divide between L Lake and PAR Pond, PAR Pond tributaries, and potentiometric head contours upgradient of PAR Pond.

## 3.3 Model Grid

A rectangular grid frame was drawn to encompass the model extent and be oriented roughly in the direction of plume movement (Figure 3-2). A rectilinear, non-uniform grid was then constructed within this frame to provide maximum resolution (50 ft spacing) in the plume area and a lower resolution elsewhere (maximum grid spacing of 100 ft). The model has 225 rows and 239 columns. The lower left (west) corner of the model has coordinates of SRS-Northing 30514.3 ft and SRS-Easting 57922.1 ft in the SRS plant coordinate system. The model grid is rotated 18.4 degrees from SRS plant north. The model bounding box is 18,200 ft by 18,350 ft in the x and y directions, respectively.

Vertically, the model layering is based on hydrostratigraphic surface elevations and data provided by SRS. Thirteen model layers are used, with multiple model layers within hydrostratigraphic units that could have variability in properties, hydraulic heads, or concentrations with depth (Figure 3-3).

After the 2010 SRS reevaluation of the hydrostratigraphic “picks” in and near PArea (Amidon 2010), additional boreholes were installed in 2011 (SRNS 2011b) and 2014 (SRNS 2014). These picks are based on geologic interpretation of borehole logs and were used to generate a three-dimensional representation of the area hydrostratigraphy. This representation is called the “solid model” in GMS. The variability in layer elevations is indicative of natural variability and data density. In particular, the upper layers appear more undulating near the P-Area Reactor building because there are more boreholes and cone penetrometer data present to define layer elevations. Deeper layers, such as the CBCU and CBAU have gradually varying elevations because there are relatively sparse boreholes that define geologic unit elevations.

The following hydrogeologic layers are used in the solid model, from land surface downward:

- A/AA: model layer 1,
- TZ: model layer 2,
- TCCZ: model layer 3,
- LAZ: subdivided into
  - ULAZ (model layer 4)
  - MC-LAZ (model layer 5), and
  - LLAZ (model layer 6),
- GCU: model layer 7,
- GAU: subdivided into
  - UGA (model layer 8),
  - MGA (model layer 9), and
  - LGA (model layers 10 and 11),
- CBCU: model layer 12, and
- CBAU: model layer 13.

Figures 3-3 and 3-4 show cross sections along model row 100 and model column 170, respectively, with the locations of the sections identified in Figure 3-2. The sequence of model layering, relative thickness, and hydrostratigraphic trends across the model domain are illustrated in Figures 3-3 and 3-4.

Appendix A identifies all of the hydrostratigraphic picks (Table A-1) used in developing the solid model, as well as the explanations (Table A-2) for changes or removals. The Table A-1 dataset includes recently obtained data from boreholes in P Area (SRNS 2011b and 2014) plus borehole and cone penetrometer data from the surrounding region (i.e., L Area). The borehole pick data at seven wells in the study area were discarded because elevations of the CBCU were too high or the UGA were too low compared to nearby boreholes or cone penetrometer locations

(Table A-2). Data were added at locations to improve surfaces and to insure the CBCU approximates the regional slope. The wells with modified picks are identified in Appendix A, Table A-2 and A-3. Kriging (using Mining Visualization System, (MVS), (CTech 2012) software (version 9.82; release date 10/18/2012)) was used to perform interpolation/extrapolation of layer surfaces in three dimensions from the borehole pick data, with a forced minimum thickness of 2 feet. The variogram model parameters were determined automatically from the data and are shown in Table 3-1, note the nugget for all was zero (0). The MVS data was exported as a grid of x, y, z data, which was imported as scatter data into GMS. This data was then interpolated to TINs by nearest neighbor (TZ, TCCZ, ULAZ, MC-LAZ, LLAZ, GCU, CBAU) or inverse distance weighted methods (UGA, MGA). In contrast to the other layers, the layer elevations for the CBCU were developed solely in GMS. Layer thicknesses for the CBCU and CBAU were set to match the 2011 uniform values of 151 and 174 ft.

**Table 3-1 Kriging Parameters for Solid Model Development**

| Unit Top | Variogram Model | Range (ft) | Sill ($ft^2$) |
|---|---|---|---|
| Transmissive Zone | Spherical | 16,921 | 380 |
| Tan Clay Confining Zone | Spherical | 11,720 | 325 |
| Upper Lower Aquifer Zone | Spherical | 35,094 | 1,431 |
| Middle Clay of the Lower Aquifer Zone | Spherical | 14,207 | 614 |
| Lower Lower Aquifer Zone | Spherical | 6,470 | 540 |
| Gordon Confining Unit | Spherical | 13,764 | 833 |
| Upper Gordon Aquifer | Spherical | 33,527 | 1,908 |
| Middle Silt of the Gordon Aquifer | Spherical | 22,463 | 1,432 |
| Lower Gordon Aquifer | Spherical | 6,470 | 326 |

Two model layers are used to represent the LGA hydrostratigraphic unit. In this case, layer thickness was determined by dividing the hydrostratigraphic unit thickness by two. The LGA hydrostratigraphic unit thickness (approximately 140 ft) was divided in order to have similar layer thickness to the UGA (approximately 70 ft).

In addition to the surface elevations derived from Kriging of borehole pick data, the top of the model (top of layer 1) is defined by topography, as derived from the LIDAR data. The topography is especially important along Steel Creek and in wetlands. The top is identical to that of the 2011 model (SRNS 2011a). Figure 3-5 shows the topographic elevations used in the model in feet above mean sea level. Figures 3-6 through 3-16 show the elevations of each hydrostratigraphic unit, and Figures 3-17 through 3-26 show the hydrostratigraphic unit thicknesses (note that thickness maps are not provided for the CBCU or CBAU because the thicknesses of these units are assumed to be uniform).

## 3.4 Hydrogeologic Properties

Hydraulic conductivity values ($K_x$, $K_y$, $K_z$) are specified in each model cell. The value of hydraulic conductivity is much higher in aquifer zones than in confining zones and may vary considerably within an aquifer or confining zone. Typically, hydraulic conductivity values are initialized for each hydrostratigraphic layer based on prior studies, such as the previous model SRNS 2011a, and the values are adjusted during flow model calibration to achieve a good match between modeled and observed head and/or flux conditions.

Table 3-2 lists reasonable ranges for the hydraulic conductivities based on prior modeling reports at SRS (Bills et al. 2000; Council et al. 2002; Flach et al. 1998, 1999; GeoTrans 2002, 2003, 2009; HSI GeoTrans 1998; SRNS 2011a). Prior modeling at SRS has shown that the horizontal-to-vertical anisotropy to approximate 100 to 1. The initial conductivity zonation from the previous model (SRNS 2011a) was used as initial conditions for this model. Adjustment to these initial hydraulic conductivity values was considered in the flow model calibration, as discussed in Chapter 4.0.

**Table 3-2 Reasonable Ranges for Hydraulic Conductivities**

| Hydrogeologic Unit | Horizontal Hydraulic Conductivity ($K_x = K_y$) (ft/day) | Vertical Hydraulic Conductivity ($K_z$) (ft/day) |
|---|---|---|
| 'A' and 'AA' Horizons | 1 – 30 | $K_x \times 0.01$ |
| Transmissive Zone | 1 – 60 | $K_x \times 0.01$ |
| Tan Clay Confining Zone | $K_z \times 100$ | 0.0005 – 0.1 |
| Lower Aquifer Zone | 0.001 – 100 | $K_x \times 0.01$ |
| Gordon Confining Unit | $K_z \times 100$ | 0.00001 – 0.0007 |
| Gordon Aquifer Unit (composite of Upper/Middle/Lower) | 20 – 40 | $K_x \times 0.01$ |
| Middle Silt Gordon Aquifer Unit | $K_z \times 100$ | $5e^{-7}$ – 0.4 |
| Crouch Branch Confining Unit | $K_z \times 10$ to $K_z \times 1000$ | 0.000045 - 0.008 |
| Crouch Branch Aquifer Unit | 10 - 25 | $K_x \times 0.02$ to $K_x \times 0.001$ |

Transport modeling requires specification of values for effective porosity (n), dispersivity ($\alpha_L$, $\alpha_H$, and $\alpha_V$), and sorption coefficient ($K_d$). A value of 0.3 was used as the default effective porosity value for all hydrogeologic units, as done in the 2011 model. This is a typical value for effective porosity for sands, silts, and clays.

Dispersivity is a parameter that describes the degree of plume spreading and is often determined by calibration to an existing plume. Dispersivity values depend on the scale of the plume and are typically higher in highly heterogeneous formations. As a practical rule of thumb, the longitudinal dispersivity ($\alpha_L$) should be no greater than one-tenth of the problem length scale, the horizontal-transverse dispersivity ($\alpha_H$) should be about one-tenth of $\alpha_L$, and the vertical dispersivity ($\alpha_V$) should be about one-hundredth of $\alpha_L$. Dispersivity values were set to 2011 values of 10 ft (longitudinal), 0.1 ft (horizontal-transverse), and 0.01 ft (vertical). Dispersivity was treated as a space-uniform parameter during transport model calibration (Chapter 4.0).

The bulk density ($\rho_b$) and sorption coefficient ($K_d$) determine the degree to which tritium and the CVOCs (PCE and TCE) mass is adsorbed to solids in the porous medium (an equilibrium sorption is assumed). Greater adsorption effectively results in slower movement of the CVOCs; whereas, tritium would not be expected to be slowed. A bulk density of 1.48 kg/L (92.4 lb/ft$^3$ or 4.19e$^7$ mg/ft$^3$) was used throughout the model domain. Sorption is a function of the constituent organic-carbon partition coefficient ($K_{oc}$) and fractional organic content ($F_{oc}$) of the sediment.

$$K_d = F_{oc} K_{oc} \tag{3}$$

Organic-carbon partition coefficients ($K_{oc}$) for both TCE and PCE are 265 L/Kg (from Lester and Council 2008) and half-lives for TCE and PCE are assumed to be 25 yrs (personal communication, Jeff Ross, 2015). The assumed organic carbon content in the solids ($F_{oc}$) by hydrostratigraphic unit is found in Table 3-3, along with the calculated $K_d$ used in the model. For tritium, a $K_d$ of zero is used for all hydrostratigraphic units.

The retardation factor (R) describes the adsorption process through the use of the contaminant specific sorption coefficient, the material specific bulk density and total porosity. R can also be defined as the ratio of the average groundwater velocity to the velocity of the contaminants. A retardation factor of 1.0 results in the contaminant moving along with the groundwater. A factor of 2.0 results in the contaminant moving at one-half the velocity of groundwater.

The equation for retardation factor is:

$$R = (1 + K_d(\rho_b/n)) \tag{4}$$

Where:

R = retardation factor

$K_d$ = equilibrium sorption coefficient

$\rho_b$ = bulk density

$n$ = total porosity (assumed to equal effective porosity)

**Table 3-3 Fractional Organic Content, $K_d$, and Retardation by Hydrostratigraphic Unit**

| Layer | $F_{oc}$ (%) | $K_d$ (L/kg) | R | $F_{oc}$ Source |
|---|---|---|---|---|
| 'A' and 'AA' Horizons/Transmissive Zone | 1.0 | 2.65 | 14.1 | 1 |
| Tan Clay Confining Zone | 1.2 | 3.18 | 16.7 | 2 |
| Lower Aquifer Zone | 0.3 | 0.80 | 4.9 | 3 |
| Gordon Confining Unit | 0.3 | 0.80 | 4.9 | 3 |
| Gordon Aquifer Unit | 0.3 | 0.80 | 4.9 | 3 |
| Crouch Branch Confining Unit | 0.8 | 2.12 | 11.5 | 2 |
| Crouch Branch Aquifer Unit | 0.3 | 0.80 | 4.9 | 3 |

Source 1: Average total organic carbon content of the 27- to 30-ft-depth intervals of boreholes RAG001, RAG003, and RAG005 are from the *RCRA Facility Investigation/Remedial Investigation (RFI/RI) Report with Baseline Risk Assessment and Corrective Measures Study (CMS/FS) for the R-Area Operable Unit (U)* (SRNS 2009).

Source 2: Fraction of organic carbon ($F_{oc}$) value represents 2 times the average lignite percentage of the layer in six borings (P19TA, P20TA, P24TA, PPC1, GCB7LI, and LAW1TD) from P-, R-, and L-Areas. Total organic carbon is assumed to be 2 times the visible lignitic carbon.

Source 3: Default Savannah River Site value from *Sampling and Analysis of Fraction of Organic Carbon (foc) in Soil* (Ohio EPA 2003).

## 3.5 Groundwater Flow Boundary Conditions

Flow boundary conditions provide the sources and sinks of groundwater in the model. Three types of boundaries are used in the P-Area model: specified head, head-dependent flux, and specified flux boundaries.

Specified head boundaries are used on the model perimeter for the model layers representing aquifers (Figure 3-27 through 3-30) for sections not along groundwater divides. The head values specified are based on both the results from prior groundwater models (Flach et al. 1998, 1999; GeoTrans 2004; SRNS 2011a) and extrapolation from observed head values in P Area. The adjustment of the specified head values for calibration is discussed in Chapter 4.0.

Head-dependent flow boundaries are used to model creeks and wetlands within the model domain. The head-dependent flow boundaries are placed in the uppermost active model layer. In most areas, the uppermost layer is layer 1 (A/AA); however, where the TZ outcrops, the uppermost layer is layer 2; where the TCCZ outcrops the uppermost layer is layer 3. The creeks are modeled with the Drain package (Figure 3-31) and can only receive inflow from groundwater if the water table elevation is higher than the stream stage (drain elevation). The drain elevations were derived from the surface elevation of the solid model. The drain elevations are set at 1 foot below the solid model ground surface.

Drain conductances were set at the calibrated value of the 2011 model, which was an arbitrarily high value of 100 $ft^2$/day/ft for the wetlands and 200 $ft^2$/day/ft for the creeks so that flow from the aquifers would not be limited. Wetland locations were derived from multiple sources including the National Wetlands Inventory and topographic maps; the wetlands also were modeled as seepage faces in the Drain package. The P-Area Discharge Canal was modeled with the River package with the head stage set to the bottom riverbed elevation to emulate the Drain package. This technique allows the P-Area Discharge Canal to behave as a groundwater sink while enabling easy differentiation of its flux from that of the other drains. As with the drains, the riverbed conductances were set to calibrated values in the 2011 model of 100 or 500 $ft^2$/day/ $ft^2$.

A specified flux is applied at the model top (uppermost active layer) in upland areas to model precipitation recharge (Figure 3-32). The recharge zones have a base recharge rate of 17.0 in./yr, 8.5 in./yr in the industrialized areas, and zero recharge in areas of groundwater discharge. A no-flow condition (specified flux of zero) is also assumed at the model bottom (base of the CBAU).

There are no extraction wells or other boundary conditions within the model domain. One production well exists at the railroad yard with and average extraction rate of 0.23 gallons per minute (gpm) (Sept 2013- Sept 2014). This well was deemed insignificant to the flow model and not included.

## 3.6 Initial Conditions

Because the groundwater flow is assumed to be at steady state, initial conditions for hydraulic head are not relevant. The heads from the 2011 model were used as a starting condition and then used the final heads as starting heads for the final run.

Initial concentrations for CVOCs and tritium are shown in the plumes developed from the 2014/15 sampling events (Figures 2-6 through 2-10). Development of the transport model initial conditions is discussed further in Chapter 5.0.

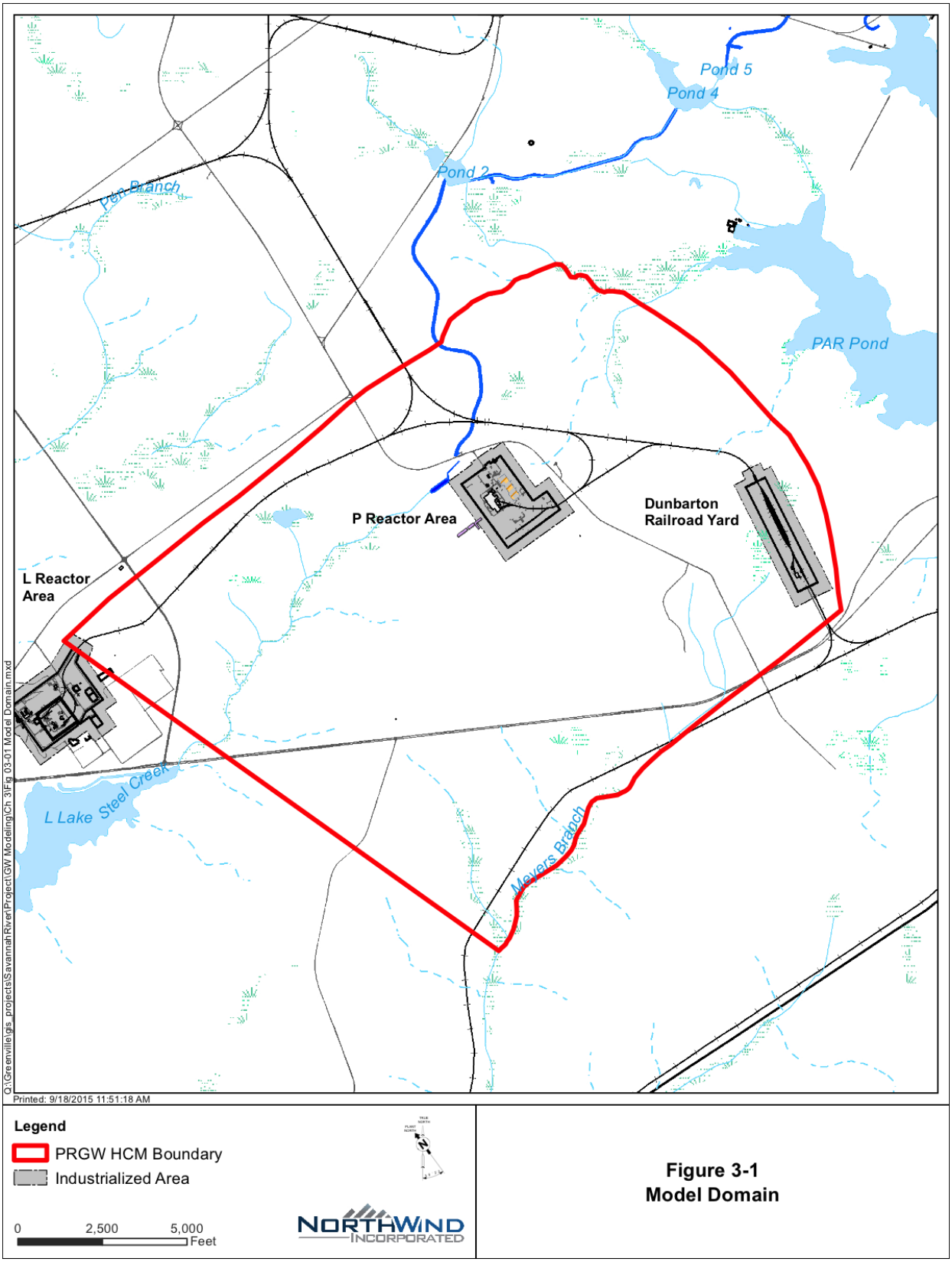


**Figure 3-1 Model Domain**

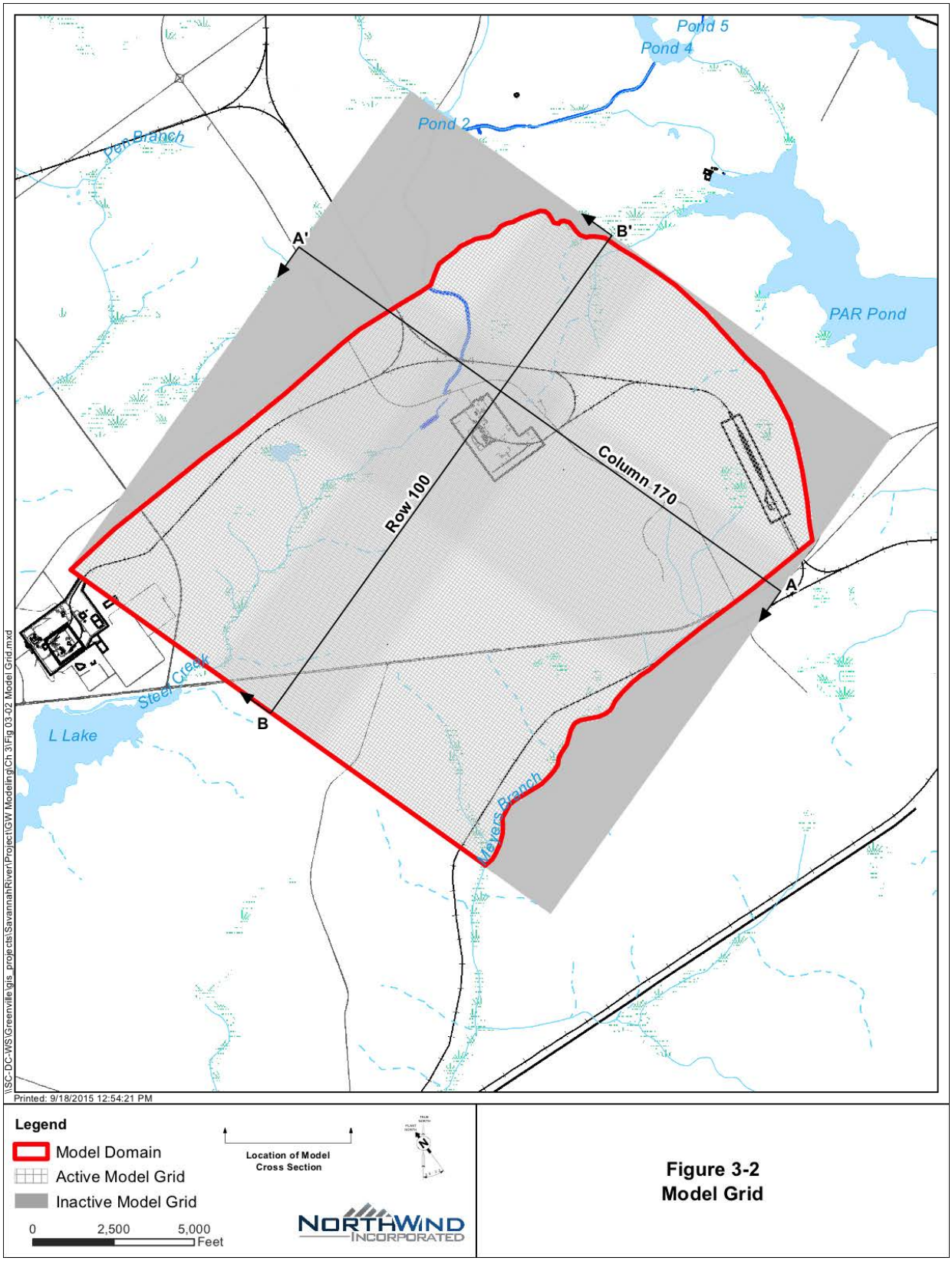


**Figure 3-2 Model Grid**

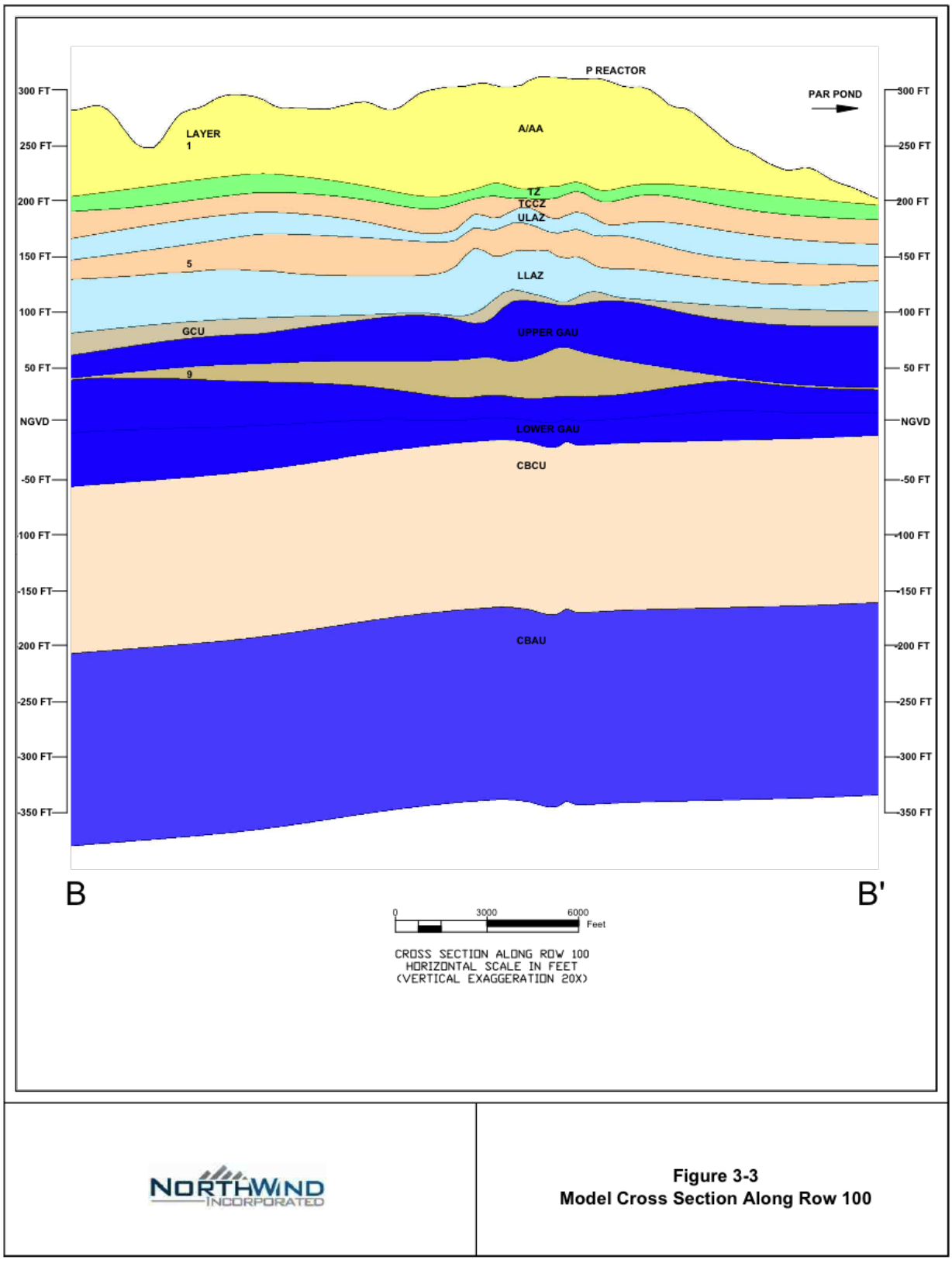


**Figure 3-3 Model Cross Section Along Row 100**

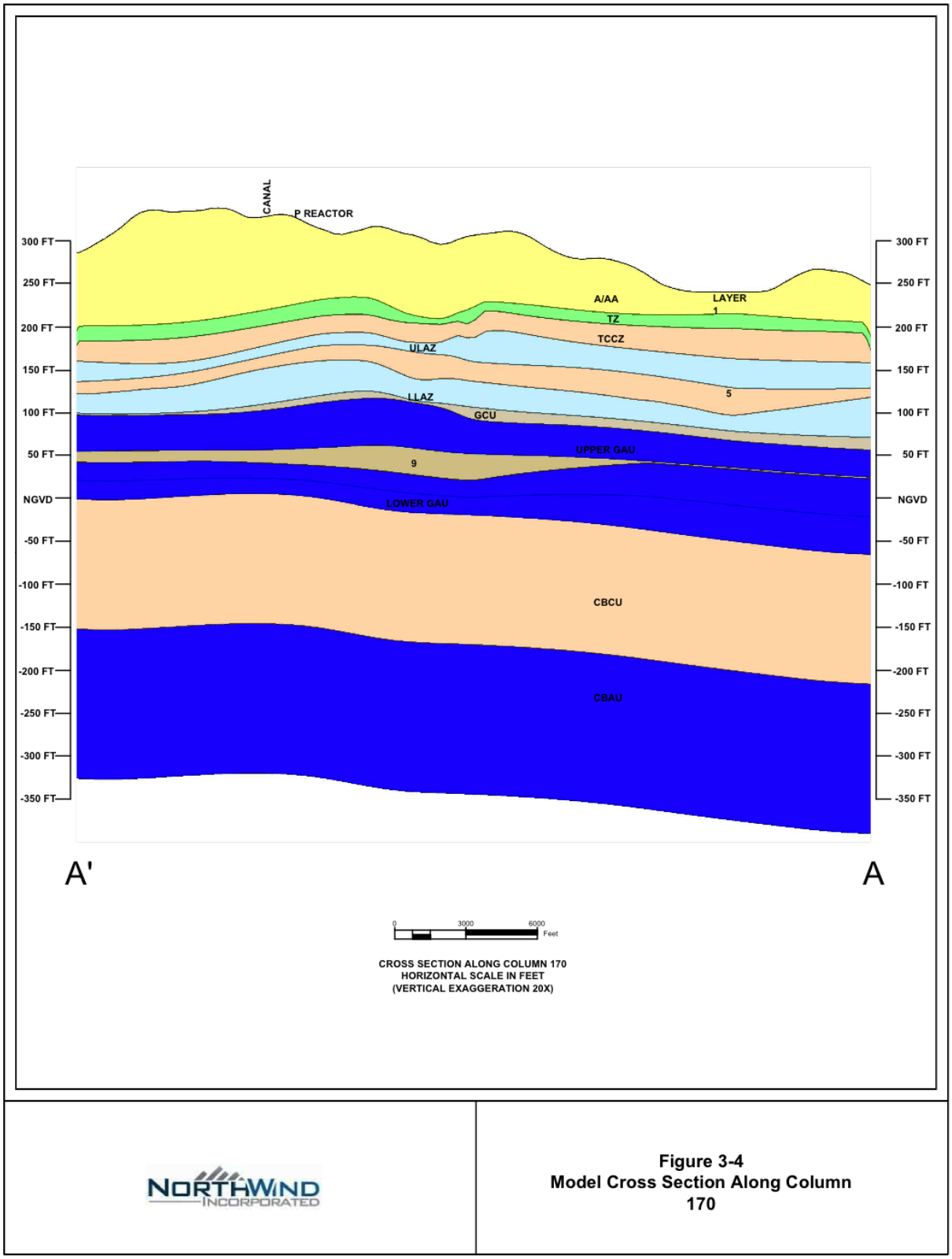


**Figure 3-4 Model Cross Section Along Column 170**

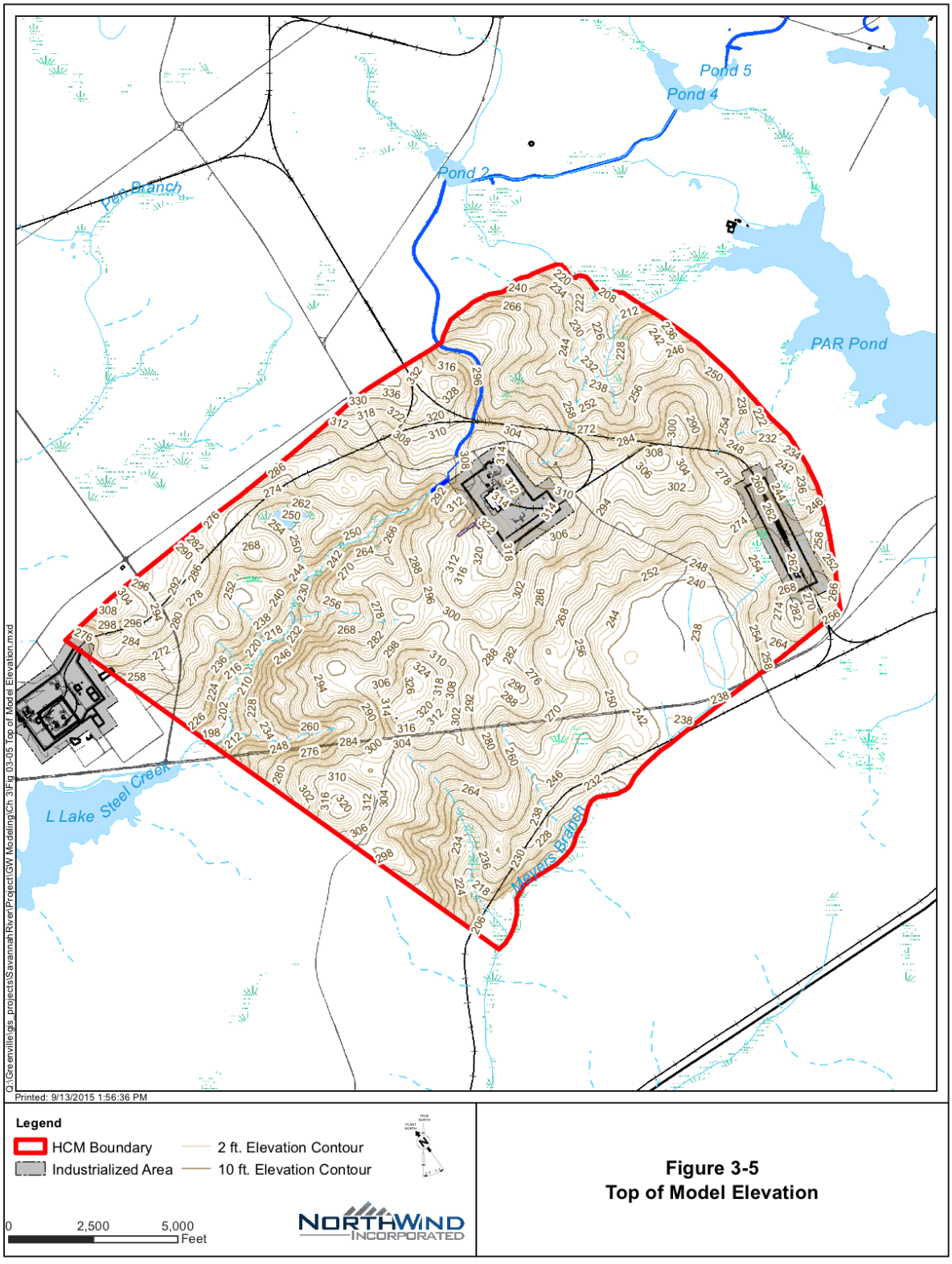


**Figure 3-5 Topography**

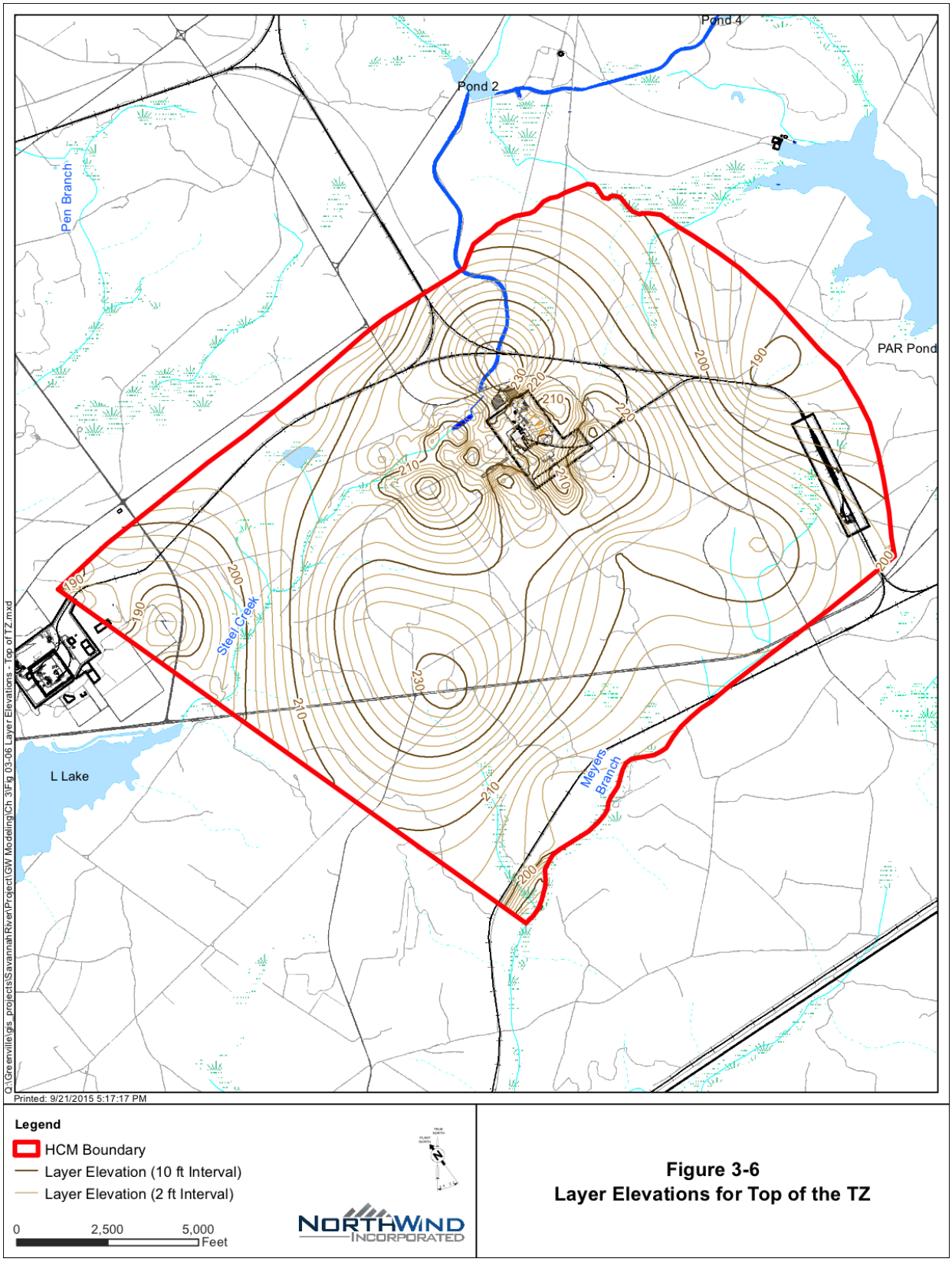


**Figure 3-6 Layer Elevations – Top of TZ**

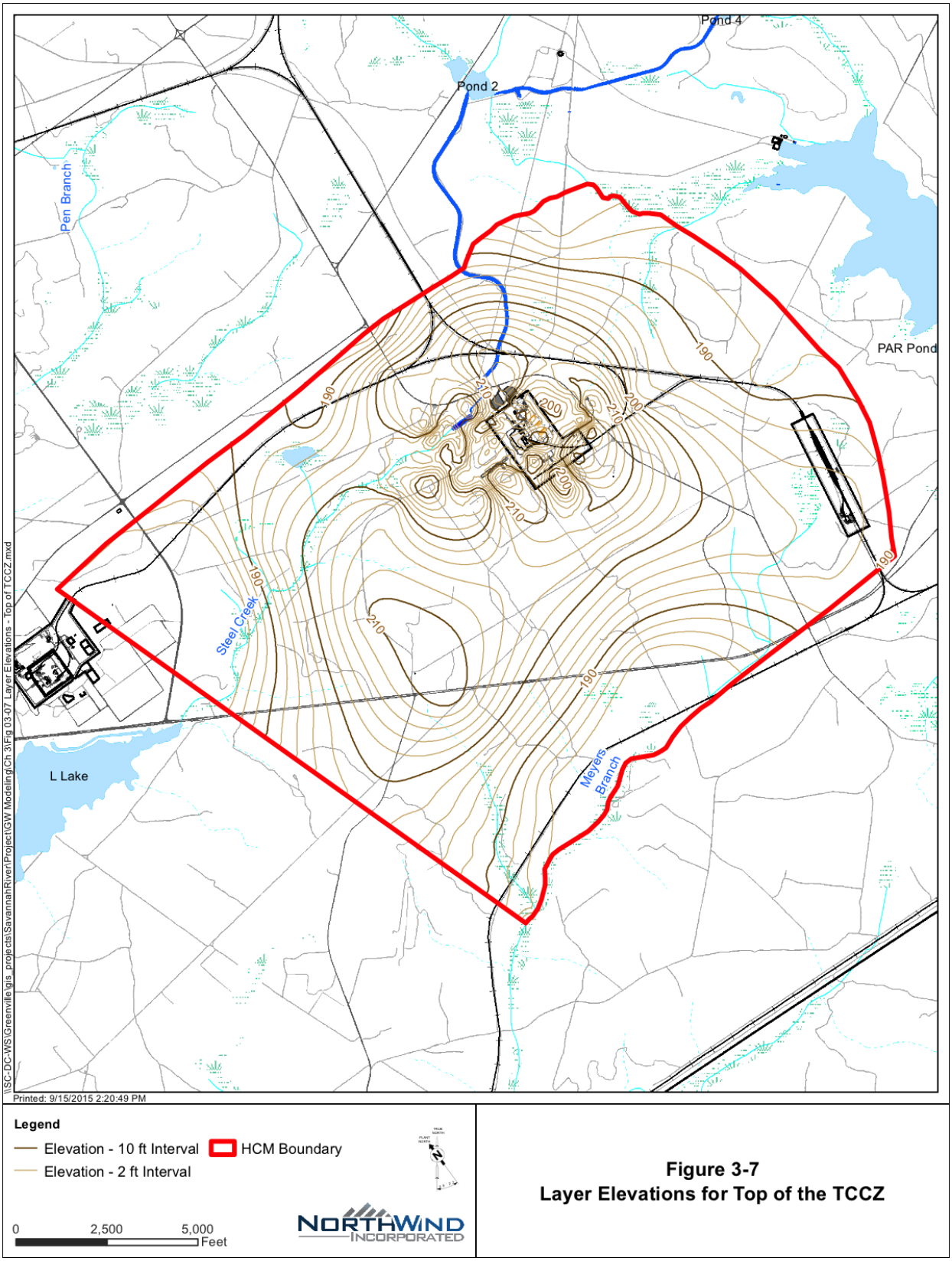


**Figure 3-7 Layer Elevations – Top of TCCZ**

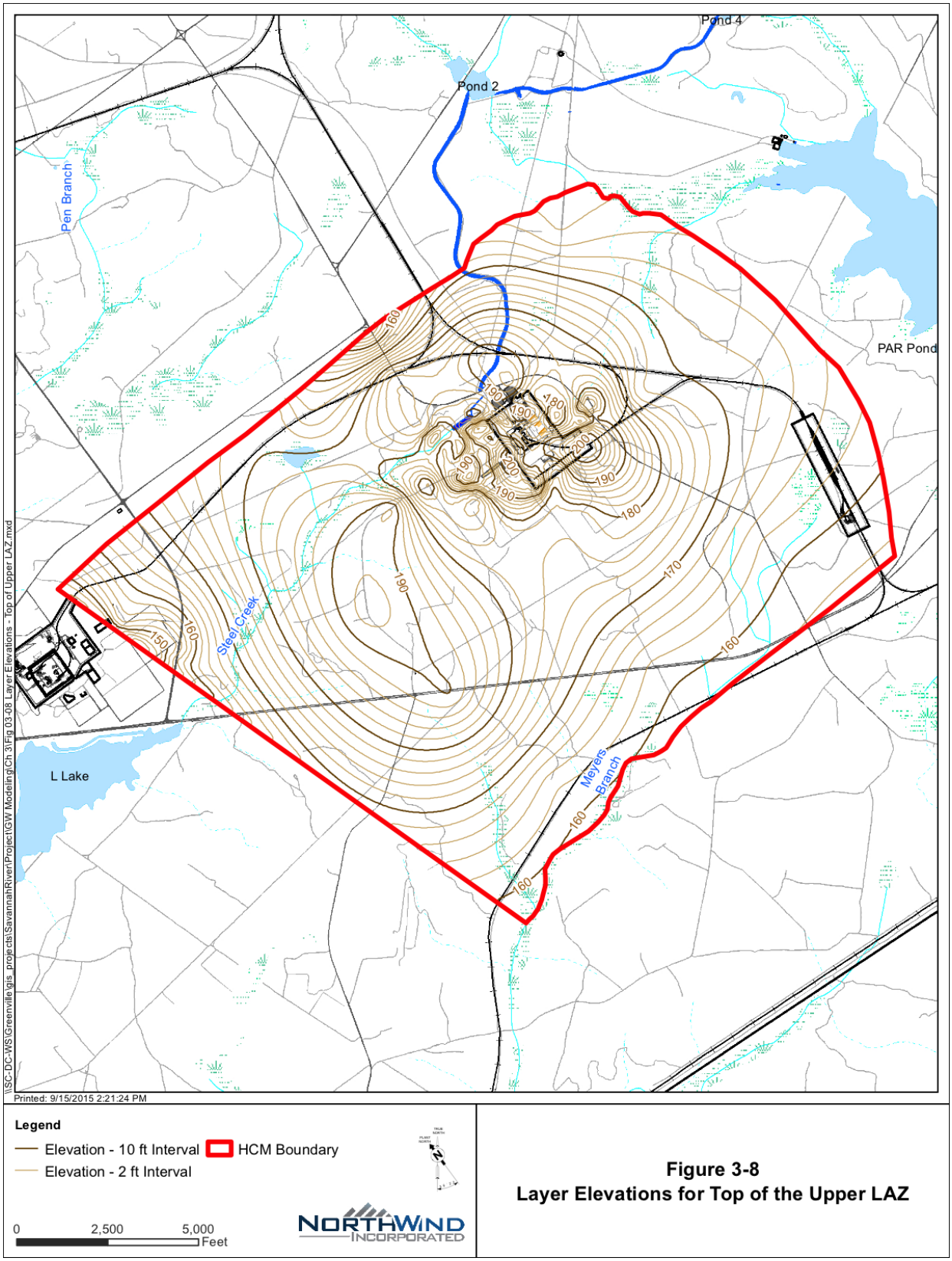


**Figure 3-8 Layer Elevations – Top of Upper LAZ**

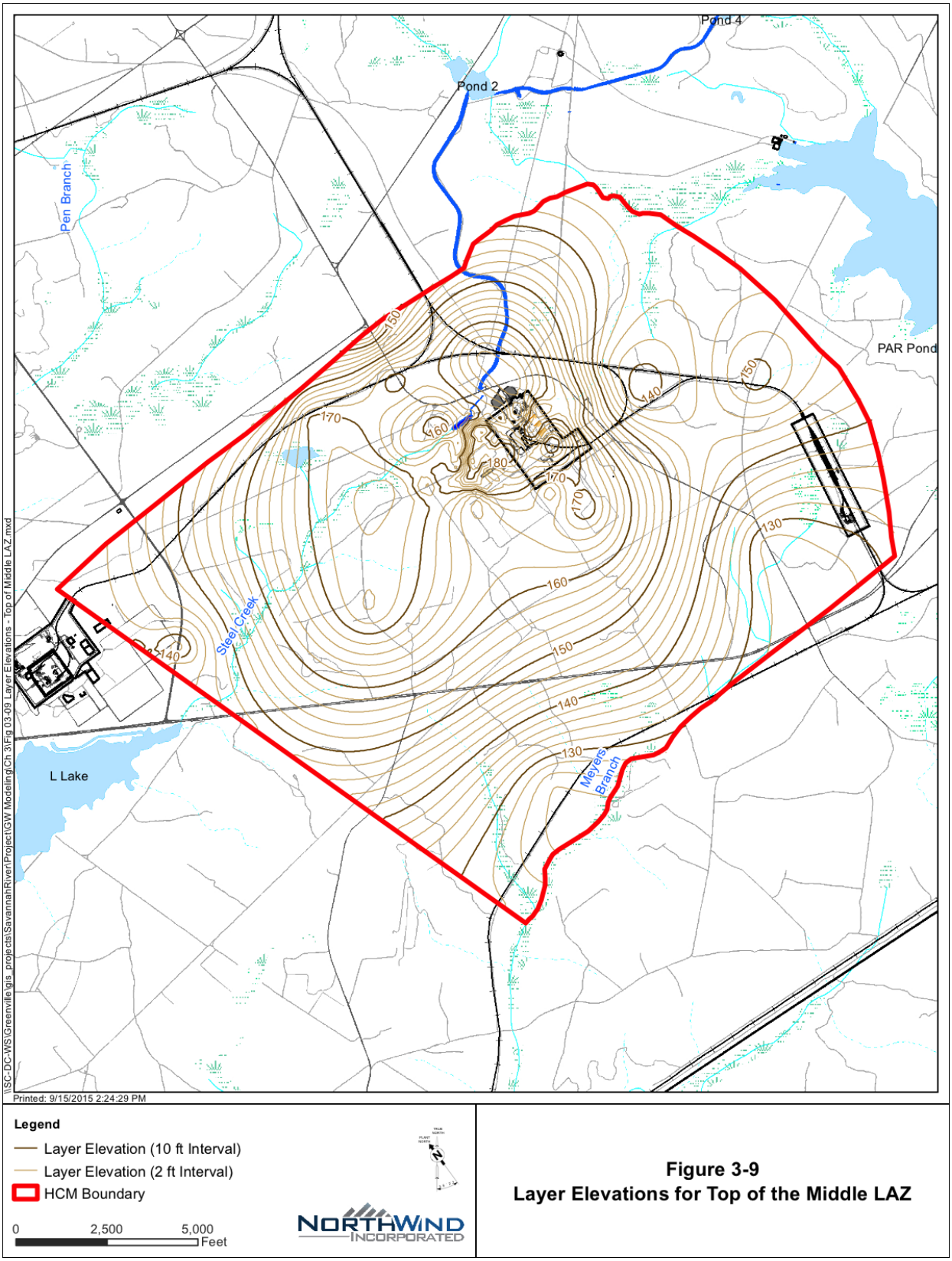


**Figure 3-9 Layer Elevations – Top of MC-LAZ**

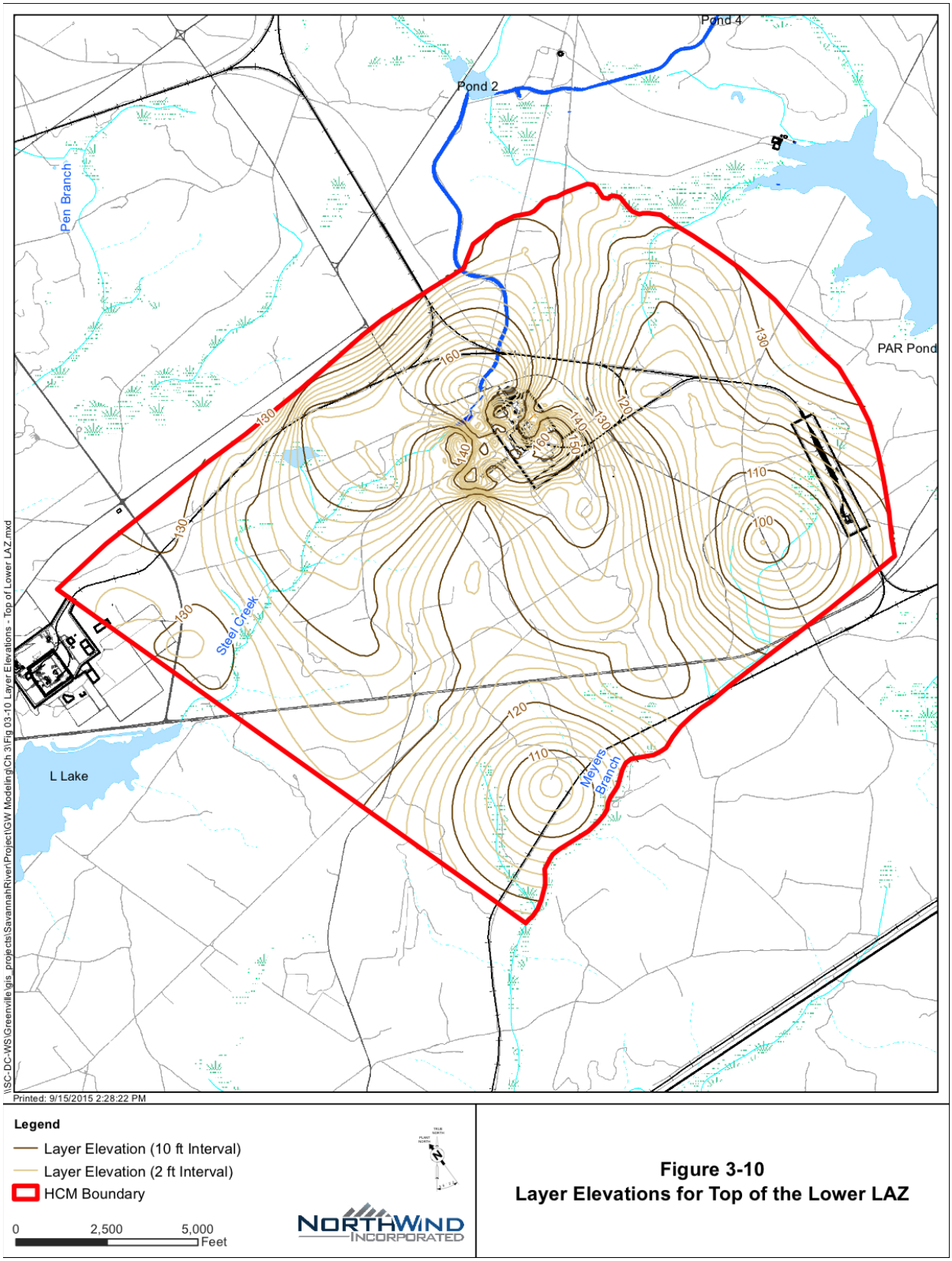


**Figure 3-10 Layer Elevations – Top of Lower LAZ**

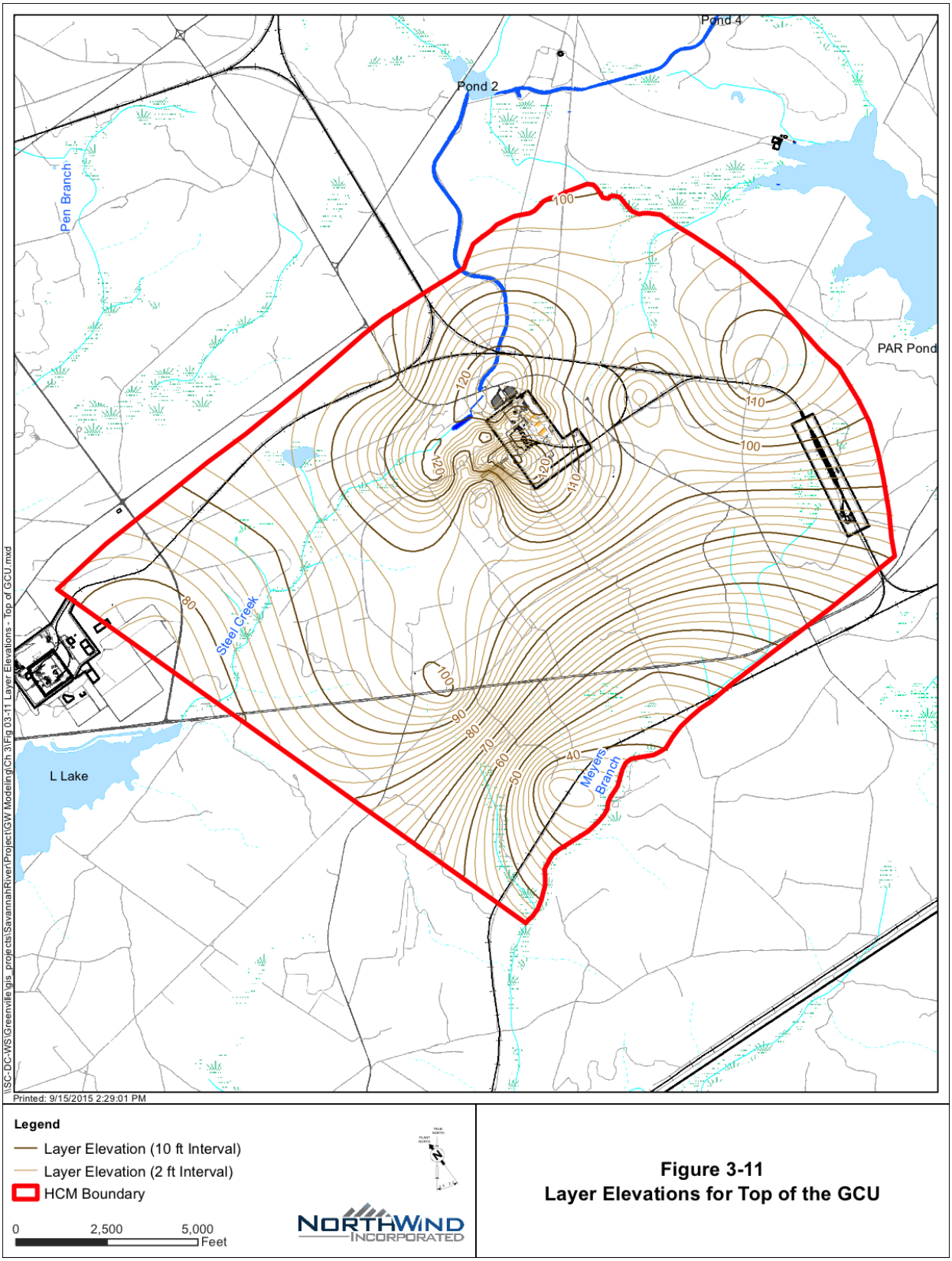


**Figure 3-11 Layer Elevations – Top of GCU**

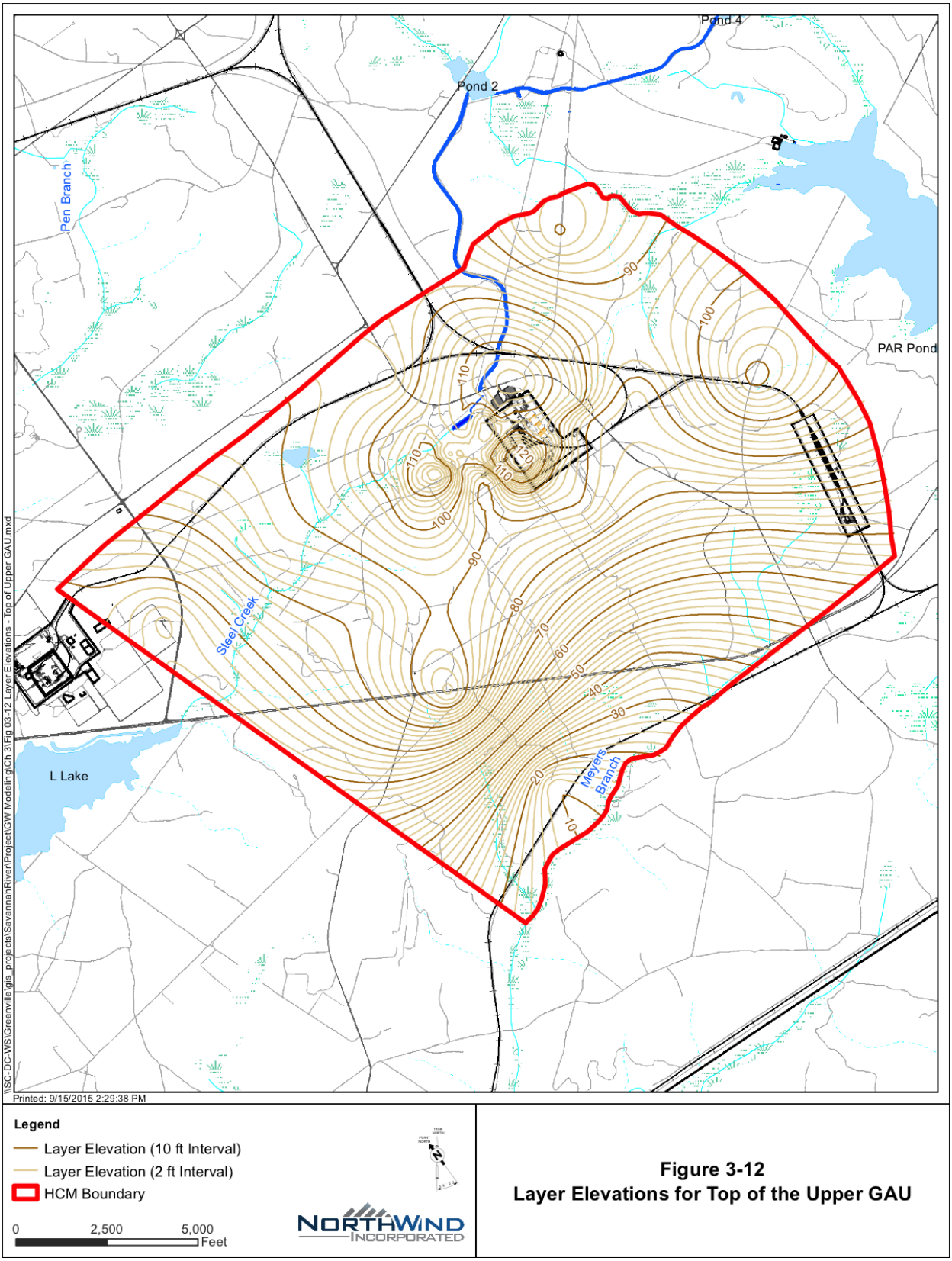


**Figure 3-12 Layer Elevations – Top of Upper GAU**

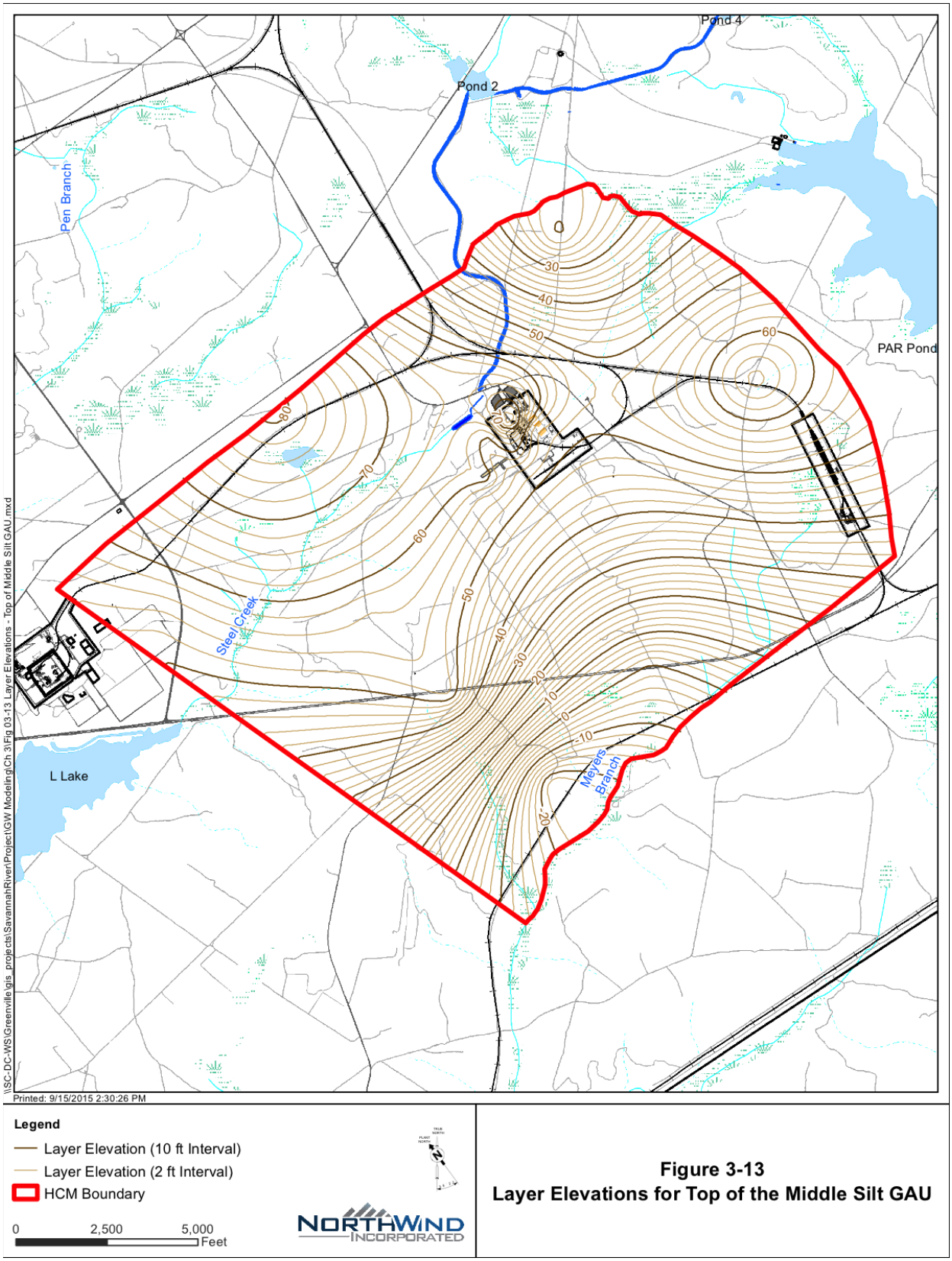


**Figure 3-13 Layer Elevations – Top of Middle Silt GAU**

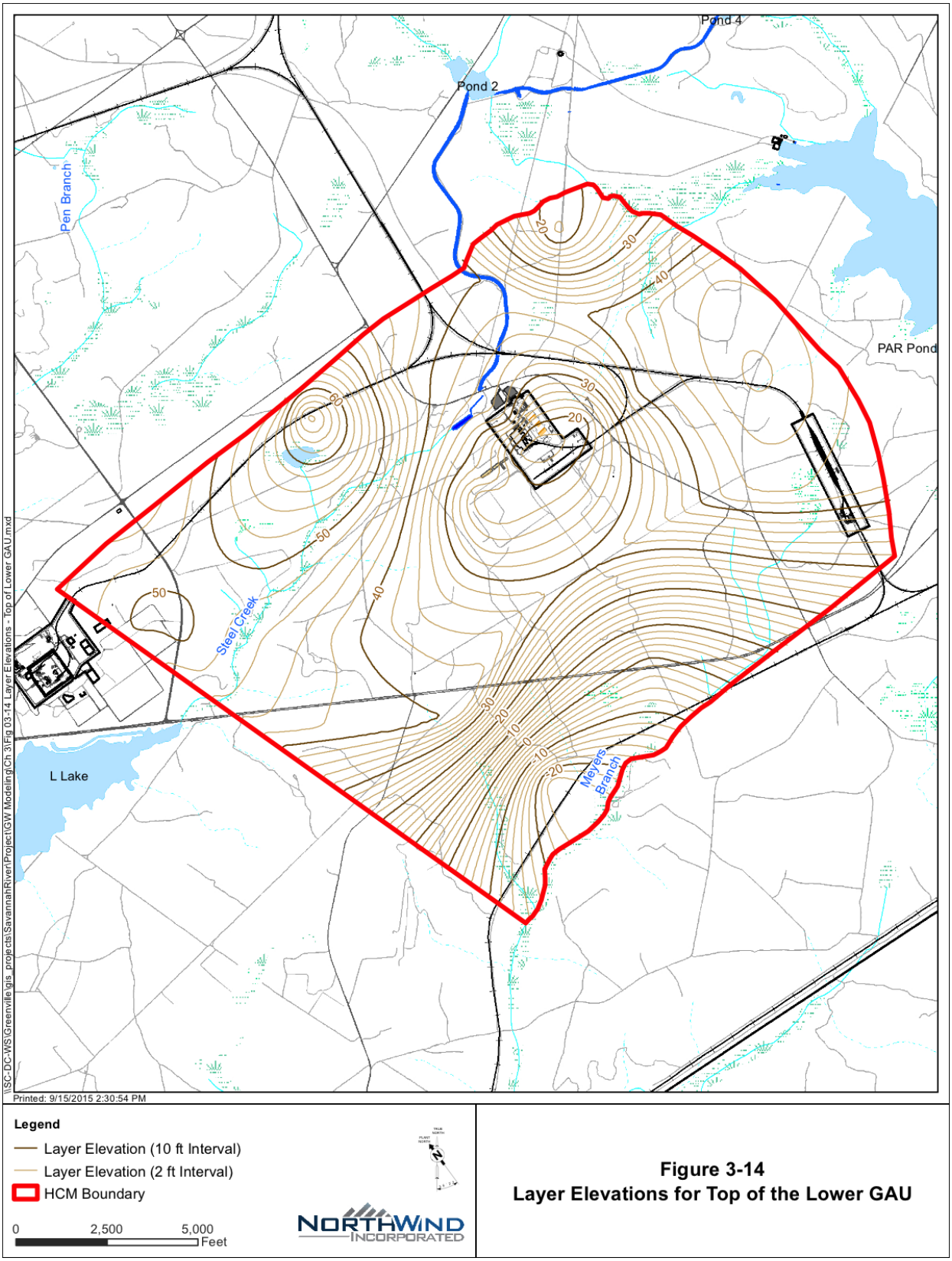


**Figure 3-14 Layer Elevations – Top of Lower GAU**

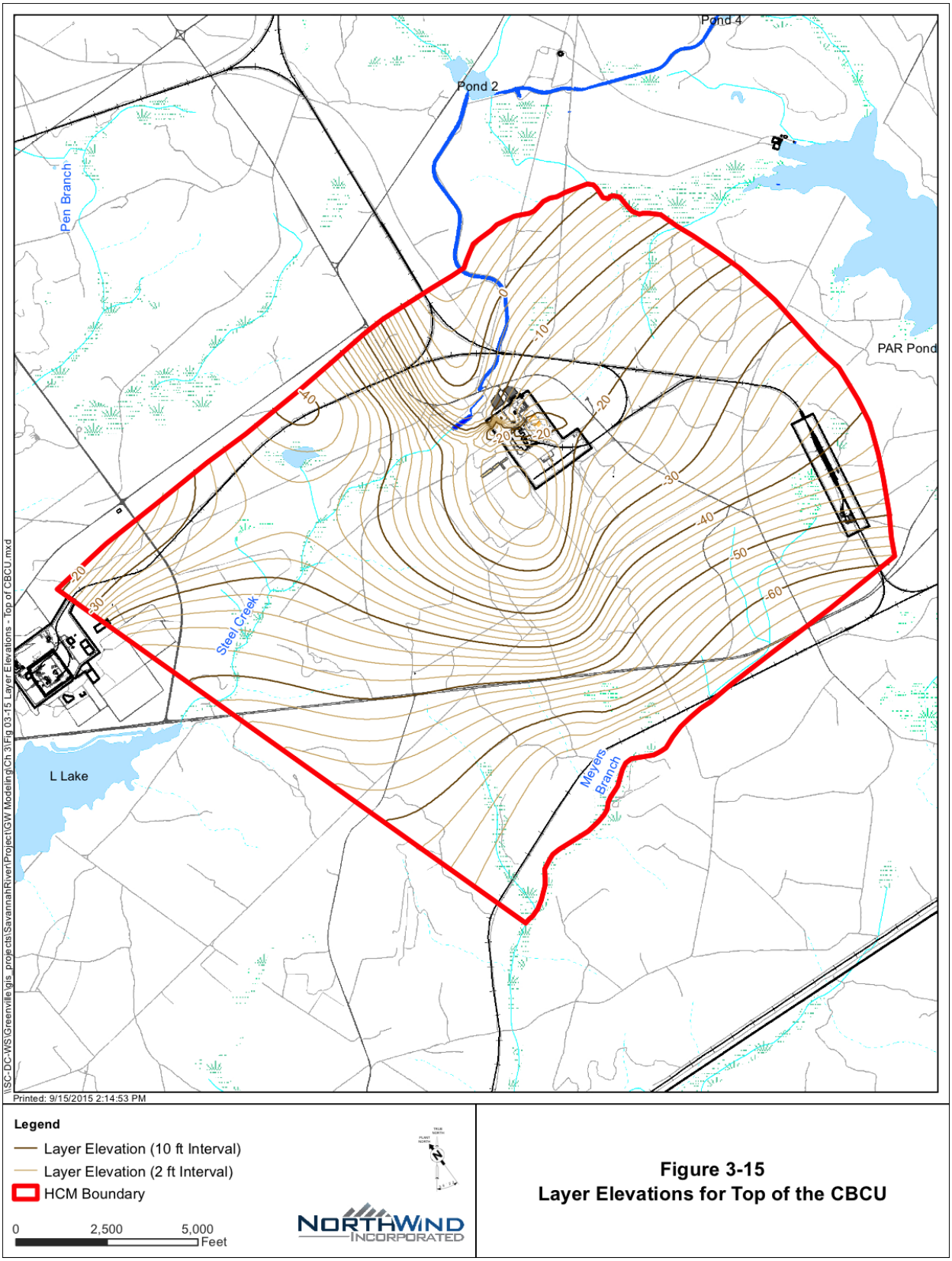


**Figure 3-15 Layer Elevations – Top of CBCU**

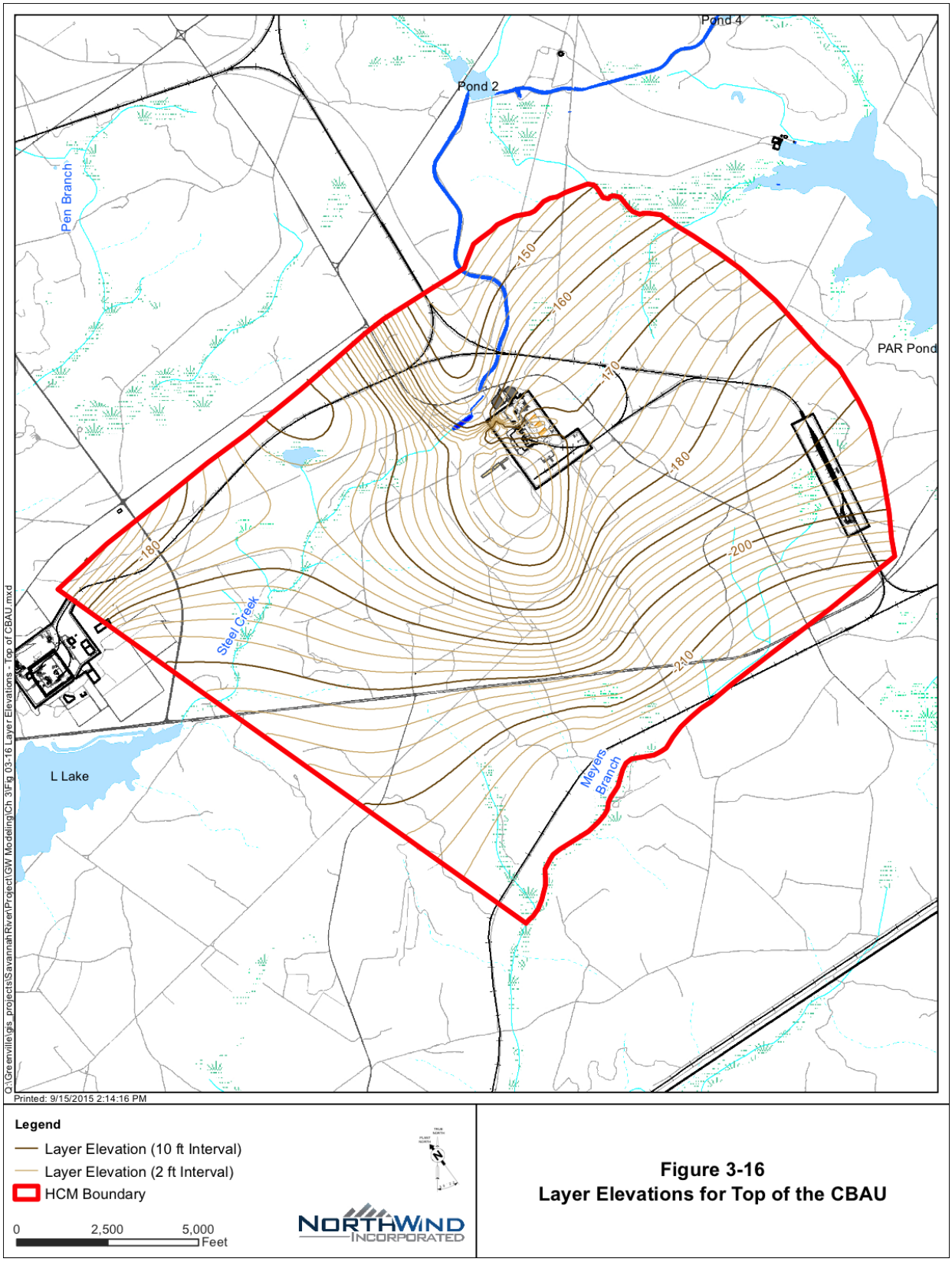


**Figure 3-16 Layer Elevations – Top of CBAU**

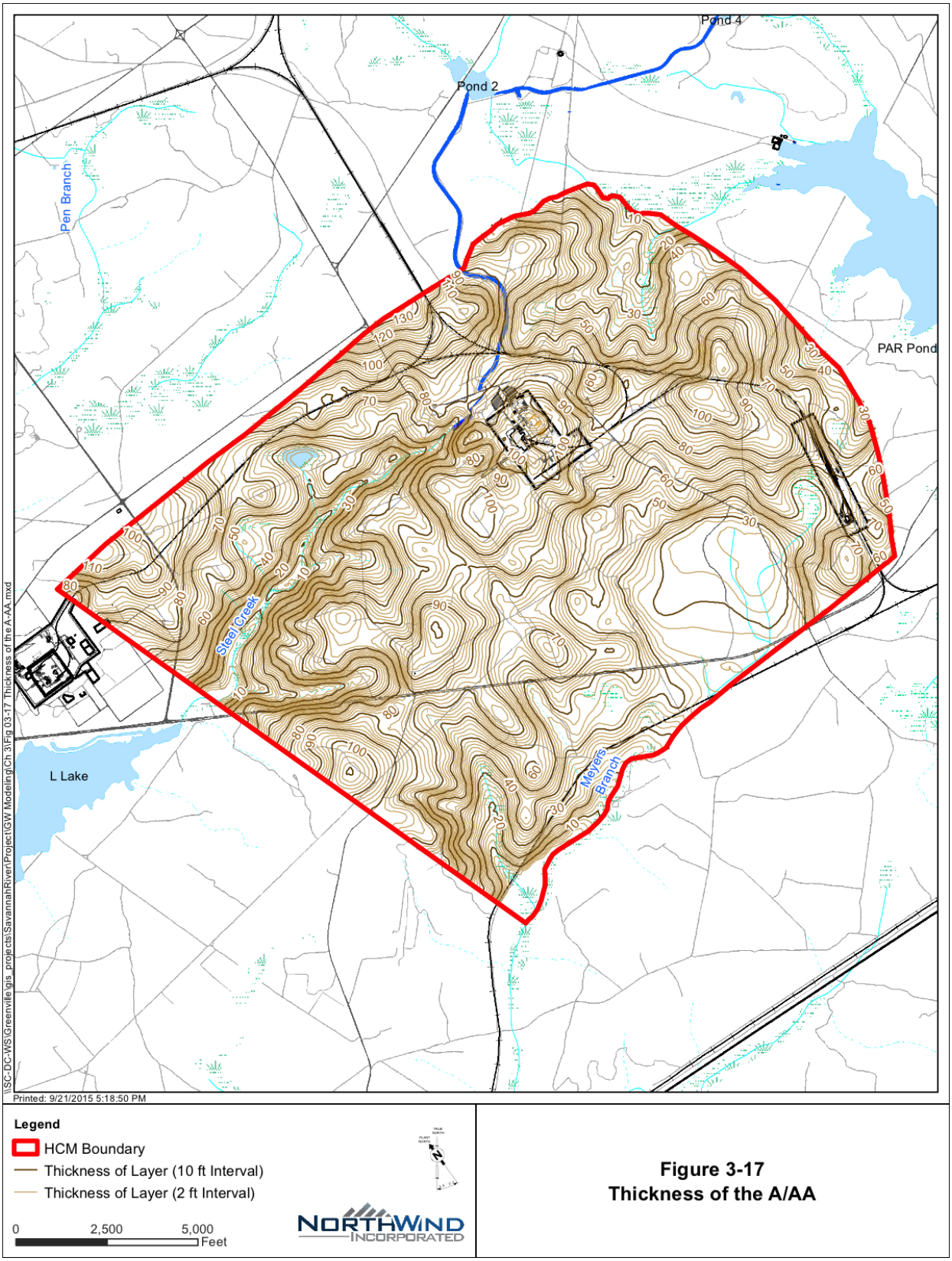


**Figure 3-17 Thickness of the A-AA**

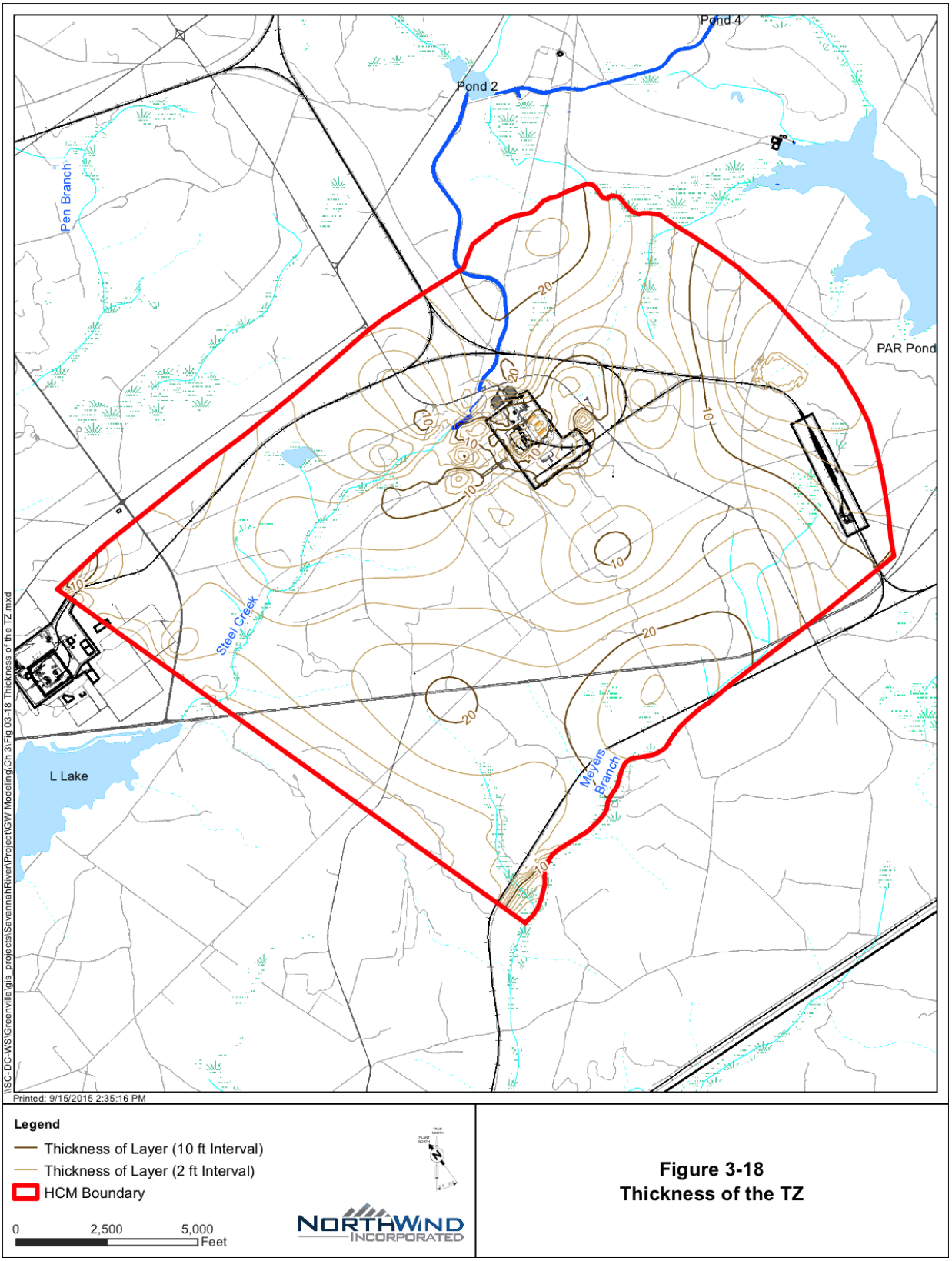


**Figure 3-18 Thickness of the TZ**

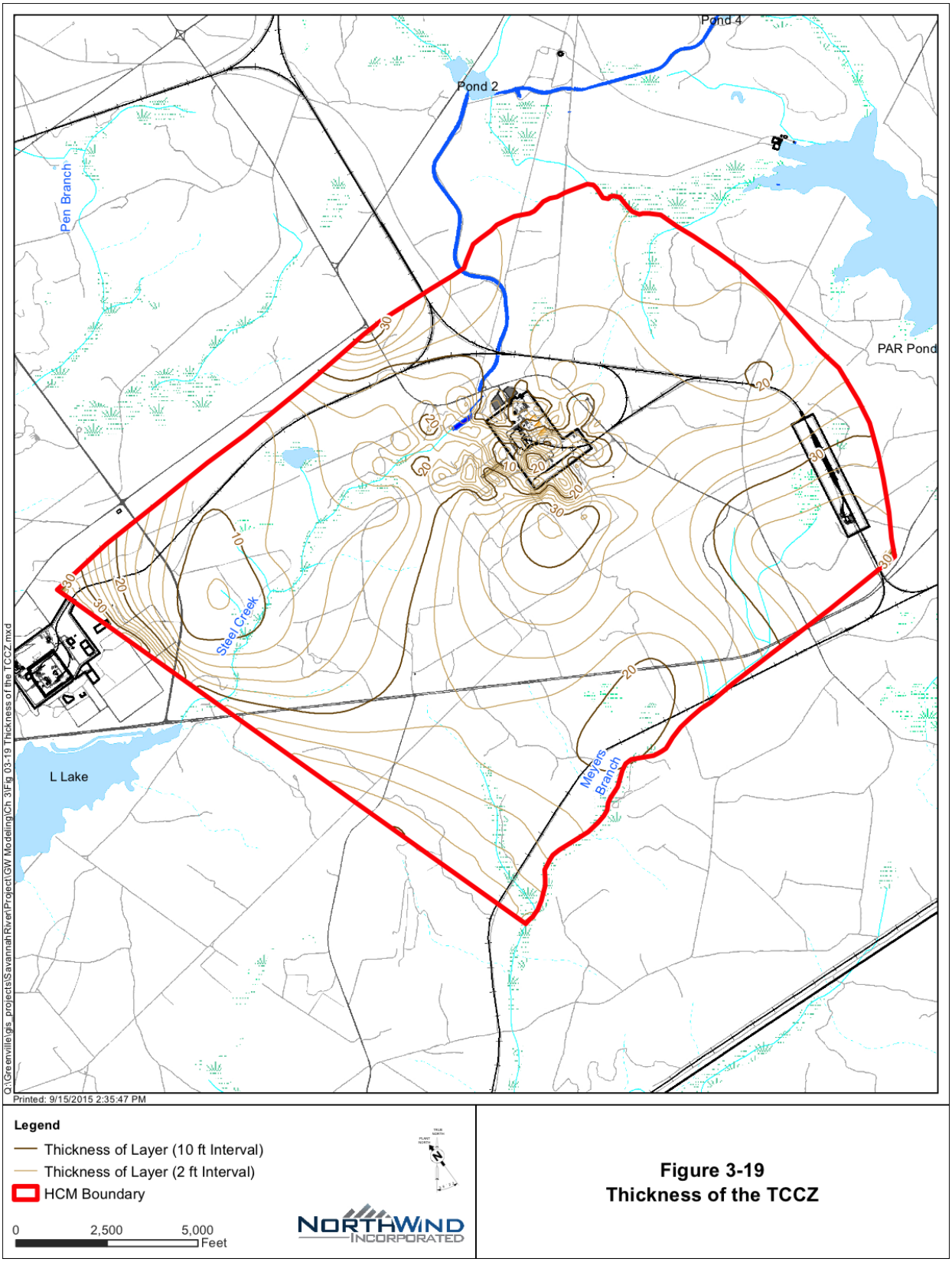


**Figure 3-19 Thickness of the TCCZ**

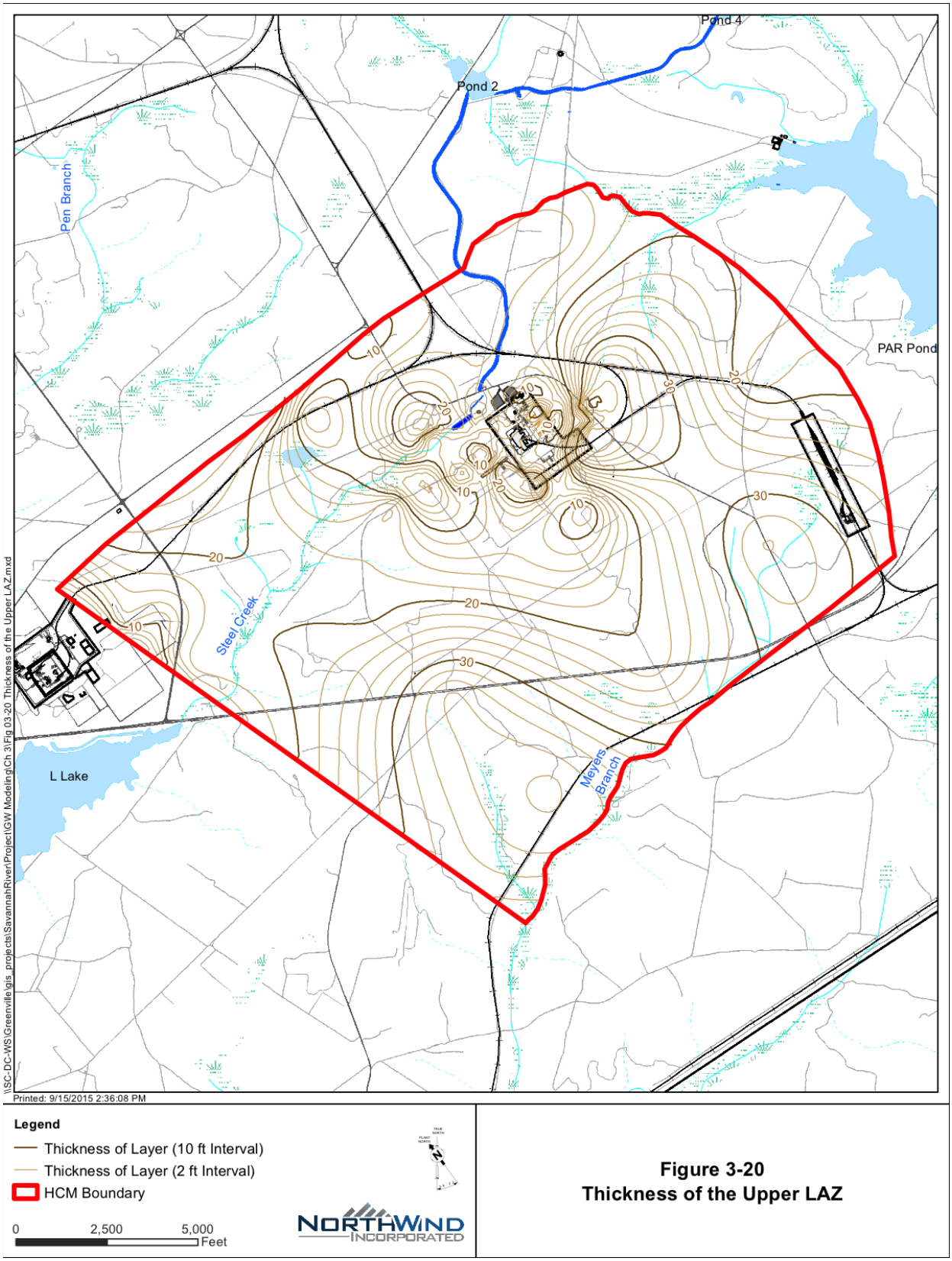


**Figure 3-20 Thickness of the Upper LAZ**

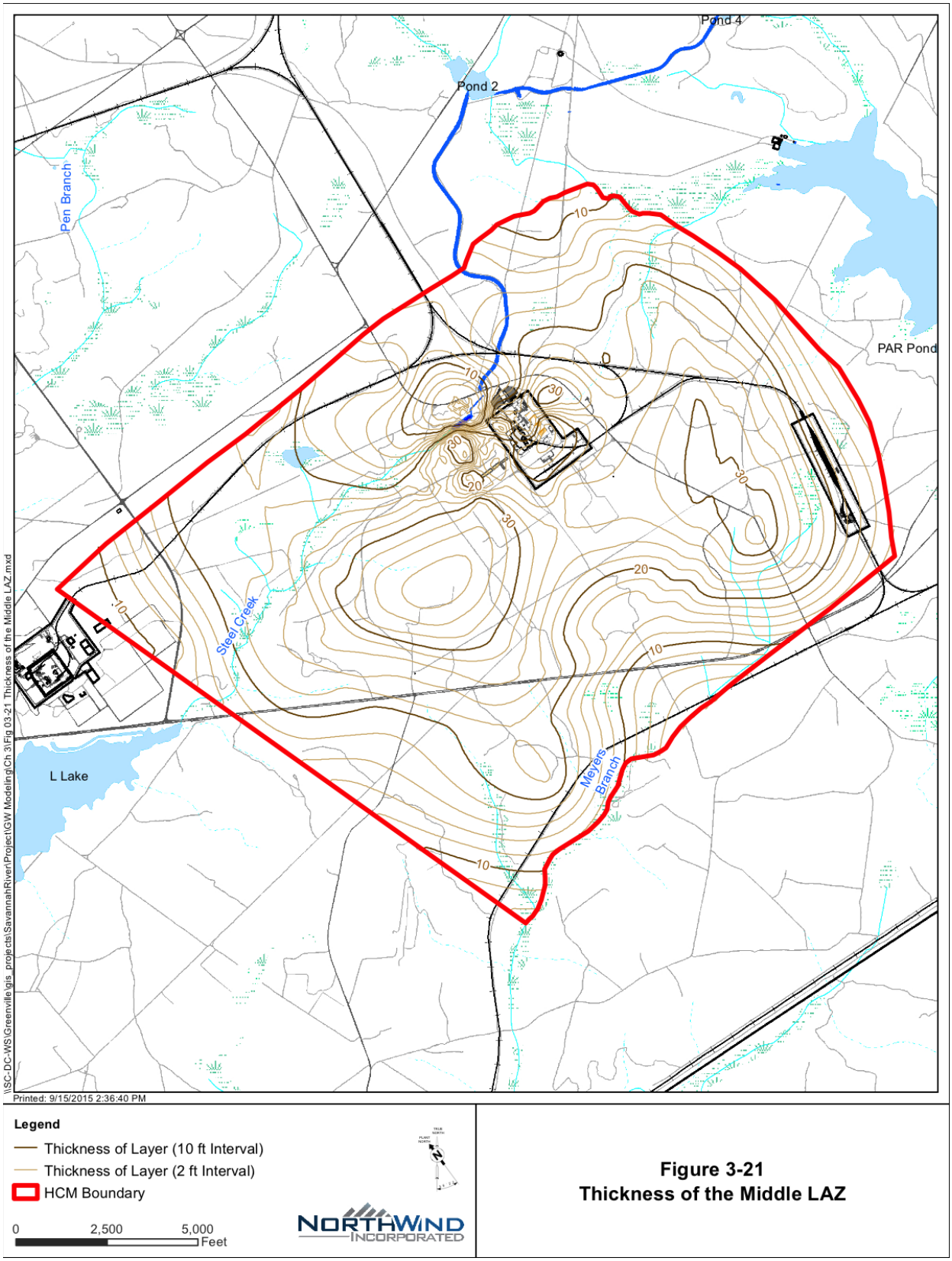


**Figure 3-21 Thickness of the Middle LAZ**

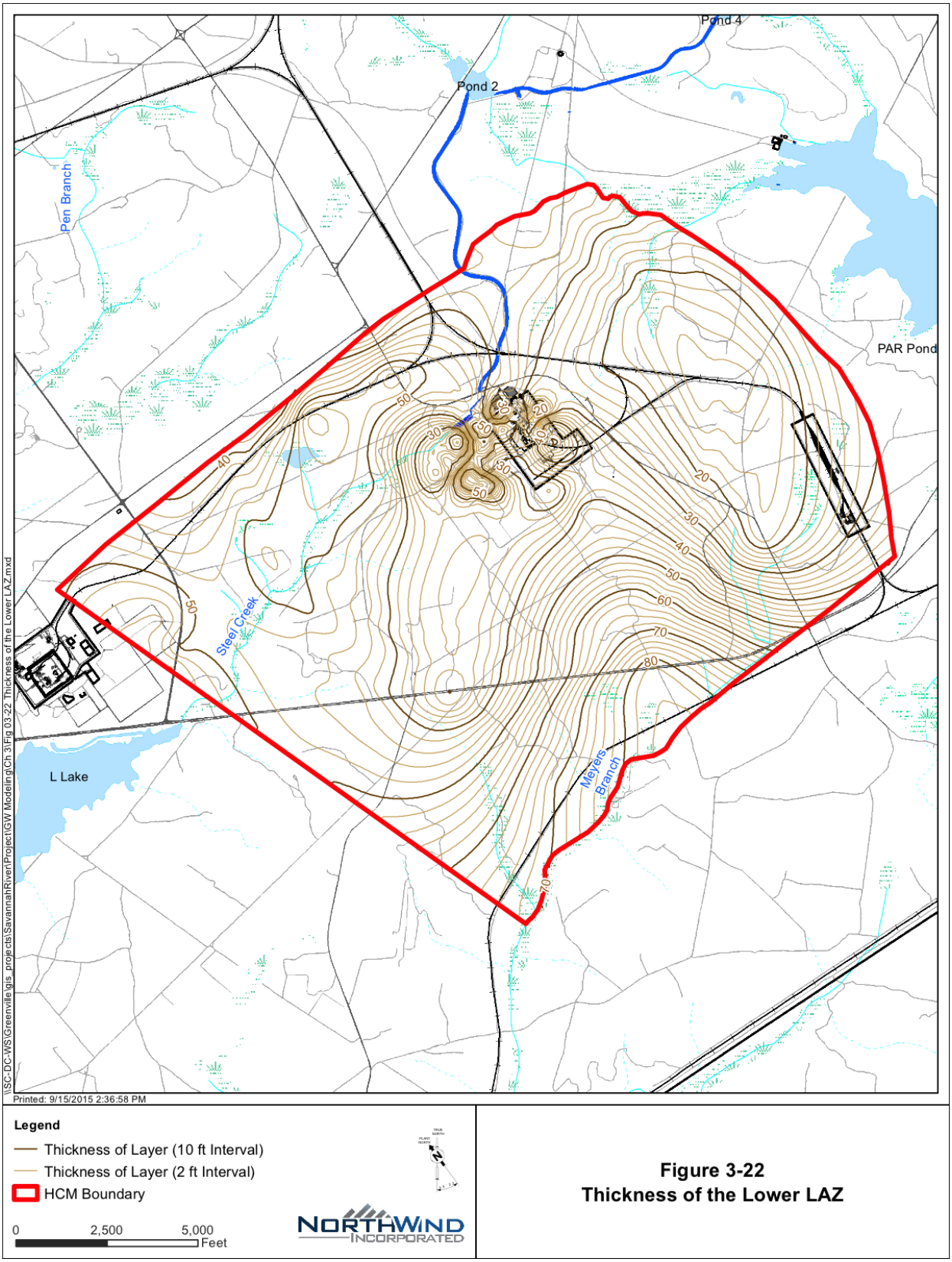


**Figure 3-22 Thickness of the Lower LAZ**

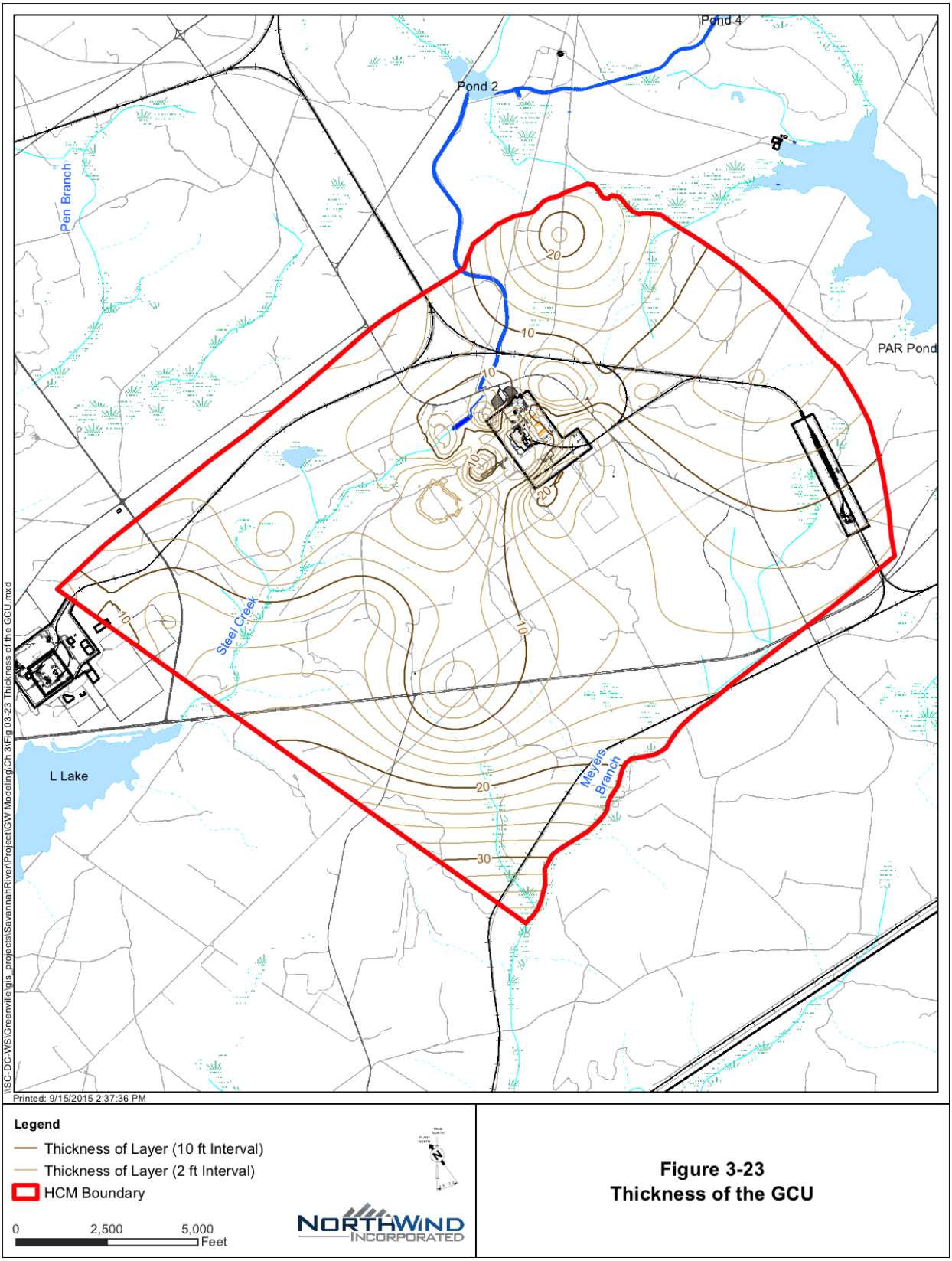


**Figure 3-23 Thickness of the GCU**

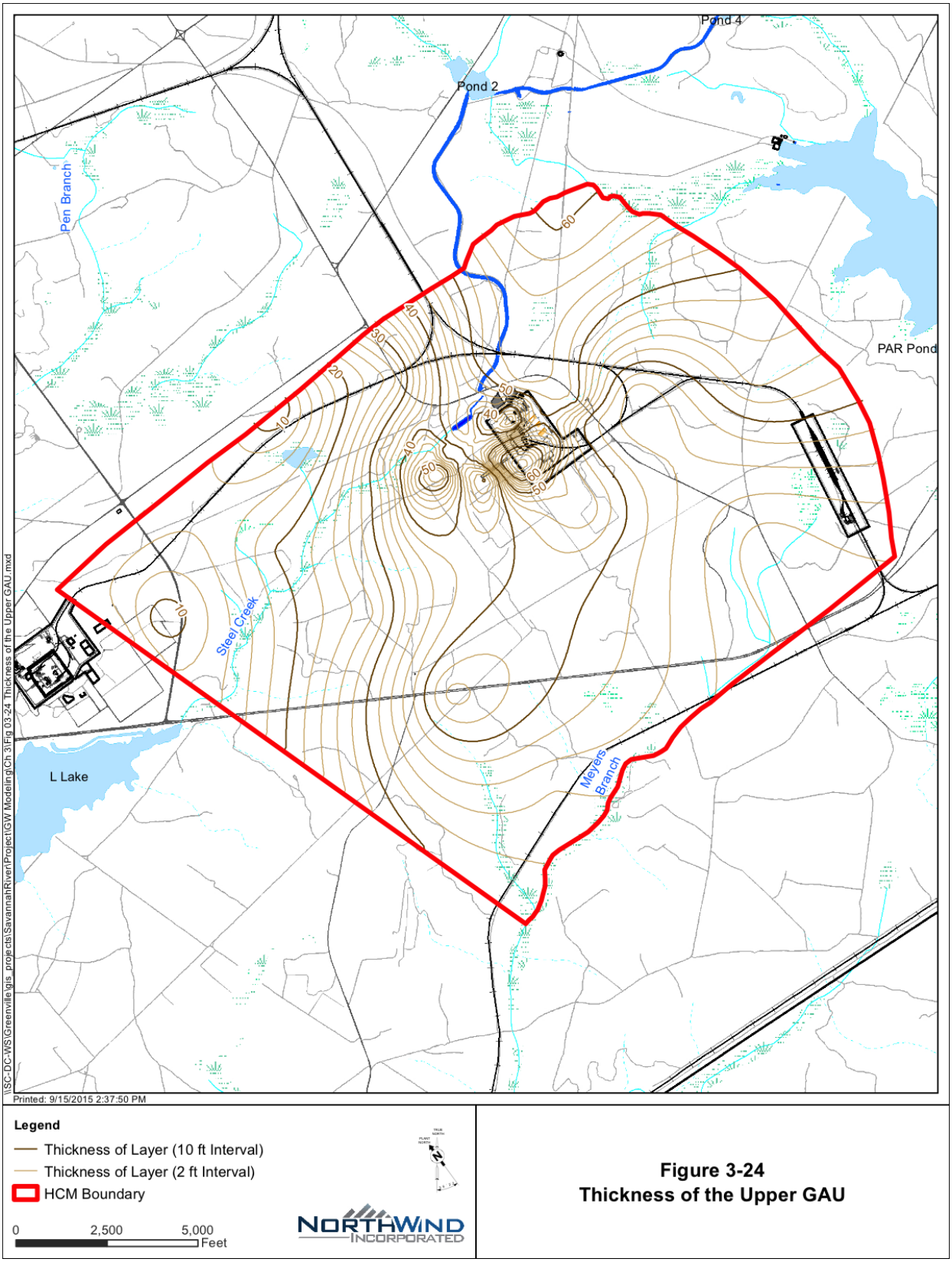


**Figure 3-24 Thickness of the Upper GAU**

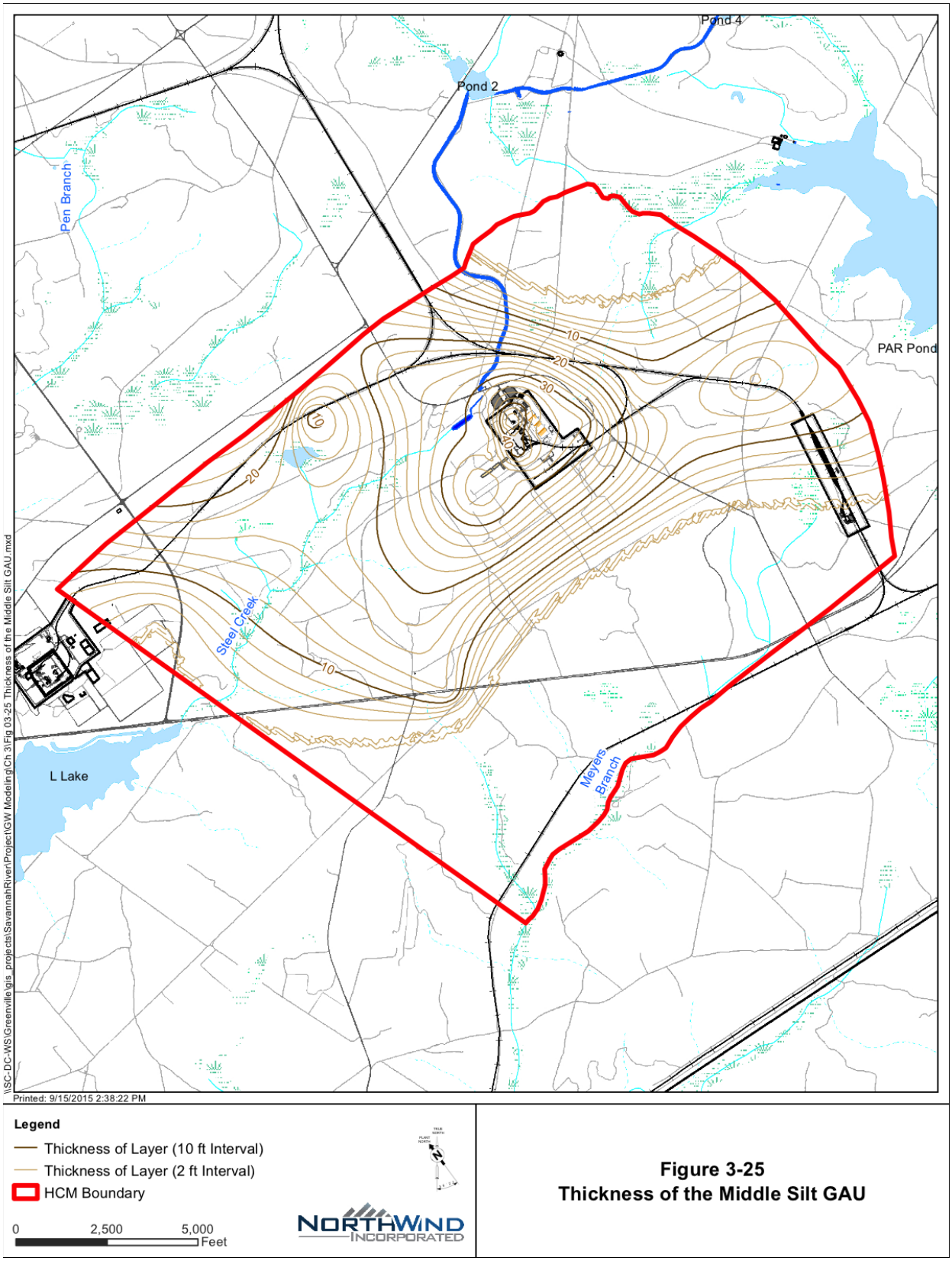


**Figure 3-25 Thickness of the Middle Silt GAU**

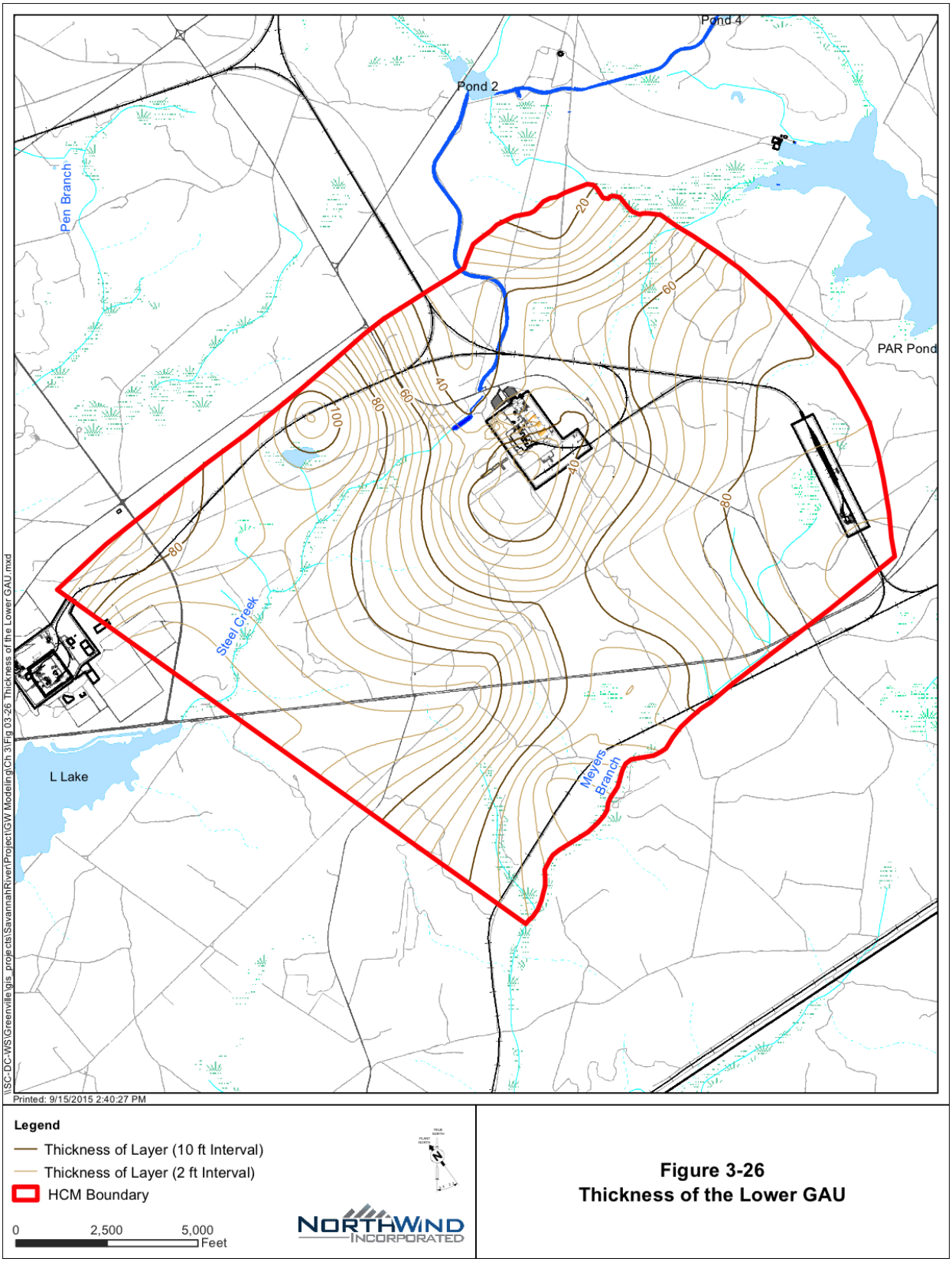


**Figure 3-26 Thickness of the Lower GAU**

**(This page intentionally left blank)**

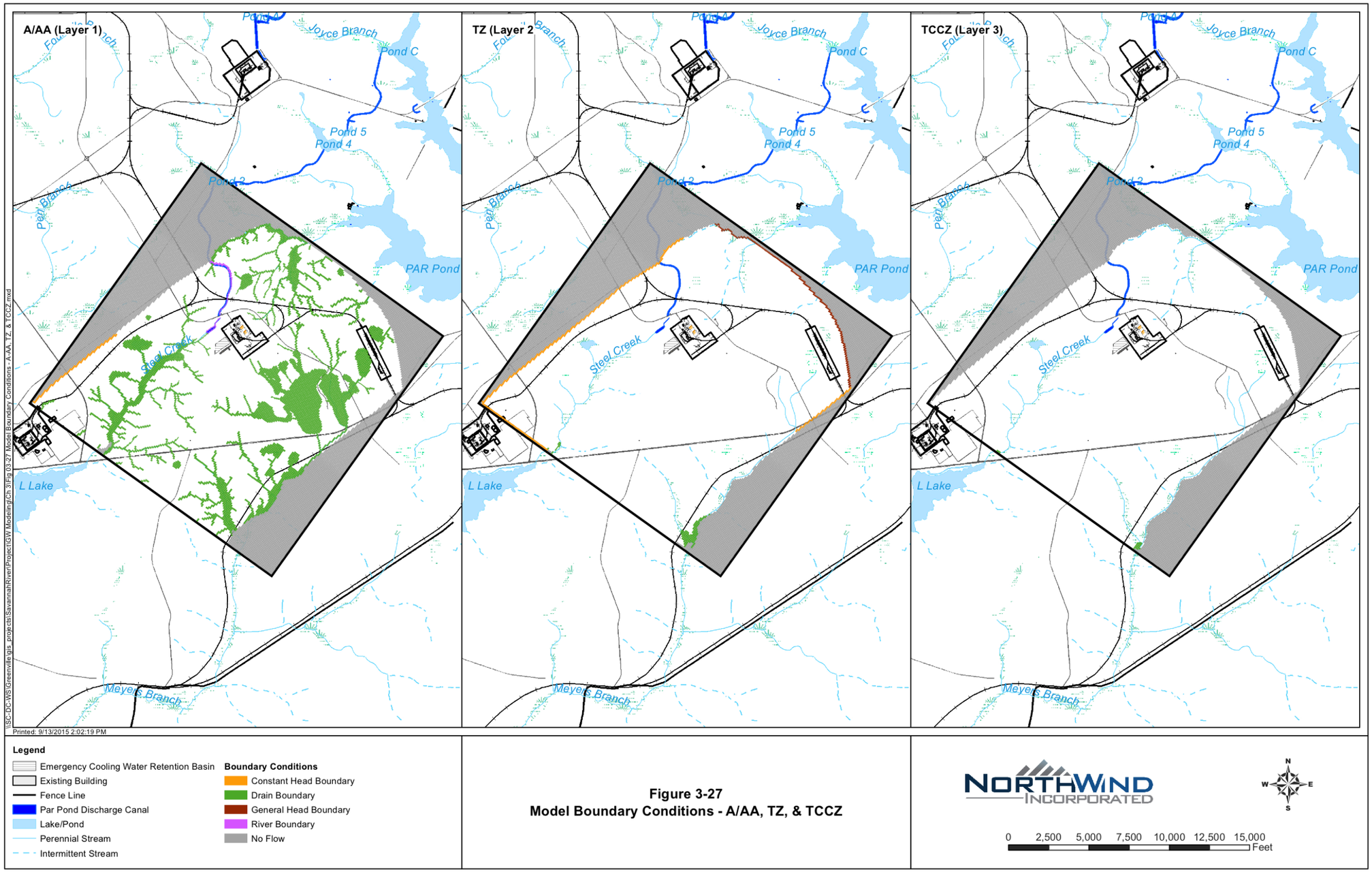


**Figure 3-27 Model Boundary Conditions: A/AA, TZ, and TCCZ**

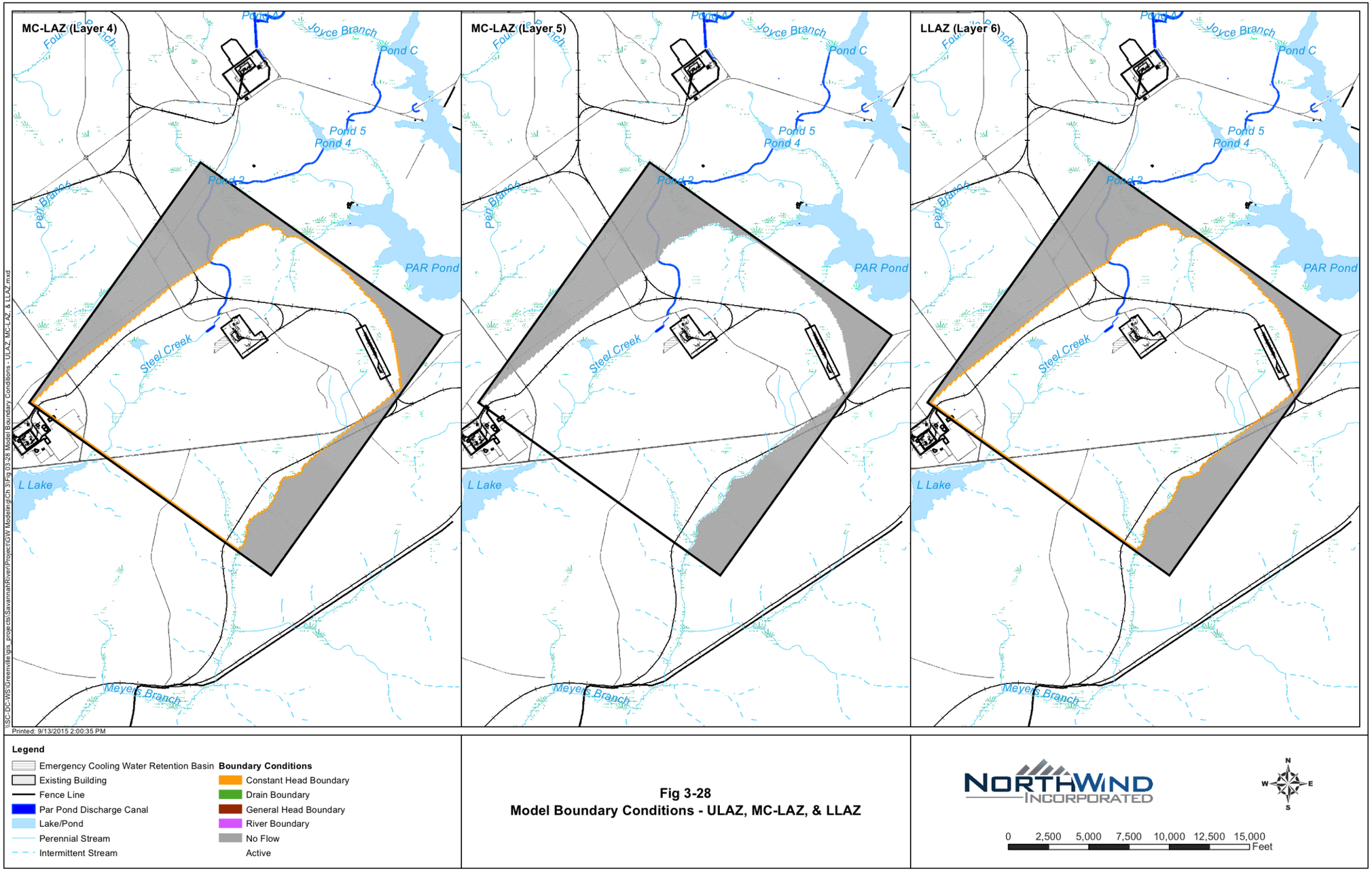


**Figure 3-28 Model Boundary Conditions: ULAZ, MC-LAZ, and LLAZ**

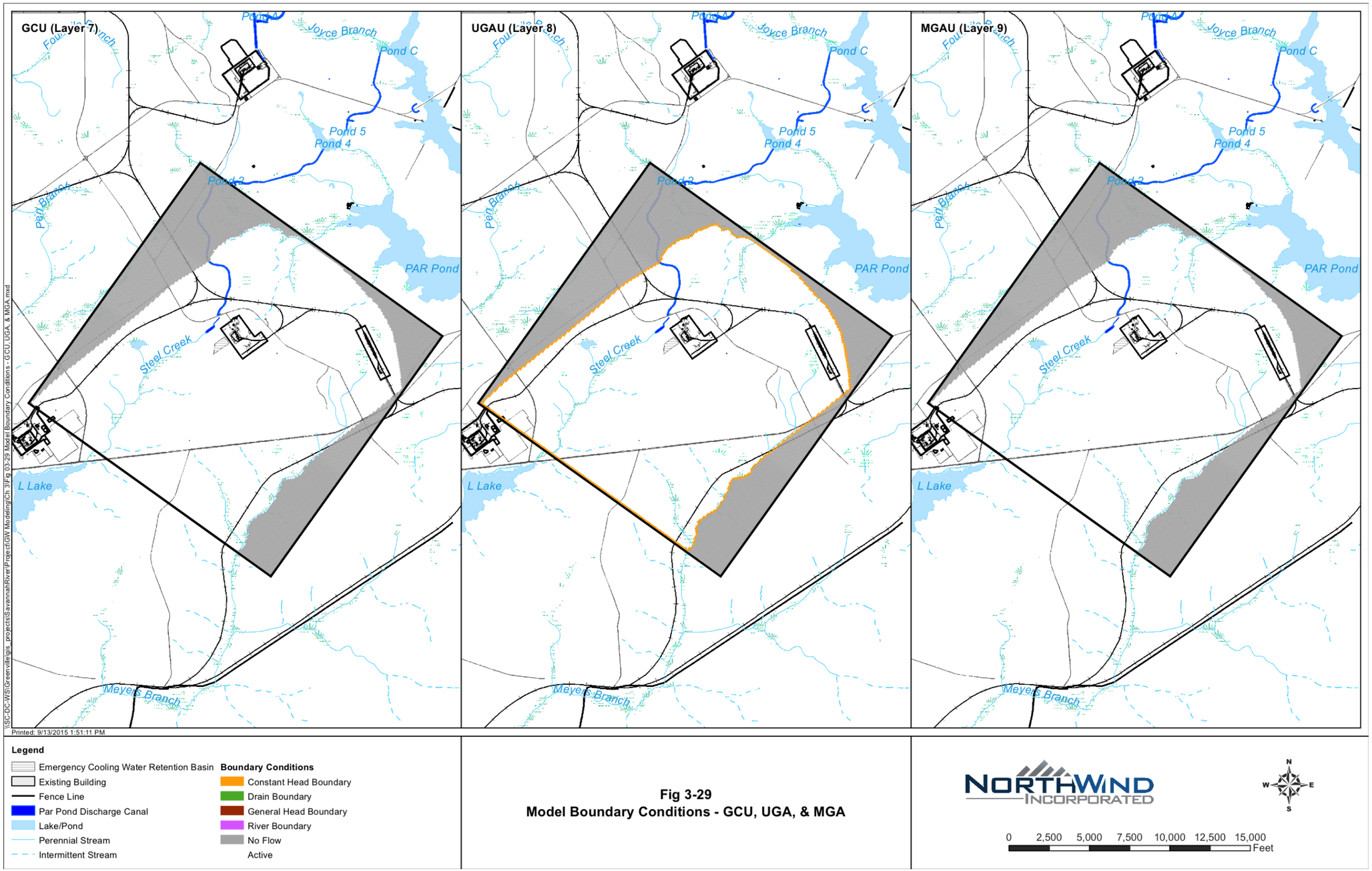


**Figure 3-29 Model Boundary Conditions: GCU, UGA, and MGA**

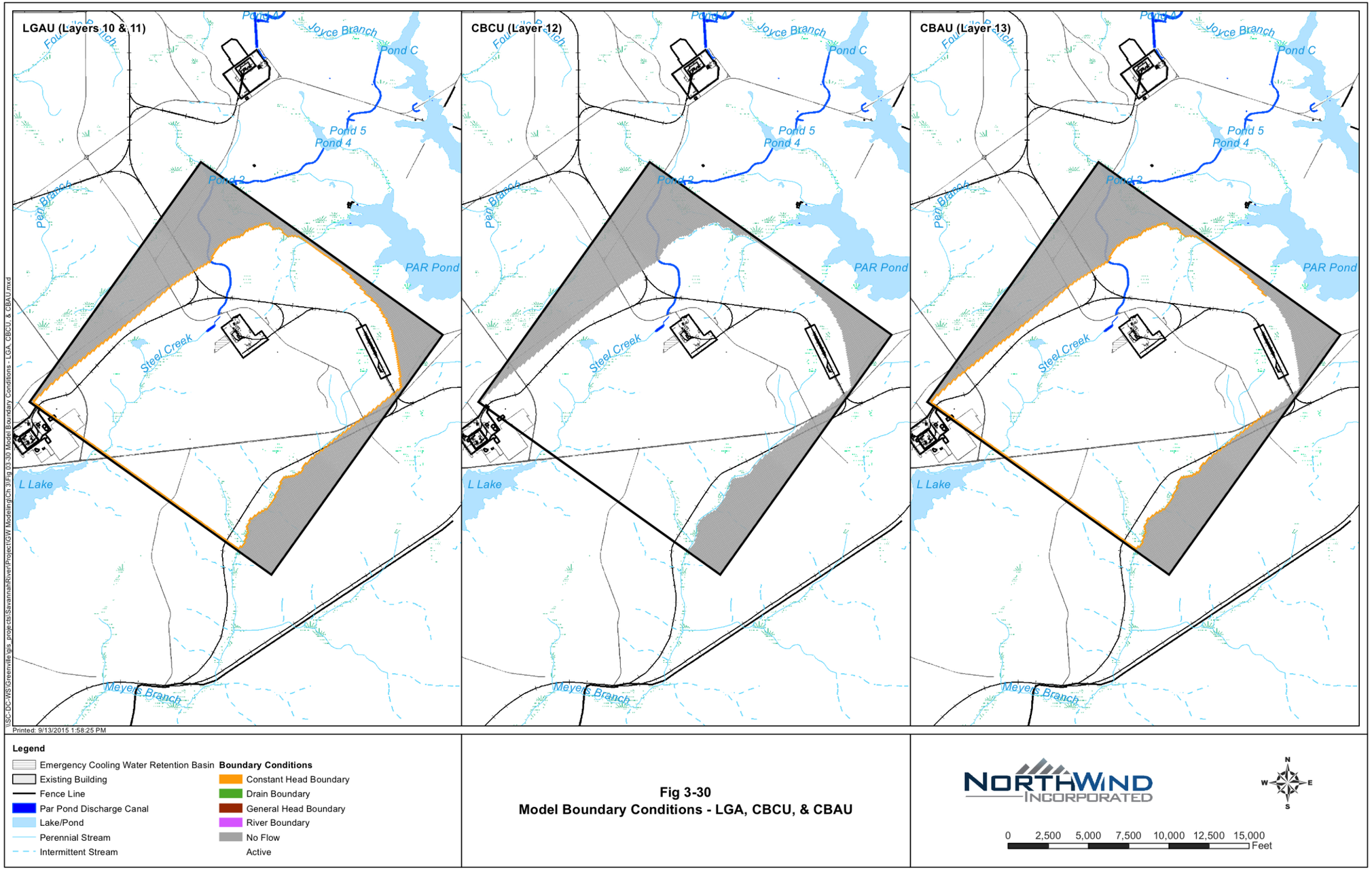


**Figure 3-30 Model Boundary Conditions: LGA, CBCU, and CBAU**

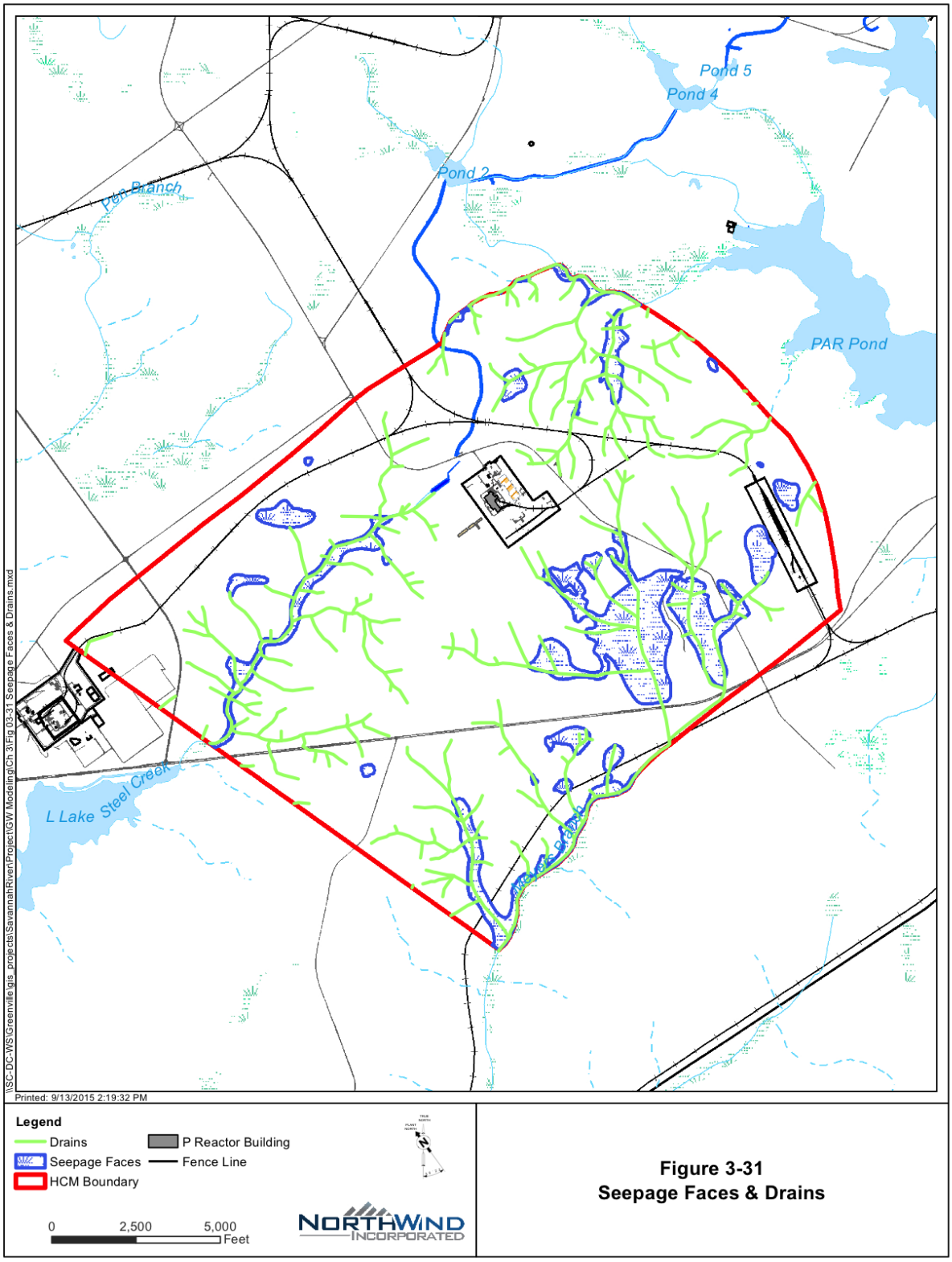


**Figure 3-31 Seepage Faces and Drains**

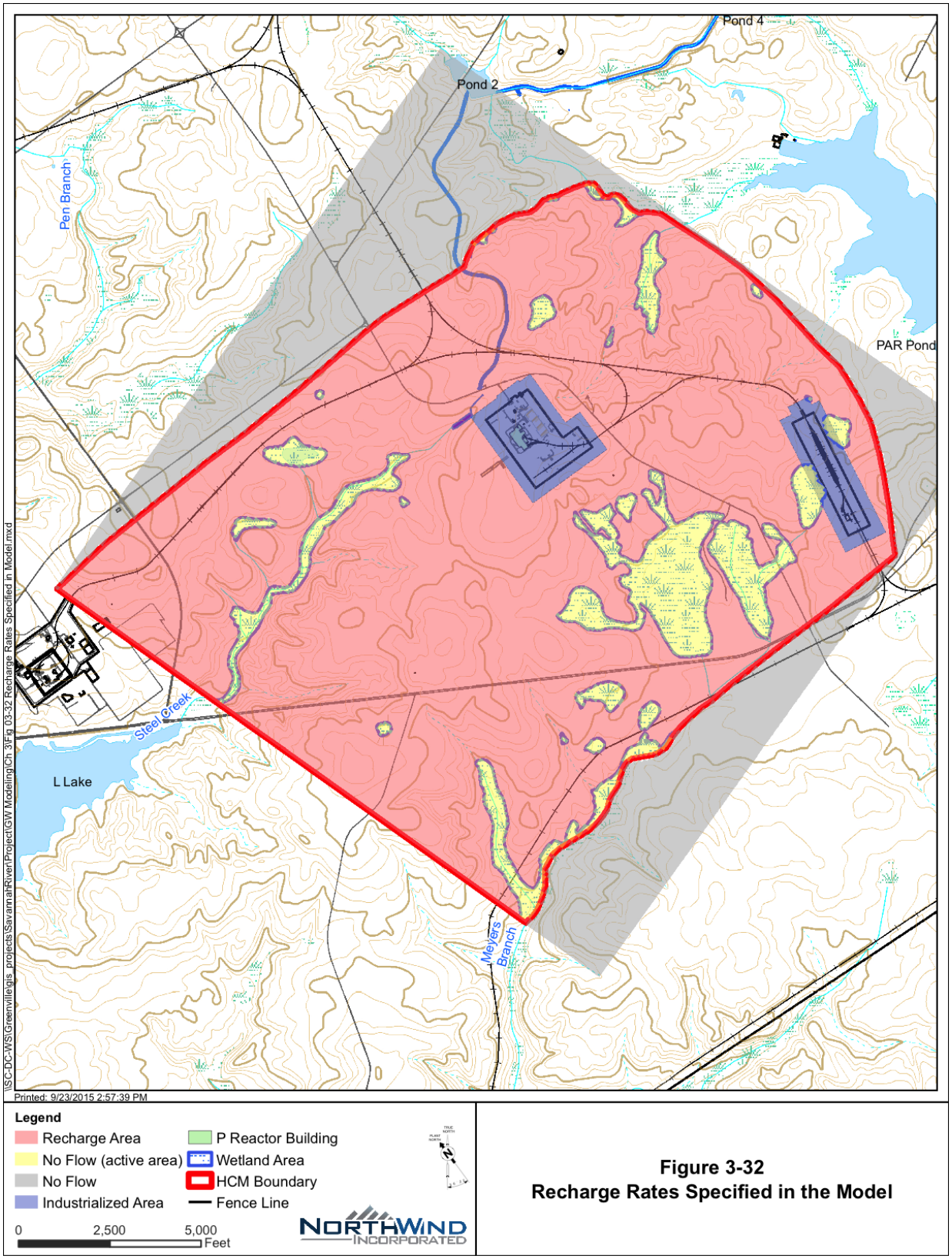


**Figure 3-32 Recharge Rates Specified in the Model**

# 4.0 MODEL CALIBRATION

This chapter describes the flow model calibration goals and results. Calibration improves consistency between modeled and observed conditions.

## 4.1 Calibration Goals

For each simulation, a head residual (or error) is computed for each head target (Section 2.6) by subtracting the observed head from the simulated head. The statistics for these residuals are then compared to commonly accepted criteria for groundwater flow model calibration. Specifically, a calibration is sought that has a mean error within 0.5 ft of zero and has a root-mean-square error (RMSE) less than 5% of the observed head range across the area of interest. For this model, the RMSE should be less than 5.5 ft to achieve this criterion (in the plume area, the maximum observed head is 282.0 ft and the minimum is 172.2 ft). The RMSE is calculated by squaring each residual, taking the mean of the squares, and then taking the square root of that mean (when the mean error is zero, the RMSE is the same as the standard deviation). Another measure of calibration quality is the mean absolute error (MAE), which is calculated as the mean of the absolute value of each residual. The MAE is less affected by extreme outliers. When the MAE is much lower than the RMSE, a few poorly matched head targets are having a large effect on the statistics.

## 4.2 Calibration Results

Calibration is accomplished by adjusting model parameters and boundary conditions from their assumed (initial) values, within reasonable limits, until the model matches observed conditions as well as possible. In this analysis, the main parameters are the horizontal and vertical hydraulic conductivities of the different aquifer zones and confining units.

Figures 4-1 through 4-3 show the hydraulic conductivity zones for model layers 1 through 11, as defined during calibration. Horizontal hydraulic conductivities in the UGA, LGA, CBCU, and CBAU were set to one value throughout the model domain at 75, 15, 0.1, and 25 ft/day, respectively. Vertical hydraulic conductivities in the UGA, LGA, CBCU, and CBAU were set to one value throughout the model domain at 0.075, 0.0015, 0.001, and 0.25 ft/day, respectively.

Specification of zones in the A/AA and TZ layers improved calibration of A/AA and TZ targets near Steel Creek and PAR Pond. The triangular zone of higher conductivity in the TCCZ corresponds to a similar zone found in the L-Area model (GeoTrans 2004) that was added to improve calibration of that model. Zones in the LAZ and GCU were used to create the mounding and steep gradients found in the LAZ. This resulted in much of the GCU having a vertical conductivity lower than the values presented for the GCU in Table 3-2. The hydraulic heads on the model boundary were also adjusted during calibration to reproduce observed conditions. Adjustments were made by extrapolating trends from head targets near model boundaries to the boundary. Through a trial-and-error process, the model was adjusted until a final RMSE of 3.40 ft was achieved, which is 3.1% of the range in measured water levels (Table 4-1) and is consistent with the calibration goal of 5.5 ft or less. The mean error of +0.45 ft is below the target mean error of ±0.5 ft.

Figures 4-4 through 4-11 show the modeled head contours in the aquifer zones along with head residuals at individual targets. Modeled versus observed head is shown in Figure 4-12. The figure shows a reasonable match without bias. A histogram of residuals is shown in Figure 4-13. Residuals were within 12 ft for all 133 head targets, with a normal distribution.

**Table 4-1 Head Calibration Statistics**

| Statistic | Value |
|---|---|
| Number of Head Targets | 133 |
| Mean Error (ft) | 0.45 |
| Mean Absolute Error (ft) | 2.56 |
| Root Mean Square Error (ft) | 3.40 |

The overall water budget for this model is shown in Figure 4-14. Table 4-2 summarizes the water balance for various stream segments and includes all drains (wetlands) feeding those stream segments. Segment SC-02 includes both the drain cells and the river cells of the canal that drain towards SC-02. Total Canal comprises the flux to the river cells that drain towards PAR Pond.

**Table 4-2 Water Balance Summary for Stream Segments**

| Stream Segment | Groundwater Flux to Stream Segment (cfs) |
|---|---|
| SC-02 | 0.03 |
| SC-03 | 0.10 |
| SC-04 | 0.56 |
| Total Steel Creek | 3.16 |
| Total PAR Pond | 0.40 |
| Total Meyers Branch | 2.07 |
| Total Canal | 0.07 |

cfs = cubic feet per second.

A particle tracking analysis was completed to assess the flow model's ability to predict plume movement. The analysis was conducted by releasing particles from twelve locations as shown in Figures 4-15 and 4-16. The twelve locations were selected based on the probable source locations of the COCs (tritium, PCE, and TCE) as well as the observed maximum concentration locations in the vicinity of P Area. It is important to note that particle tracking includes only the effects of advection flow and neglects dispersion, sorption, and degradation. The results of this particle tracking show the future flow path of contamination from the twelve source locations. The particle tracks correlate with the location of the historical plumes to the southwest of the reactor area and indicate that plumes sourced northeast of the reactor area will discharge to PAR Pond. The results indicate that the contaminants from north of the P-Reactor Building (source of tritium and CVOCs) and southwest and south of the Emergency Cooling Water Basin (source of tritium at the PRSB) travel towards Steel Creek. Times shown are for when the particle first reaches a boundary condition (drain or constant head). Figure 4-16 shows a profile view of the forward particle tracks from the vertical plane of section A-A' (see Figure 4-17). As can be seen from this figure, generally, particles placed in A/AA within the P-Reactor Building area travel vertically downward at a much slower velocity into ULAZ then travel at a much faster rate to the eastern model boundary. The GMS particle tracking program has the particles enter constant

head cells in the ULAZ, then exit and travel vertically through to the general head boundary in the TZ. Particles placed in A/AA away from, and west of P-Reactor Area travel vertically downward into TZ then travel west through TZ and discharge into Steel Creek and the P-Area Reactor Discharge Canal. The current model does not depict plume depths that match actual measurements. The reasons for this flow include higher recharge at the seepage basin during operation or from old production well conduits in the area.

### *4.2.1 Calibrated Values for Model Parameters*

The aquifer parameters of the calibrated flow model are listed in Table 4-3. This model is considered to be a calibrated model and meets the criteria for developing a calibrated flow model. Table 4-3 also lists some of the transport parameters that are used for developing the transport models presented in Chapter 6.0.

**Table 4-3 Aquifer Parameters for the Calibrated Model**

| Parameter | Value |
|---|---|
| Hydraulic Conductivity ($K_h/K_v$ ft/day) | See Figures 4-1 through 4-3<br>Upper Gordon Aquifer Unit (75/0.075)<br>Lower Gordon Aquifer Unit (15/0.0015)<br>Crouch Branch Confining Unit (0.1/0.001)<br>Crouch Branch Aquifer Unit (25/0.25) |
| Effective Porosity | 0.3 |
| Upland Recharge Rate | See Figure 3-32 |
| Creek Drain Conductance | 200 $ft^2$/day |
| Seepage Area Drain Conductance | 100 $ft^2$/day |
| Canal River Conductance | 100 or 500 $ft^2$/day |

## 4.3 Flow Model Sensitivity Analysis

Sensitivity analysis is performed on groundwater models to assess the effects of parameter, boundary condition, or conceptualization uncertainty on the calibrated results. The procedure generally involves changing a single aspect (parameter, boundary condition, etc.) of the model

by a pre-determined amount (usually within a reasonable range of certainty) and comparing the result to the calibrated model. This procedure is repeated several times where independent changes are made to assess low and high ranges of uncertainty for a suite of parameters.

The process of calibrating a model involves making independent changes and noting the result; consequently, the analyst has an indication of model sensitivity prior to performing the formal sensitivity analysis that is documented. During the model calibration, hydraulic conductivity was identified as a key element of the model. In this study, a formal flow-model sensitivity analysis on hydraulic conductivity and recharge was conducted.

The sensitivity of the flow model to horizontal ($K_h$) and vertical ($K_v$) hydraulic conductivity changes was comprehensively evaluated by making simulations with perturbations (factors of 0.8 and 1.2, minimum and maximum expected values from Table 3-2) to individual hydrostratigraphic layers and comparing the key model calibration statistics for each sensitivity simulation to those of the calibrated model. These results, shown in Table 4-4, indicate that the model is most sensitive to changes in hydraulic conductivity in the following units: A/AA, TZ, TCCZ, and ULAZ, as well as recharge.

**Table 4-4 Results of the Flow Calibration Sensitivity Analysis**

| Unit | Base Kh | Base Kv | Kv/Kh | Multiplier | Kh | Kv | ME | MAE | RMS |
|---|---|---|---|---|---|---|---|---|---|
| A/AA Z1 | 15 | 0.15 | 0.01 | 0.8 | 12 | 0.12 | 0.56 | 2.58 | 3.43 |
| | 15 | 0.15 | | 1.2 | 18 | 0.18 | 0.35 | 2.54 | 3.39 |
| | 15 | 0.15 | | 0.07 | 1 | 0.01 | 1.34 | 3.01 | 4.14 |
| | 15 | 0.15 | | 2 | 30 | 0.3 | 0.05 | 2.60 | 3.43 |
| A/AA Z2 | 10 | 0.1 | 0.01 | 0.8 | 8 | 0.08 | 0.79 | 2.57 | 3.46 |
| | 10 | 0.1 | | 1.2 | 12 | 0.12 | 0.16 | 2.62 | 3.41 |
| | 10 | 0.1 | | 0.1 | 1 | 0.01 | 4.40 | 5.41 | 7.24 |
| | 10 | 0.1 | | 3 | 30 | 0.3 | -1.27 | 3.26 | 4.21 |
| A/AA Z3 | 1 | 0.01 | 0.01 | 0.8 | 0.8 | 0.008 | 0.99 | 2.80 | 3.78 |
| | 1 | 0.01 | | 1.2 | 1.2 | 0.012 | 0.01 | 2.60 | 3.33 |
| | 1 | 0.01 | | 1 | 1 | 0.01 | 0.45 | 2.56 | 3.40 |
| | 1 | 0.01 | | 30 | 30 | 0.3 | -7.82 | 8.97 | 11.99 |
| TZ Z1 | 30 | 0.3 | 0.01 | 0.8 | 24 | 0.24 | 0.45 | 2.56 | 3.40 |
| | 30 | 0.3 | | 1.2 | 36 | 0.36 | 0.57 | 2.57 | 3.43 |
| | 30 | 0.3 | | 0.03 | 1 | 0.01 | 0.34 | 2.56 | 3.38 |
| | 30 | 0.3 | | 2 | 60 | 0.6 | 1.57 | 2.95 | 3.90 |
| TZ Z2 | 20 | 0.2 | 0.01 | 0.8 | 16 | 0.16 | 0.45 | 2.56 | 3.40 |
| | 20 | 0.2 | | 1.2 | 24 | 0.24 | 1.20 | 2.77 | 3.70 |
| | 20 | 0.2 | | 0.05 | 1 | 0.01 | -0.26 | 2.66 | 3.43 |
| | 20 | 0.2 | | 3 | 60 | 0.6 | 5.60 | 6.70 | 8.99 |
| TZ Z3 | 15 | 0.15 | 0.01 | 1.6 | 24 | 0.24 | 0.45 | 2.56 | 3.40 |
| | 15 | 0.15 | | 2 | 30 | 0.3 | 0.22 | 2.54 | 3.38 |
| | 15 | 0.15 | | 0.07 | 1 | 0.01 | 1.26 | 3.16 | 4.72 |
| | 15 | 0.15 | | 4.00 | 60 | 0.6 | -0.13 | 2.74 | 3.52 |
| TZ Z4 | 30 | 0.3 | 0.01 | 0.8 | 24 | 0.24 | 0.45 | 2.56 | 3.40 |
| | 30 | 0.3 | | 1.2 | 36 | 0.36 | 0.56 | 2.60 | 3.44 |
| | 30 | 0.3 | | 0.03 | 1 | 0.01 | 0.34 | 2.54 | 3.37 |
| | 30 | 0.3 | | 2 | 60 | 0.6 | 1.17 | 2.94 | 4.16 |

**Table 4-4 (continued)**

| Unit | Base Kh | Base Kv | Kv/Kh | Multiplier | Kh | Kv | ME | MAE | RMS |
|---|---|---|---|---|---|---|---|---|---|
| TCCZ Z1 | 10 | 0.1 | 0.01 | 0.8 | 8 | 0.08 | 0.45 | 2.56 | 3.40 |
| | 10 | 0.1 | | 1.2 | 12 | 0.12 | 0.46 | 2.56 | 3.40 |
| | 10 | 0.1 | | 0.005 | 0.05 | 0.0005 | 0.43 | 2.56 | 3.40 |
| | 10 | 0.1 | | 1 | 10 | 0.1 | 0.45 | 2.56 | 3.40 |
| TCCZ Z2 | 0.2 | 0.002 | 0.01 | 0.8 | 0.16 | 0.0016 | 0.67 | 2.62 | 3.47 |
| | 0.2 | 0.002 | | 1.2 | 0.24 | 0.0024 | 1.03 | 2.89 | 3.89 |
| | 0.2 | 0.002 | | 0.25 | 0.05 | 0.0005 | -0.08 | 2.57 | 3.28 |
| | 0.2 | 0.002 | | 50 | 10 | 0.1 | 2.64 | 5.76 | 7.56 |
| ULAZ Z1 | 100 | 1 | 0.01 | 0.8 | 80 | 0.8 | 0.45 | 2.56 | 3.40 |
| | 100 | 1 | | 1.2 | 120 | 1.2 | 1.02 | 2.62 | 3.52 |
| | 100 | 1 | | 0.002 | 0.2 | 0.002 | 9.08 | 9.74 | 13.23 |
| | 100 | 1 | | 0.4 | 40 | 0.4 | 3.06 | 3.97 | 5.10 |
| ULAZ Z2 | 10 | 0.01 | 0.001 | 0.8 | 8 | 0.008 | 0.45 | 2.55 | 3.40 |
| | 10 | 0.01 | | 1.2 | 12 | 0.012 | 0.45 | 2.56 | 3.40 |
| | 10 | 0.01 | | 0.02 | 0.2 | 0.0002 | 0.55 | 2.64 | 3.53 |
| | 10 | 0.01 | | 4 | 40 | 0.04 | 0.50 | 2.60 | 3.43 |
| ULAZ Z3 | 1 | 0.001 | 0.001 | 0.8 | 0.8 | 0.0008 | 0.60 | 2.58 | 3.43 |
| | 1 | 0.001 | | 1.2 | 1.2 | 0.0012 | 0.30 | 2.56 | 3.39 |
| | 1 | 0.001 | | 0.2 | 0.2 | 0.0002 | 0.98 | 2.66 | 3.57 |
| | 1 | 0.001 | | 40 | 40 | 0.04 | -3.11 | 4.86 | 6.62 |
| MC-LAZ Z1 | 0.1 | 0.00001 | 0.0001 | 0.8 | 0.08 | 0.000008 | 0.45 | 2.56 | 3.40 |
| | 0.1 | 0.00001 | | 1.2 | 0.12 | 0.000012 | 0.45 | 2.56 | 3.40 |
| | 0.1 | 0.00001 | | 2 | 0.2 | 0.00002 | 0.44 | 2.57 | 3.40 |
| MC-LAZ Z2 | 0.1 | 0.001 | 0.01 | 0.8 | 0.08 | 0.0008 | 0.44 | 2.55 | 3.39 |
| | 0.1 | 0.001 | | 1.2 | 0.12 | 0.0012 | 0.44 | 2.56 | 3.41 |
| | 0.1 | 0.001 | | 2 | 0.2 | 0.002 | 0.42 | 2.58 | 3.42 |

**Table 4-4 (continued)**

| Unit | Base Kh | Base Kv | Kv/Kh | Multiplier | Kh | Kv | ME | MAE | RMS |
|---|---|---|---|---|---|---|---|---|---|
| LLAZ Z1 | 0.05 | 0.0005 | 0.01 | 0.8 | 0.04 | 0.0004 | 0.46 | 2.55 | 3.40 |
| | 0.05 | 0.0005 | | 1.2 | 0.06 | 0.0006 | 0.43 | 2.56 | 3.40 |
| | 0.05 | 0.0005 | | 4 | 0.2 | 0.002 | 0.23 | 2.69 | 3.52 |
| LLAZ Z2 | 0.5 | 0.001 | 0.002 | 0.8 | 0.4 | 0.0008 | 0.48 | 2.58 | 3.42 |
| | 0.5 | 0.001 | | 1.2 | 0.6 | 0.0012 | 0.42 | 2.54 | 3.39 |
| | 0.5 | 0.001 | | 0.4 | 0.2 | 0.0004 | 0.59 | 2.66 | 3.51 |
| | 0.5 | 0.001 | | 80 | 40 | 0.08 | 0.19 | 2.64 | 3.44 |
| LLAZ Z3 | 15 | 0.1 | 0.0067 | 0.8 | 12 | 0.08 | 0.46 | 2.57 | 3.40 |
| | 15 | 0.1 | | 1.2 | 18 | 0.12 | 0.44 | 2.55 | 3.40 |
| | 15 | 0.1 | | 0.013 | 0.2 | 0.0013 | 0.64 | 2.67 | 3.58 |
| GCU Z1 | 0.0001 | 0.000005 | 0.05 | 0.8 | 0.00008 | 0.000004 | 0.44 | 2.56 | 3.40 |
| | 0.0001 | 0.000005 | | 1.2 | 0.00012 | 0.000006 | 0.45 | 2.56 | 3.40 |
| | 0.0001 | 0.000005 | 0.01 | 10 | 0.001 | 0.00001 | 0.45 | 2.56 | 3.41 |
| | 0.0001 | 0.000005 | | 700 | 0.07 | 0.0007 | 0.49 | 2.71 | 3.74 |
| GCU Z2 | 0.05 | 0.0005 | 0.01 | 0.8 | 0.04 | 0.0004 | 0.45 | 2.56 | 3.40 |
| | 0.05 | 0.0005 | | 1.2 | 0.06 | 0.0006 | 0.44 | 2.55 | 3.40 |
| | 0.05 | 0.0005 | | 0.02 | 0.001 | 0.00001 | 0.61 | 2.69 | 3.61 |
| | 0.05 | 0.0005 | | 1.4 | 0.07 | 0.0007 | 0.44 | 2.55 | 3.39 |
| GCU Z3 | 0.00001 | 0.000001 | 0.1 | 0.8 | 8E-06 | 8E-07 | 0.45 | 2.56 | 3.40 |
| | 0.00001 | 0.000001 | | 1.2 | 1.2E-05 | 1.2E-06 | 0.44 | 2.56 | 3.40 |
| | 0.00001 | 0.000001 | 0.01 | 100 | 0.001 | 0.00001 | 0.27 | 2.53 | 3.40 |
| | 0.00001 | 0.000001 | | 7000 | 0.07 | 0.0007 | -0.82 | 3.19 | 4.82 |
| GCU Z4 | 0.05 | 0.0005 | 0.01 | 0.8 | 0.04 | 0.0004 | 0.45 | 2.56 | 3.40 |
| | 0.05 | 0.0005 | | 1.4 | 0.07 | 0.0007 | 0.44 | 2.56 | 3.40 |

**Table 4-4 (continued)**

| Unit | Base Kh | Base Kv | Kv/Kh | Multiplier | Kh | Kv | ME | MAE | RMS |
|---|---|---|---|---|---|---|---|---|---|
| GCU Z5 | 0.01 | 0.0001 | 0.01 | 0.8 | 0.008 | 0.00008 | 0.45 | 2.56 | 3.40 |
| | 0.01 | 0.0001 | | 1.2 | 0.012 | 0.00012 | 0.44 | 2.56 | 3.40 |
| | 0.01 | 0.0001 | | 0.1 | 0.001 | 0.00001 | 0.47 | 2.56 | 3.42 |
| | 0.01 | 0.0001 | | 7 | 0.07 | 0.0007 | 0.41 | 2.55 | 3.38 |
| UGA Z1 | 75 | 0.0005 | | 1.2 | 90 | 0.09 | 0.47 | 2.56 | 3.40 |
| | 75 | 0.0005 | | 0.267 | 20 | 0.2 | 0.12 | 2.62 | 3.54 |
| MGA Z1 | 0.0001 | 0.000001 | 0.01 | 0.8 | 0.00008 | 8E-07 | 0.45 | 2.56 | 3.40 |
| | 0.0001 | 0.000001 | | 1.2 | 0.00012 | 1.2E-06 | 0.45 | 2.56 | 3.40 |
| MGA Z2 | 1 | 0.001 | 0.001 | 0.8 | 0.8 | 0.0008 | 0.43 | 2.55 | 3.40 |
| | 1 | 0.001 | | 1.2 | 1.2 | 0.0012 | 0.45 | 2.57 | 3.41 |
| MGA Z3 | 0.05 | 0.00005 | 0.001 | 0.8 | 0.04 | 0.00004 | 0.44 | 2.56 | 3.40 |
| | 0.05 | 0.00005 | | 400 | 20 | 0.2 | 0.56 | 2.66 | 3.62 |
| MGA Z4 | 0.0001 | 0.000001 | 0.01 | 0.8 | 0.00008 | 8E-07 | 0.45 | 2.56 | 3.40 |
| | 0.0001 | 0.000001 | | 200000 | 20 | 0.2 | 0.58 | 2.69 | 3.63 |
| LGA Z1 | 15 | 0.0005 | 3.33E-05 | 0.8 | 12 | 0.0012 | 0.49 | 2.57 | 3.41 |
| | 15 | 0.0005 | 3.33E-05 | 2.667 | 40 | 0.4 | 0.27 | 2.56 | 3.41 |
| CBCU Z1 | 0.1 | 0.0005 | 0.005 | 0.8 | 0.08 | 0.0008 | 0.45 | 2.56 | 3.40 |
| | 0.1 | 0.0005 | | 1.2 | 0.12 | 0.0012 | 0.44 | 2.56 | 3.40 |
| CBAU Z1 | 25 | 0.0005 | 0.00002 | 0.8 | 20 | 0.2 | 0.45 | 2.56 | 3.40 |
| | 25 | 0.0005 | | 1.2 | 30 | 0.3 | 0.44 | 2.56 | 3.40 |
| Recharge | 17 | | | 0.8 | 14 | | -2.64 | 3.82 | 4.80 |
| (in/yr) | 17 | | | 1.2 | 20 | | 2.91 | 4.06 | 5.19 |
| | 17 | | | 0.65 | 11 | | -5.28 | 6.10 | 7.72 |
| | 17 | | | 1.24 | 21 | | 3.25 | 4.36 | 5.55 |

**Note:** Base case - mean error (ME) = 0.445, mean absolute error (MAE) = 2.557, and root-mean-square error (RMSE) = 3.399.
Kh = Horizontal hydraulic conductivity,
Kv = Vertical hydraulic conductivity

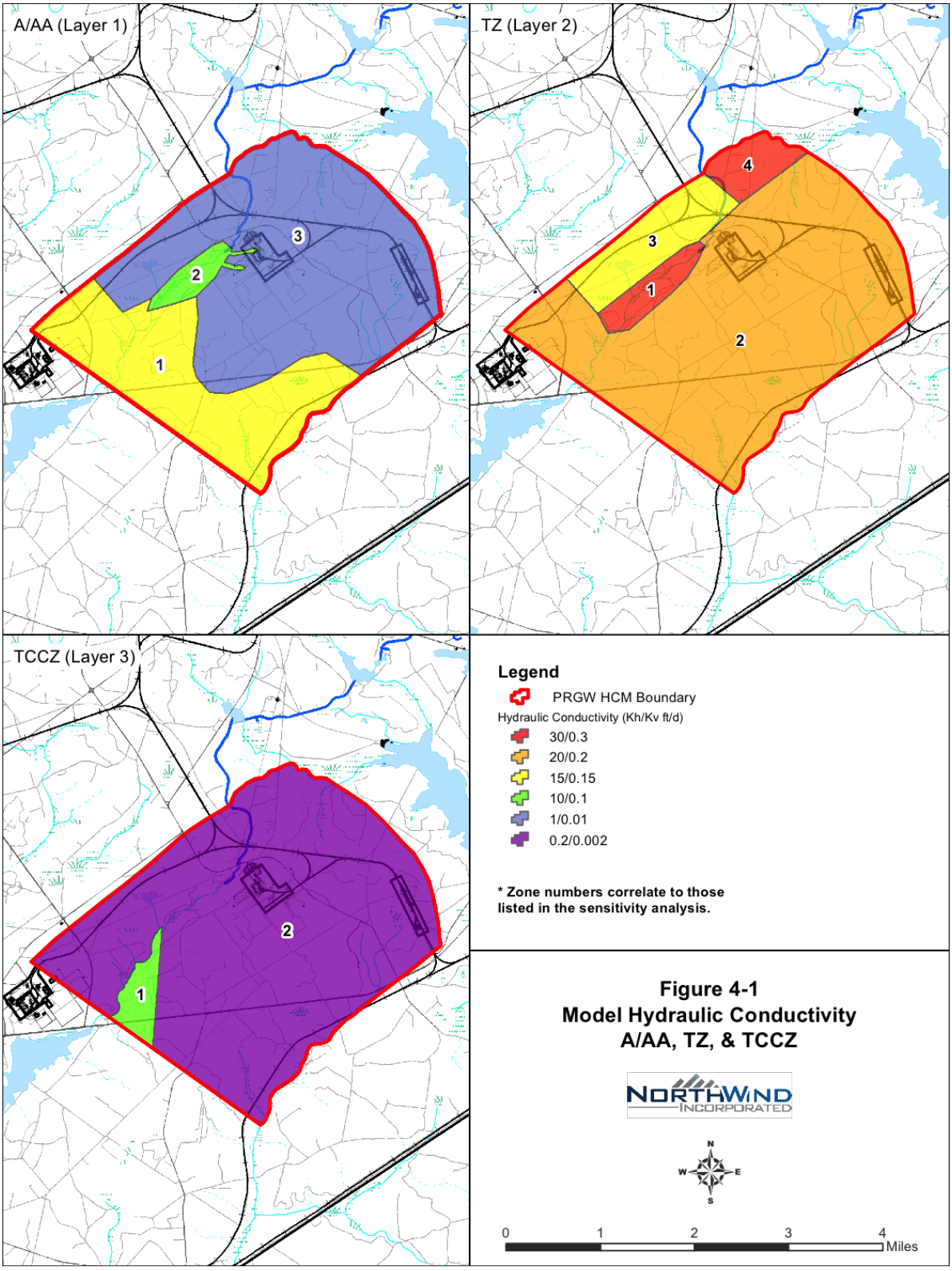


**Figure 4-1 Model Hydraulic Conductivity: A/AA (Layer 1), TZ (Layer 2), and TCCZ (Layer 3)**

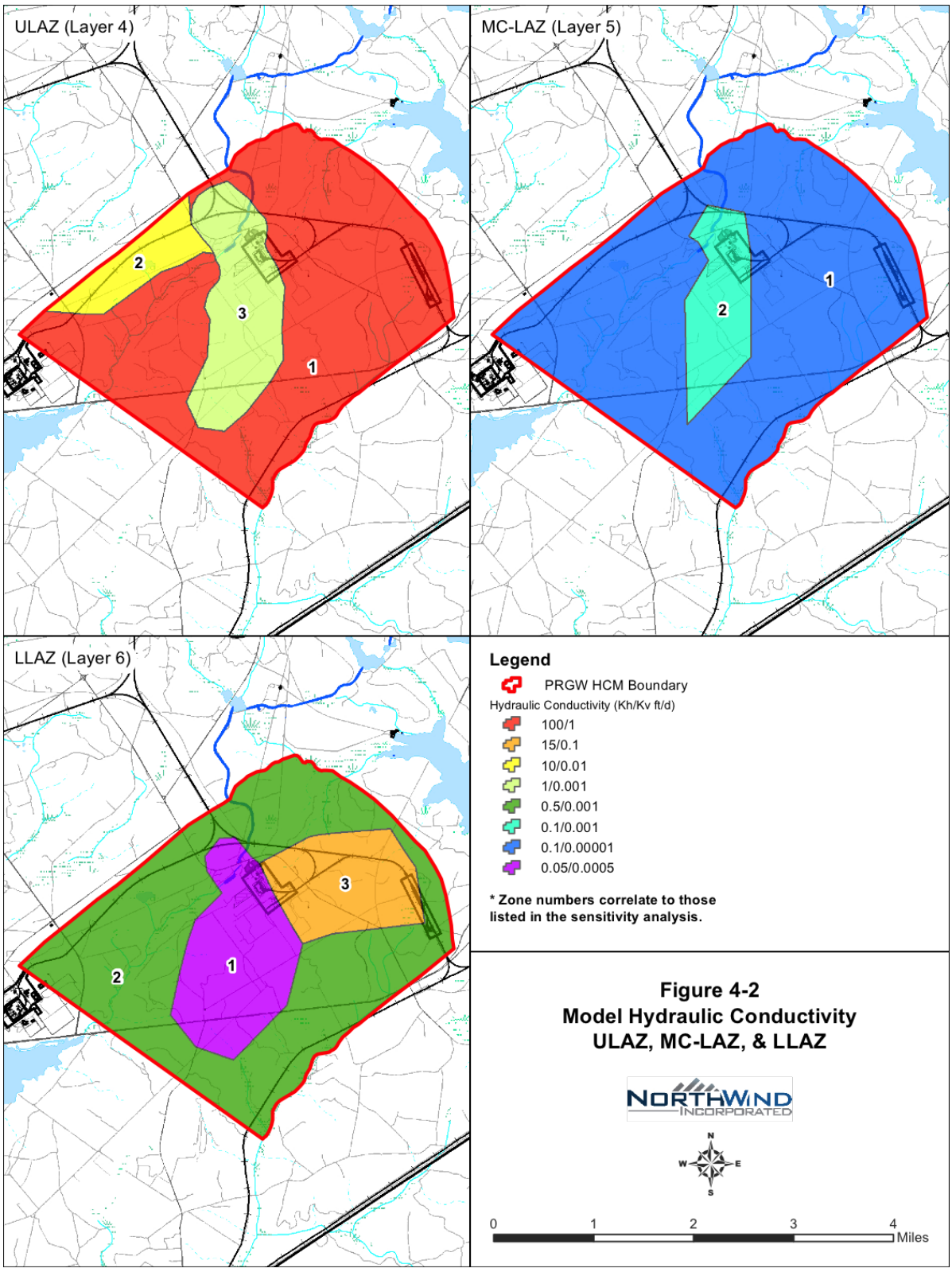


**Figure 4-2 Model Hydraulic Conductivity: ULAZ (Layer 4), MC-LAZ (Layer 5), and LLAZ (Layer 6)**

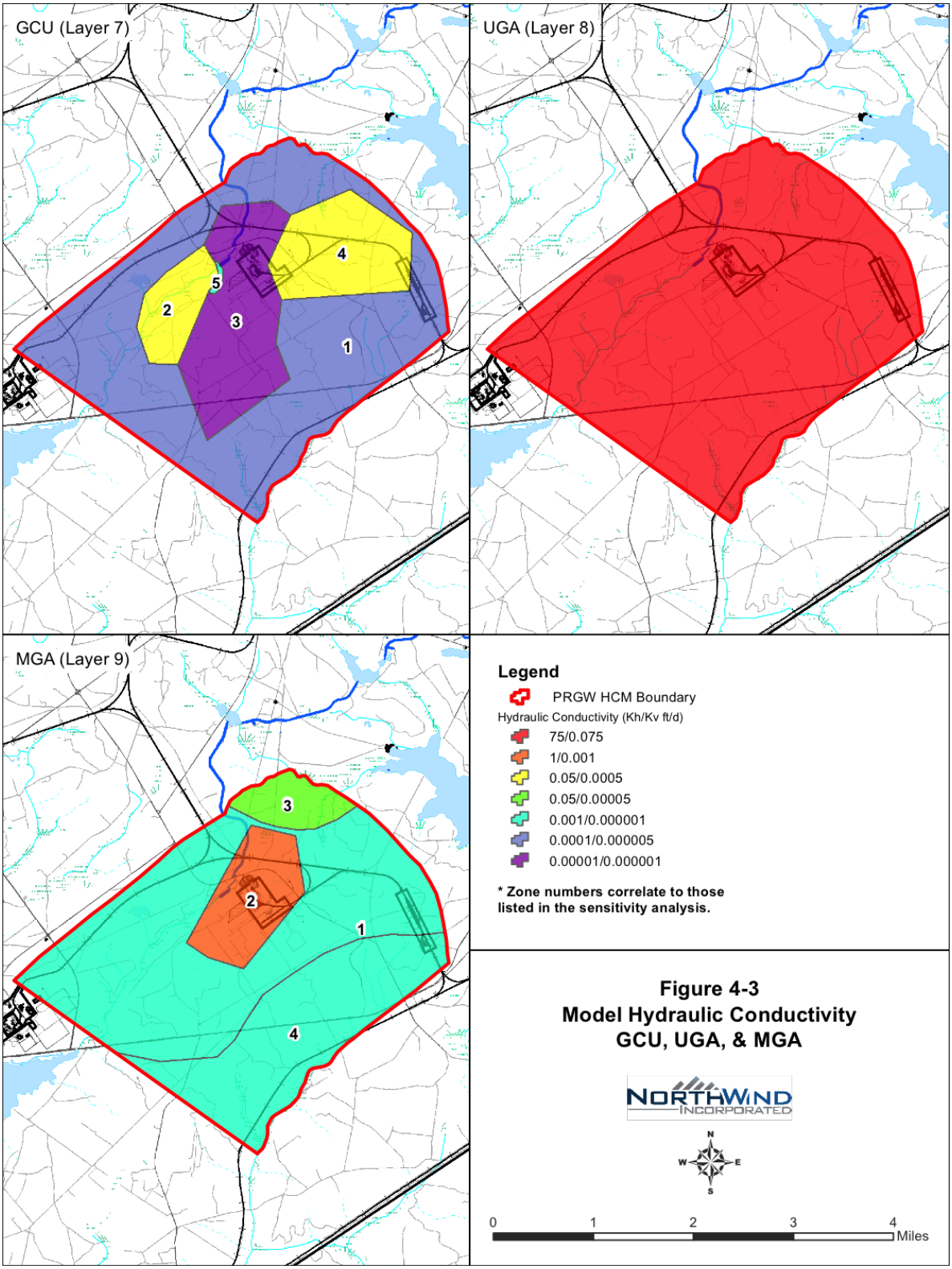


**Figure 4-3 Model Hydraulic Conductivity: GCU (Layer 7), UGA (Layer 8), and MGA (Layer 9)**

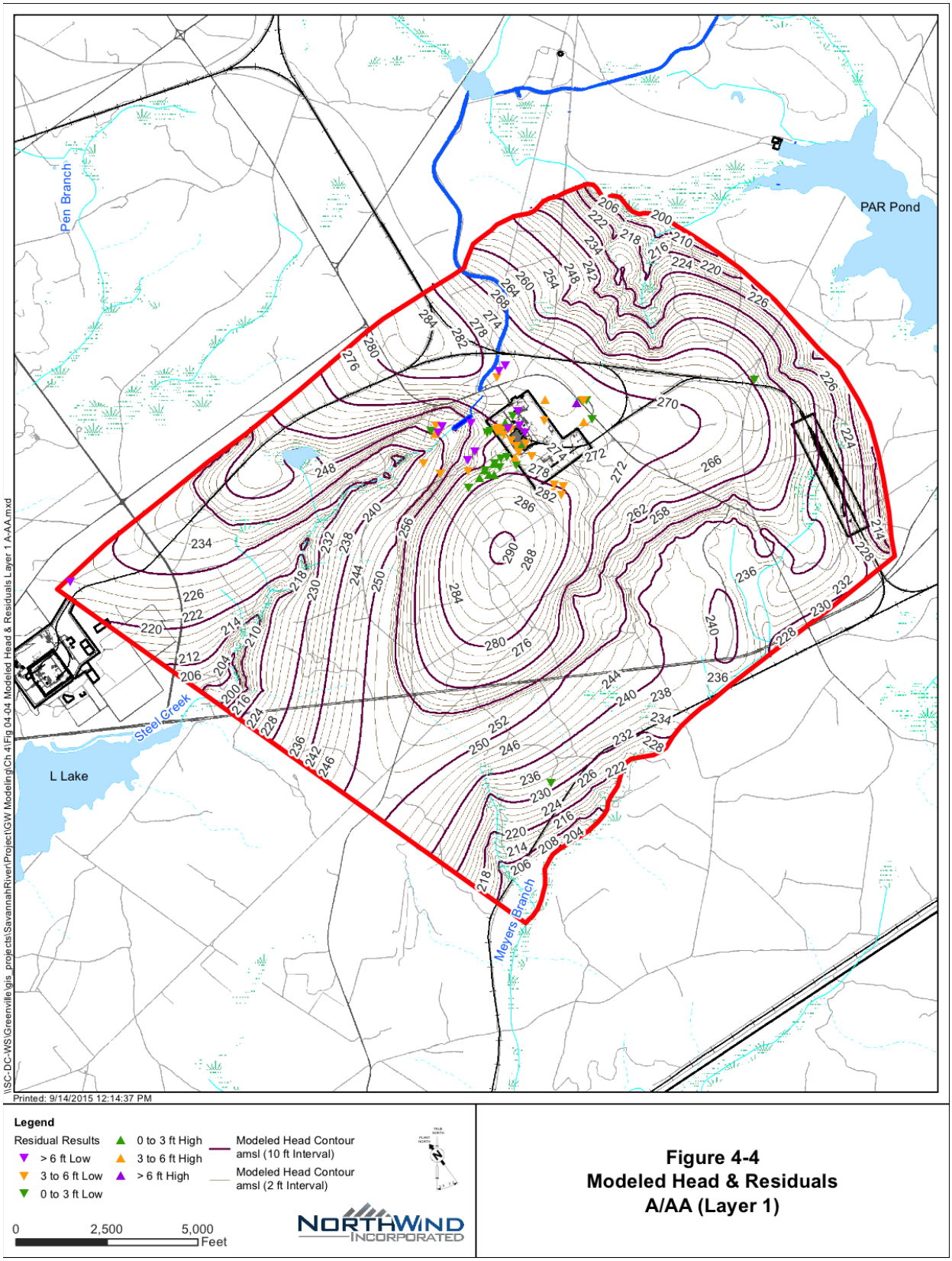


**Figure 4-4 Modeled Head and Residuals A/AA (Layer 1)**

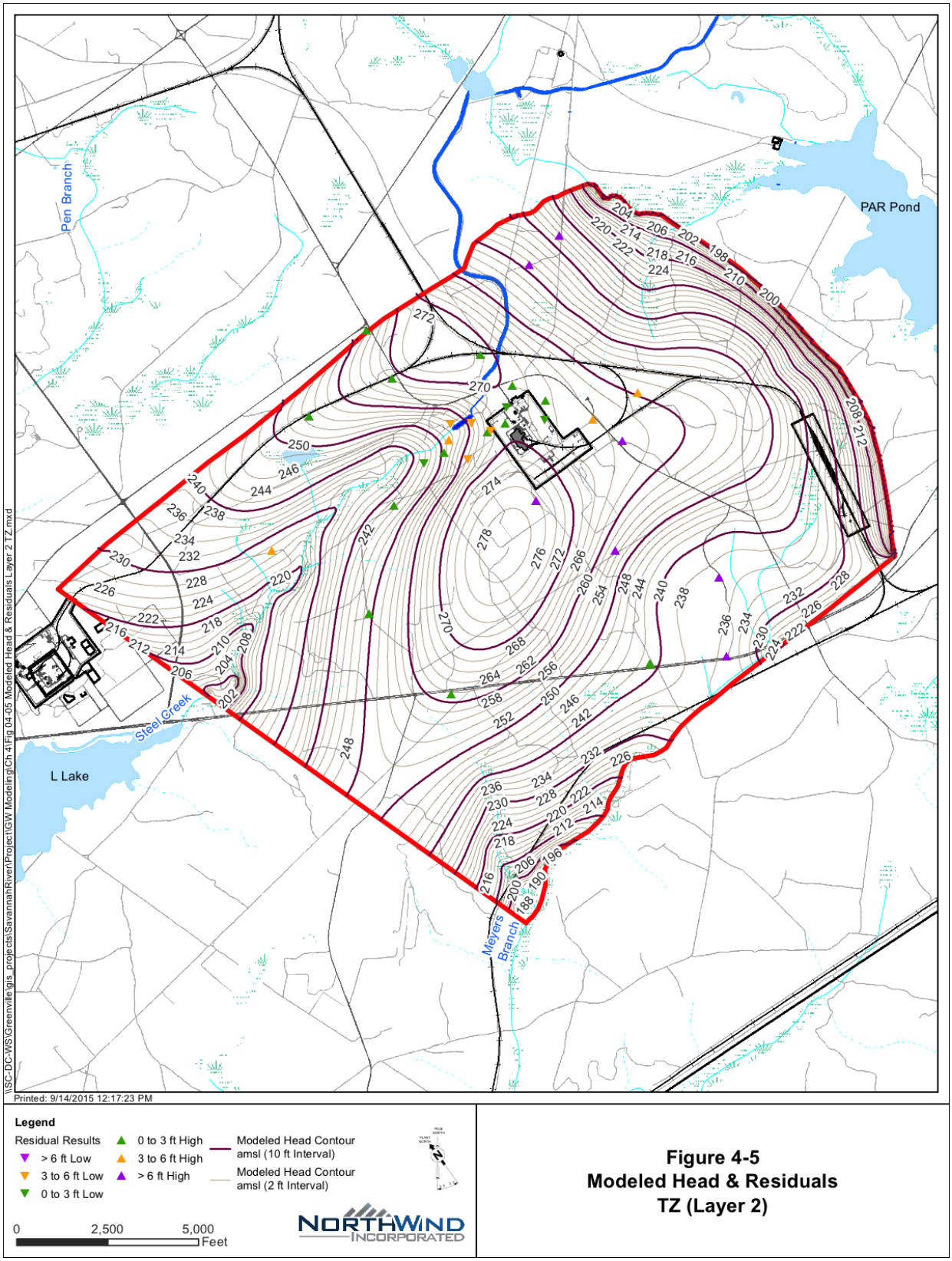


**Figure 4-5 Modeled Head and Residuals TZ (Layer 2)**

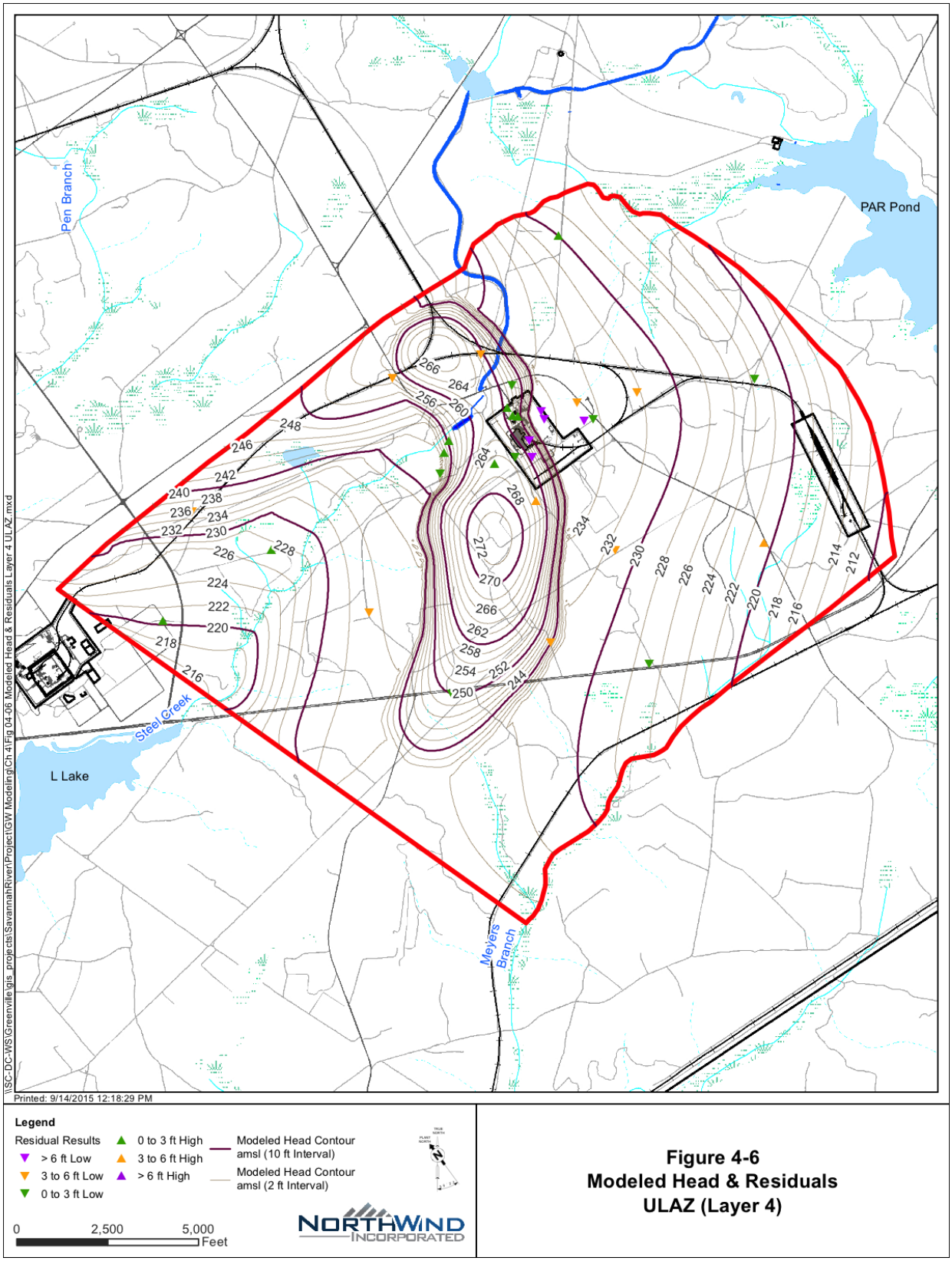


**Figure 4-6 Modeled Head and Residuals ULAZ (Layer 4)**

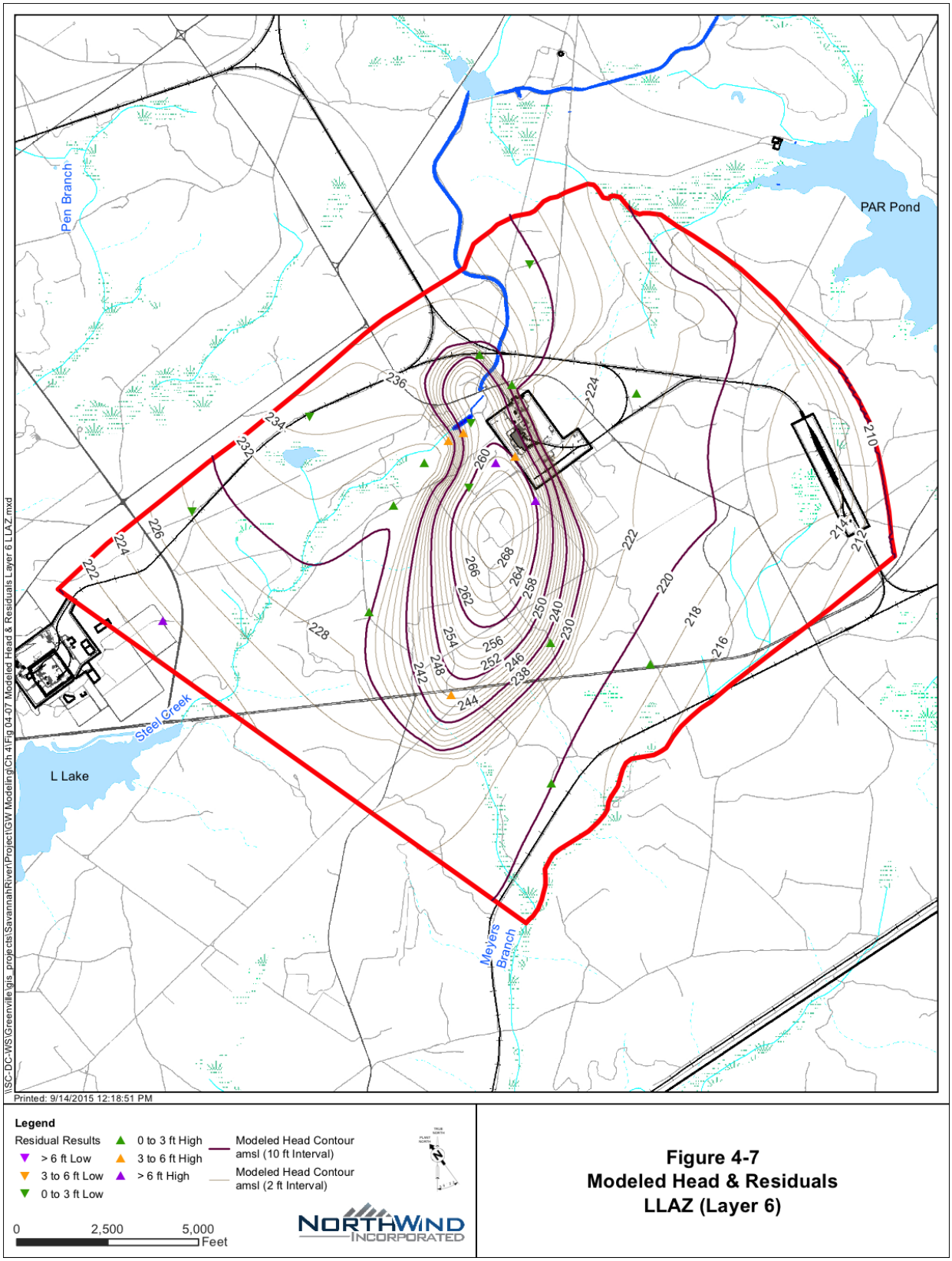


**Figure 4-7 Modeled Head and Residuals LLAZ (Layer 6)**

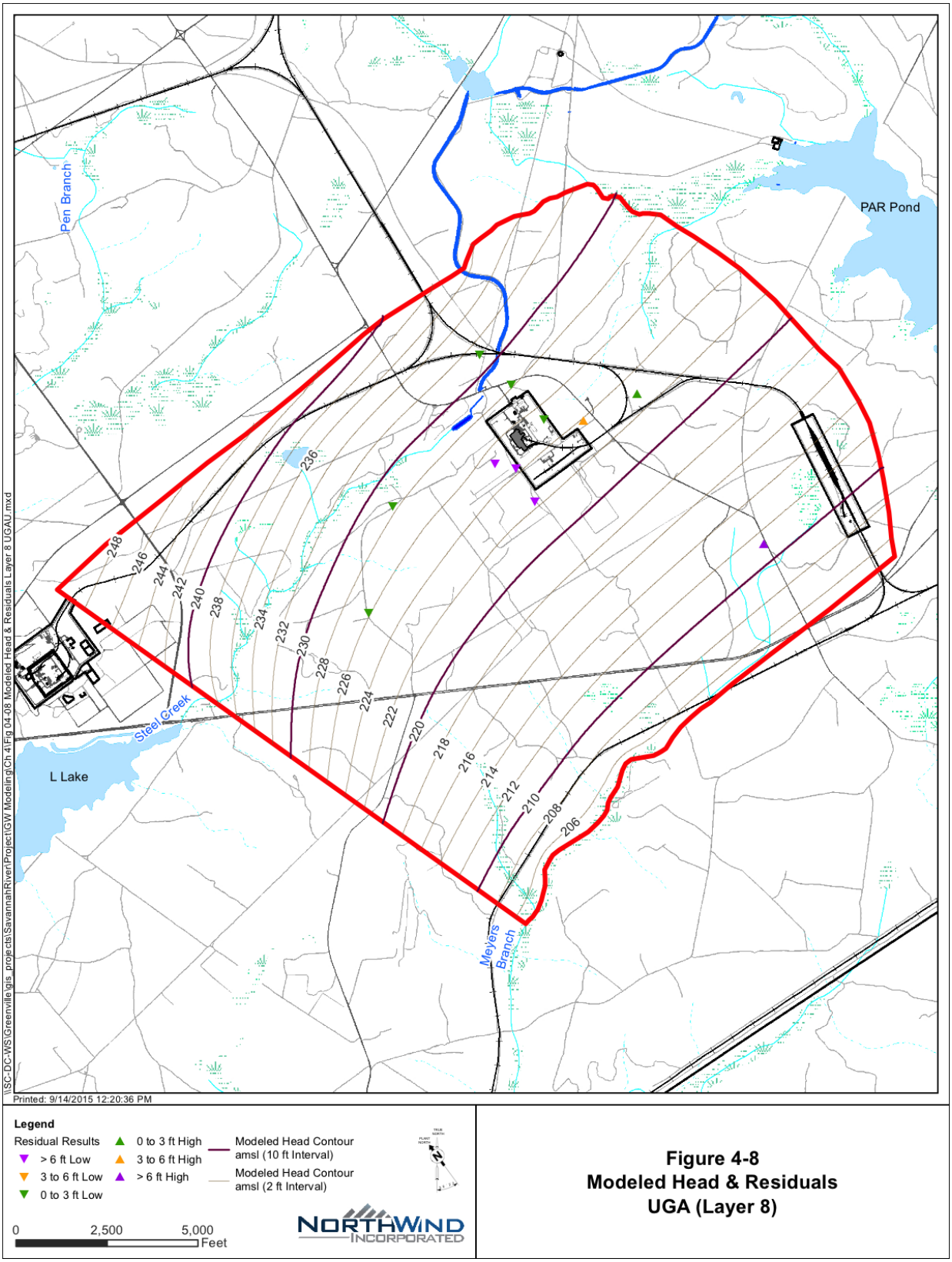


**Figure 4-8 Modeled Head and Residuals UGA (Layer 8)**

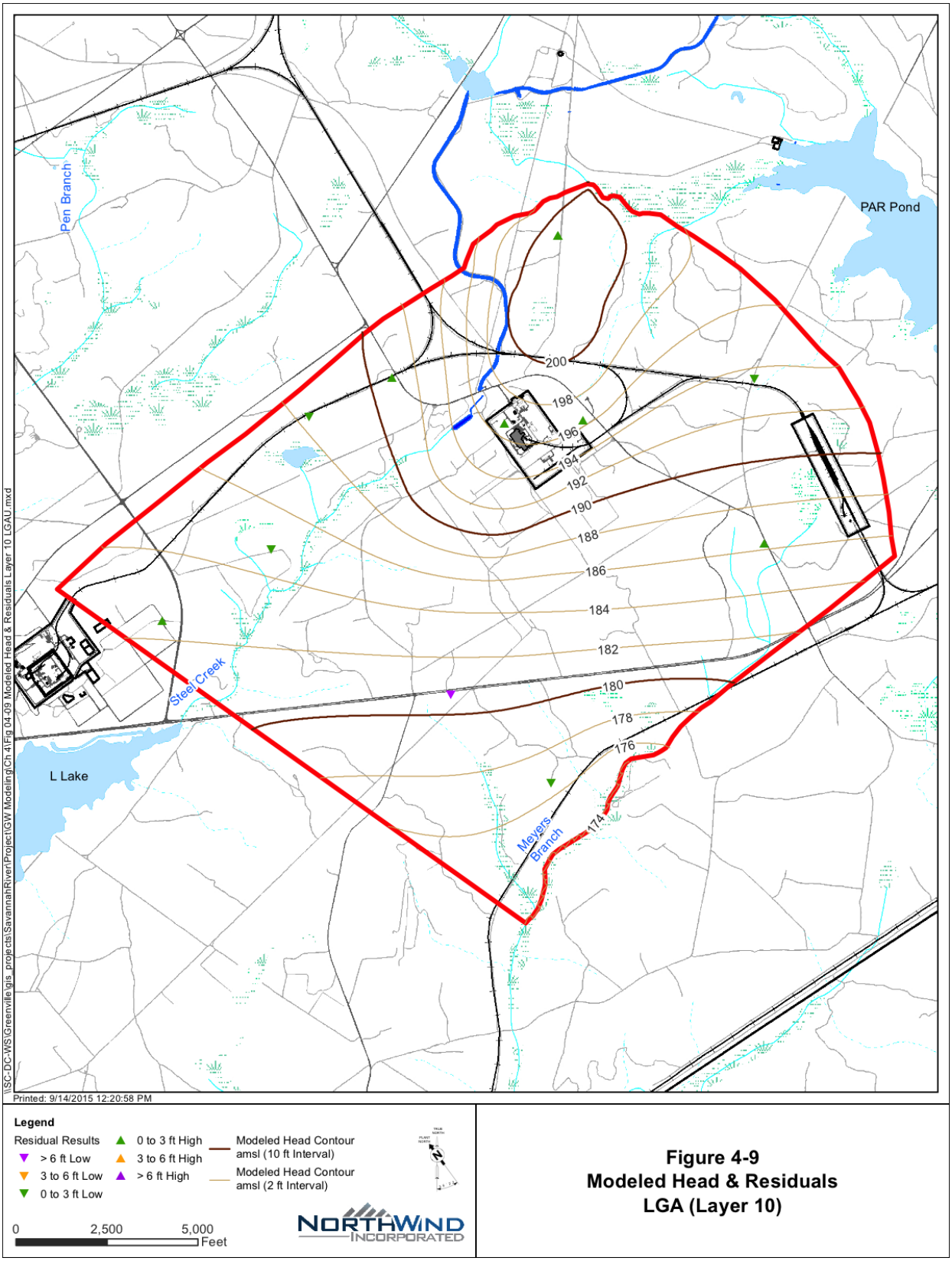


**Figure 4-9 Modeled Head and Residuals LGA (Layer 10)**

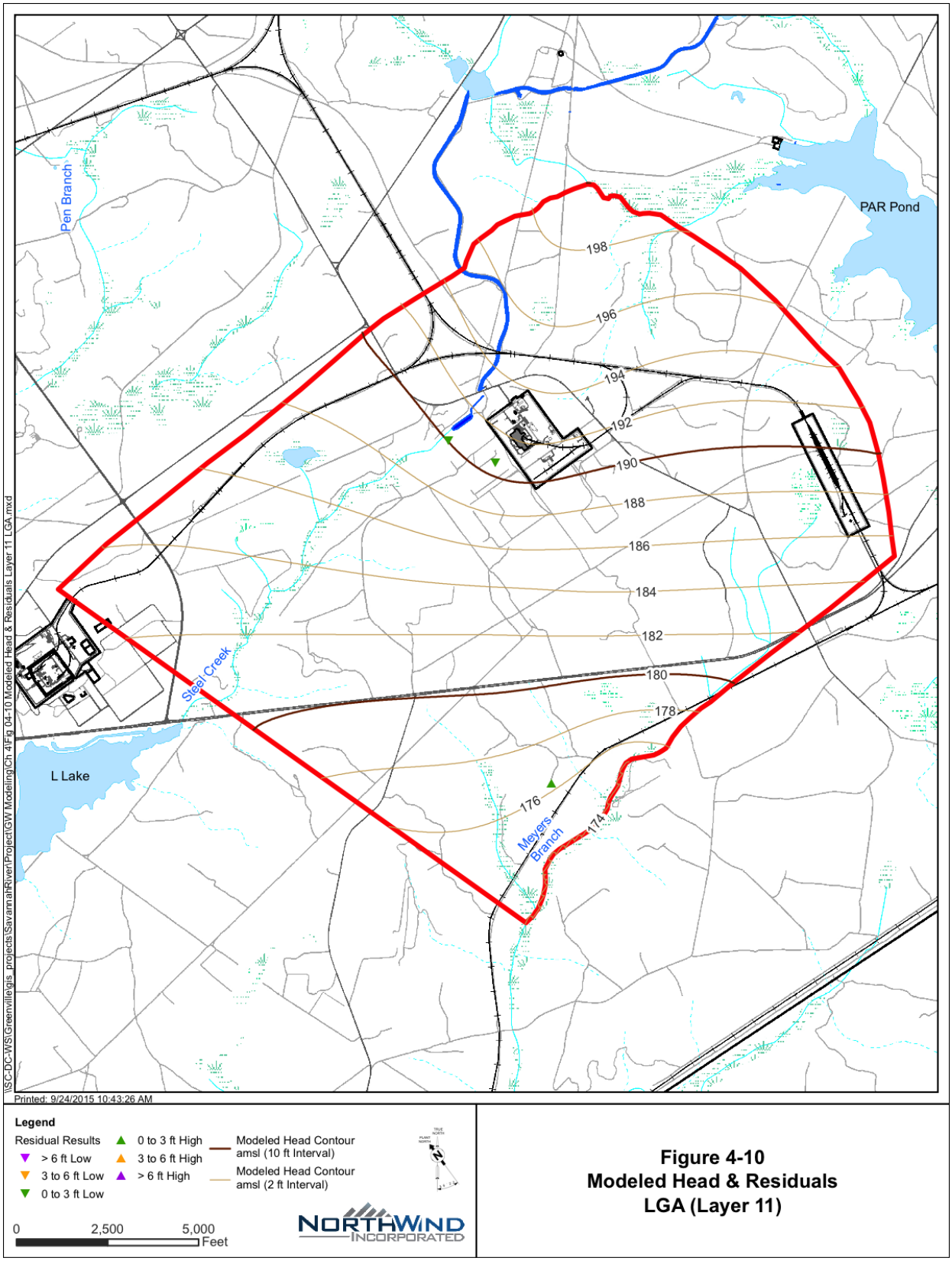


**Figure 4-10 Modeled Head and Residuals LGA (Layer 11)**

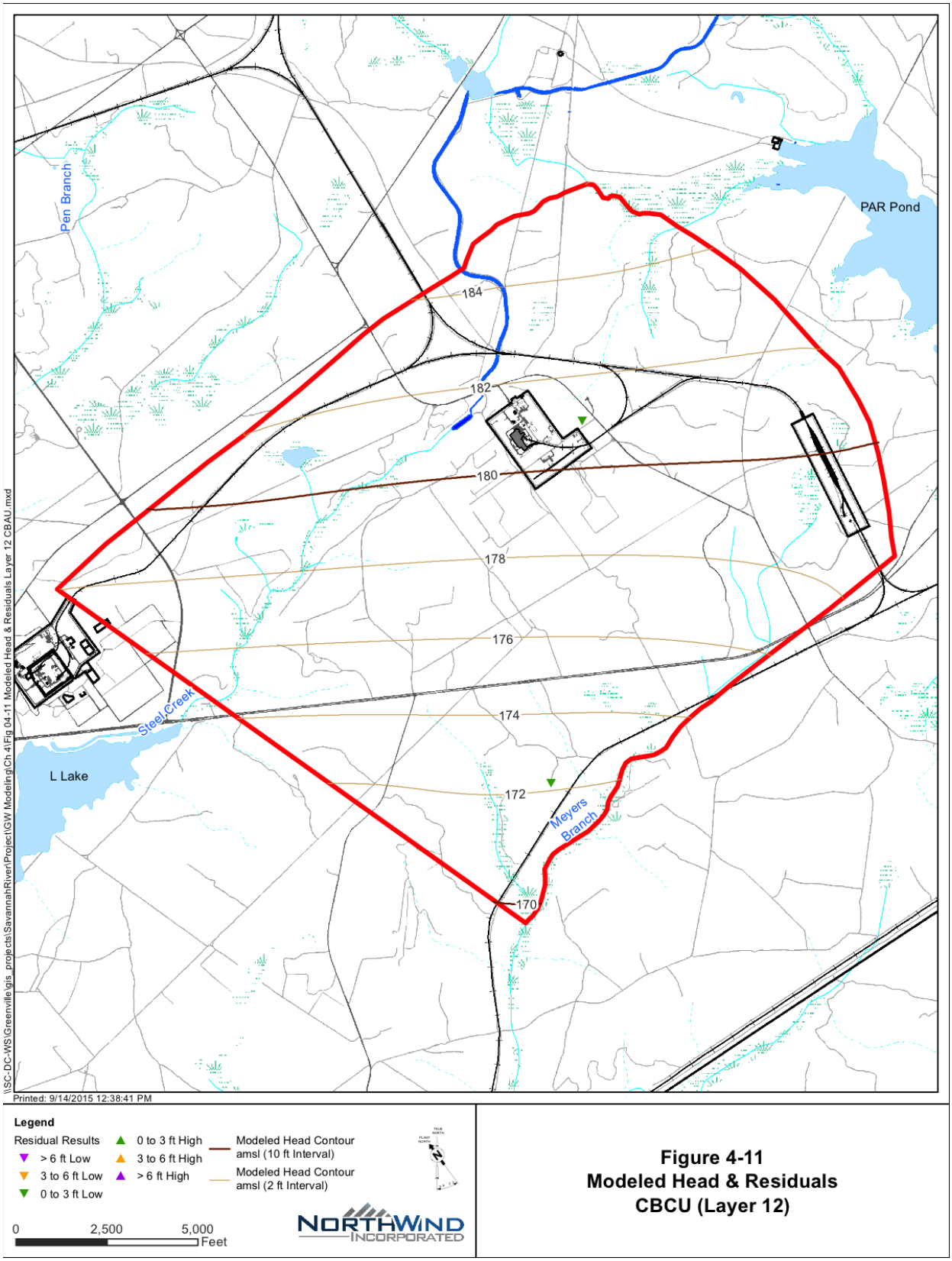


**Figure 4-11 Modeled Head and Residuals CBCU (Layer 12)**

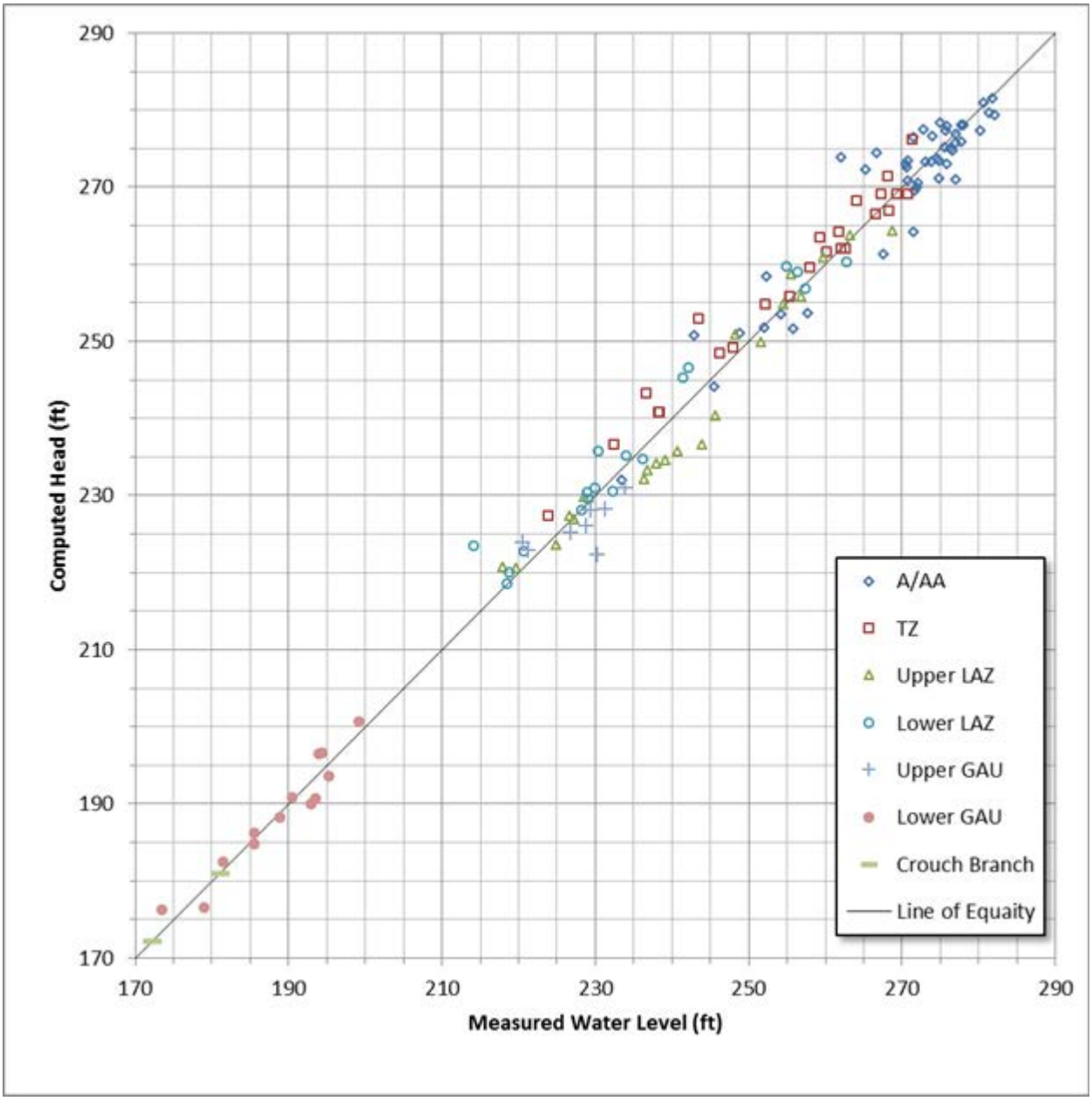


**Figure 4-12 Modeled versus Observed Head**

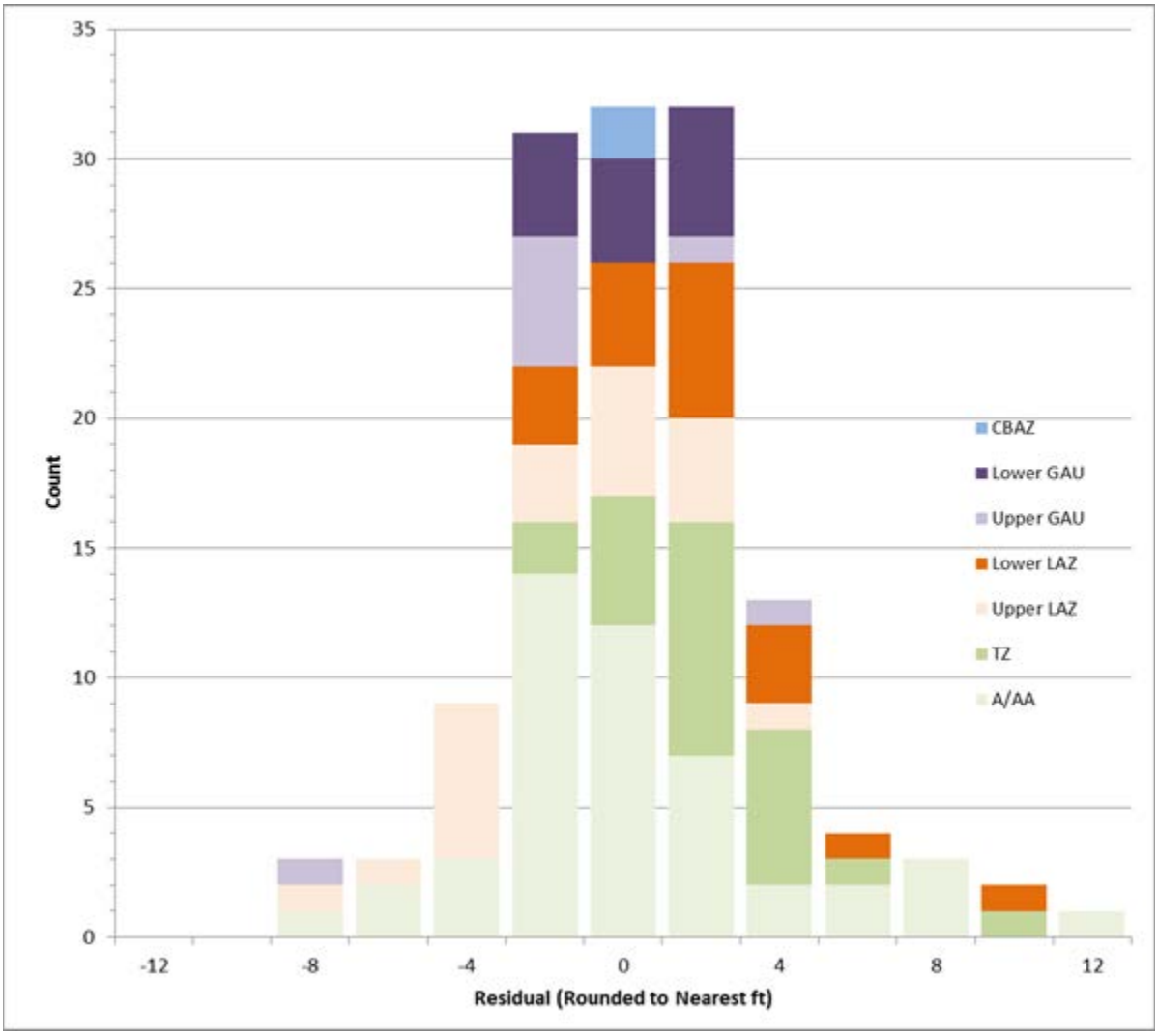


**Figure 4-13 Histogram of Residuals**

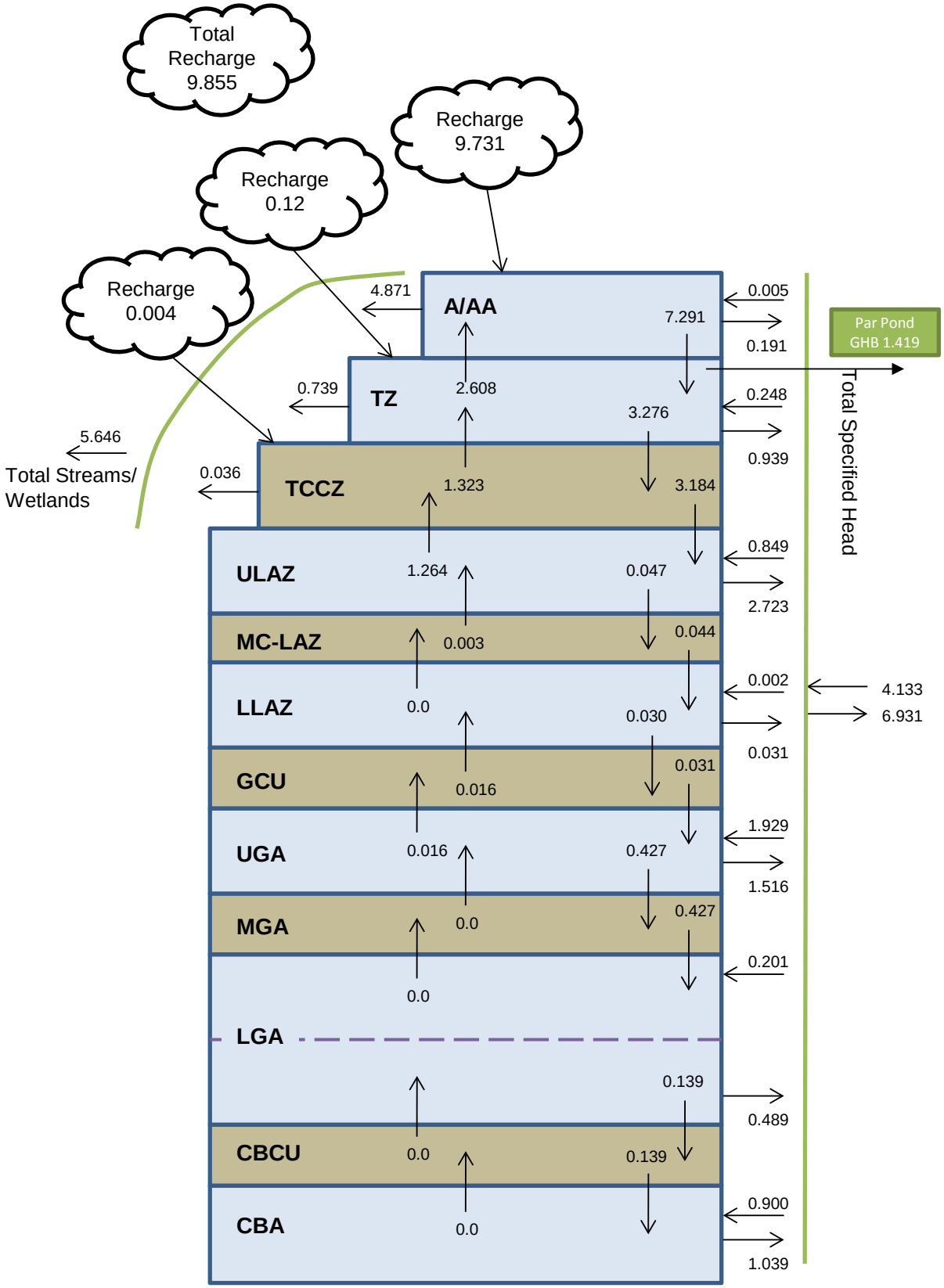


**Figure 4-14 Water Balance in cfs**

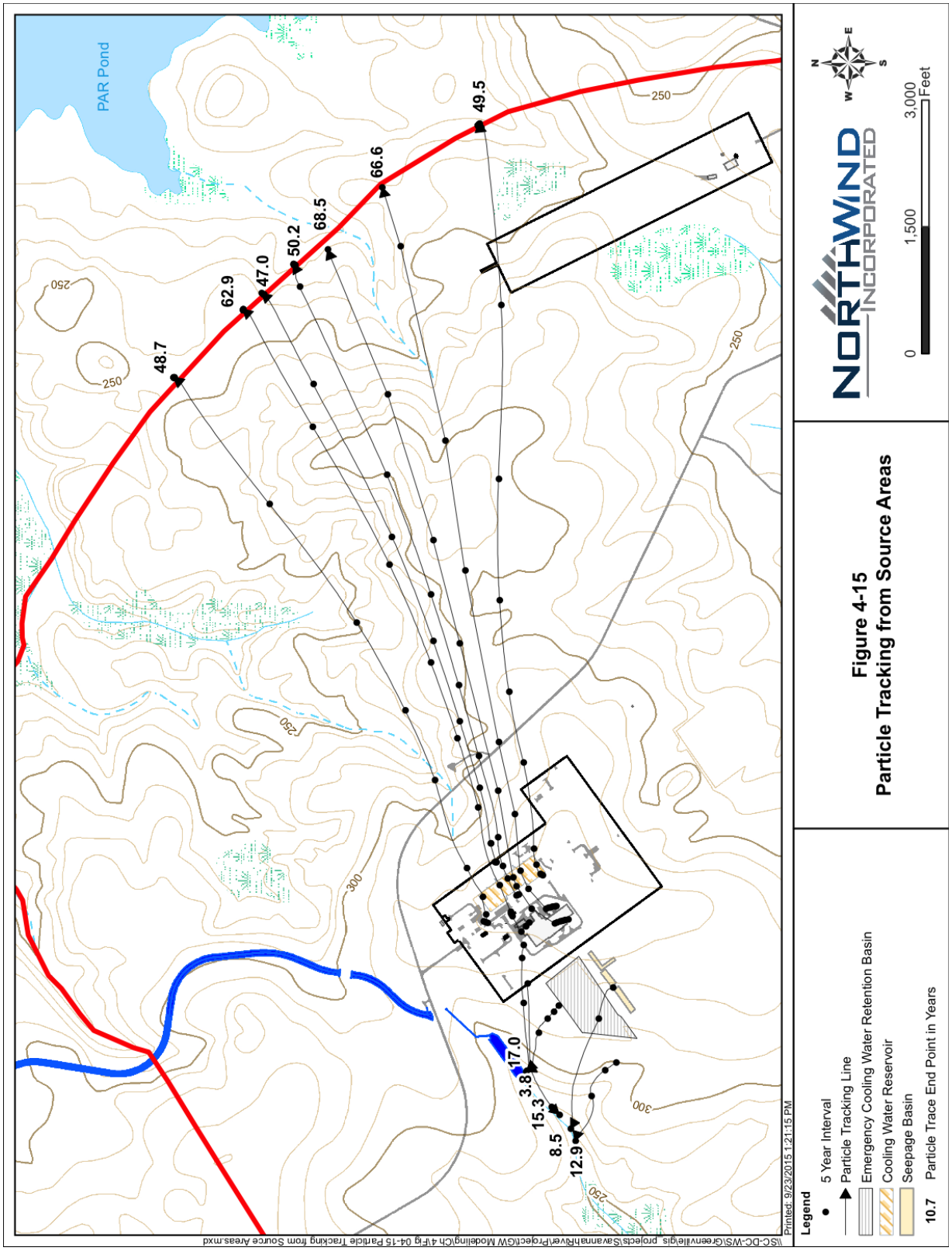


**Figure 4-15 Particle Tracking from Source Areas**

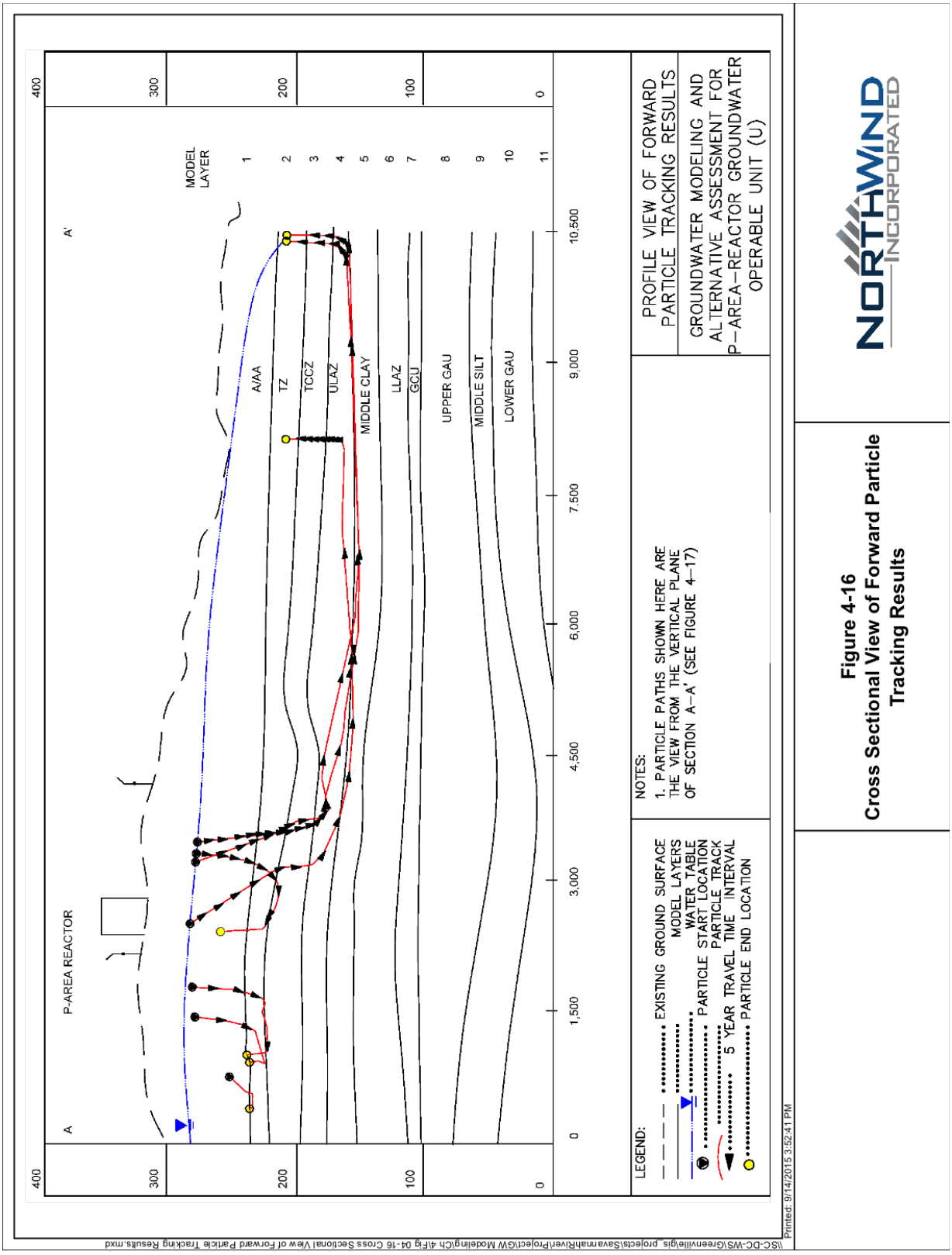


**Figure 4-16 Cross Sectional View of Forward Particle Tracking Results**

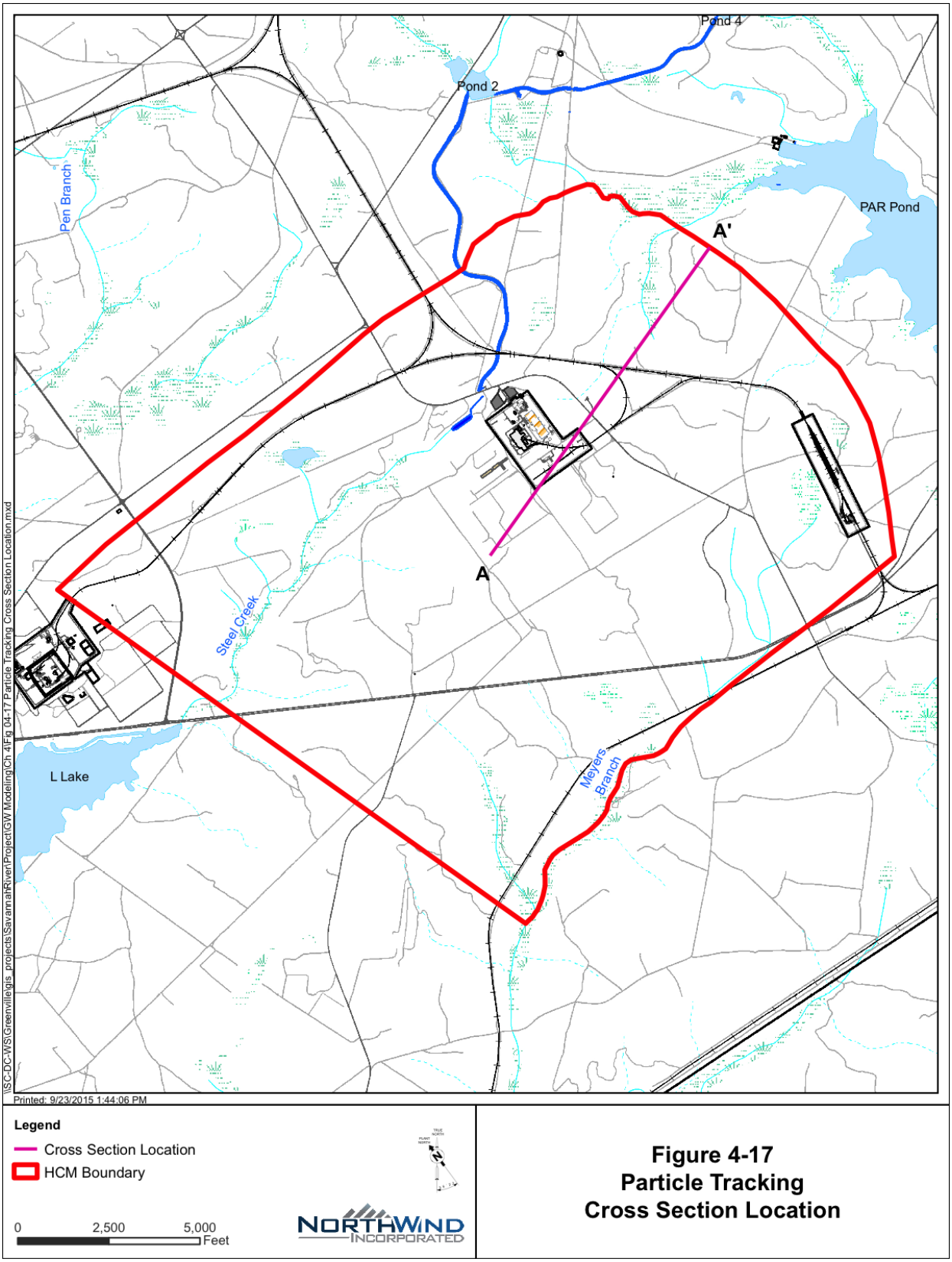


**Figure 4-17 Particle Tracking Cross Section Location**

# 5.0 TRANSPORT MODEL PREDICTIONS

The steady state hydraulic heads computed by the calibrated groundwater flow model are used in the contaminant transport model to assess the future transport of tritium, PCE, and TCE. The contaminant transport simulation estimates future groundwater concentrations and mass discharges to surface water bodies within the P-Area HCM. The transport model includes attenuation of the contaminants through natural processes (i.e., advection, dispersion, sorption, and/or radioactive decay).

The transport model uses the steady-state calibrated flow field and current condition (2014/2015) of the groundwater plumes to predict future concentrations and mass discharge of tritium, PCE, and TCE. Surface units that were previously identified as source areas have been addressed and the modeled plumes are assumed to be the only source of contamination in the transport model.

## 5.1 Initial Conditions

Figures 2-6 through 2-10 show the initial groundwater concentration plumes for PCE, TCE, and tritium. Each figure has three plots, one for each constituent showing the interpreted concentrations in the A/AA and TZ (layers 1 and 2), the TCCZ (layer 3), and the ULAZ (layers 4 and 5). Tritium plumes for the LLAZ (layer 6) and the GCU (layer 7) are also presented. These concentration plumes represent the transport model initial conditions. Theses plumes are derived from analytical data by the following procedures:

- At each DPT location or well and for each contaminant, the measured concentration from the 2014 DPT sampling event (SRNS 2014) and routine 2014-2015 groundwater monitoring well sampling were used to modify the 2011 isoconcentration (SRNS 2011b). If concentration data existed in 2014 and 2015 at the same location, then the 2014 data were used to correspond to available DPT collected data. If more than one depth was measured at a location, the highest concentration was used for that unit. This approach may have overestimated the total plume mass by assigning the higher concentration for the whole unit thickness. Plume isoconcentration contours stopped just prior to Steel Creek, based on SRS data that shows there is no underflow in A/AA or TZ of contaminants. This approach would underestimate the early time discharge to Steel Creek.

- For each hydrostratigraphic unit in the UTRA (A/AA, TZ, TCCZ, and LAZ) and the GCU, and for each constituent, concentration values were assigned to the model cells based on interpolation of the revised isoconcentration contours and measured 2014/15 concentration values.

- The two-dimensional plumes are assigned to the three-dimensional model grid. Layers 1 and 2 were assigned the A/AA and TZ concentrations, respectively. Layer 3 was assigned the TCCZ concentrations, and layers 4 through 5 were each assigned the LAZ concentrations. This approach may have overestimated the total plume mass as the same plume was used for more than one layer and each plume is assumed to be present across the entire thickness of a layer.

- Because tritium had measured concentrations at greater depths, plumes for the LLAZ (layer 6) and the GCU (layer 7) were developed. One well, PSB002AA, which is recorded as being screened in the upper portion of the Gordon Aquifer, had tritium concentration of 5,860 pCi/mL in March 2015, while a second well nearby and screened in the GCU (PGW033A) had a concentration flagged as non-detect at less than 0.243 pCi/mL. Comparison of the heads from wells PSB002AA and PGW033A (238.2 ft amsl) to a nearby well screened lower in the GAU (PGW 03A at 230.2 ft amsl), suggests that PSB002AA is actually screened in the GCU, and it is considered so for modeling purposes.

- In this analysis, the LLAZ, GCU, GAU, CBCU, and CBAU (layers 7 through 13) were assigned an initial concentration of zero for all constituents, except for tritium in the LLAZ and GCU as described above. There have been only two TCE detections (21.7 μg/L at PG-33 on Oct 2, 2002 and 5.66 μg/L at PG-37 on August 26, 2003) in the GAU above the MCL (5 μg/L). All TCE concentrations in the GAU are mostly non-detects or slightly above the method detection limit. The groundwater model does not predict the presence of contamination in the GAU, CBCU, or CBAU, as evidenced by the particle tracking results (Section 4.2) and the transport model results presented below. Additionally, extensive characterization in 2010 did not detect TCE at depth below the LAZ and therefore, the detection of TCE in the GAU from the earlier investigation is considered an anomaly or associated with sampling/analytical error.

## 5.2 Calibrated Transport Model Results

The parameters of the calibrated transport model are listed in Table 5-1.

**Table 5-1 Calibrated Transport Model Parameters**

| Parameter | Value |
|---|---|
| Effective Porosity | 0.3 |
| Dispersivity | 10 ft (longitudinal)<br>1.0 ft (horizontal-transverse)<br>0.1 ft (vertical) |
| Bulk Density | 1.48 kg/L |
| Half-life | 25 years for TCE/PCE<br>12.3 years for Tritium |
| $K_d$ and Retardation | See Table 3-3 |

### *5.2.1 Baseline Model Results*

Transport simulations for the baseline scenario representing the current conditions for tritium and CVOCs are presented below.

#### 5.2.1.1 Tritium Simulation Results

Transport of tritium was simulated under steady state flow conditions for a model period of 100 years. The MODPATH and MT3DMS (Zheng 1999) solutions show that migration of tritium through groundwater is primarily towards Steel Creek (Figures 5-1 to 5-4), and that the tritium plume does not exit into Steel Creek past stream gauge location SC-04 at concentrations exceeding the MCL (20 pCi/mL).

However, the predicted concentration of tritium in groundwater discharging to stream gauge location SC-03 is greater than the MCL and is predicted to remain above the MCL for approximately 30 years from calendar year (CY) 2015 (i.e., the time 0.0 of the simulation period or the start time). As shown in Figure 5-1 (TZ), the tritium plume discharge to surface water bodies is limited to Steel Creek between locations SC-01 and SC-04. Results of the tritium transport baseline simulation indicate that tritium concentrations will be reduced to below the

MCL much faster in the shallow aquifers (A/AA, TZ) than deeper aquifers (ULAZ, LLAZ, GCU) (see Figures 5-1 through 5-4). In the ULAZ the plume extends past SC-04 and heads towards L Lake in year 25 but degrades to below MCL prior to reaching the lake and is gone by year 100. In LLAZ (i.e., model layer 6), tritium is expected to be present in the groundwater at a concentration exceeding its MCL for more than 100 years (Figure 5-3). A cross-section of the base case tritium plume at 25 yr is provided in Figure 5-5 that shows higher concentrations of tritium at depths at the source than adjacent to Steel Creek.

The farthest downgradient wells within the model domain (three well clusters PGW014, PGW026 and PGW027) located near Steel Creek were used to evaluate predicted breakthrough. In particular, wells PGW014DU, PGW026DL, and PGW027DU (all assumed to be in layer 2, TZ) were used to analyze the current impact to the wells associated with movement of contaminated groundwater reaches to Steel Creek. The predicted future tritium concentrations in groundwater at those locations are shown in Figure 5-6. The model results indicate that the predicted maximum tritium concentration in groundwater at location PGW014DU is 546 pCi/mL (Model Year 3) and that the predicted tritium concentration will exceed the MCL for up to 32 years (Table 5-2). At PGW026DL the maximum tritium concentration in groundwater is 151 pCi/mL (Model Year 10) and it will take 29 years to drop below the MCL. At PGW027DU the maximum concentration is 2757 pCi/mL (Model Year 2) and it will take 22 years to drop below the MCL. At PSB002AA, a well in the GCU (layer 7), the maximum concentration is the starting concentration and it takes 77 years to drop below the MCL. No vertical transport of tritium into the GAU above the MCL occurs over time. Observed tritium concentration in groundwater at well PGW014DU ranged from 13.5 pCi/mL in 2004 to 8.4 pCi/mL in 2014, at well PGW026DL it ranged from 54.2 pCi/mL in 2011 to 121 pCi/mL in 2015 and at well PGW027DU it ranged from 4020 pCi/mL in 2011 to 1300 pCi/mL in 2015. The concentration at PSB002AA ranged from 3430 pCi/mL in 2011 to 5860 pCi/mL in 2015.

**Table 5-2 Predicted Future Tritium Concentrations in Groundwater**

| Location | Maximum Tritium Concentration (pCi/mL) | Time of Maximum Tritium Concentration (yr) | Time to Reach MCL (yr) |
|---|---|---|---|
| **Groundwater at Well PGW014DU** | 546 | 3 | 32 |
| **Groundwater at PGW026DL** | 151 | 10 | 29 |
| **Groundwater at PGW027DU** | 2757 | 2 | 22 |
| **Groundwater at PSB002AA** | 5630 | 0 | 77 |
| **Groundwater Discharge into Steel Creek[a]** | 2139 | 0 | 27 |
| **Surface Water at SC-04** | 430 | 3 | 17 |

[a]Groundwater discharge to Steel Creek represents the maximum concentration for the entire reach of Steel Creek and P-Area Discharge Canal.

MCL = Maximum contaminant level.

Figure 5-7 shows the tritium discharging into the portion of the canal draining towards Steel Creek and to the entire reach of Steel Creek, including the wetlands draining into Steel Creek. The transport model predicts that the tritium discharge rate into Steel Creek ranges from a peak discharge rate of 106 Ci/yr in the 3rd year to 0.4 Ci/yr in the 30th year with an average rate of 27.5 Ci/yr over the first 30 years. The observed activity flux found at SC-04 was 111 Ci/yr in November 2014. At the P-Area Reactor Discharge Canal, the peak discharge rate is 3.2 Ci/yr at year 10. The predicted maximum tritium concentration through time in groundwater discharging anywhere into Steel Creek is 2,139 pCi/mL at model year 0 and decreasing below the MCL after 27 years (Figure 5-8).

Tritium predicted to discharge to Steel Creek (including the canal that drains to Steel Creek) and flow past SC-04 is shown in Figure 5-9. The tritium concentration in surface water at SC-04 was estimated by dividing the model-predicted flux by the average measured stream flow at SC-04 [that accounts for both groundwater discharge and surface runoff of 0.276 cubic feet per second

(cfs)]. Location SC-04 was chosen for this evaluation because it was the point furthest downstream evaluated in the model, un-impacted from contaminated groundwater discharge, and can be used to estimate the effectiveness of the various future alternatives. The calculated tritium concentrations in surface water (SC-04) indicate that the tritium concentration would be below the MCL within 18 years and that concentrations decrease from 430 pCi/mL in the 3rd year to 19.2 pCi/mL (i.e., below the MCL) in the 17th year (Figure 5-9). The observed tritium concentration in surface water at SC-04 ranged from a maximum of 906 pCi/mL in 2002 to a minimum concentration of 227 pCi/mL in 2015. The calculated tritium concentration in surface water is comparable with the measured tritium concentration.

As stated above, the transport model indicates that the tritium plume elongates along Steel Creek (Figure 5-1) through time, but that the groundwater plume is not predicted to reach stream gauge location SC-04 at concentrations exceeding its MCL. However, the calculated surface water concentration of tritium in Steel Creek is significantly higher than the MCL at location SC-04 (Figure 5-9). This indicates that tritium released into the creek between SC-02 and SC-04 impacts the surface water at SC-04. The model also shows that tritium entering into Steel Creek downstream of location SC-01 (Figure 5-1). The plume does move past SC-04 in the ULAZ towards L Lake, but the plume degrades and disperses before reaching L Lake for the entire 100 year simulation.

The model predicts that tritium will not impact any other surface water bodies in the vicinity of P Area, including PAR Pond and the canals and tributaries of PAR Pond within the modeled timeframe.

#### 5.2.1.2 CVOC Simulation Results

Transport of CVOCs was simulated for a period of 300 years under steady-state flow conditions using MT3DMS (Zheng 1999). Figures 5-10 through 5-13 show predicted TCE plumes in the TZ, ULAZ, and LLAZ after 5, 25, 100 and 300 years of simulation, respectively. The predicted PCE plumes change little over 100 years of simulation and are shown in Figures 5-14 through 5-16.

These results indicate that migration of TCE through groundwater is primarily westward towards Steel Creek in the A/AA and TZ units and eastward towards PAR Pond in the ULAZ. However, TCE does not migrate to PAR Pond or unnamed tributaries within the period of simulation (300 years). A longer simulation time would find the ULAZ plume extending to the constant head boundaries. The transport simulations suggest that PCE and TCE are expected to be present in the groundwater above MCLs for more than 300 years. Cross sections of the TCE plume at 25 and 100 years are provided in Figures 5-17 and 5-18, respectively.

The predicted transport model breakthrough curve in groundwater for TCE for layer 2 (TZ) wells PGW014DU and PGW026DL is shown in Figure 5-19. These locations were chosen, as they are near the centerline of the observed TCE plume at Steel Creek. The model results indicate that TCE concentrations will exceed the MCL in groundwater for over 100 years at the PGW026DL, while at PGW014DU, the concentration drops to the MCL by year 50. The peak TCE concentration in groundwater occurs at Model Year 0 at the starting concentration for both PGW014DU and PGW026DL (Table 5-3). The highest starting concentration for TCE in the A/AA and TZ is at PGW026DL, which was drawn with a tight contour around it (Figure 2-7). Once that small high passes through there is only lower concentration portions of the starting plume moving towards Steel Creek that are shown in Figure 5-19. The observed TCE concentrations in groundwater at well PGW014DU ranged from 396 µg/L in January 2004 to 130 µg/L in August 2014, in well PGW026DL ranged from 5,200 µg/L in June 2011 to 4,500 µg/L in 2014 to 4900 µg/L in Feb 2015.

Figure 5-20 shows the total TCE discharge to the canal and Steel Creek for the first 100 years. The transport model predicts TCE entering Steel Creek at a peak rate of 19 kg/yr in Model Year 8 with an average rate of 7.7 kg/yr over the first 100 years. The maximum concentration discharging into Steel Creek and the canal is 351 µg/L in Model Year 10 (Table 5-3 and Figure 5-21). Based on the TCE discharge results of the transport model, the predicted TCE concentration in surface water at SC-04 was estimated by dividing the predicted TCE mass discharge to Steel Creek (including the wetlands) by the average measured stream flow at SC-04 (0.276 cfs). The calculated TCE concentration in surface water (at SC-04) suggests that the TCE concentration would not fall below the MCL within 100 years (Figure 5-21) and that the concentration would peak at 79 µg/L in Model Year 8 (Figure 5-22). However, the maximum

TCE concentration observed in surface water at SC-04, to date, has been 0.78 µg/L in March 2015 and 28 µg/L in March 2015 for SC-03 (Figure 2-12). The fact that the model predicts current and future TCE concentrations in surface water that are much higher than observed TCE concentrations suggests that there may be wetland or surface water TCE attenuation processes that are not accounted for in the groundwater model. In particular, the model does not take into consideration volatilization in the stream or increased biodegradation in wetland sediments. While TCE and PCE do migrate eastward towards PAR Pond, they do not reach PAR Pond within the period of simulation (300 years).

**Table 5-3 Predicted Future TCE Concentration in Groundwater**

| Location | Groundwater at Well PGW014DU | Groundwater at PGW026DL | Groundwater Discharge into Steel Creek[a] | Surface Water at SC-04 |
|---|---|---|---|---|
| Maximum TCE Concentration (µg/L) | 130 | 4500 | 351 | 79 |
| Time of Maximum TCE Concentration (yr) | 0 | 0 | 10 | 8 |
| Time to Reach MCL (yr) | 47 | >300 | >100 | >100 |

[a]Groundwater discharge to Steel Creek represents the maximum concentration for the entire reach of Steel Creek and P-Area Discharge Canal.

MCL = Maximum contaminant level.
TCE = Trichloroethene.

## 5.3 Transport Model Sensitivity Analysis

Predictive sensitivity analysis is performed on groundwater models to assess the effects of parameter, boundary condition, or conceptualization uncertainty on the results. The procedure generally involves changing a single aspect (parameter, boundary condition, etc.) of the model by a pre-determined amount (usually within a reasonable range of certainty) and comparing the results to the original model results. This procedure is repeated several times where independent changes are made to assess low and high ranges of uncertainty for a suite of parameters. Key transport-model parameters were varied to assess the change on model predictions. The parameters included: porosity, dispersivity, degradation rates of CVOCs and sorption coefficient ($K_d$) for both CVOC and for tritium.

In one set of sensitivity simulations, the first-order degradation rates for TCE and PCE were multiplied and divided by two (i.e., half-life changed from 25 to 12.5 yr and 50 yr). Degradation of CVOCs is assigned to the dissolved phase and not the sorbed phase, as bacteria that degrade CVOCs are most efficient in the dissolved phase. The results are summarized in Figure 5-23 for concentration versus time in wells PGW014DU and PGW026DL. Figures 5-24 and 5-25 show the plumes in the TZ and ULAZ, respectively, with a half-life of 12.5 yr, which is similar to the half-life of 10 yr used in the 2011 model (SRNS 2011a). The increased degradation rates slightly reduced the concentration of TCE at PGW026DL in Model Year 100 from 233 to 194 μg/L, a decrease of approximately 39 μg/L (Figure 5-23), while the decreased degradation rate slightly increased the concentration of TCE at PGW026DL in Model Year 100 from 233 to 256 μg/L, an increase of approximately 23 μg/L.

For the sensitivity of CVOC sorption coefficient, the $K_d$ for all layers and CVOC constituents were divided by 10. This resulted in faster plume movement, as shown in Figures 5-26 to 5-28, and consequently increased discharge into Steel Creek. This results in the TCE concentration dropping below MCL in Model Year 29 rather than Model Year 49 for well PGW014DL (Figure 5-26). Figure 5-26 indicate that the plume is greatly reduced after 100 yr with the reduction in $K_d$.

To approximate the observed retardation of the tritium plume at the Site a sensitivity of $K_d$ was completed with tritium assuming a $K_d$ equal to 0.1 and 1. These values result in retardation values of approximately 1.5 and 6. Note the half-life was applied to both the dissolved and sorbed phases, as the tritium decays while sorbed to the soils. Increasing the $K_d$ results in the plume taking longer to reach concentrations below the MCL at downgradient locations (Figures 5-29 and 5-30). While the basecase takes 22 years for PGW027DU to drop below the MCL for a $K_d$ of 0.1 it takes 33 years and for a $K_d$ of 1 it takes over 100 years (Figures 5-29 and 5-30).

Another analysis was performed to evaluate the impact of using an effective porosity 0.3 versus 0.25 and longitudinal dispersivity of 10 ft versus 5 ft. This evaluation was performed by using the tritium transport model. In this case, the tritium transport model was re-run by varying the porosity from 0.3 to 0.25, longitudinal dispersivity from 10 to 5 ft, horizontal transverse dispersivity from 1 to 0.5 ft, and vertical transverse dispersivity from 0.1 to 0.05 ft throughout

the model domain at the same time. The results of this analysis indicate that the model has low sensitivity to the combined effects of these parameters, but that the plumes move through faster. As shown on Figure 5-31, the time it takes for the concentrations of tritium to drop below the MCL is reduced by about 3 years when both porosity and dispersivity are reduced.

In general, the sensitivity analysis indicates that lack of precise knowledge regarding CVOC degradation rates, formation porosity, and dispersivities will not have significant effect on modeling results. However, model predictions are sensitive to the degree to which CVOCs and tritium are adsorbed to mineral grains (i.e. the sorption coefficient, $K_d$). Sensitivity runs show that dividing the TCE $K_d$ by 10 (i.e. changing it from about 3 L/kg to 0.3), results in faster predicted plume movement, lower future TCE concentrations in groundwater, and shorter times to fall below the MCL. Conversely, increasing the tritium $K_d$ from zero to 0.1 or 1 L/kg would result in higher future tritium concentrations in the out-years, and longer times needed to fall below the MCL.

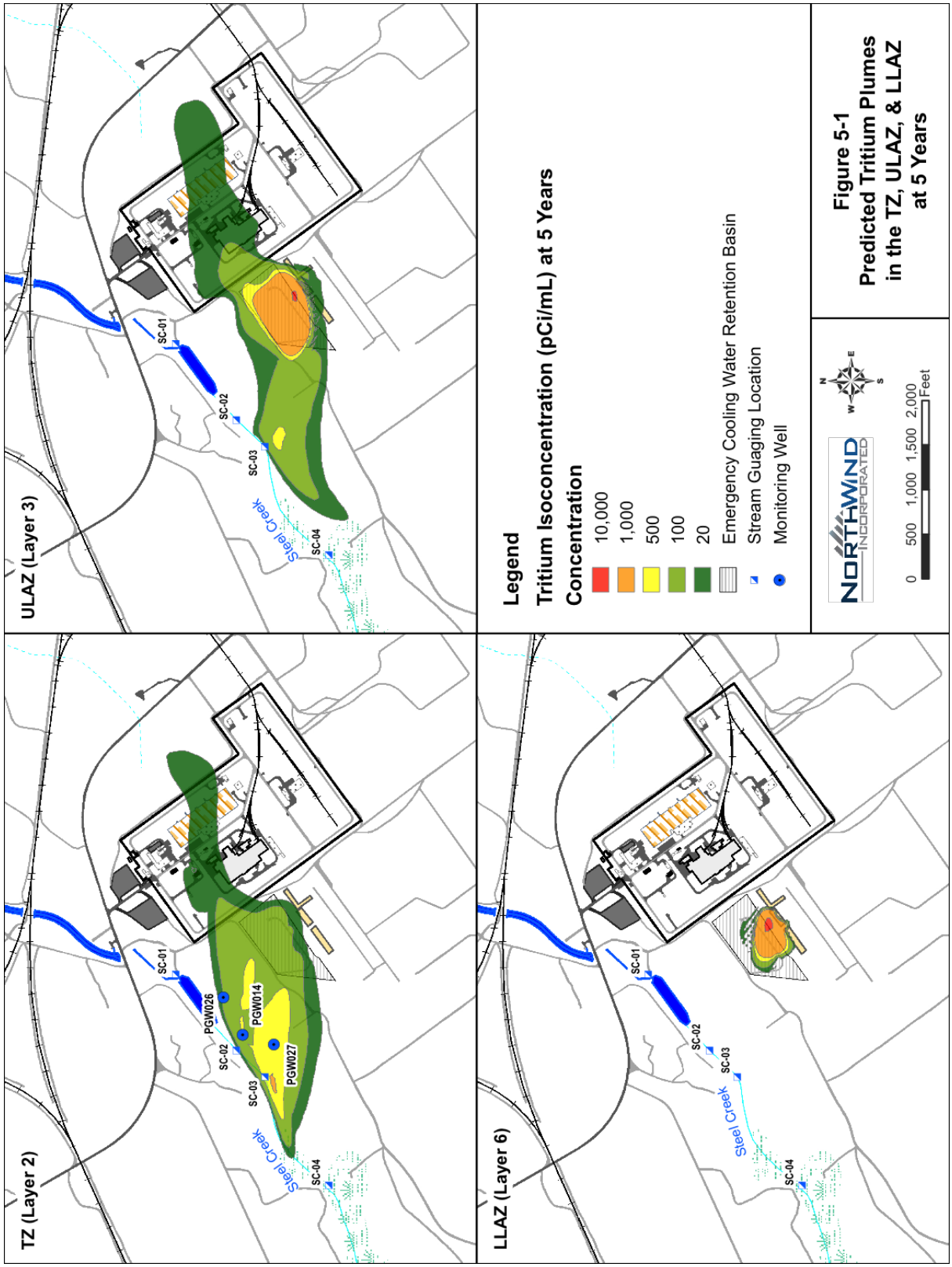


**Figure 5-1 Predicted Tritium Plumes in the TZ, ULAZ, & LLAZ at 5 Years**

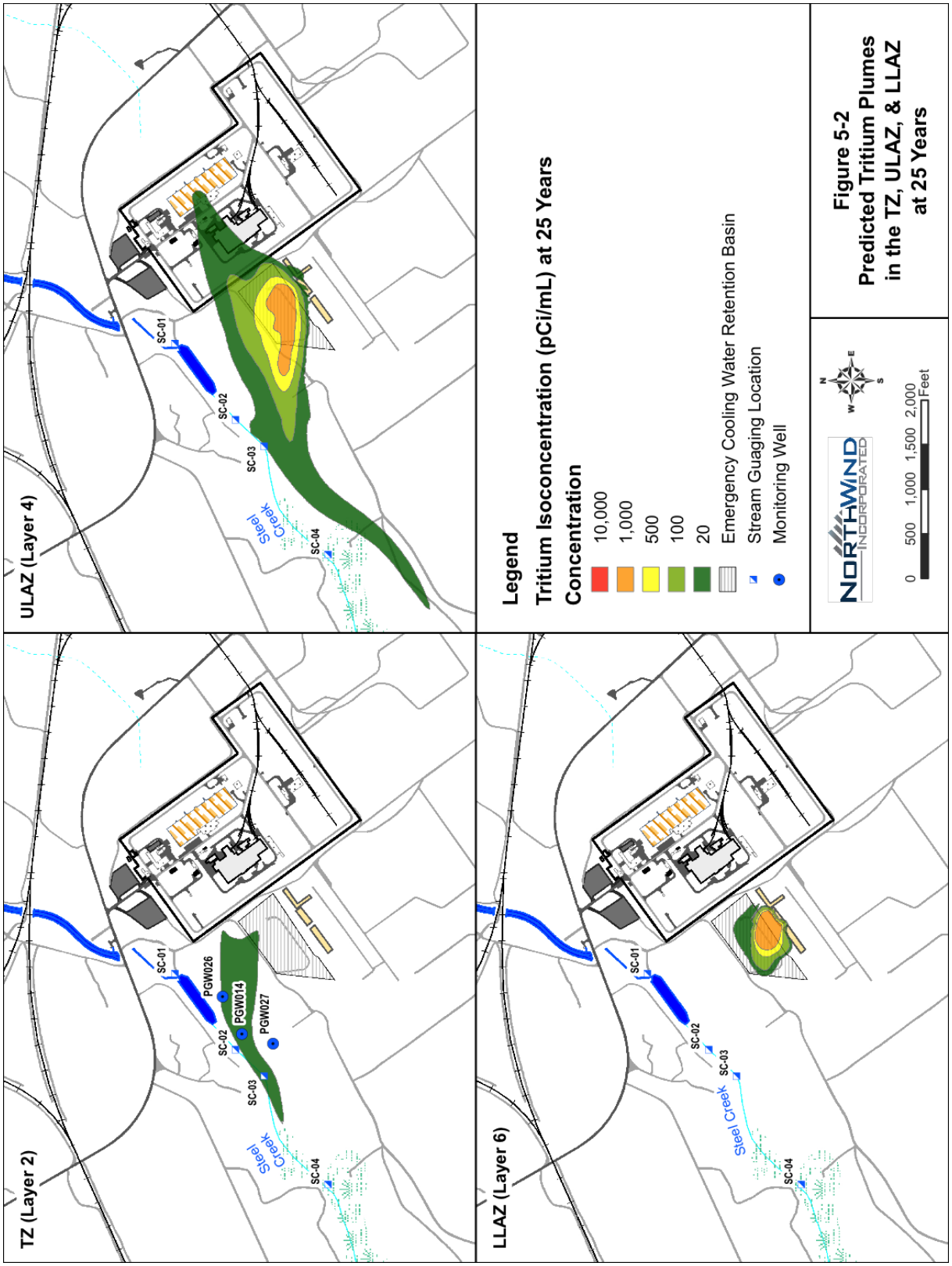


**Figure 5-2 Predicted Tritium Plumes in the TZ, ULAZ, & LLAZ at 25 Years**

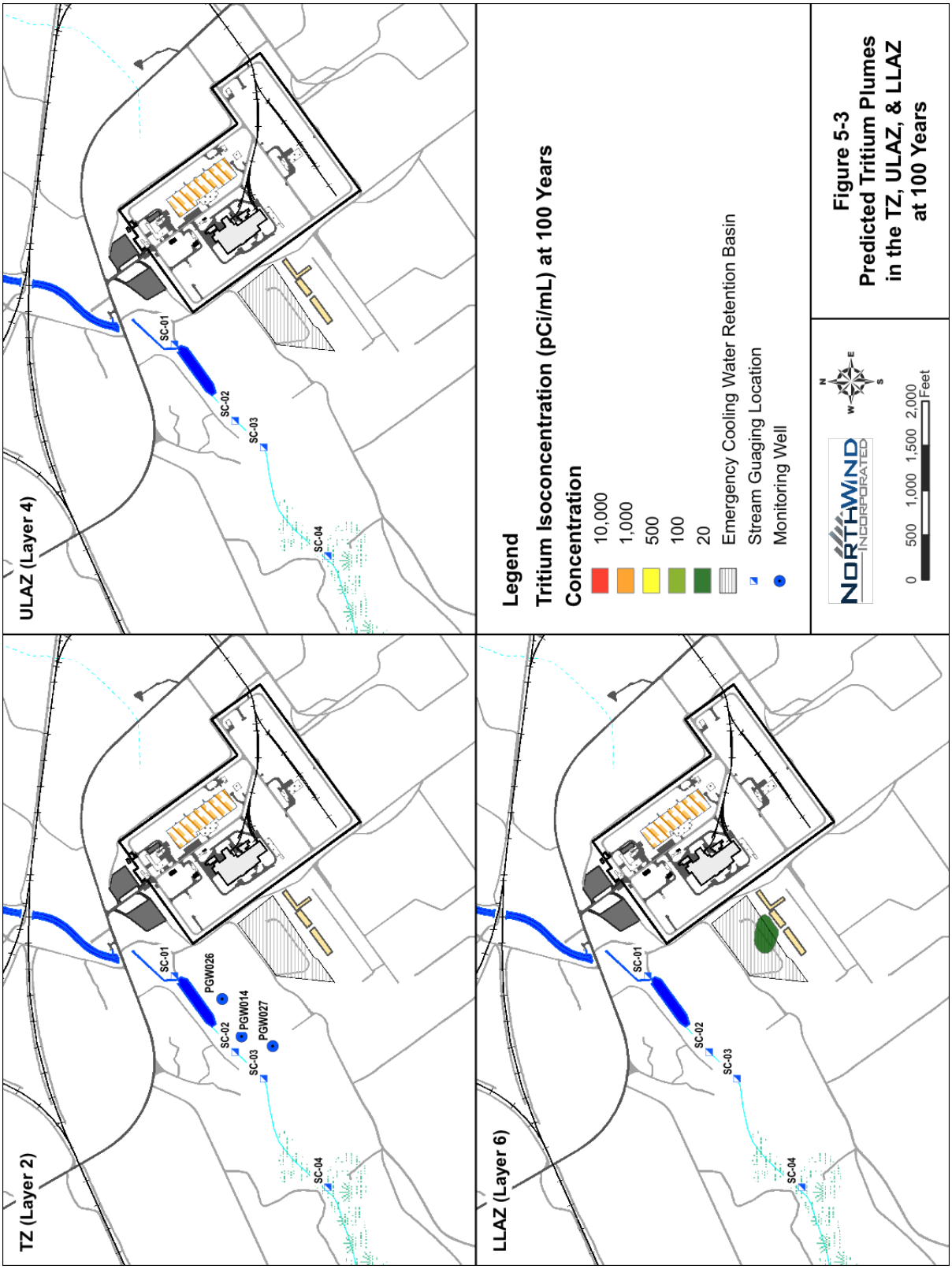


**Figure 5-3 Predicted Tritium Plumes in the TZ, ULAZ, & LLAZ at 100 Years**

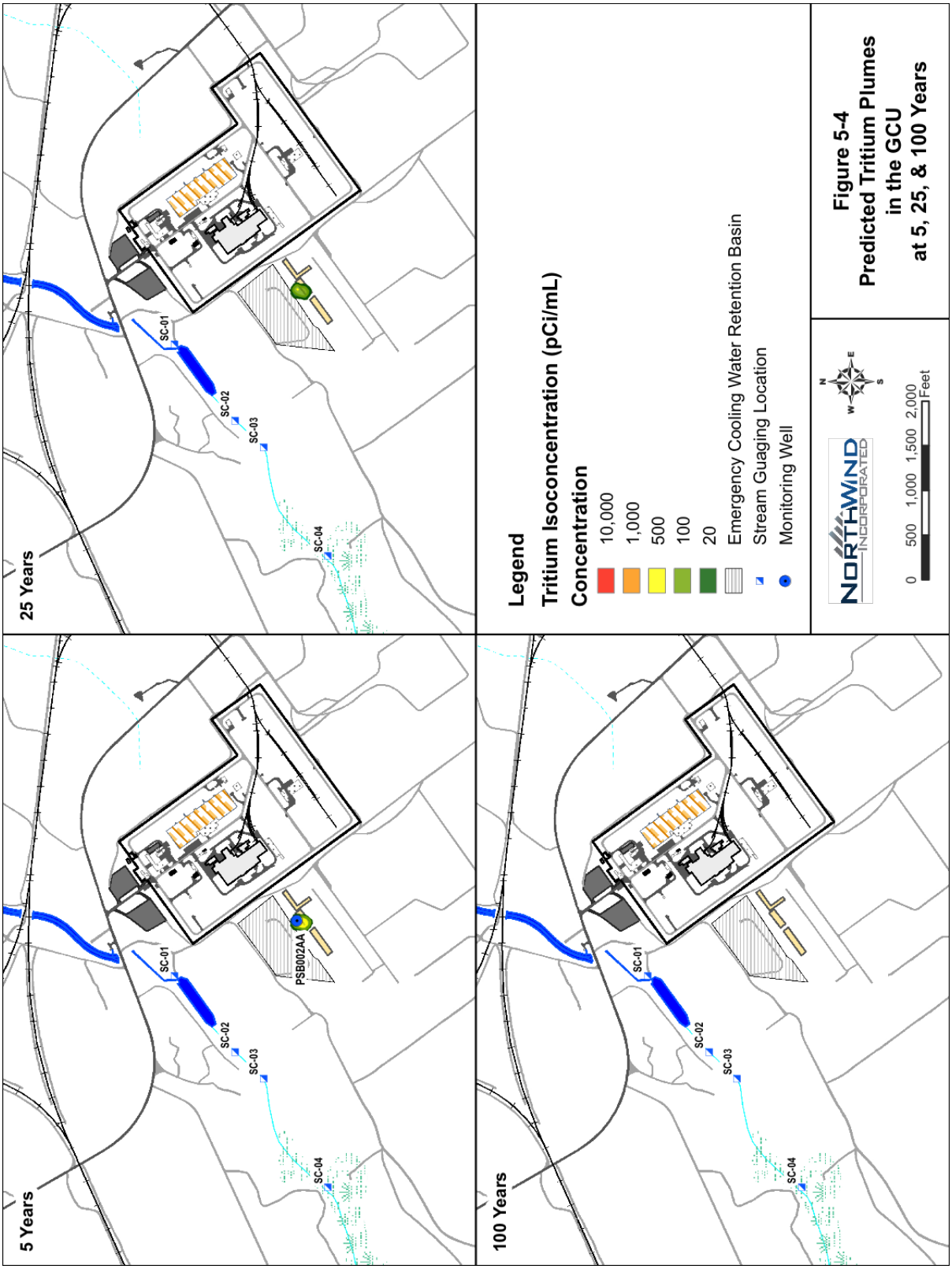


**Figure 5-4 Predicted Tritium Plumes in the GCU at 5, 25, and 100 Years**

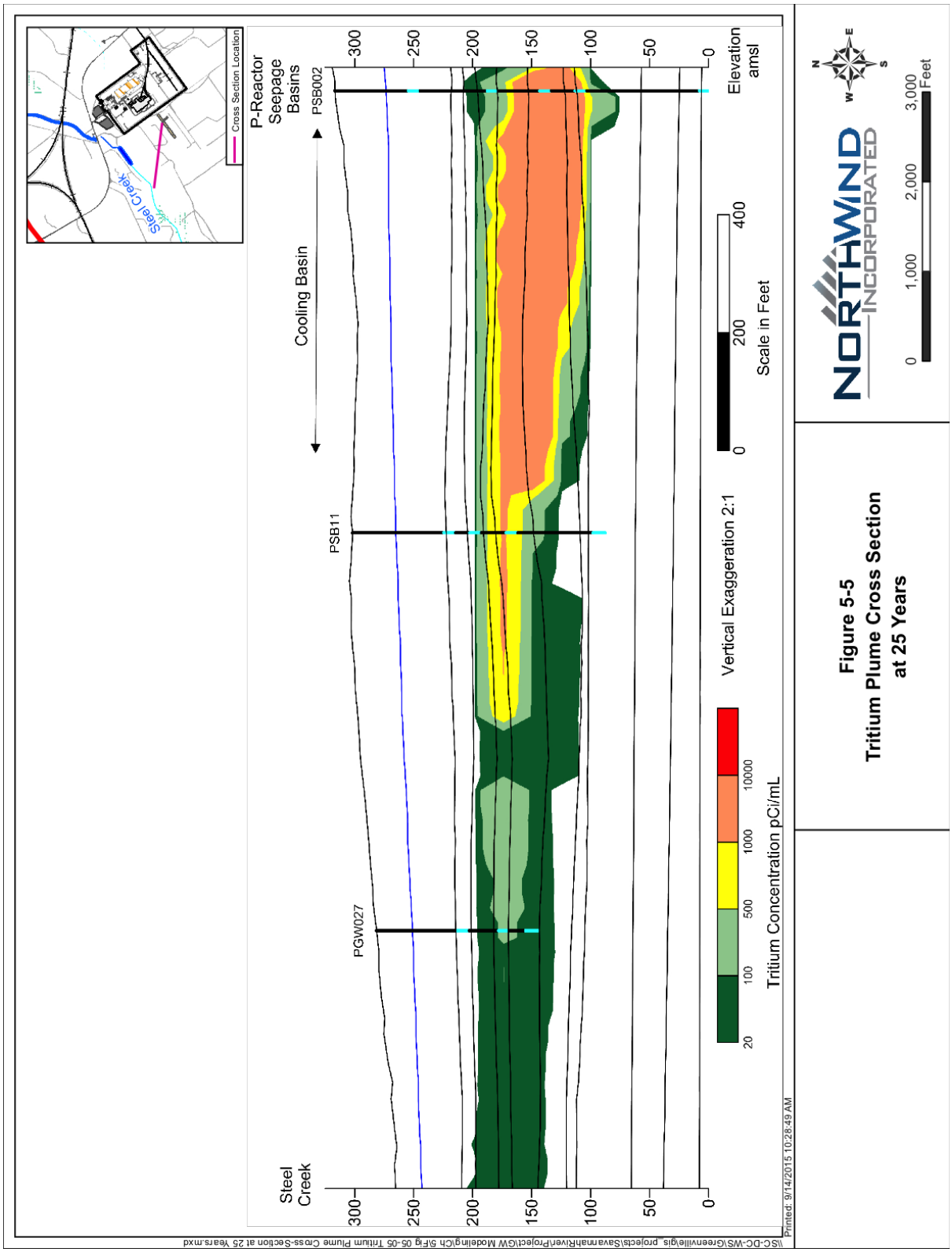


**Figure 5-5 Tritium Plume Cross Section at 25 Years**

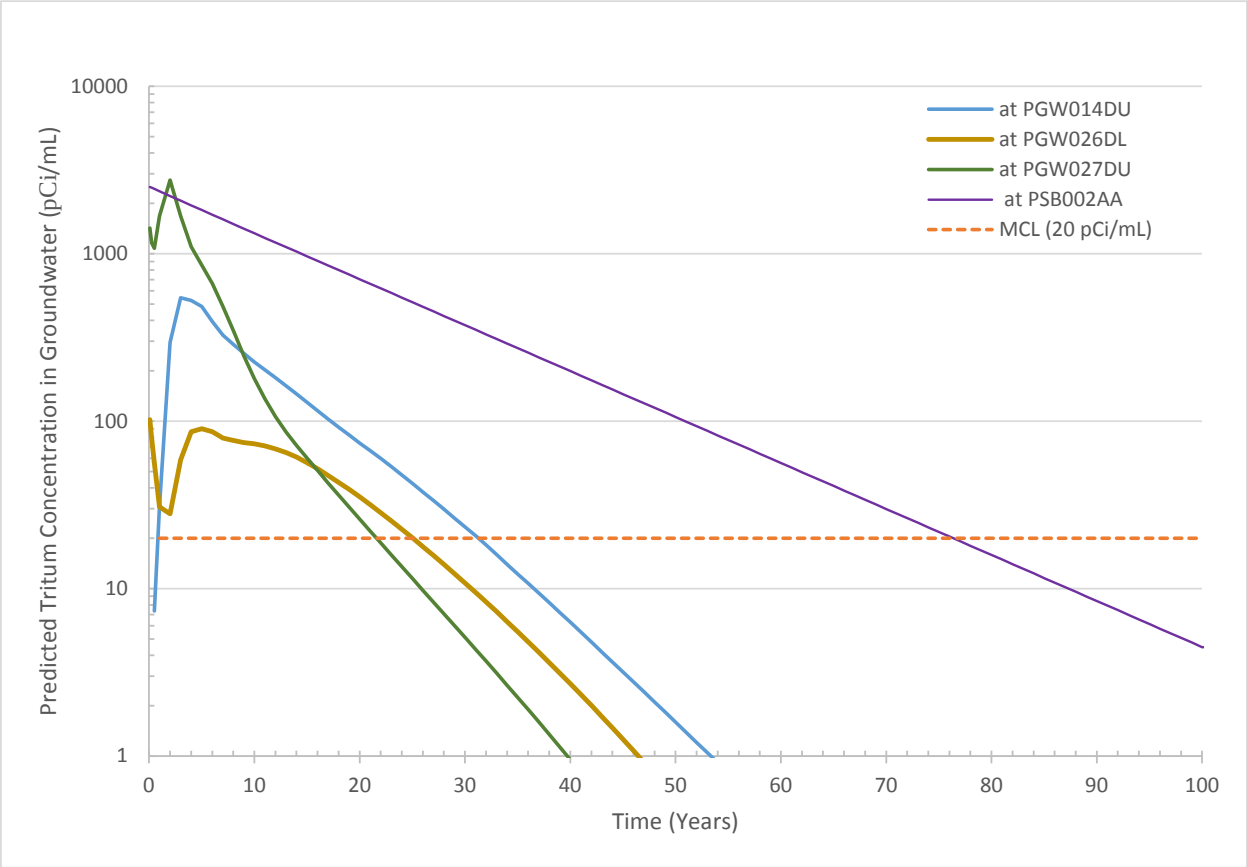


**Figure 5-6 Predicted Groundwater Tritium Concentration at Wells near Steel Creek in TZ (Layer 2) at PGW014DU, PGW026DL, and PGW027DU**

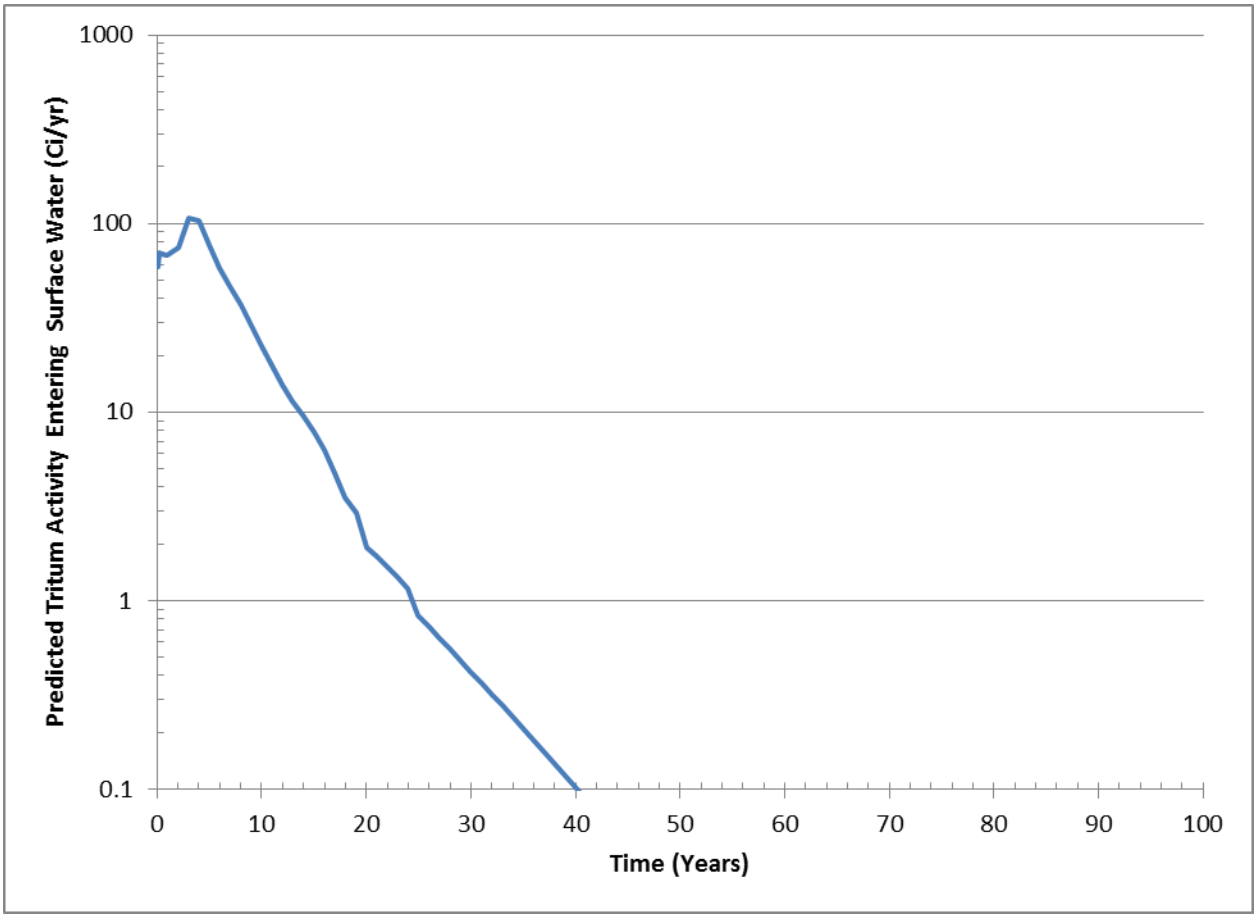


**Figure 5-7 Predicted Groundwater Activity Flux of Tritium Discharging to P-Area Discharge Canal and Steel Creek Passing SC-04**

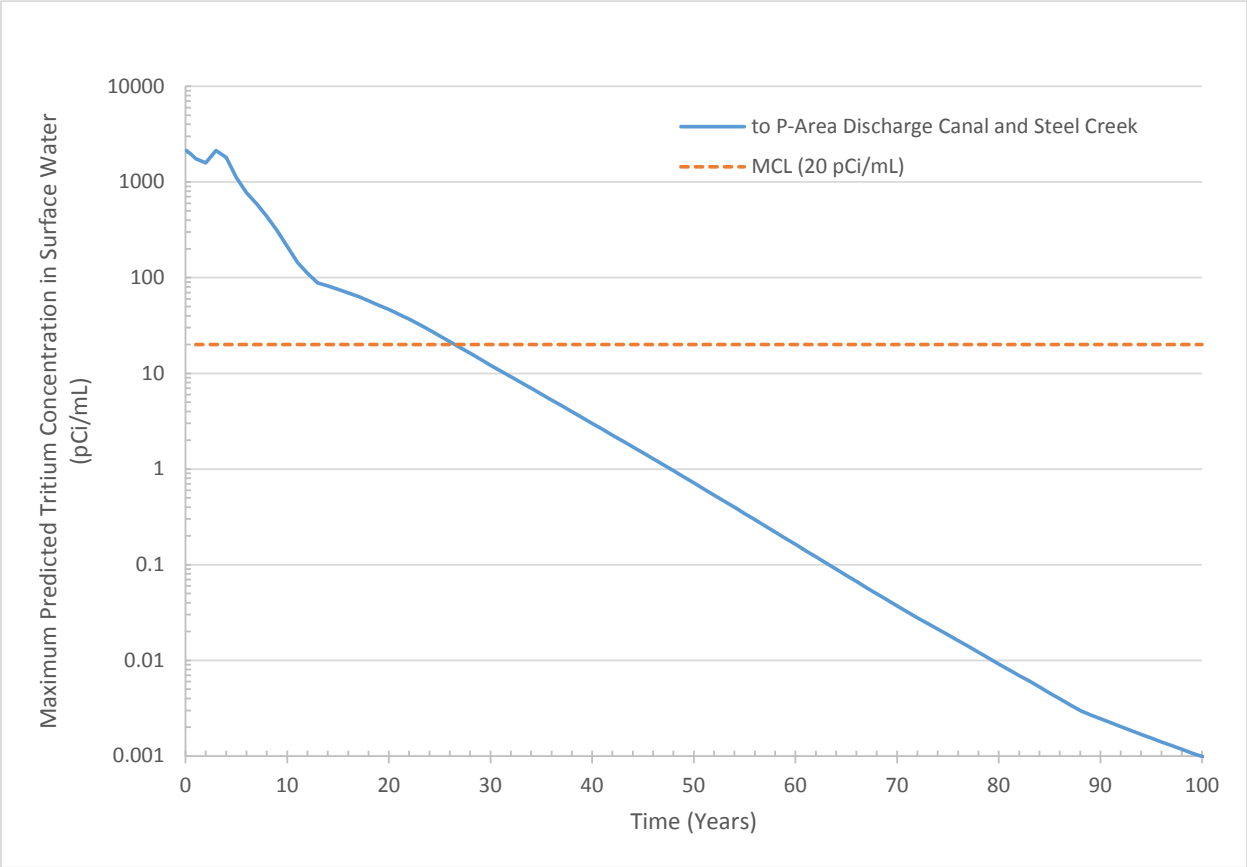


**Figure 5-8 Maximum Predicted Groundwater Tritium Concentration Discharging into P-Area Discharge Canal and Steel Creek**

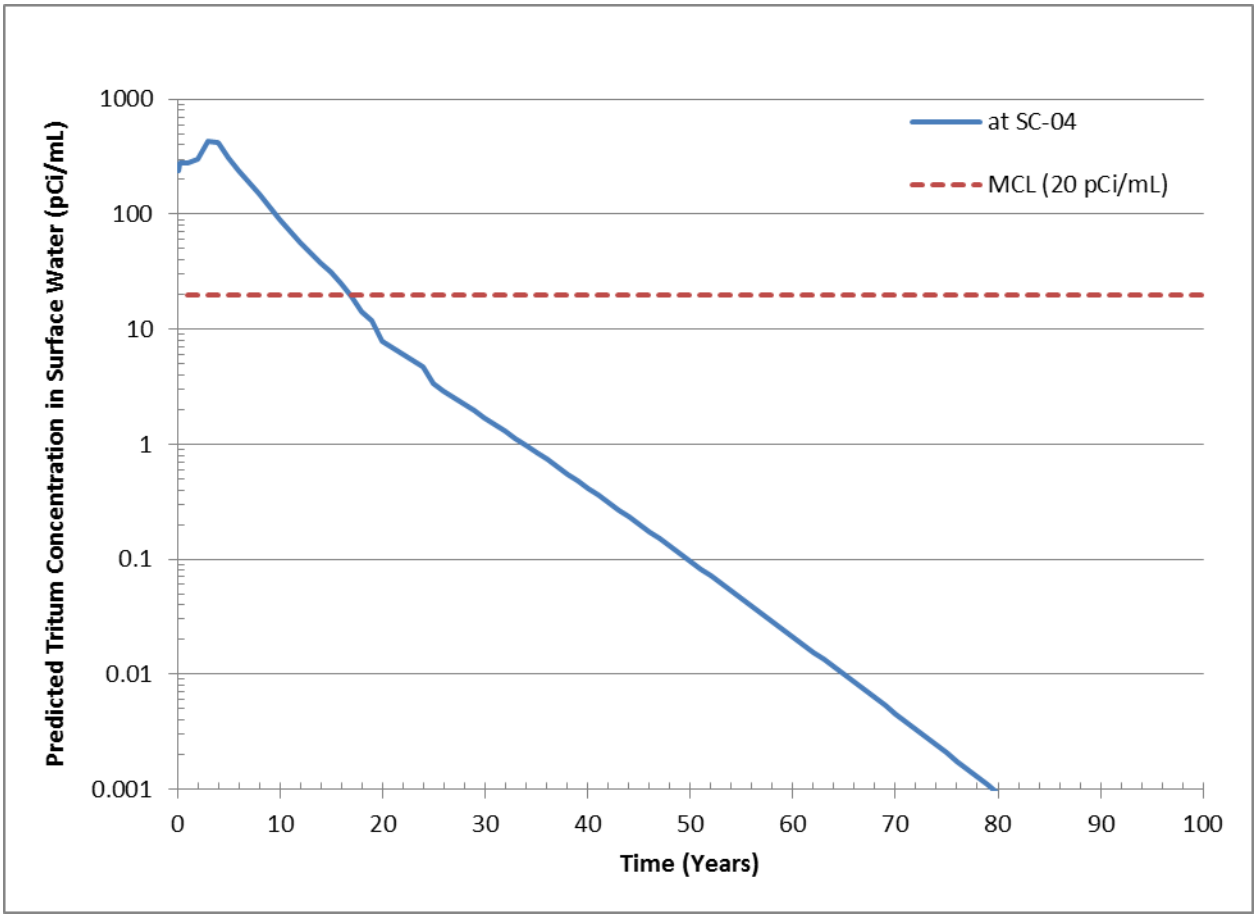


**Figure 5-9 Predicted Surface Water Tritium Concentration in Steel Creek at SC-04**

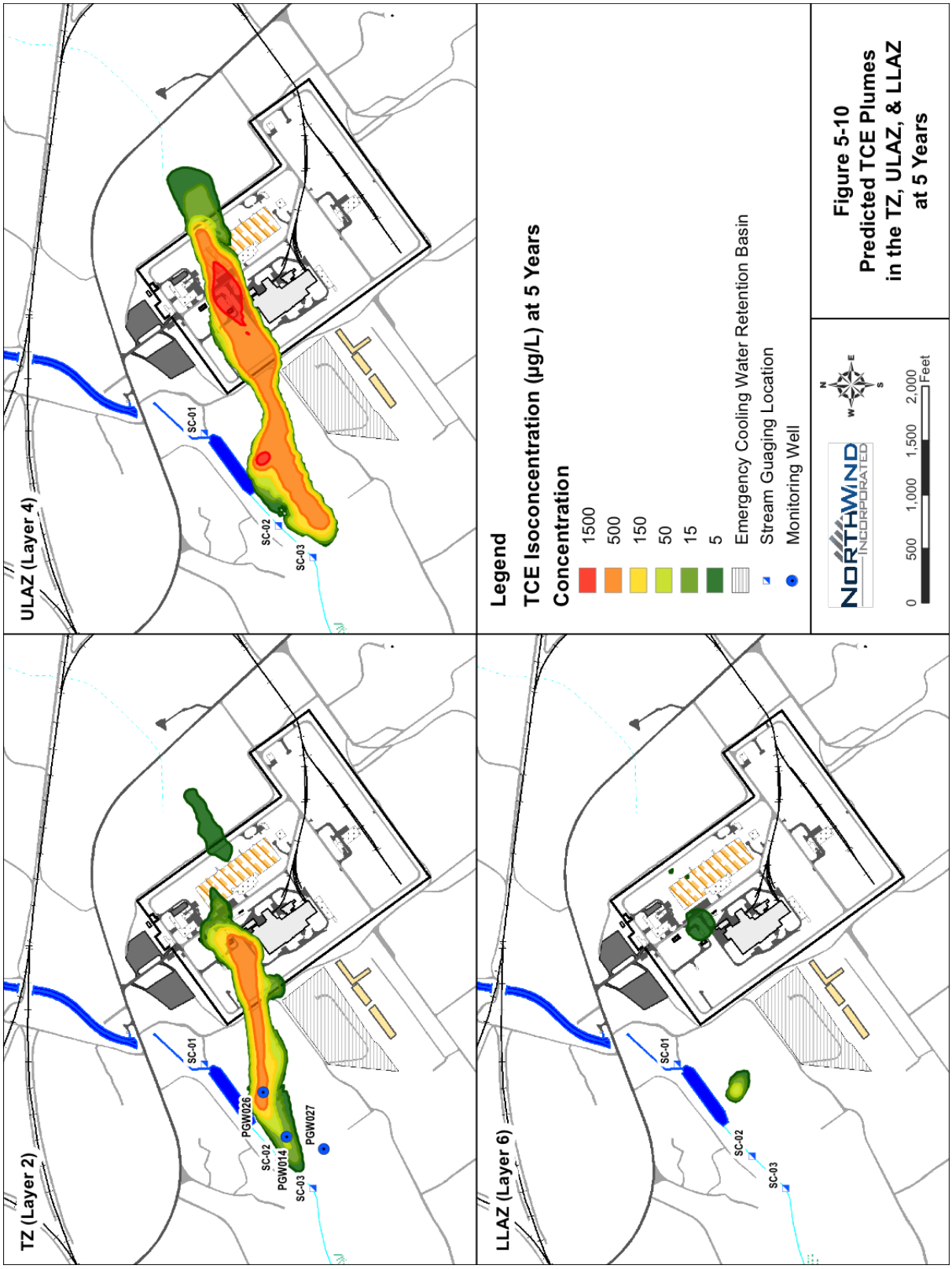


**Figure 5-10 Predicted TCE Plumes in the TZ, ULAZ, & LLAZ at 5 Years**

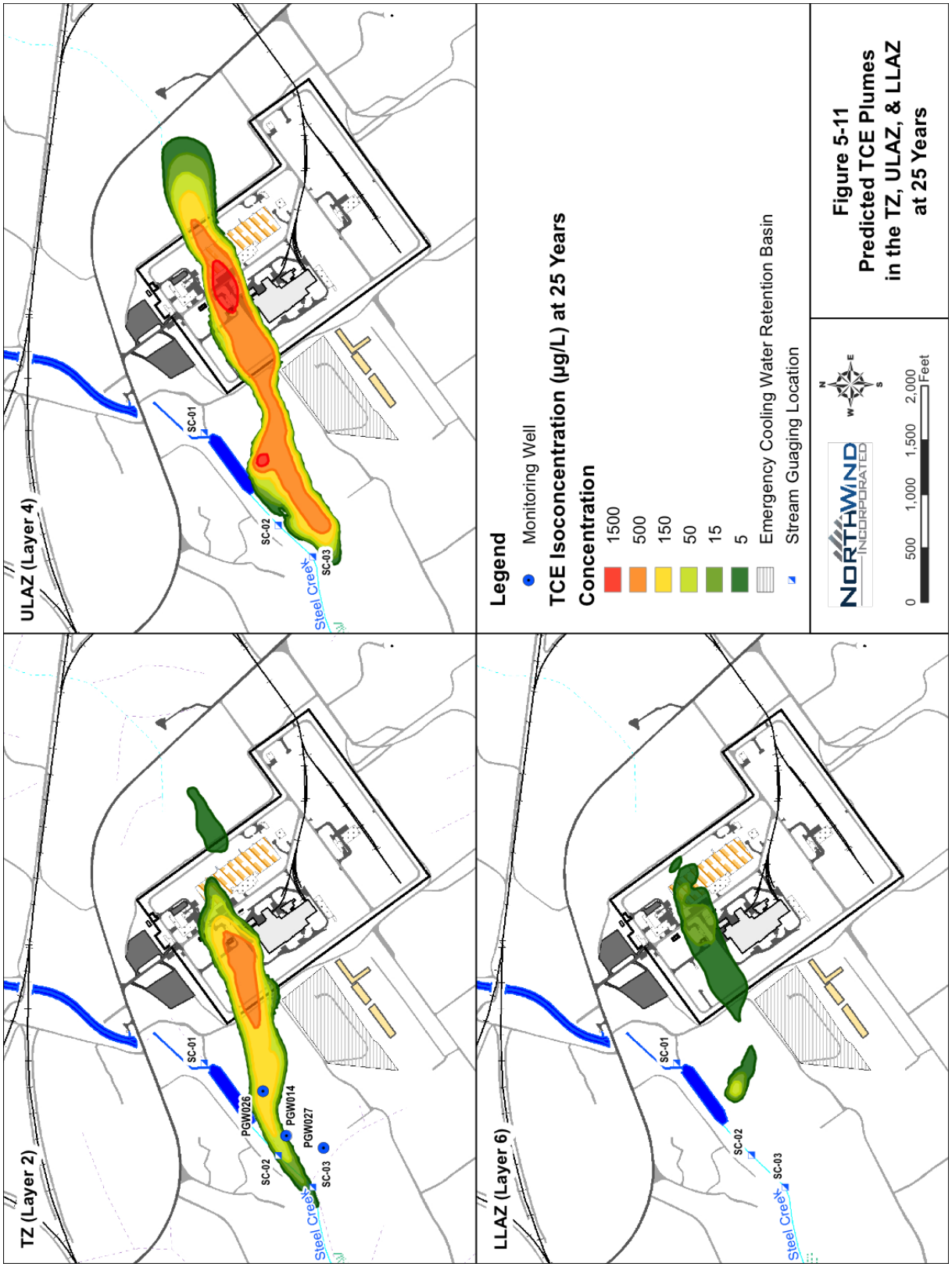


**Figure 5-11 Predicted TCE Plumes in the TZ, ULAZ, & LLAZ at 25 Years**

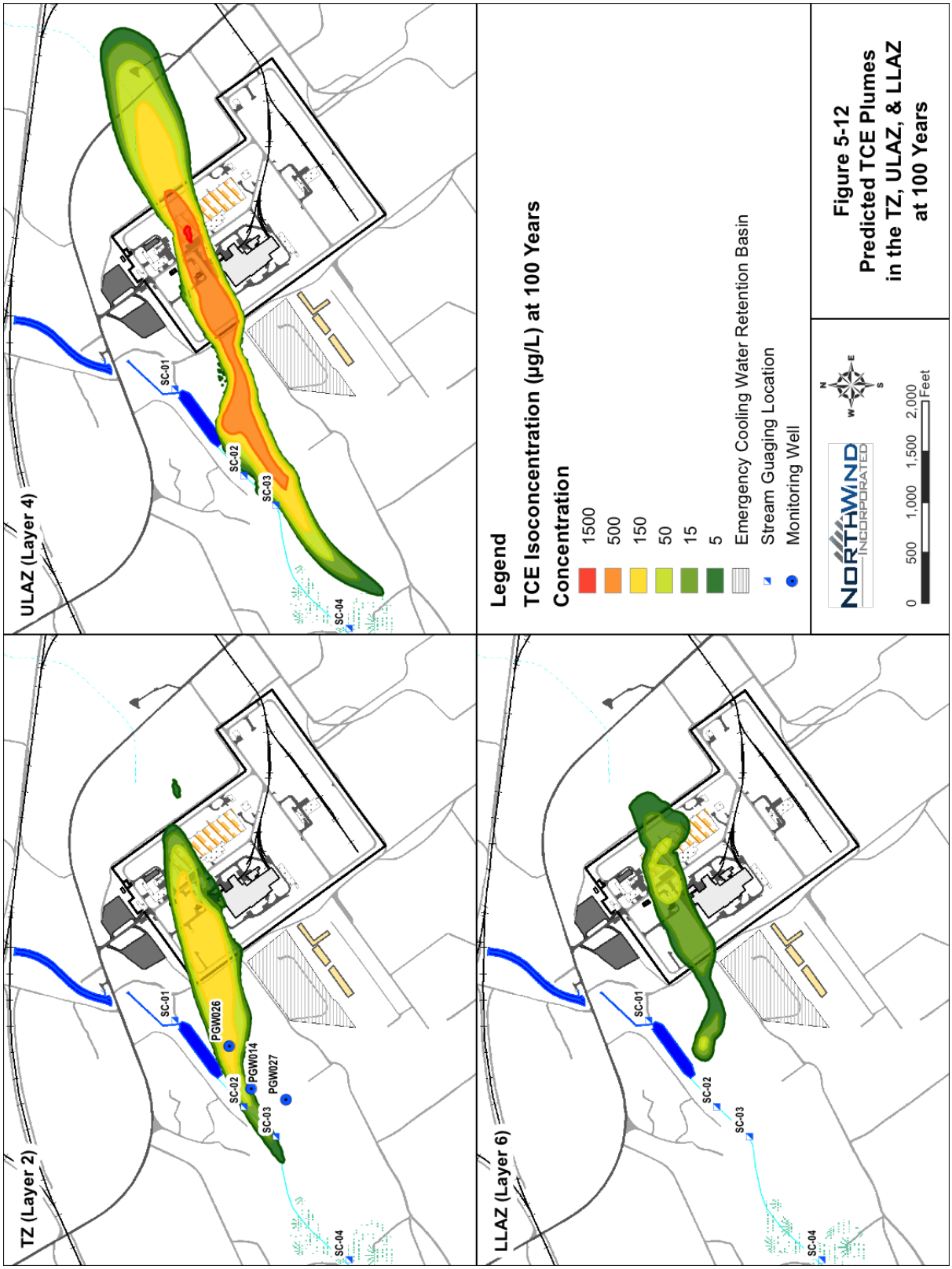


**Figure 5-12 Predicted TCE Plumes in the TZ, ULAZ, & LLAZ at 100 Years**

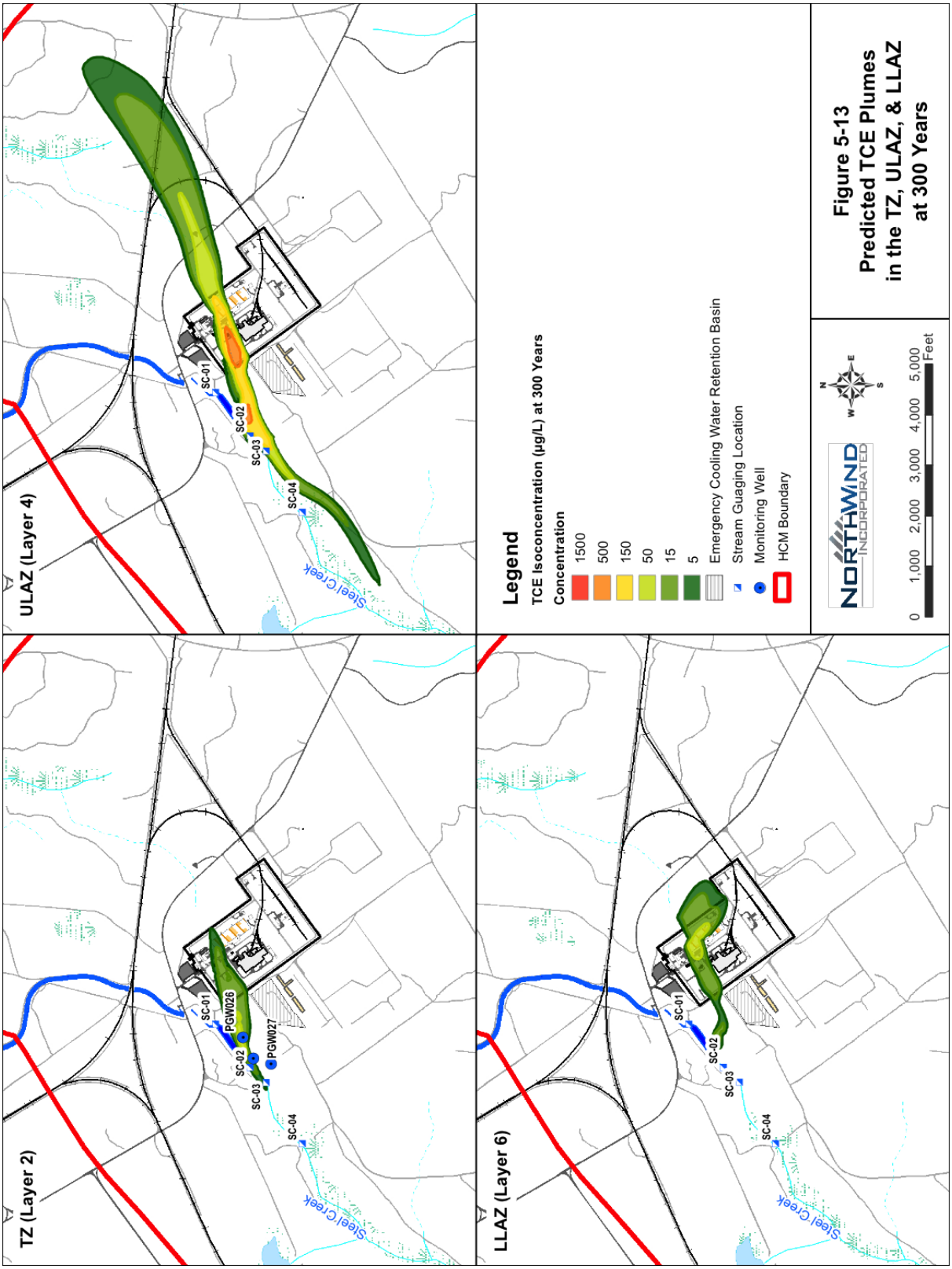


**Figure 5-13 Predicted TCE Plumes in the TZ, ULAZ, & LLAZ at 300 Years**


**Figure 5-14 Predicted PCE Plumes in the TZ, ULAZ, & LLAZ at 5 Years**

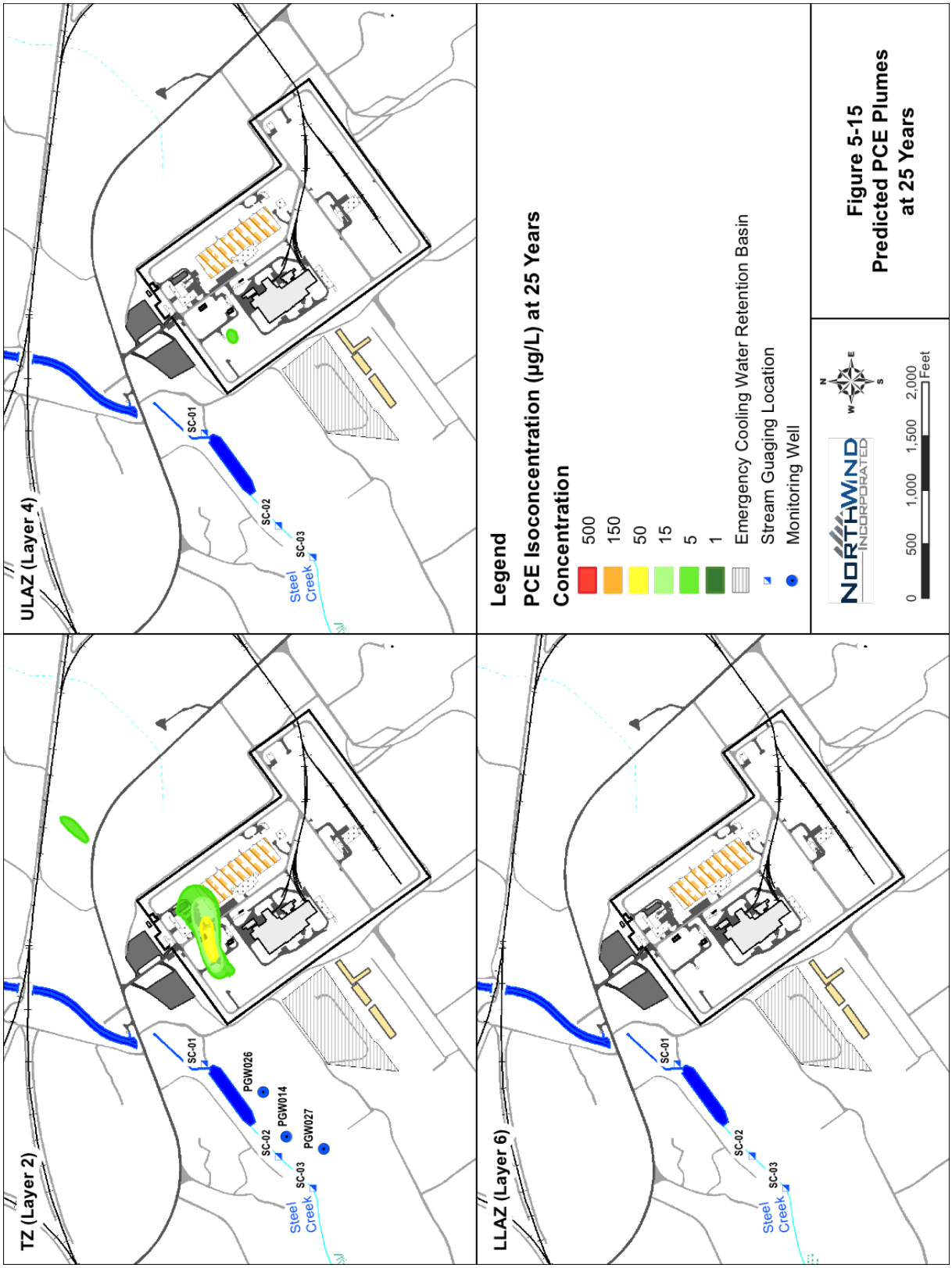


**Figure 5-15 Predicted PCE Plumes in the TZ, ULAZ, & LLAZ at 25 Years**

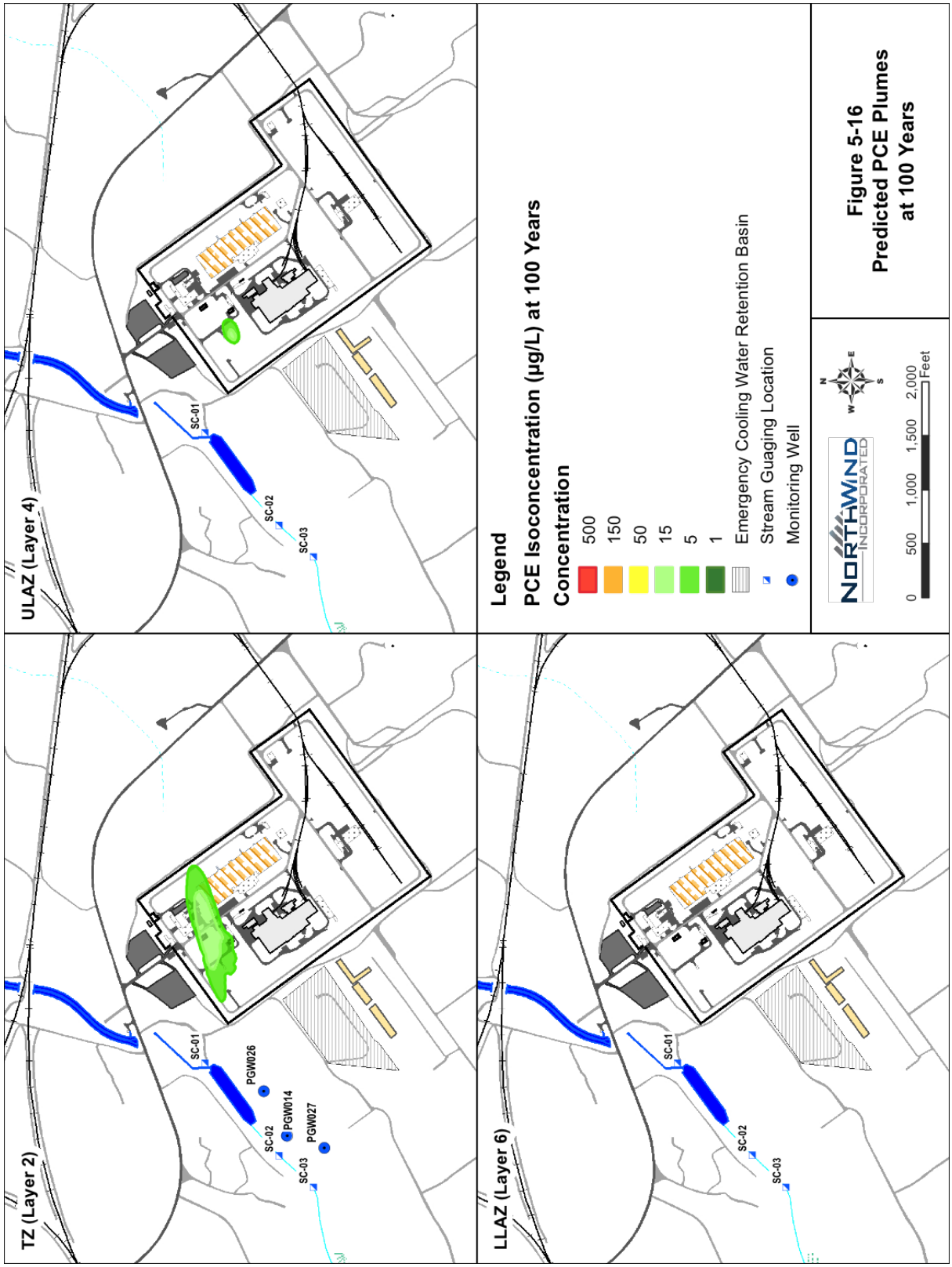


**Figure 5-16 Predicted PCE Plumes in the TZ, ULAZ, & LLAZ at 100 Years**

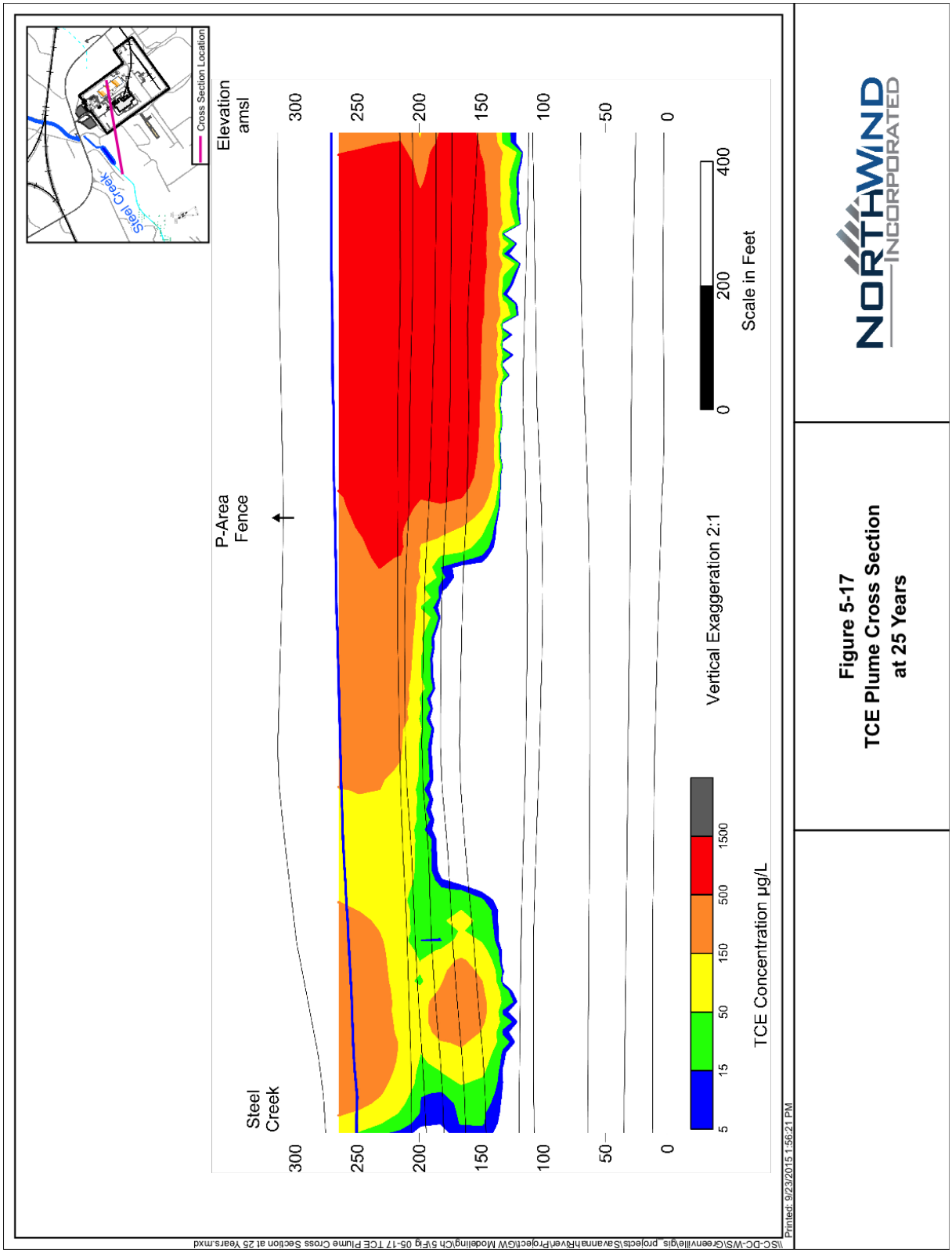


**Figure 5-17 TCE Plume Cross Section at 25 Years**

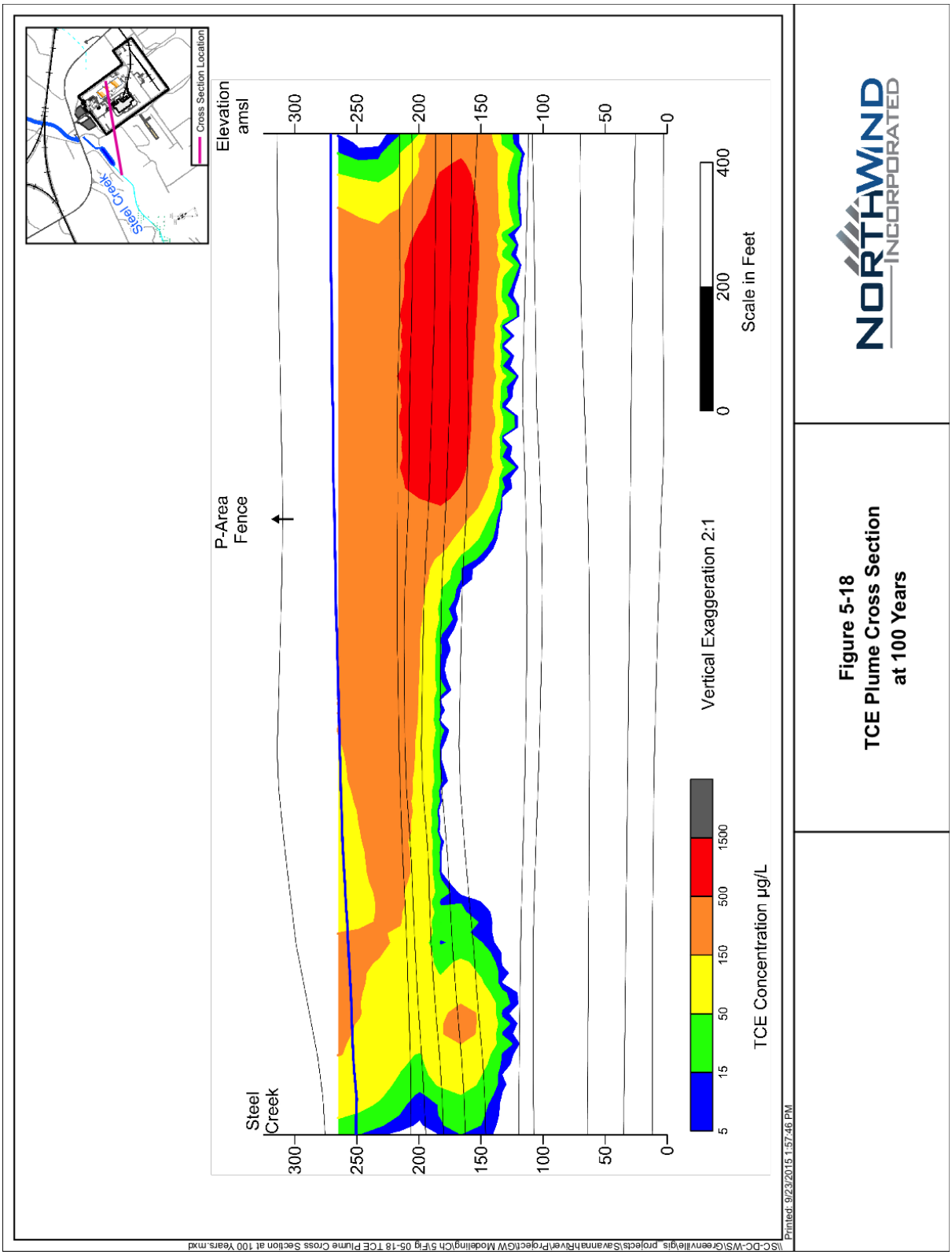


**Figure 5-18 TCE Plume Cross Section at 100 Years**

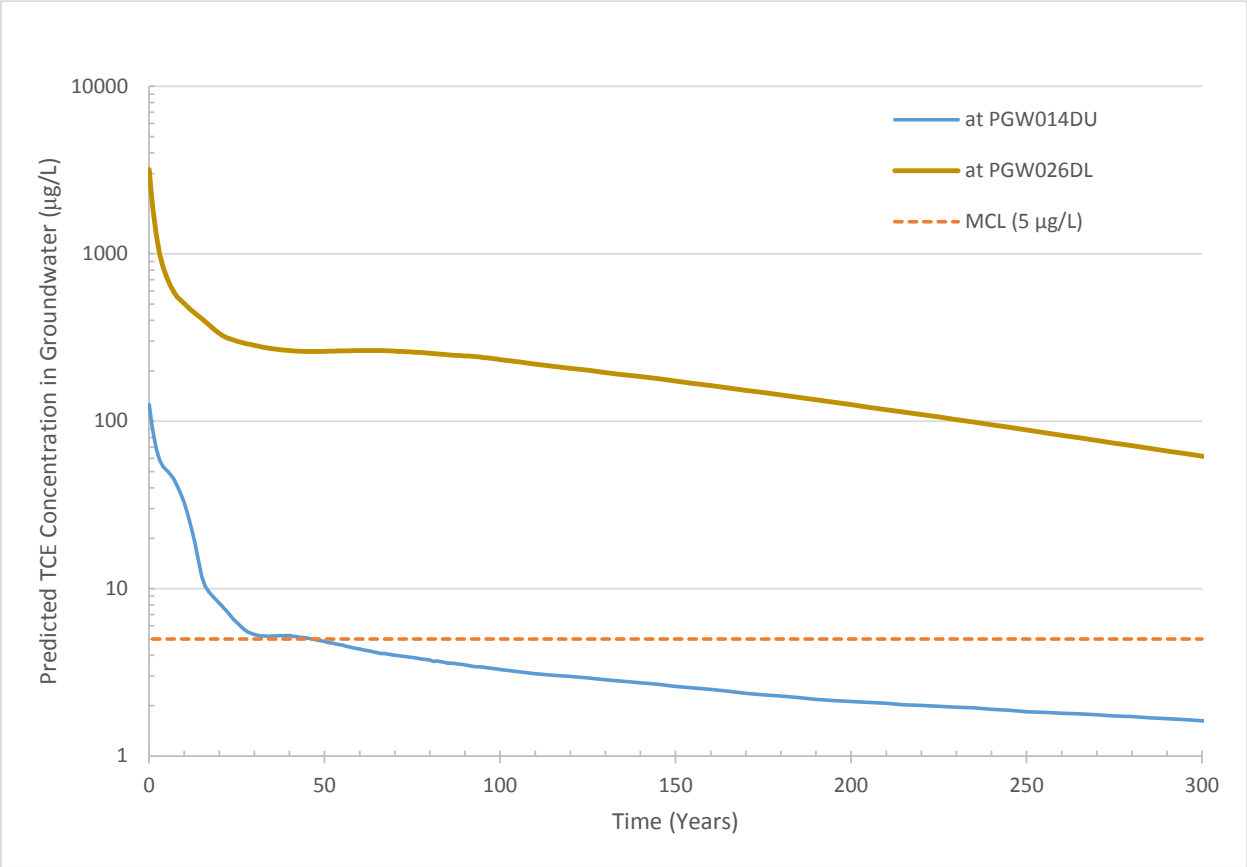


**Figure 5-19 Predicted Groundwater TCE Concentration at Wells near Steel Creek in TZ (Layer 2) at PGW014DU and PGW026DL for 300 Years.**

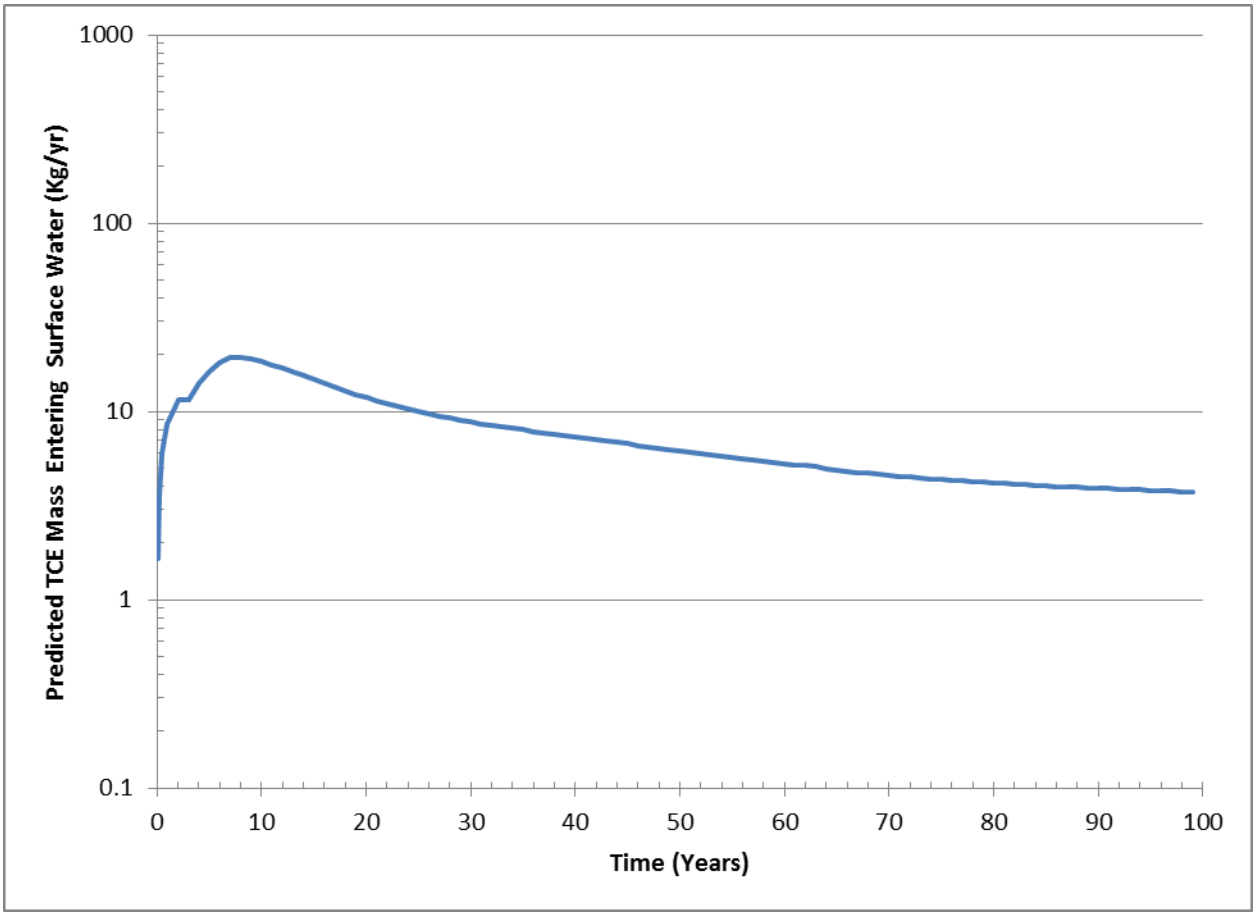


**Figure 5-20 Predicted Groundwater Mass Flux of TCE Discharging to P-Area Discharge Canal and Steel Creek for 100 Years**

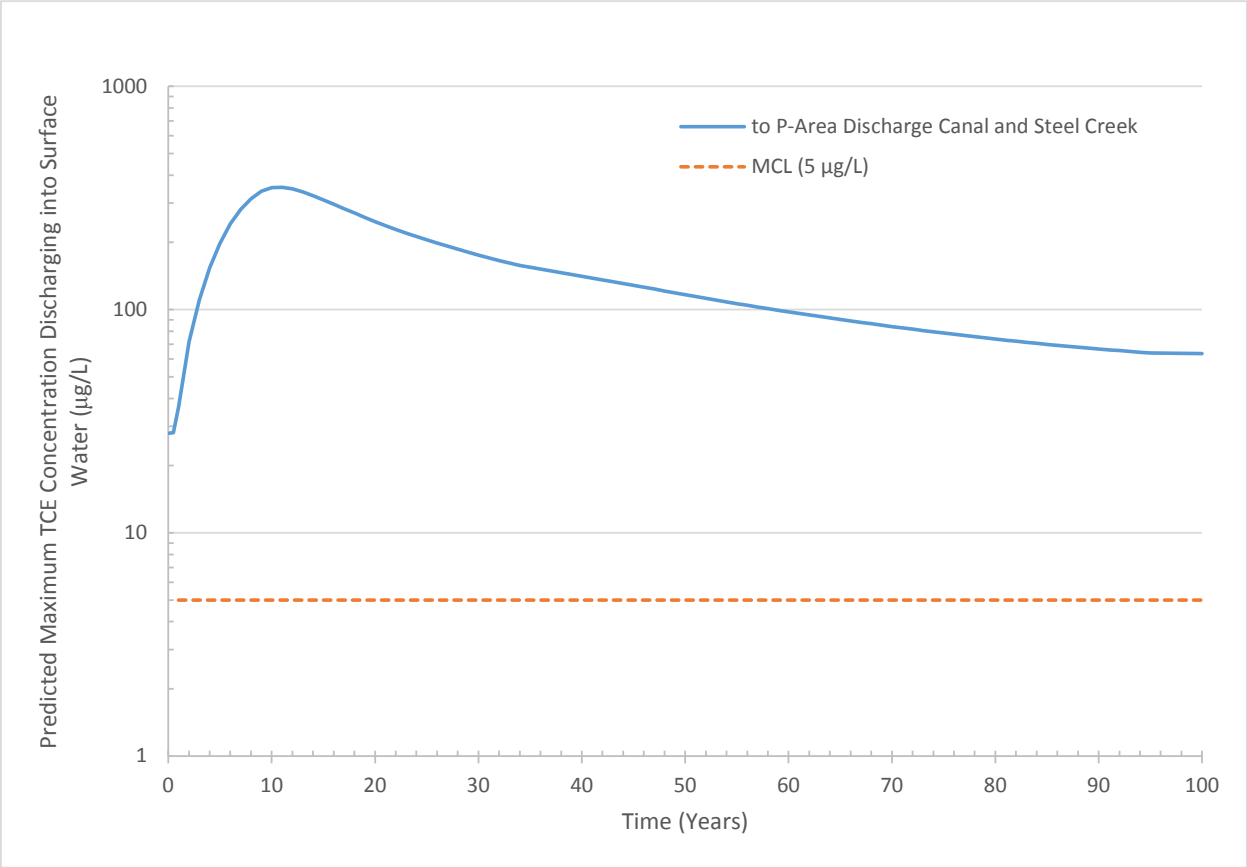


**Figure 5-21 Predicted Maximum Groundwater TCE Concentration Discharging into P-Area Discharge Canal and Steel Creek for 100 Years**

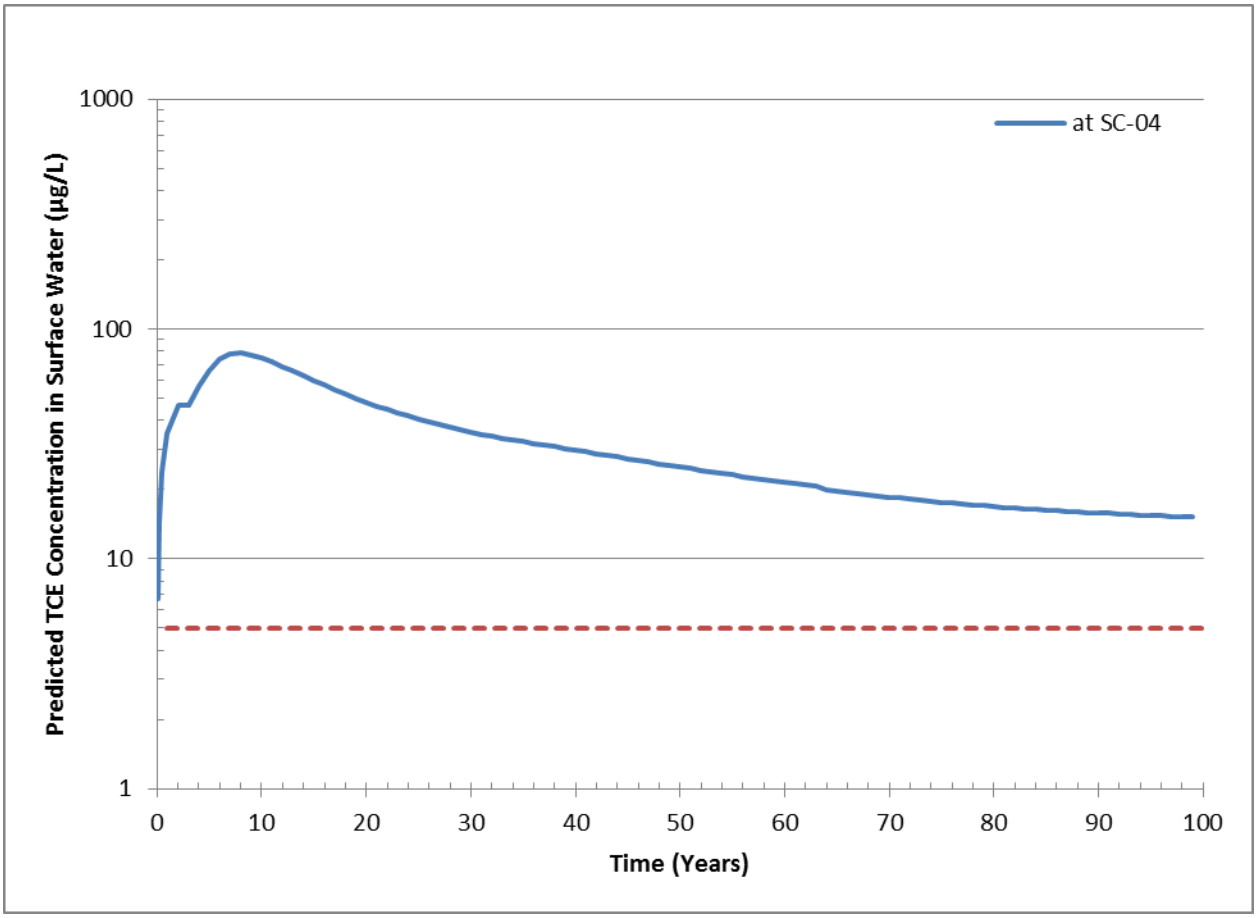


**Figure 5-22 Predicted Surface Water TCE Concentration in Steel Creek at SC-04 for 100 Years**

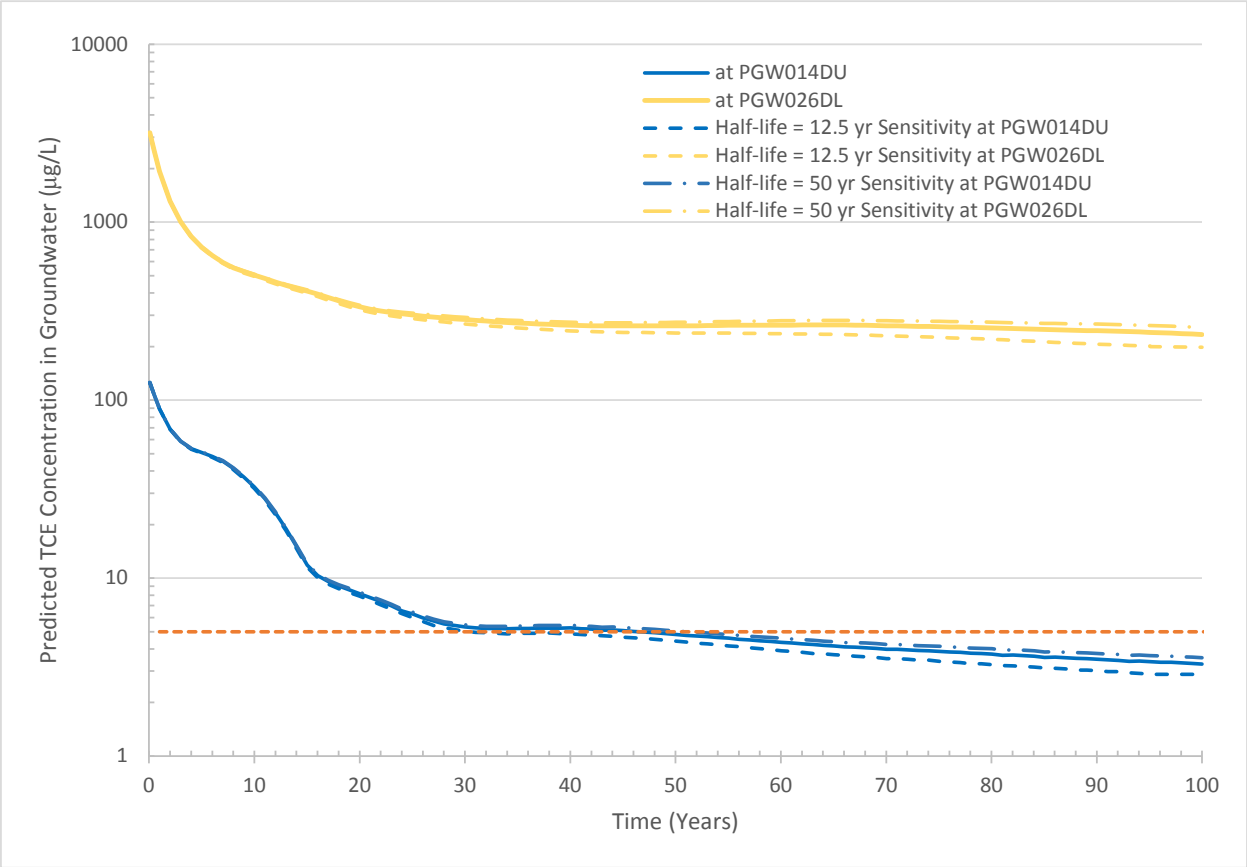


**Figure 5-23 Degradation Sensitivity Analysis for TCE Transport in Groundwater at Wells PGW014DU and PGW026DL Concentration vs Time**


**Figure 5-24 Comparison of Degradation Sensitivity (Half-life = 12.5 yr) Analysis Plume for TCE in the TZ at 100 years**

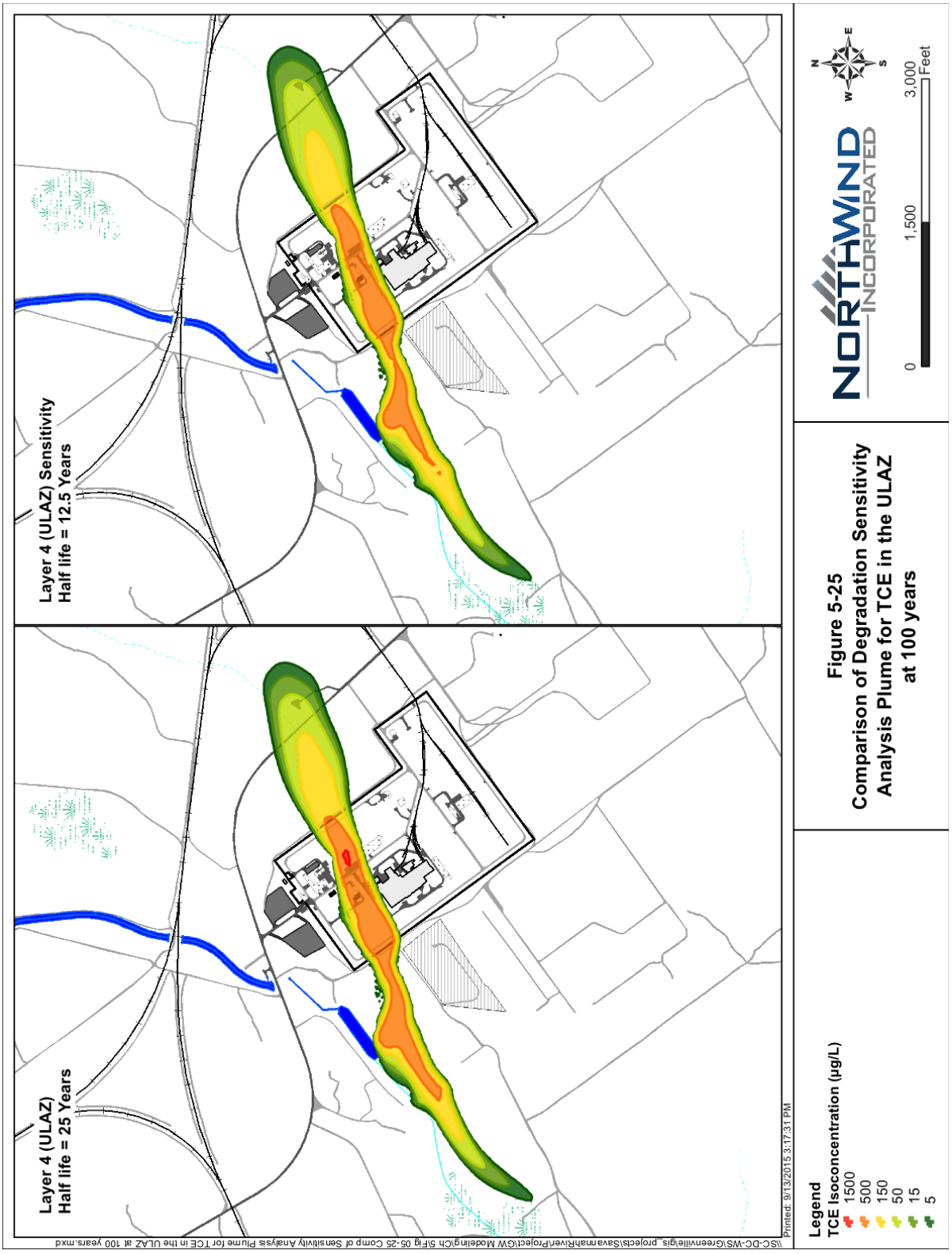


**Figure 5-25 Comparison of Degradation Sensitivity (Half-life = 12.5 yr) Analysis Plume for TCE in the ULAZ at 100 years**

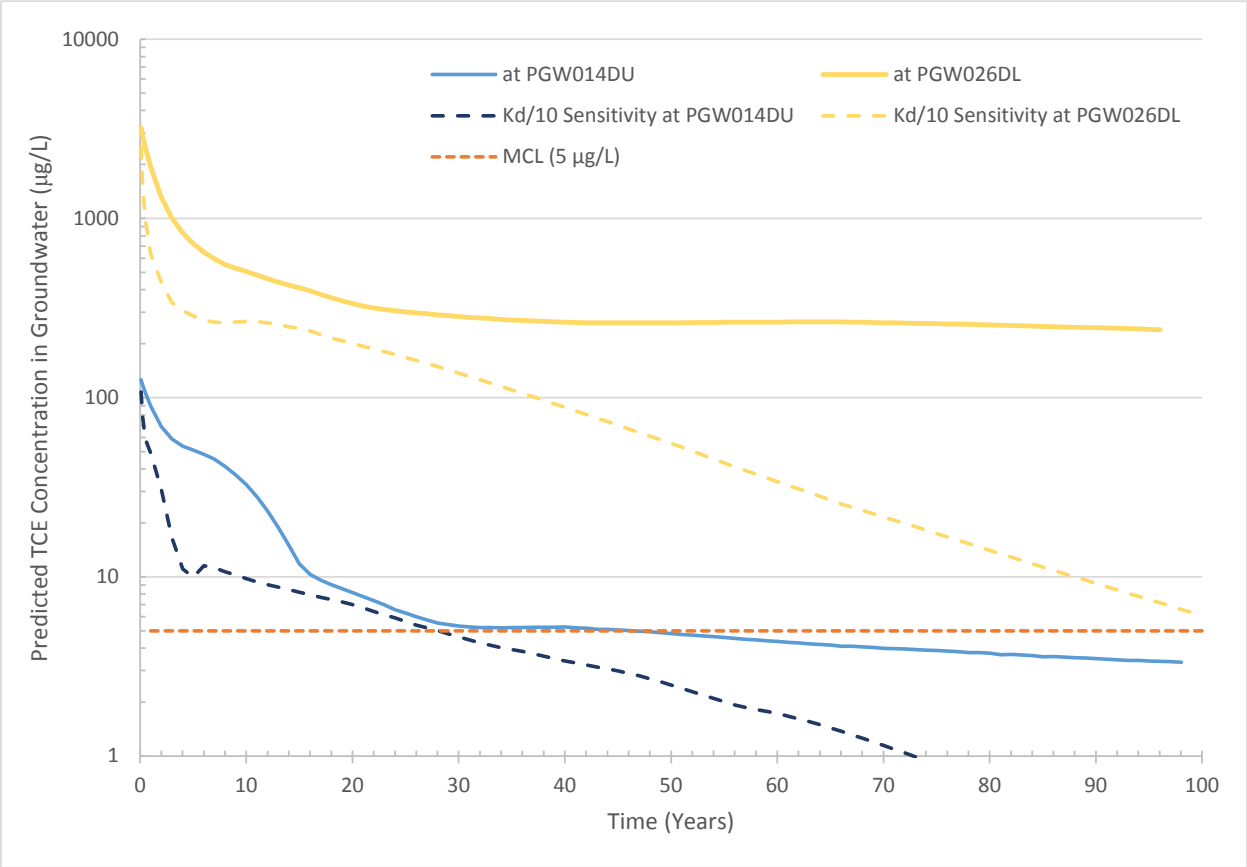


**Figure 5-26 Comparison of $K_d$/10 Sensitivity Analysis Plume for TCE at 100 years**

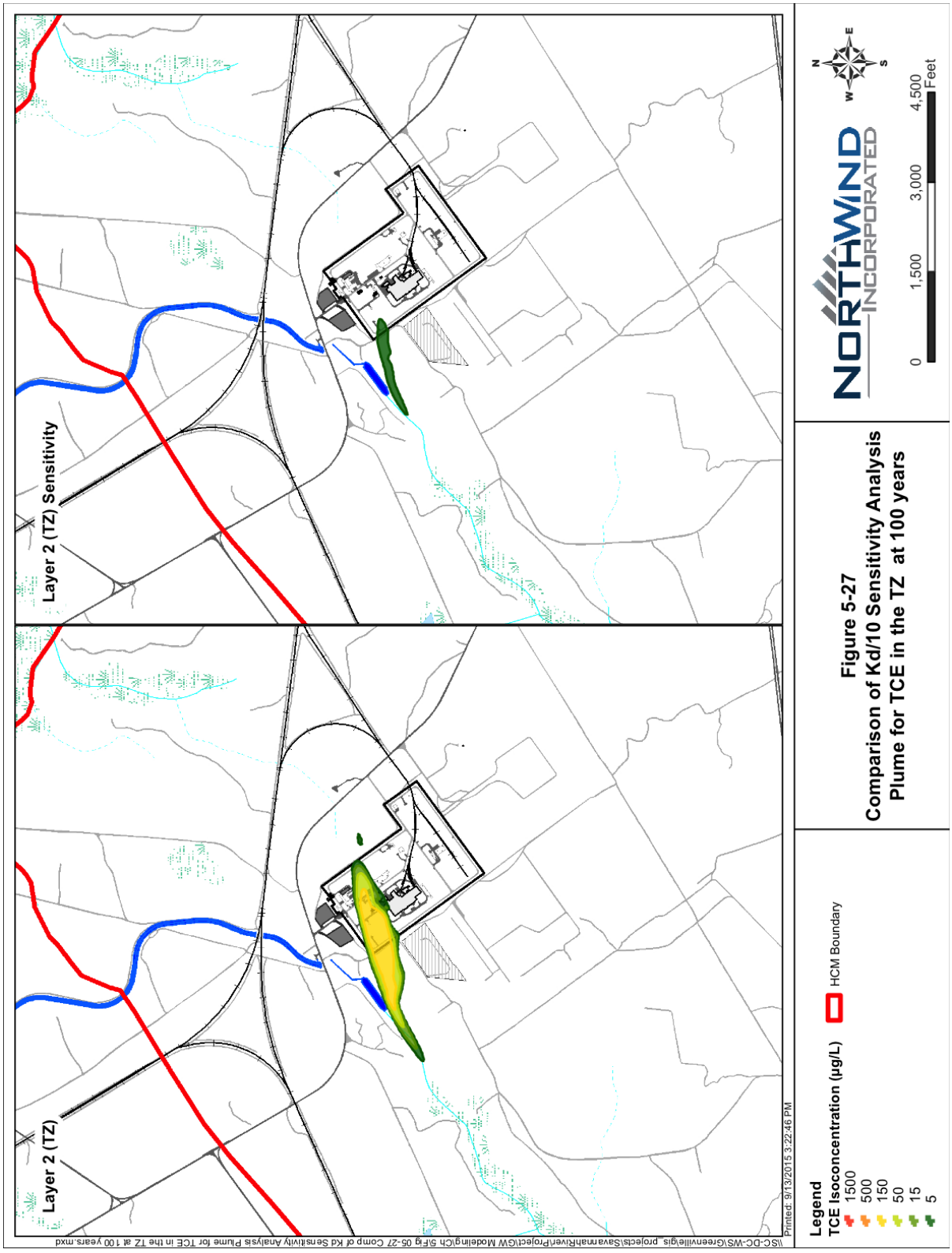


**Figure 5-27 Comparison of $K_d$/10 Sensitivity Analysis Plume for TCE in the TZ at 100 years**

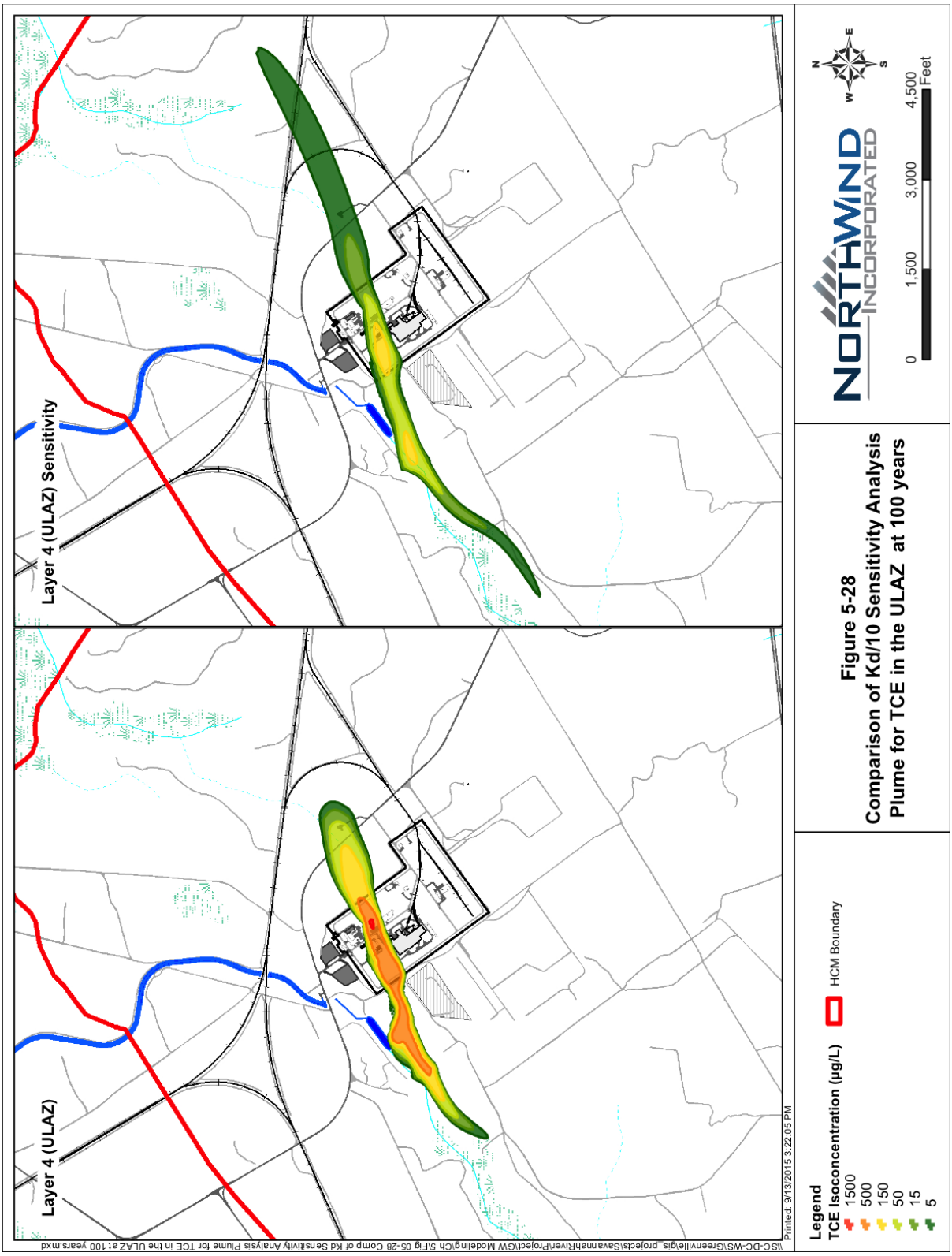


**Figure 5-28 Comparison of $K_d$/10 Sensitivity Analysis Plume for TCE in the ULAZ at 100 years**

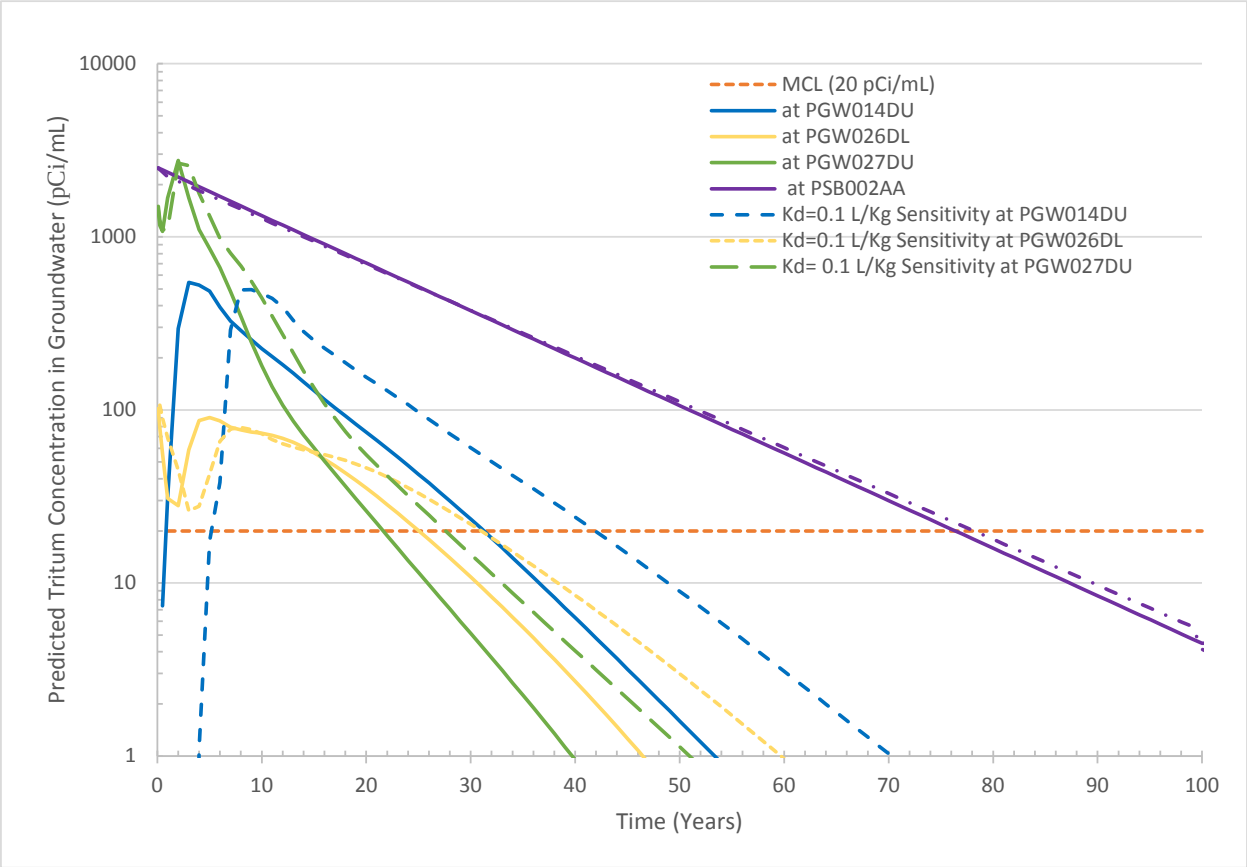


**Figure 5-29 $K_d$=0.1 L/Kg Sensitivity Analysis for Tritium Transport in Groundwater at Wells PGW014DU, PGW026DL, and PGW027DU Concentration vs Time**

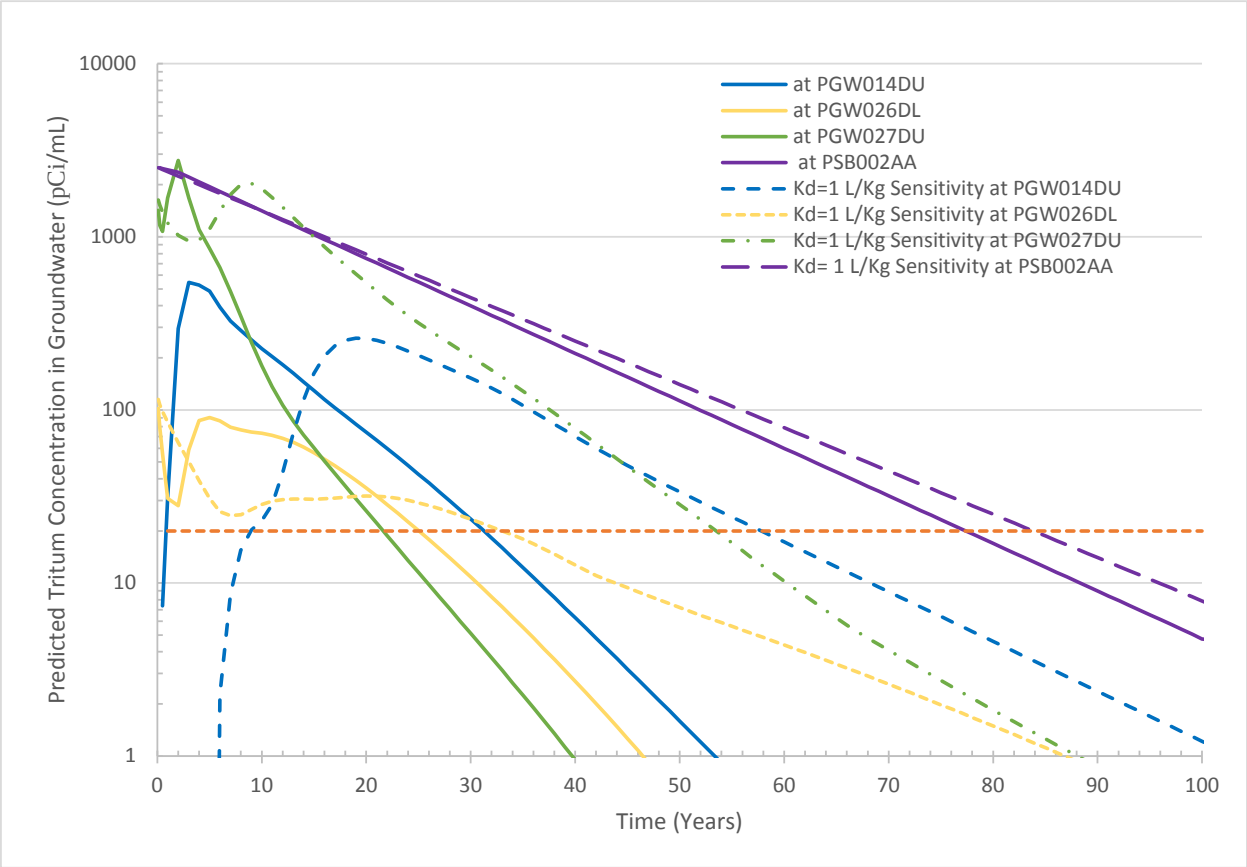


**Figure 5-30 $K_d$=1 L/Kg Sensitivity Analysis for Tritium Transport in Groundwater at Wells PGW014DU, PGW026DL, and PGW027DU Concentration vs Time**

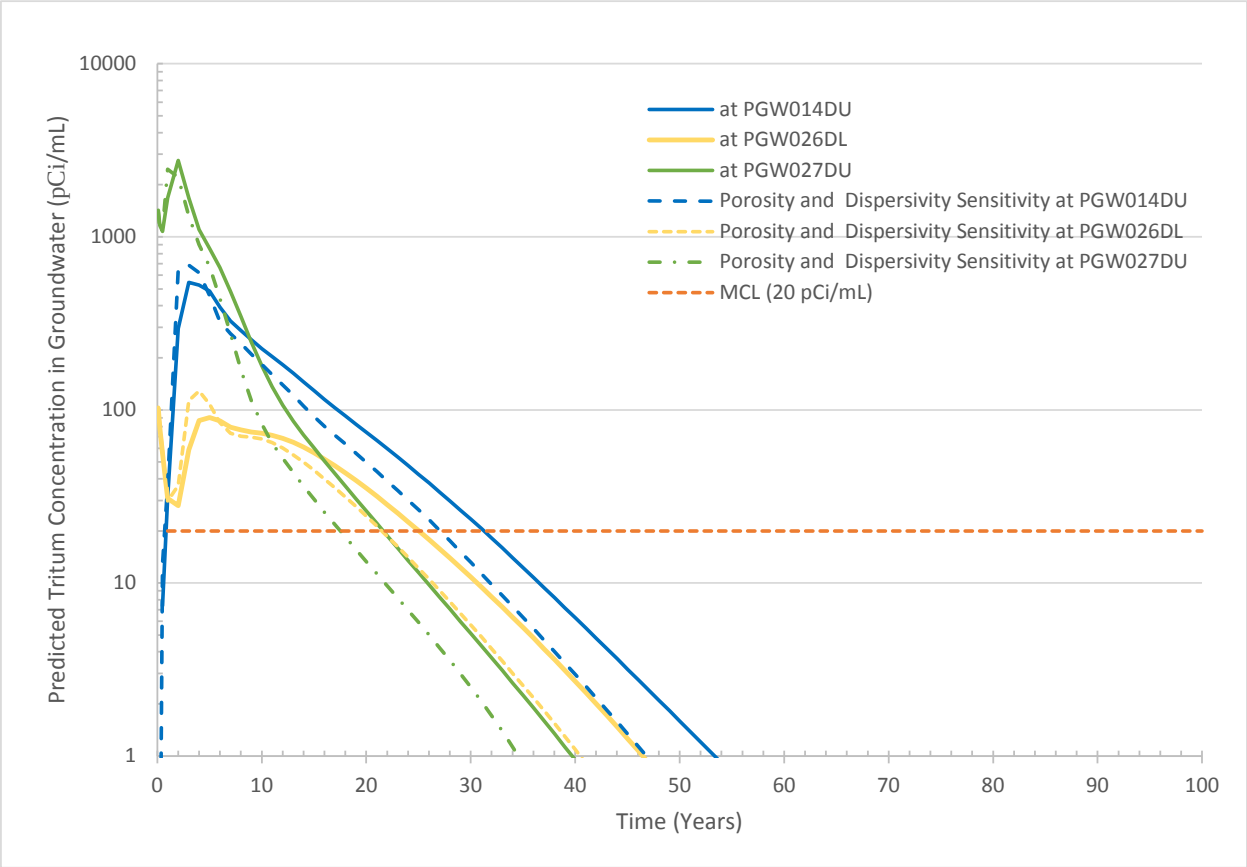


**Figure 5-31 Sensitivity Analysis for Tritium Transport in Groundwater at Well PGW014DU, PGW026DL, and PGW027DU Concentration vs Time**

**(This page intentionally left blank)**

## 6.0 UNCERTAINTIES

The groundwater model described in this report, like all models of this type, is a simplified representation of a complex natural system. Furthermore, this simplified representation is based on limited information about the natural system and about the contaminants that have been introduced into the natural system. Numerous modeling assumptions are made based on available information and professional judgment to complete the modeling exercise. Uncertainties in these assumptions are an important source of uncertainty in the model results. Uncertainties are inherent to groundwater models, and an understanding of uncertainties helps illuminate the limitations that should be placed on interpretation of model results.

It is possible to perform a detailed uncertainty analysis to show the effect of uncertainty in model assumptions (parameter values) on model results (predicted concentrations, flows, etc.). However, this type of analysis is complicated and does not address all sources of uncertainty, including uncertainty in the HCM. A detailed uncertainty analysis is beyond the scope of the current study.

Uncertainties in the groundwater flow model are limited, to some extent, through the process of model calibration. By matching average observed water levels at groundwater wells, some confidence is gained that the model can reasonably predict groundwater heads that would result from changes in the flow system (e.g., pumping more or less water). It should be noted, however, that the flow model calibration exercise provides information about certain model parameters/assumptions but not others. The calibration to head does help identify reasonable choices of hydraulic conductivities for the various hydrostratigraphic units and zones (as shown in the sensitivity analysis of Chapter 5.0); this calibration does not help select the appropriate assumptions for transport model parameters such as dispersivity, effective porosity, CVOC biodegradation rates, or sorption coefficients. These transport parameter values were taken from the scientific literature including other studies at SRS.

The base case tritium transport model assumes a sorption coefficient of zero (i.e., no sorption), which may lead to significant uncertainty in the model results. Because there is no sorption of tritium, migration of tritium is not retarded; therefore, higher concentrations of tritium at

downgradient distances are predicted than if some form of retardation had been included in the model, thereby perhaps producing larger plumes of tritium than actually present. It should be noted that the transport model is highly dependent on the accuracy of the calibrated flow model as the migration and flow paths are totally dependent on the groundwater flow prediction. Given the current vertical extent of tritium in deeper horizons than predicted by the flow model, clearly some uncertainty in the flow model exists. However, the impact of this uncertainty is not significant, especially when the model is ultimately used to compare the merits of different alternatives in helping to reduce concentrations (as opposed to using the model to predict the exact concentrations that will result from a given alternative).

For the CVOCs modeled (PCE and TCE), uncertainties in natural biodegradation rates and sorption coefficients lead to significant uncertainty in modeling results. The available data at P Area are presently not sufficient for derivation of biodegradation rates in groundwater; thus, assumptions for these rates were based on literature values. Similarly, there is significant uncertainty in sorption coefficients ($K_d$) and their spatial distribution. Uncertainty in degradation rates and sorption coefficients is significant, and the predicted concentrations in a given CVOC transport simulation may have significant uncertainty, depending upon the combination of parameters. For example, degradation of the dissolved part of a plume that has a large sorbed component may appear insignificant; while the same degradation rate may appear significant when combined with little or no sorption. These uncertainties do not invalidate the model, especially when the model is used to compare the merits of different alternatives in helping to reduce concentrations (as opposed to using the model to predict the exact concentrations that will result from a given alternative).

There are important uncertainties in the HCM that are not easily addressed through numerical modeling studies. For instance, the different stratigraphic layers and layer elevations have been revised several times during the present study to better account for observed gradients and new information obtained during recent drilling. While the model presented here uses a reasonable interpretation of layering based on available information, the layer definitions and interpolated elevations are not certain and may be important for certain types of model results, such as predictions of concentrations in deeper, less well-defined aquifer units.

In addition, heterogeneity in the spatial and vertical distribution of hydraulic parameters is generally significantly more complex than represented in the model. The simplification of heterogeneity may result in the model not being able to represent localized features or complex responses, such as the apparent retardation of plumes as they move through lenses of low hydraulic conductivity. Related to simplification of heterogeneity is not accounting for potential localized groundwater flow and contaminant pathways, such as improperly abandoned boreholes or natural breaches in confining beds.

Importantly, biodegradation processes and volatilization of CVOCs that may be occurring in the in and near Steel Creek are not accounted for in this groundwater study. These processes may be the most important attenuation mechanisms for CVOCs (GeoTrans 2003).

Another uncertainty in the model results is stream flow in Steel Creek. Measured Steel Creek flow was not a calibration target in this model application. However, the modeled Steel Creek flows at SC-04 (0.56 cfs) are higher than the reported measured value (0.27 cfs). These differences could be the result of model error or uncertainty in measured streamflows due to inaccuracies in the measurement method or not accounting for wetland or tributary flow.

Although not strictly an uncertainty in the groundwater model, the geometry of the contaminant plumes that were used as the starting point of the model is an important contributor to the model predictions. Inaccuracies in the baseline plume may make a significant contribution to discrepancies between measured contaminant concentrations and model results, thus leading to the interpretation that the model needs to be revised where the baseline plume was actually the source of the discrepancy. For example, uncertainty in the configuration of the baseline plume near Steel Creek and well PGW014DU may contribute to the model predicted increase in concentrations in that well. The extent of low concentration water in this area could be larger than conceptualized, and may result in a less rapid and more muted increase in tritium concentrations in well PGW014DU. Uncertainty in plume configuration is likely to be most prevalent on the distal end of the plumes where DPT data are sparse. There is also uncertainty in the vertical characterization of plumes. Due to data resolution with depth and model discretization, initial concentrations are assumed to be the same across an entire model layer. This assumption is likely to cause overestimation of plume mass. Uncertainty in the model

predictions also could be introduced due to the selection of boundary conditions for the contaminant source. For example, in this analysis, no existing or continuing sources are assumed to exist at this site because actions are complete to remediate the sources. However, plume longevity could be different than predicted if there is remaining contamination in the vadose zone or low hydraulic conductivity units.

## 7.0 CONCLUSIONS AND RECOMMENDATIONS

The groundwater flow and contaminant transport model described in this report is based on data and knowledge that were acquired from previous studies of the groundwater system underlying the regional P Area. The flow model was calibrated and appears to provide a reasonable representation of the long-term average groundwater flow field. The transport model predicts plume movement and discharge to Steel Creek and the P-Area Discharge Canal. The base case Tritium model appears to over-predict the velocity of the plume and the discharge of contamination to Steel Creek. A sensitivity simulation that uses a sorption coefficient to represent a slower moving component of the tritium plume, potentially due to unaccounted-for heterogeneity, appears to provide a more realistic representation of the future plume behavior relative to currently observed results. Similarly, there is some overestimation of CVOC concentrations in Steel Creek when low values of retardation or degradation are assumed. After consideration of historical plume behavior, it appears that the true $K_d$s for CVOCs and tritium at P Area lie between the basecase conditions and the upper bound sensitivity values. Therefore, the best interpretation of model results would be to consider the basecase and sensitivity predictions to be extremes, with the true situation somewhere in the middle. Despite these differences between the transport model and observed or expected responses, the flow and transport models appear to be useful tools for the future assessment of remedial alternatives.

A number of improvements have been made to the model since it was originally developed in 2011. Most of these improvements result from new or additional data that have been collected. There were eight water level data points (shown in Table B-2) that could not be used because they appeared to be have some discrepancies associated with them. Examples of discrepancies include water levels that were approximately 10 feet higher or lower than expected based on spatial trends or measurements at nearby wells. It is recommended that SRS further explore the nature of these data discrepancies and provide support for the proper use of these data.

SRS should continue to collect data that can be used to verify the groundwater flow and transport model. Agreement of model results with observed data will help support the current model; differences of model results and observed data should lead to modifications to the HCM and groundwater flow and transport model.

This model, like all models, is subject to limitations that arise from uncertainties and assumptions that are made in simplifying a complex natural system. However, the limited calibration of the model provides some confidence that the model is a reasonable representation of the natural system (especially for groundwater flow). Despite the uncertainties with the model, it establishes a reasonable baseline is an effective tool for future evaluation of the relative merits of various remedial alternatives. Prediction of absolute responses (e.g. attain MCL within a certain number of years) is less certain than relative results (e.g. Scenario X is more effective than Scenario Y) because the latter analysis is a comparison of the results of changes within the same framework.

## 8.0 REFERENCES

Aadland, R.K. and H.W. Bledsoe 1990. *Classification of Hydrostratigraphic Units at the Savannah River Site, South Carolina (U)*, WSRC-RP-90-987, Westinghouse Savannah River Company, Savannah River Site, Aiken, SC.

Aadland, R.K., J.A. Gellicic, and P.A. Thayer, 1995. *Hydrogeologic Framework of West-Central South Carolina*, Report 5, Water Resources Division, South Carolina Department of Natural Resources, Columbia, SC.

Amidon, M., 2010. Savannah River National Laboratory, mark.amidon@srnl.doe.gov., TO 319 Gordon Aquifer Picks and Well Assignments. July 8.

Andersen, Pete and Grogin, Lisa, 2008. *Memorandum to David Noffsinger: Determination of Steady State Calibration Head Targets for the Regional A/M Area Model*, 20 June 2008.

Bills, T.L., K.E. Brewer, A.L. Stieve, and M.S. Rabin, 2000. *Groundwater Flow Modeling for C-Area Groundwater Operable Unit (U)*, WSRC-RP-2000-4096, Rev. 0, Westinghouse Savannah River Company, Savannah River Site, Aiken, SC.

BYU (Brigham Young University) 2000. United States Department of Defense Groundwater Modeling System, Version 6.5.4, Provo, UT.

Clement, T.P., 1998. RT3D, *A Modular Computer Code for Simulating Reactive Multi-species Transport in 3-Dimensional Groundwater Systems*, PNNL-SA-11720, Battelle Pacific Northwest National Laboratory, Richland, WA.

Council, G.W., L.M. Grogin, and T.L. Fogle, 2002. *Groundwater Modeling for the Chemicals, Metals, and Pesticides Pits (U)*, WSRC-RP-2002-4195, Rev. 0, Westinghouse Savannah River Company, Savannah River Site, Aiken, SC.

Flach, G.P., M.K. Harris, R.A. Hiergesell, A.D. Smits, and K.L. Hawkins, 1998. *Hydrogeological and Groundwater Flow Model for C-, K-, L-, and P-Reactor Areas* (U), WSRC-TR-98-00285, Rev. 0, Westinghouse Savannah River Company, Savannah River Site, Aiken, SC.

Flach, G.P., M.K. Harris, R.A. Hiergesell, A.D. Smits, and K.L. Hawkins, 1999. *Regional Groundwater Flow Model for C-, K-, L-, and P-Areas* (U), WSRC-TR-99-00248, Rev. 0, Westinghouse Savannah River Company, Savannah River Site, Aiken, SC.

GeoTrans, Inc., 2002. *Groundwater Modeling for the Northeast Plume of the Mixed Waste Management Facility (U),* WSRC-RP-2002-4072, Rev. 0, Westinghouse Savannah River Company, Savannah River Site, Aiken, SC.

GeoTrans, Inc., 2003. *Groundwater Flow and TCE Transport Modeling for the C-Area Burning/Rubble Pit (U),* WSRC-TR-2003-4066, Rev. 0, Westinghouse Savannah River Company, Savannah River Site, Aiken, SC.

GeoTrans, Inc., 2004. *Groundwater Flow and Transport Model of the L-Area Southern Groundwater Operable Unit (U),* WSRC-RP-2004-4082, Westinghouse Savannah River Company, Savannah River Site, Aiken, SC.

GeoTrans, Inc, 2009. *A Regional A/M Area Groundwater Flow and Contaminant Transport Model (U),* SRNS-TR-2009-00154 Rev. 0, Savannah River Nuclear Solutions, Savannah River Site, Aiken, SC.

Harbaugh, A., Banta, E., Hill, M., and M. McDonald, 2000. *MODFLOW-2000, The U.S. Geological Survey Modular Ground-Water Model – User Guide to Modularization Concepts and the Ground-Water Flow Processes,* U.S. Geological Survey Open-File Report 00-92.

HSI GeoTrans, Inc., 1998. *Groundwater Flow and Solute Transport Modeling Report, K-Area Burning/Rubble Pit and Rubble Pile,* WSRC-RP-98-5052, Westinghouse Savannah River Company, Savannah River Site, Aiken, SC.

Lester, B.H. and G.W. Council, 2008. *R-Area Groundwater Plume Transport Analysis*, ERD-EN-2008-0061, Washington Savannah River Company, Savannah River Site, Aiken, SC.

Newfields and GeoTrans, 2004, *Head Calibration Targets for SRS Groundwater Modeling*, Rev0, WSRC-RP-2004-4059, May 2004.

Ohio EPA (Ohio Environmental Protection Agency) 2003. *Sampling and Analysis of Fraction of Organic Carbon (foc) in Soil*, VAP TDC Document VA30007.03.019, Division of Emergency and Remedial Response, Ohio Environmental Protection Agency.

Price, V, Fallaw, W.C., and McKinney, 1991, Geologic Setting of the New Production Reactor Reference Site within the Savannah River Site. WSRC-RP-91-96 / ESH-EMS-90171 80p.

SRNS (Savannah River Nuclear Solutions) 2009. *RCRA Facility Investigation/Remedial Investigation (RFI/RI) Report with Baseline Risk Assessment and Corrective Measures Study (CMS/FS) for the R-Area Operable Unit (U)*, WSRC-RP-2008-4035, Rev. 1.1, Savannah River Nuclear Solutions, Aiken, SC, July

SRNS 2011a. *Groundwater Modeling and Alternatives Assessment for the P-Area Reactor Groundwater Operable Unit*, SRNS-RP-2010-01746, Savannah River Nuclear Solutions, Aiken, SC, March 2011.

SRNS 2011b. *Field Summary Report for Groundwater Pre-Characterization Activities at the P-Area Reactor Groundwater Operable Unit*, SRNS-RP-2011-00296, Savannah River Nuclear Solutions, Aiken, SC, May 2011.

SRNS 2014. *Groundwater Characterization and Well Installation Field Summary Report for the P-Area Groundwater Operable Unit*, SRNS-RP-2014-00540, Savannah River Nuclear Solutions, Aiken, SC, Nov 2011.

WSRC (Westinghouse Savannah River Company) 2004. *P-Area Reactor Groundwater Operable Unit Hydrogeological Conceptual Model (U)*, WSRC-RP-2004-4086, Westinghouse Savannah River Company, Savannah River Site, Aiken, SC.

Zheng, C., 1999. *MT3DMS: A Modular Three-Dimensional Multi-Species Transport Model for Simulation of Advection, Dispersion, and Chemical Reactions of Contaminants in Groundwater Systems, Documentation and User's Guide*, SERDP-99-1, U. S. Army Corps of Engineers, Engineer Research and Development Center, 221 p.

Zullo, V.A., Harris, W.B. and Price, V. eds., 1990, Savannah River Region: Transition Between the Gulf and Atlantic Coastal Plains, 144p.

**(This page intentionally left blank)**

# APPENDIX A:

# HYDROSTRATIGRAPIC PICKS

**(This page intentionally left blank)**

**Table A-1 Hydrostratigraphic Picks (reported as elevation in feet)**

| Name | SRS X | SRS Y | Ground Surface (ft msl) | TZ (ft msl) | TCCZ (ft msl) | ULAZ ft msl) | MCLAZ (ft msl) | LLAZ (ft msl) | GCU (ft msl) | UGA (ft msl) | MGA (ft msl) | LGA (ft msl) | CBCU (ft msl) |
|---|---|---|---|---|---|---|---|---|---|---|---|---|---|
| LSW20 | 54001.94 | 45491.87 | 268.77 | 181.34 | 167.23 | 154.01 | 144.33 | 132.33 | 75.38 | 60.69 | 52.77 | 52.00 | |
| P12R | 59955.52 | 48492.96 | 292.80 | 203.90 | 191.43 | 178.91 | 152.52 | 126.47 | 94.48 | 88.85 | 81.80 | 51.80 | -40.20 |
| CMP15A | 52896.79 | 51357.17 | 274.70 | 240.73 | 208.57 | 165.40 | | | 94.76 | 87.16 | | | |
| LAW1TD | 50640.49 | 44564.08 | 217.10 | 178.88 | | 108.62 | | | 65.84 | 43.81 | | | -40.75 |
| LAW2A | 49637.58 | 45626.49 | 222.80 | 178.48 | | 120.59 | | | 69.01 | 42.36 | | | -20.73 |
| LAW3A | 52266.18 | 45585.80 | 246.00 | 177.61 | | 112.64 | | | 74.77 | 69.75 | | | -48.80 |
| LCO5A | 50865.79 | 44987.16 | 230.00 | 187.97 | | 122.60 | | | 77.32 | 65.96 | | | |
| LSCPT10 | 52421.77 | 47268.08 | 263.20 | 199.22 | 179.51 | | | | | | | | |
| LSCPT11 | 52444.40 | 47567.82 | 265.40 | 205.09 | | | | | | | | | |
| LSCPT20 | 53529.54 | 43861.28 | 237.10 | | 173.97 | 154.03 | | | | | | | |
| LSCPT21 | 53869.78 | 43853.90 | 239.40 | 191.60 | 178.92 | 161.67 | | | | | | | |
| LSCPT54 | 52580.25 | 47835.08 | 277.50 | 181.82 | | | | | | | | | |
| LSCPT88 | 53854.09 | 44600.58 | 255.70 | 185.96 | 164.14 | 150.76 | 134.92 | 124.39 | | | | | |
| LSCPT89 | 53597.28 | 44371.09 | 246.90 | 194.75 | 181.73 | 157.80 | 143.40 | 131.41 | | | | | |
| LSCPT9 | 52951.51 | 46054.75 | 259.90 | 195.23 | 181.82 | 154.56 | | | | | | | |
| LSW17 | 48535.66 | 41479.61 | 268.30 | 190.52 | | 132.42 | | | 67.06 | 41.42 | | | |
| P13TA | 59999.94 | 35599.99 | 252.40 | 200.39 | 183.60 | 162.58 | 123.95 | 101.71 | 32.23 | 10.20 | -23.97 | | -67.89 |
| P15TA | 51241.44 | 47383.73 | 253.00 | 182.74 | | 132.87 | | | 83.30 | 62.21 | | | -22.21 |
| P19TA | 60034.58 | 55295.88 | 297.40 | | | 176.28 | | | 119.33 | 117.23 | | | 25.59 |
| P24TA | 66565.16 | 43096.20 | 313.30 | 214.13 | 184.51 | 171.91 | 158.62 | 136.83 | 106.05 | 90.71 | 50.94 | 18.30 | -19.70 |
| PAS001C | 65188.89 | 39736.71 | 262.60 | 209.47 | 201.71 | 177.78 | 160.96 | | | 73.44 | | | |

**Table A-1 (continued)**

| Name | SRS X | SRS Y | Ground Surface (ft msl) | TZ (ft msl) | TCCZ (ft msl) | ULAZ ft msl) | MCLAZ (ft msl) | LLAZ (ft msl) | GCU (ft msl) | UGA (ft msl) | MGA (ft msl) | LGA (ft msl) | CBCU (ft msl) |
|---|---|---|---|---|---|---|---|---|---|---|---|---|---|
| PBRPCPT10LT | 62756.24 | 45303.14 | 279.45 | 210.43 | 195.24 | 181.20 | | | | 110.09 | | | |
| PBRPCPT1LT | 63111.06 | 45569.35 | 288.21 | 213.66 | 206.31 | 183.67 | | | | | | | |
| PBRPCPT2LT | 63083.88 | 45238.36 | 278.83 | 209.87 | 196.74 | 172.90 | | | | | | | |
| PBRPCPT3LT | 63037.04 | 45187.17 | 278.62 | 197.19 | 180.10 | 158.50 | | | | | | | |
| PBRPCPT4LT | 62982.92 | 45150.41 | 276.54 | 197.19 | 173.35 | 168.22 | | | | 102.57 | | | |
| PBRPCPT5LT | 62916.18 | 45132.64 | 275.45 | 198.09 | 182.32 | 158.50 | | | | 111.90 | | | |
| PBRPCPT6LT | 63002.42 | 45480.49 | 286.23 | 224.98 | 217.33 | 192.37 | | | | 105.40 | | | |
| PBRPCPT7LT | 62949.11 | 45453.44 | 283.97 | 220.39 | 212.14 | | | | | 108.46 | | | |
| PBRPCPT8LT | 62192.51 | 45432.04 | 283.14 | 210.43 | 193.63 | | | | | 106.03 | | | |
| PBRPCPT9LT | 62836.88 | 45365.86 | 280.69 | 210.66 | 201.46 | 180.51 | | | | 109.42 | | | |
| PCL4 | 63191.00 | 48651.01 | 332.00 | 198.54 | 181.95 | 147.54 | 140.53 | 128.49 | | | | | |
| PG2A | 64807.36 | 44337.66 | 313.24 | 217.29 | 200.85 | 194.10 | 166.41 | | | 106.92 | | | |
| PG31 | 63158.97 | 44095.01 | 298.00 | 213.59 | 194.69 | 173.82 | 159.78 | 130.90 | 101.03 | 97.36 | | | |
| PG32 | 63372.24 | 44337.96 | 310.60 | 215.91 | 191.18 | 171.72 | 160.99 | 128.19 | | 100.55 | | | |
| PG33 | 62950.07 | 44649.35 | 279.60 | 220.25 | 204.54 | 183.59 | 170.21 | 149.84 | 113.60 | 95.60 | | | |
| PG34 | 62985.76 | 44335.81 | 287.70 | 214.14 | 202.50 | 182.35 | 169.11 | 140.48 | 110.69 | 105.94 | | | |
| PG5 | 64628.27 | 44445.04 | 309.80 | 204.87 | 194.92 | 176.24 | 165.36 | | | 106.99 | | | |
| PGCPT01 | 64868.17 | 44323.61 | 313.70 | 211.94 | 203.32 | 185.28 | 173.33 | 162.49 | | 107.63 | | | |
| PGCPT02 | 64784.88 | 44325.99 | 313.40 | 210.13 | 201.39 | 183.37 | 167.91 | 155.29 | | 106.76 | | | |
| PGCPT03 | 64652.09 | 44318.37 | 312.20 | 221.35 | 210.64 | 177.99 | | | | 104.60 | | | |
| PGCPT04 | 64541.96 | 44323.01 | 311.90 | 219.14 | 211.47 | 207.47 | 185.04 | 174.63 | | 103.60 | | | |

**Table A-1 (continued)**

| Name | SRS X | SRS Y | Ground Surface (ft msl) | TZ (ft msl) | TCCZ (ft msl) | ULAZ ft msl) | MCLAZ (ft msl) | LLAZ (ft msl) | GCU (ft msl) | UGA (ft msl) | MGA (ft msl) | LGA (ft msl) | CBCU (ft msl) |
|---|---|---|---|---|---|---|---|---|---|---|---|---|---|
| PGCPT05 | 64628.27 | 44445.00 | 309.80 | 209.33 | 197.20 | | | | | 106.99 | | | |
| PGCPT06 | 64639.56 | 44487.51 | 309.30 | 221.91 | 215.51 | 177.41 | | | | 108.14 | | | |
| PGCPT07 | 64646.16 | 44565.11 | 309.10 | 222.14 | 208.97 | 177.52 | | | | 110.39 | | | |
| PGCPT08 | 64752.75 | 43049.20 | 318.30 | 231.12 | 224.60 | | | | | 123.02 | | | |
| PGCPT100 | 64891.07 | 44171.13 | 314.60 | 213.99 | 205.78 | 185.01 | | | | 107.54 | | | |
| PGCPT102 | 64698.67 | 44170.33 | 314.70 | 213.83 | 203.18 | 183.73 | | | | 107.21 | | | |
| PGCPT103 | 64779.41 | 44476.90 | 310.80 | 209.35 | 197.32 | 176.44 | | | | 110.43 | | | |
| PGCPT104 | 65076.69 | 44619.44 | 312.00 | 221.08 | 219.28 | 190.15 | | | | 112.04 | | | |
| PGCPT105 | 65185.32 | 44619.46 | 313.50 | 213.47 | 206.83 | 187.46 | | | | 111.10 | | | |
| PGCPT106 | 65450.39 | 44641.96 | 314.90 | 214.58 | 202.57 | 184.26 | | | | 113.65 | | | |
| PGCPT107 | 64422.36 | 43028.78 | 321.00 | 206.76 | 201.68 | 187.86 | 173.33 | | | 123.91 | | | |
| PGCPT108 | 64480.05 | 42925.28 | 319.30 | 217.06 | 203.60 | | | | | 121.77 | | | |
| PGCPT11 | 64817.25 | 44781.30 | 310.10 | 221.53 | 214.51 | 186.91 | | | | 114.86 | | | |
| PGCPT110 | 64483.89 | 44516.95 | 308.20 | 219.89 | 212.44 | 191.11 | | | | 101.18 | | | |
| PGCPT111 | 64505.86 | 44588.80 | 308.00 | 212.47 | 204.42 | 200.87 | | | | 99.84 | | | |
| PGCPT112 | 65925.65 | 44426.39 | 312.90 | 210.77 | 201.28 | 178.75 | | | | 112.26 | | | |
| PGCPT113 | 65828.16 | 43509.95 | 316.60 | 211.76 | 203.85 | 177.44 | | | | 101.28 | | | |
| PGCPT115 | 66758.96 | 43614.46 | 290.40 | 215.13 | 206.45 | 189.03 | | | | 103.47 | | | |
| PGCPT116 | 66420.63 | 43400.22 | 301.50 | 212.56 | 207.28 | 187.71 | | | | 96.61 | | | |
| PGCPT117 | 66742.06 | 44168.91 | 295.20 | 214.38 | 211.06 | 184.97 | | | | 107.30 | | | |
| PGCPT118 | 66581.58 | 42983.32 | 309.00 | 240.02 | 232.05 | 201.44 | | | | 90.68 | | | |

**Table A-1 (continued)**

| Name | SRS X | SRS Y | Ground Surface (ft msl) | TZ (ft msl) | TCCZ (ft msl) | ULAZ ft msl) | MCLAZ (ft msl) | LLAZ (ft msl) | GCU (ft msl) | UGA (ft msl) | MGA (ft msl) | LGA (ft msl) | CBCU (ft msl) |
|---|---|---|---|---|---|---|---|---|---|---|---|---|---|
| PGCPT119 | 66838.57 | 43022.19 | 305.60 | 218.02 | 210.91 | | | | | 89.51 | | | |
| PGCPT12 | 64519.95 | 44742.19 | 306.20 | 220.32 | 207.82 | 184.84 | | | | 99.88 | | | |
| PGCPT120A | 66838.18 | 43365.90 | 296.50 | 229.81 | 223.36 | 208.33 | | | | 95.20 | | | |
| PGCPT121 | 67902.95 | 44005.89 | 299.00 | 214.24 | 204.28 | 181.61 | 144.52 | | 105.70 | 94.18 | | | |
| PGCPT122 | 65165.07 | 42309.89 | 306.40 | 204.97 | 186.65 | | | | | 95.08 | | | |
| PGCPT123 | 65060.68 | 42198.30 | 306.20 | 204.08 | 192.20 | | | | | 95.19 | | | |
| PGCPT124 | 65479.47 | 42140.60 | 307.00 | 226.61 | 213.39 | | | | | 92.98 | | | |
| PGCPT125 | 65050.45 | 41921.39 | 302.20 | 202.75 | 193.12 | 186.20 | 168.48 | 141.26 | | 93.48 | | | |
| PGCPT126 | 64742.46 | 42099.88 | 304.50 | 216.40 | 206.30 | 174.07 | 160.52 | 139.75 | | 94.84 | | | |
| PGCPT127 | 65178.08 | 41140.59 | 290.10 | 224.27 | 210.62 | 177.71 | 172.90 | 146.16 | | 89.13 | | | |
| PGCPT15 | 64256.66 | 44706.48 | 306.50 | 225.89 | 220.28 | 206.67 | 179.27 | 159.27 | | 101.30 | | | |
| PGCPT18 | 64273.16 | 44856.70 | 302.10 | 210.17 | 205.02 | 178.13 | | | | 103.61 | | | |
| PGCPT23 | 62916.36 | 45132.38 | 275.50 | 205.94 | 195.28 | 173.30 | | | | | | | |
| PGCPT24 | 63203.37 | 45175.39 | 278.10 | 206.67 | 190.18 | 171.12 | 154.81 | | | | | | |
| PGCPT25 | 63576.27 | 45186.60 | 285.80 | 206.31 | 189.33 | 180.72 | | | | 107.52 | | | |
| PGCPT26 | 63876.34 | 45204.08 | 293.50 | 215.81 | 208.53 | 183.04 | | | | 109.63 | | | |
| PGCPT27 | 64110.85 | 45215.90 | 295.60 | 209.20 | 186.48 | 182.71 | 169.22 | | | 110.64 | | | |
| PGCPT29 | 64369.67 | 44401.08 | 311.10 | 225.51 | 219.74 | 201.87 | | | | 100.74 | | | |
| PGCPT35 | 65312.19 | 44211.03 | 316.30 | 222.91 | 216.30 | 197.68 | | | | 109.12 | | | |
| PGCPT36 | 65192.55 | 44293.38 | 314.80 | 221.75 | 211.34 | 194.75 | 182.81 | 161.40 | | 108.88 | | | |
| PGCPT37 | 64957.47 | 44311.09 | 313.40 | 213.89 | 207.36 | 189.83 | | | | 108.10 | | | |

**Table A-1 (continued)**

| Name | SRS X | SRS Y | Ground Surface (ft msl) | TZ (ft msl) | TCCZ (ft msl) | ULAZ ft msl) | MCLAZ (ft msl) | LLAZ (ft msl) | GCU (ft msl) | UGA (ft msl) | MGA (ft msl) | LGA (ft msl) | CBCU (ft msl) |
|---|---|---|---|---|---|---|---|---|---|---|---|---|---|
| PGCPT38 | 64954.37 | 44201.71 | 314.20 | 216.54 | 207.29 | 186.97 | | | | 107.40 | | | |
| PGCPT39 | 64953.98 | 44463.38 | 311.70 | 219.15 | 207.08 | 181.17 | | | | 109.35 | | | |
| PGCPT40 | 65050.19 | 44461.55 | 312.70 | 218.46 | 210.55 | 193.04 | | | | 109.05 | | | |
| PGCPT44 | 64688.40 | 44026.40 | 316.80 | 216.45 | 205.57 | 187.87 | 173.34 | | | 110.86 | | | |
| PGCPT46 | 64658.77 | 43534.61 | 316.40 | 225.56 | 198.02 | 193.60 | 180.34 | 162.06 | | 123.86 | | | |
| PGCPT49 | 65252.88 | 43807.80 | 314.90 | 212.66 | 203.00 | 178.49 | | | | 106.30 | | | |
| PGCPT50 | 65294.08 | 43419.67 | 315.70 | 201.47 | 193.09 | 185.20 | 172.14 | | | 108.14 | | | |
| PGCPT51 | 65477.58 | 43175.09 | 315.90 | 209.49 | 200.37 | 195.05 | 186.84 | 171.28 | | 109.36 | | | |
| PGCPT52 | 66101.00 | 42882.67 | 314.20 | 216.18 | 211.97 | 196.39 | | | | 91.82 | | | |
| PGCPT55 | 64501.41 | 43030.81 | 320.40 | 213.15 | 203.91 | 188.93 | 175.09 | | | 123.82 | | | |
| PGCPT57 | 65813.80 | 44849.03 | 318.20 | 224.86 | 206.09 | | | | | 117.19 | | | |
| PGCPT58 | 63368.66 | 43253.21 | 313.50 | 211.28 | 202.39 | 195.30 | 182.50 | 165.46 | | 88.87 | | | |
| PGCPT59 | 62071.49 | 44214.60 | 286.70 | 192.51 | 183.02 | 163.27 | | | | 120.92 | | | |
| PGCPT61 | 61288.46 | 44718.27 | 262.00 | 204.74 | 194.63 | | | | | 101.58 | | | |
| PGCPT62 | 61252.39 | 44900.18 | 254.10 | 203.52 | 194.41 | 177.59 | 174.76 | 156.61 | 108.43 | 102.17 | | | |
| PGCPT63A | 61462.70 | 45365.90 | 256.00 | 220.67 | 199.79 | 179.28 | | | | 103.76 | | | |
| PGCPT64 | 62231.55 | 45318.90 | 267.50 | 217.53 | 198.63 | 183.02 | 162.16 | | 116.83 | 106.89 | | | |
| PGCPT65 | 63040.67 | 44777.19 | 275.80 | 222.64 | 204.40 | 186.17 | 172.33 | 143.06 | | 103.94 | | | |
| PGCPT66 | 63269.96 | 44885.63 | 274.60 | 217.27 | 200.11 | 181.88 | 168.48 | 142.38 | | | | | |
| PGCPT67 | 63725.77 | 44805.19 | 289.10 | 220.13 | 213.56 | 203.20 | 192.15 | 169.00 | | 109.32 | | | |
| PGCPT68 | 63880.87 | 44883.67 | 297.40 | 214.25 | 207.00 | 195.60 | 172.11 | 166.59 | | 109.25 | | | |

**Table A-1 (continued)**

| Name | SRS X | SRS Y | Ground Surface (ft msl) | TZ (ft msl) | TCCZ (ft msl) | ULAZ ft msl) | MCLAZ (ft msl) | LLAZ (ft msl) | GCU (ft msl) | UGA (ft msl) | MGA (ft msl) | LGA (ft msl) | CBCU (ft msl) |
|---|---|---|---|---|---|---|---|---|---|---|---|---|---|
| PGCPT69 | 64035.85 | 44891.80 | 304.70 | 210.85 | 205.11 | 199.03 | 185.19 | 170.02 | | 107.80 | | | |
| PGCPT70 | 64152.35 | 44879.41 | 304.70 | 208.04 | | | | 205.11 | | 104.85 | | | |
| PGCPT81 | 64660.18 | 44079.50 | 316.10 | 214.97 | 205.84 | 184.47 | | | | 108.40 | | | |
| PGCPT86 | 66238.19 | 42437.44 | 314.70 | 227.12 | 216.72 | 206.03 | | | | 89.86 | | | |
| PGCPT87 | 65719.65 | 42427.19 | 312.00 | 230.24 | 225.06 | 201.13 | | | | 93.09 | | | |
| PGCPT88 | 65202.44 | 42427.85 | 310.80 | 201.81 | 195.30 | 179.37 | | | | 95.06 | | | |
| PGCPT89 | 64491.06 | 42421.01 | 319.10 | 218.82 | 209.49 | 204.49 | | | | 101.11 | | | |
| PGCPT90 | 66035.09 | 43726.87 | 314.20 | 203.20 | 195.23 | 169.26 | | | | 104.90 | | | |
| PGCPT92 | 66052.66 | 44197.17 | 311.40 | 207.27 | 197.30 | 178.31 | | | 111.50 | 110.22 | | | |
| PGCPT93 | 65330.33 | 44345.61 | 314.80 | 221.34 | 214.21 | | | | | 109.90 | | | |
| PGCPT95 | 65280.32 | 44380.17 | 315.30 | 217.23 | 209.75 | | | | | 109.89 | | | |
| PGCPT96 | 65251.13 | 44505.48 | 314.50 | 209.68 | 201.22 | | | | | 110.86 | | | |
| PGCPT98 | 65263.36 | 44308.31 | 314.68 | 220.22 | 211.67 | 195.79 | 184.69 | 161.89 | | 109.43 | | | |
| PGW010B | 64129.79 | 36650.90 | 255.86 | 204.86 | 181.13 | 161.66 | 141.56 | 133.71 | 51.43 | 36.86 | 0.00 | | -55.14 |
| PGW011A | 68997.47 | 47643.40 | 276.06 | 206.70 | 183.42 | 162.01 | 149.83 | 140.06 | 102.48 | 79.06 | 19.06 | | |
| PGW012A | 71046.58 | 41285.21 | 275.48 | 188.56 | 188.56 | 168.62 | 151.92 | 127.65 | 115.96 | 112.38 | 67.48 | 48.48 | |
| PGW013A | 60551.39 | 47636.71 | 290.20 | 203.00 | 188.00 | 174.06 | 171.14 | 155.16 | | | | 70.20 | |
| PGW014A | 63246.38 | 44871.81 | 277.77 | 204.79 | 204.79 | 185.34 | 172.48 | 142.15 | | | | | |
| PGW015A | 63019.58 | 47171.33 | 302.20 | 215.17 | 204.27 | 188.01 | 172.47 | 153.73 | 97.28 | 92.50 | 68.20 | 43.20 | |
| PGW016B | 62341.26 | 44763.81 | 284.31 | 210.11 | 200.91 | 177.51 | | | | 113.12 | | | |
| PGW017B | 64037.39 | 44894.41 | 308.03 | 211.87 | 194.42 | 170.53 | 156.51 | | | 107.82 | | | |

**Table A-1 (continued)**

| Name | SRS X | SRS Y | Ground Surface (ft msl) | TZ (ft msl) | TCCZ (ft msl) | ULAZ ft msl) | MCLAZ (ft msl) | LLAZ (ft msl) | GCU (ft msl) | UGA (ft msl) | MGA (ft msl) | LGA (ft msl) | CBCU (ft msl) |
|---|---|---|---|---|---|---|---|---|---|---|---|---|---|
| PGW018B | 62947.76 | 43488.52 | 304.85 | 211.66 | 203.84 | 177.58 | 167.92 | 150.48 | | 95.15 | | | |
| PGW019B | 65079.59 | 44658.02 | 315.85 | 225.26 | 214.25 | 191.63 | 173.71 | | | 112.93 | | | |
| PGW-01A | 65337.71 | 46263.10 | 312.99 | 232.00 | 213.22 | 192.81 | 179.28 | 161.69 | 119.91 | 112.05 | | | |
| PGW020B | 64473.46 | 43437.51 | 323.17 | 224.64 | 216.88 | 197.50 | 178.65 | 163.15 | | 127.08 | | | |
| PGW021B | 66058.12 | 44194.69 | 314.51 | 210.08 | 200.49 | 181.12 | 169.60 | | | | | | |
| PGW022B | 66710.96 | 43640.80 | 293.32 | 210.82 | 201.22 | 186.51 | 165.02 | | | 103.97 | | | |
| PGW023B | 66807.08 | 43008.99 | 309.16 | 220.81 | 202.00 | 183.49 | | | | 89.53 | | | |
| PGW024A | 65720.85 | 43787.72 | 319.34 | 224.43 | 206.54 | 182.30 | 171.01 | 158.54 | 115.32 | 105.13 | | | |
| PGW026B | 63711.96 | 44801.26 | 289.12 | 186.12 | 186.12 | 170.62 | 154.90 | 119.12 | 119.12 | 109.32 | | | |
| PGW027C | 62953.26 | 44660.07 | 279.22 | 193.26 | 193.26 | 180.02 | 167.11 | 120.60 | 120.60 | 113.66 | | | |
| PGW028C | 62525.42 | 44255.44 | 296.22 | 203.67 | 190.10 | 180.51 | 171.73 | 142.18 | 125.22 | 125.22 | | | |
| PGW02A | 57566.58 | 45311.74 | 253.84 | 206.54 | 196.11 | 183.53 | | | 89.56 | 86.89 | 66.84 | | |
| PGW031B | 65787.60 | 44025.61 | 315.30 | 207.59 | 198.97 | 189.95 | 155.91 | 128.03 | 128.03 | 109.57 | | | |
| PGW03A | 64196.18 | 42119.71 | 324.08 | 230.01 | 214.46 | 183.79 | 166.28 | 143.34 | 115.25 | 94.44 | | | |
| PGW04A | 60968.00 | 44310.53 | 280.27 | 215.73 | 206.27 | 193.65 | | | 103.81 | 100.02 | | | |
| PGW05A | 68610.06 | 37479.11 | 245.63 | 214.73 | 197.37 | 161.48 | 126.99 | 94.49 | 77.38 | 66.26 | 35.63 | | |
| PGW06A | 68202.99 | 42869.72 | 297.13 | 215.76 | 194.96 | 172.03 | 137.77 | 113.25 | 92.12 | 87.16 | 53.13 | 40.13 | |
| PGW07A | 65566.09 | 45094.93 | 323.80 | 238.70 | 217.61 | 196.78 | 180.86 | 165.72 | 129.25 | 118.40 | | | |
| PGW08A | 58720.88 | 42344.23 | 300.90 | 227.23 | 210.48 | 193.32 | 174.57 | 141.03 | | 80.90 | 55.90 | | |
| PGW09A | 59199.78 | 39183.95 | 311.78 | 233.44 | 212.33 | 190.49 | 153.64 | 130.35 | 101.45 | 98.02 | 52.78 | 38.78 | |
| PLith1 | 64332.85 | 44441.81 | 308.90 | 224.63 | 220.08 | 203.17 | | | | 99.29 | | | |

**Table A-1 (continued)**

| Name | SRS X | SRS Y | Ground Surface (ft msl) | TZ (ft msl) | TCCZ (ft msl) | ULAZ ft msl) | MCLAZ (ft msl) | LLAZ (ft msl) | GCU (ft msl) | UGA (ft msl) | MGA (ft msl) | LGA (ft msl) | CBCU (ft msl) |
|---|---|---|---|---|---|---|---|---|---|---|---|---|---|
| PLith2/S02 | 64289.28 | 44457.27 | 308.60 | 224.34 | 218.85 | 204.43 | 185.61 | 171.20 | | 99.40 | | | |
| PLith3/S04 | 64246.11 | 44417.93 | 311.40 | 220.57 | 218.16 | 201.34 | 189.61 | 172.27 | | 99.29 | | | |
| POS002 | 64295.71 | 44381.74 | 310.32 | 207.69 | 190.99 | 173.93 | | | | 99.14 | | | |
| POS003 | 64340.71 | 44363.70 | 309.30 | 203.86 | 187.62 | 168.66 | | | | 100.64 | | | |
| POS004 | 64281.48 | 44406.65 | 309.37 | 200.35 | 189.30 | 166.15 | | | | 99.18 | | | |
| POS005 | 64285.98 | 44439.24 | 308.77 | 199.30 | 186.78 | 166.70 | | | | 99.25 | | | |
| POS006 | 64277.60 | 44461.71 | 308.67 | 197.45 | 186.78 | 165.88 | | | | 99.43 | | | |
| PRGW-023 | 63043.77 | 43100.64 | 314.80 | 207.40 | 190.91 | 170.29 | 160.40 | 126.59 | 90.80 | 87.80 | 55.80 | 19.80 | |
| PRGW-026 | 63605.50 | 43450.30 | 318.00 | 221.87 | 210.96 | 175.24 | 162.05 | 136.48 | 96.99 | 89.48 | 62.00 | 27.00 | |
| PRGW-029 | 63914.09 | 43622.11 | 322.30 | 218.30 | 205.30 | 195.30 | 180.30 | 152.30 | 126.30 | 115.30 | 55.30 | 25.30 | -12.70 |
| PRGW-044 | 64249.46 | 44328.62 | 310.00 | 210.47 | 191.18 | 174.15 | 160.65 | 126.89 | 101.00 | 99.00 | 59.00 | 28.00 | -21.00 |
| PRGW-056 | 64462.44 | 44371.61 | 310.80 | | | | | | 117.80 | 102.80 | | | -26.20 |
| PRGW-058 | 64544.87 | 44649.56 | 306.90 | | | | | | | | | | -8.10 |
| PRGW-059 | 64720.68 | 44646.62 | 308.50 | 223.40 | 196.09 | 182.75 | 169.60 | 135.30 | 127.50 | 113.50 | 70.15 | 33.50 | -12.50 |
| PRGW-061 | 64958.31 | 44314.03 | 313.10 | 211.67 | 205.10 | 187.88 | 175.10 | 142.10 | 109.60 | 108.10 | 80.10 | 30.10 | -6.90 |
| PRGW-062 | 64953.09 | 44207.12 | 313.90 | | | | | | 107.90 | 107.40 | | | -17.10 |
| PRGW-082 | 65255.59 | 43805.43 | 314.80 | 220.69 | 202.59 | 178.25 | 162.33 | 133.70 | 112.60 | 106.30 | 54.74 | 19.36 | -22.20 |
| PRGW100 | 63515.78 | 43782.51 | 290.10 | | 205.88 | | 181.57 | 159.03 | 123.45 | 98.64 | 62.04 | | |
| PRGW101 | 64495.46 | 43424.63 | 320.30 | 222.79 | 214.16 | 193.21 | 174.66 | 159.79 | 134.30 | 127.30 | 60.30 | 17.30 | |
| PRGW102 | 64310.89 | 43104.80 | 329.00 | 230.49 | 218.75 | 206.22 | 176.48 | 156.90 | 129.00 | 124.50 | 54.00 | 21.00 | |
| PRSBCPT10 | 64384.43 | 43726.51 | 321.90 | 212.91 | 209.51 | 204.98 | 186.49 | | | 118.47 | | | |

**Table A-1 (continued)**

| Name | SRS X | SRS Y | Ground Surface (ft msl) | TZ (ft msl) | TCCZ (ft msl) | ULAZ ft msl) | MCLAZ (ft msl) | LLAZ (ft msl) | GCU (ft msl) | UGA (ft msl) | MGA (ft msl) | LGA (ft msl) | CBCU (ft msl) |
|---|---|---|---|---|---|---|---|---|---|---|---|---|---|
| PRSBCPT11 | 63996.09 | 44190.84 | 311.24 | 216.42 | 210.41 | 202.27 | 185.63 | 170.18 | | 101.10 | | | |
| PRSBCPT12 | 63878.82 | 43487.93 | 320.72 | 218.52 | 210.73 | 200.97 | | | | 110.03 | | | |
| PRSBCPT13 | 62999.08 | 43632.84 | 304.42 | 214.99 | 207.39 | 200.15 | 186.75 | 169.00 | | 95.54 | | | |
| PRSBCPT14 | 62952.22 | 43892.27 | 301.30 | | 213.66 | 197.76 | | | | 101.41 | | | |
| PRSBCPT7 | 64386.41 | 43010.53 | 321.57 | | 207.71 | 192.47 | 176.45 | | | 123.82 | | | |
| PRSBCPT8 | 64381.30 | 43371.38 | 321.89 | 214.11 | 204.28 | 194.79 | 180.38 | | | 125.80 | | | |
| PRSBCPT9 | 64390.41 | 43545.82 | 322.17 | 216.53 | 209.78 | 202.10 | 182.44 | | | 123.72 | | | |
| PSB011B | 63377.55 | 44146.39 | 306.86 | 229.66 | 208.86 | 204.86 | 193.86 | 152.06 | 104.86 | 104.86 | | | |
| PSB10CP | 63199.39 | 43866.41 | 306.54 | 213.09 | 207.56 | 199.57 | 180.51 | 165.62 | | 95.60 | | | |
| PSB11CP | 63770.69 | 44120.98 | 306.02 | 210.48 | 198.11 | 170.96 | | | | 104.21 | | | |
| PSB12CP | 63666.61 | 44190.82 | 308.92 | 231.19 | 215.86 | 190.71 | | | | 103.52 | | | |
| PSB8CP | 64381.97 | 43218.87 | 321.75 | 189.82 | 177.78 | | | | | 125.29 | | | |
| PSB8SB | 64381.97 | 43218.90 | 321.75 | 200.75 | 200.75 | 192.75 | 178.75 | | | 125.29 | | | |
| PSB9CP | 63738.08 | 43263.40 | 318.30 | 239.70 | 223.95 | 191.89 | | | | 96.80 | | | |
| RGW10 | 75192.97 | 58551.99 | 306.00 | 223.00 | | | | | | | | | |
| RGW4A | 74706.98 | 57917.00 | 303.00 | 195.56 | 172.62 | | | | | | | | |
| RGW9 | 75115.98 | 58650.98 | 302.00 | | 198.60 | 168.68 | | | | | | | |

**Table A-2 Hydrostratigraphic Picks Removed or Added for Developing the Solids Model**

| Well ID | Removed/Added | Reason for Change |
|---|---|---|
| LSW20 | Remove CBCU | Observed value does not correlate to L area wells. |
| PRGW-023 | Remove CBCU | Elevation is higher than surrounding area (+13.8 vs -15.8) |
| PRGW-058 | Remove GCU and UGA | Removed due to hole production |
| PGCPT24 | Remove UGA | Facilitate removal of a unreasonably thick (>30ft) GCU layer next to a thin GCU spot. |
| PBRPCPT1LT | Remove UGA | |
| PBRPCPT2LT | Remove UGA | |
| PBRPCPT3LT | Remove UGA | |
| PGCPT15 | Add LLAZ | Force MCLAZ to have a 20 ft layer |
| PGW10B | Add MGA | Force a middle silt elevation of 0 ft. |
| ControlNorth | Add CBCU | Add a point in the North to ensure a sloping surface (20ft) |
| ControlEast | Add CBCU | Add a point in the East to ensure a sloping surface (-45ft) |

**Table A-3 Hydrostratigraphic Pick Differentials**

| Bore ID | Unit | Differential (feet - elevation) | Reason |
|---|---|---|---|
| P12R | CBCU | -30.67 | OP =-9.5 / NP-40.2 : Based on GP Log |
| | CBCU | | OP -67.89 / NP 'not picked' |
| P24TA | AA | -3.59 | Revised based on PETRA interwell comparison |
| | ULAZ | -7.65 | Revised based on PETRA interwell comparison |
| | MGA | -5.97 | Revised based on PETRA interwell comparison |
| PG34 | A | -15.91 | Revised based on PETRA interwell comparison |
| | LLAZ | -12.68 | Revised based on PETRA interwell comparison |
| PGCPT70 | LLAZ | -88.91 | OP 294 / NP 205 based on cross-section |
| PRGW-059 | MGA | -14.93 | OP=85.08 / NP=70.15 |
| PRGW-082 | GCU | 5.34 | Small differences based on cross-section |
| | MGA | -3.17 | Small differences based on cross-section |
| | LGAU | -2.6 | Small differences based on cross-section |
| PRGW100 | GCU | -1.65 | Small differences based on cross-section |
| | UGA | -23.46 | OP=122/ NP=99 'estimated on cross-section' |
| | MGA | -3.49 | Small differences based on cross-section |
| PRGW101 | AA | 10.05 | OP=281 / NP=291 'based on cross-section' |
| | ULAZ | -15.88 | OP=209 / NP=193 'based on cross-section' |

Note:
OP indicates "original pick"
NP indicates "new pick"

# APPENDIX B:

# LONG TERM HEAD TARGETS

**(This page intentionally left blank)**

**Table B-1 Long-term Head Targets Used in Model Calibration**

| Well Name | SRS X (ft) | SRS Y (ft) | Mid Screen Elevation (ft msl) | Long Term Head (ft msl) | Computed Head (ft msl) | Unit | Comments |
|---|---|---|---|---|---|---|---|
| P 13D | 59999.99 | 35599.99 | 217.45 | 233.40 | 232.01 | A/AA | |
| P 24D | 66579.48 | 43098.49 | 258.3 | 265.26 | 269.39 | A/AA | |
| PAC 2 | 66980.89 | 43527.67 | 262.9 | 270.41 | 268.93 | A/AA | |
| PAC 3 | 66861.40 | 43585.58 | 267.9 | 270.73 | 269.19 | A/AA | |
| PAC 5 | 66907.10 | 43561.69 | 265.1 | 273.01 | 269.09 | A/AA | |
| PAC 6 | 66894.71 | 43580.09 | 265.2 | 273.80 | 269.12 | A/AA | |
| PAO001DU | 64830.00 | 44097.30 | 261.96 | 277.04 | 271.91 | A/AA | |
| PBP 1D | 65727.59 | 45611.28 | 274.08 | 280.13 | 271.50 | A/AA | |
| PBP 2D | 65359.87 | 45481.44 | 267.8 | 275.87 | 272.15 | A/AA | |
| PBP 3D | 65510.19 | 45603.50 | 273.89 | 277.99 | 271.98 | A/AA | |
| PCB 1A | 65070.59 | 41988.20 | 278.5 | 282.00 | 276.09 | A/AA | |
| PCB 2A | 64891.39 | 41821.39 | 272.8 | 280.63 | 277.36 | A/AA | |
| PCB 3A | 64706.30 | 42035.98 | 277.7 | 281.79 | 278.54 | A/AA | |
| PCB 4A | 64901.40 | 42170.99 | 277.9 | 281.28 | 276.91 | A/AA | |
| PDB 2 | 64743.09 | 43513.09 | 258.2 | 275.48 | 274.04 | A/AA | |
| PDB 3 | 64938.19 | 43542.20 | 258.6 | 276.54 | 273.22 | A/AA | |
| PDB 4 | 64623.79 | 43455.10 | 276.2 | 277.75 | 274.71 | A/AA | |
| PDB 5 | 64584.39 | 44106.60 | 274.2 | 274.77 | 271.67 | A/AA | |
| PGW016DU | 62338.50 | 44745.90 | 234.34 | 245.47 | 240.63 | A/AA | |
| PGW017DU | 64052.70 | 44894.80 | 250.68 | 267.58 | 258.85 | A/AA | |
| PGW018DU | 62948.10 | 43497.30 | 249.91 | 272.75 | 272.06 | A/AA | |
| PGW020DU | 64473.90 | 43422.10 | 230.23 | 271.42 | 275.35 | A/AA | |
| PGW021DU | 66058.10 | 44211.00 | 217.9 | 266.72 | 270.36 | A/AA | |

**Table B-1 (continued)**

| Well Name | SRS X (ft) | SRS Y (ft) | Mid Screen Elevation (ft msl) | Long Term Head (ft msl) | Computed Head (ft msl) | Unit | Comments |
|---|---|---|---|---|---|---|---|
| PGW022DU | 66722.10 | 43631.00 | 216.24 | 262.03 | 269.47 | A/AA | |
| PGW023DU | 66792.00 | 43009.20 | 256.15 | 270.56 | 269.44 | A/AA | |
| PGW024DU | 65720.30 | 43760.70 | 254.9 | 274.83 | 270.55 | A/AA | |
| PGW025DU | 64802.10 | 44341.00 | 218.37 | 270.67 | 271.14 | A/AA | |
| PGW-12DL | 71031.60 | 41274.90 | 210.935 | 252.36 | 252.28 | A/AA | |
| PMW001DL | 64724.92 | 44199.33 | 222.92 | 272.01 | 271.49 | A/AA | |
| PMW006DL | 64584.84 | 44296.75 | 221.07 | 271.83 | 270.73 | A/AA | |
| PRP 1A | 63032.70 | 45349.79 | 247.9 | 248.81 | 247.56 | A/AA | |
| PRP 2 | 63229.00 | 45389.48 | 249.1 | 254.16 | 249.66 | A/AA | |
| PRP 3 | 63165.48 | 45200.69 | 243.6 | 255.78 | 248.30 | A/AA | |
| PRP 4 | 63345.88 | 45268.88 | 247.9 | 257.64 | 250.18 | A/AA | |
| PRP 6 | 63185.64 | 45202.70 | 241.82 | 252.01 | 248.51 | A/AA | |
| PRP 7 | 63082.25 | 45232.25 | 236.65 | 242.87 | 247.55 | A/AA | |
| PSB 1A | 64141.40 | 43619.29 | 272.4 | 276.23 | 274.71 | A/AA | |
| PSB 2A | 63916.49 | 43612.40 | 272.2 | 275.82 | 274.80 | A/AA | |
| PSB 3A | 63590.39 | 43599.78 | 271.5 | 274.50 | 274.20 | A/AA | |
| PSB 4A | 63346.98 | 43534.18 | 270.5 | 273.96 | 274.01 | A/AA | |
| PSB 5A | 63606.49 | 43440.50 | 277.3 | 275.61 | 276.04 | A/AA | |
| PSB 6A | 63975.69 | 43435.99 | 277.1 | 276.94 | 276.37 | A/AA | |
| PSB 7A | 64300.99 | 43553.29 | 274 | 276.94 | 274.99 | A/AA | |
| PSB 8 | 64381.99 | 43218.87 | 265.75 | 277.64 | 276.71 | A/AA | |
| PSB 9 | 63734.76 | 43368.86 | 262.29 | 275.00 | 276.98 | A/AA | |
| PSB 10 | 63199.44 | 43866.43 | 260.54 | 271.55 | 267.67 | A/AA | |

**Table B-1 (continued)**

| Well Name | SRS X (ft) | SRS Y (ft) | Mid Screen Elevation (ft msl) | Long Term Head (ft msl) | Computed Head (ft msl) | Unit | Comments |
|---|---|---|---|---|---|---|---|
| PSB 11 | 63370.73 | 44120.97 | 255.02 | 271.46 | 264.35 | A/AA | |
| PGW014DU | 63266.80 | 44879.60 | 205.24 | 243.42 | 248.71 | TZ | |
| PGW015DU | 63008.80 | 47164.70 | 211.85 | 264.01 | 264.82 | TZ | |
| PGW017 C | 64044.90 | 44894.80 | 190.45 | 262.58 | 258.78 | TZ | Move From TCCZ |
| PGW019DU | 65071.70 | 44657.90 | 217.77 | 270.67 | 270.21 | TZ | |
| PGW-01DL | 65348.40 | 46256.10 | 222.75 | 268.09 | 269.82 | TZ | |
| PGW021 C | 66058.20 | 44202.90 | 201.91 | 266.56 | 267.57 | TZ | |
| PGW023 C | 66799.50 | 43008.90 | 211.58 | 261.71 | 266.92 | TZ | |
| PGW024 C | 65720.40 | 43768.10 | 214.89 | 268.30 | 268.01 | TZ | |
| PGW025 C | 64794.20 | 44340.80 | 198.17 | 269.27 | 270.31 | TZ | Move From TCCZ |
| PGW-02DL | 57556.80 | 45296.40 | 199.215 | 223.87 | 227.93 | TZ | |
| PGW-03DL | 64222.30 | 42119.60 | 218.33 | 271.35 | 280.72 | TZ | |
| PGW-04DL | 60996.50 | 44311.10 | 208.345 | 236.66 | 238.76 | TZ | |
| PGW-06DL | 68228.90 | 42885.30 | 202.34 | 258.01 | 262.77 | TZ | |
| PGW-07DL | 65562.80 | 45066.70 | 226.64 | 267.28 | 270.20 | TZ | |
| PGW-08DL | 58702.60 | 42322.80 | 219.255 | 247.91 | 249.39 | TZ | |
| PGW-09DL | 59210.70 | 39197.60 | 215.105 | 260.19 | 260.80 | TZ | |
| PGW-10CU | 64124.10 | 36663.80 | 193.64 | 238.31 | 240.23 | TZ | |
| PGW-10DL | 64120.50 | 36656.10 | 202.6 | 238.29 | 240.21 | TZ | |
| PGW-11DL | 69018.10 | 47623.90 | 202.315 | 232.40 | 241.45 | TZ | |
| PGW-13DL | 60552.50 | 47654.90 | 192.47 | 252.22 | 253.39 | TZ | |
| PRP 5 | 63566.00 | 45198.61 | 205.3 | 255.38 | 251.66 | TZ | |
| RGW 4D | 63213.95 | 48641.73 | 187.06 | 262.08 | 264.54 | TZ | |

**Table B-1 (continued)**

| Well Name | SRS X (ft) | SRS Y (ft) | Mid Screen Elevation (ft msl) | Long Term Head (ft msl) | Computed Head (ft msl) | Unit | Comments |
|---|---|---|---|---|---|---|---|
| RGW 5D | 67886.04 | 47468.15 | 189.17 | 246.19 | 252.37 | TZ | Move From TCCZ |
| RGW 6D | 67118.08 | 42053.05 | 205.14 | 259.24 | 266.86 | TZ | Move From TCCZ |
| LSW 20DL | 54002.06 | 45491.78 | 149.915 | 219.67 | 220.55 | ULAZ | |
| PGW014 C | 63260.40 | 44876.90 | 180.25 | 248.24 | 250.96 | ULAZ | Move From TCCZ |
| PGW015 C | 63016.80 | 47163.00 | 179.75 | 256.83 | 253.11 | ULAZ | |
| PGW019 C | 65087.50 | 44657.90 | 182.92 | 255.53 | 258.44 | ULAZ | |
| PGW-01C | 65357.30 | 46250.10 | 181.61 | 259.73 | 254.91 | ULAZ | |
| PGW020 C | 64473.70 | 43429.70 | 185.22 | 268.76 | 265.80 | ULAZ | |
| PGW022 C | 66716.50 | 43635.90 | 186.07 | 239.13 | 235.85 | ULAZ | |
| PGW023 B | 66807.10 | 43009.00 | 171.67 | 237.98 | 235.35 | ULAZ | |
| PGW024 B | 65720.70 | 43780.10 | 174.88 | 243.92 | 237.89 | ULAZ | |
| PGW-02CU | 57551.30 | 45309.90 | 181.95 | 226.66 | 227.13 | ULAZ | |
| PGW-03C | 64213.30 | 42119.80 | 170.55 | 263.13 | 266.96 | ULAZ | |
| PGW-05C | 68607.70 | 37496.50 | 142.385 | 217.82 | 221.01 | ULAZ | |
| PGW-06C | 68220.20 | 42880.10 | 149.645 | 236.38 | 233.14 | ULAZ | |
| PGW-07C | 65564.10 | 45076.40 | 186.14 | 254.47 | 251.75 | ULAZ | |
| PGW-08C | 58708.70 | 42330.30 | 183.31 | 236.71 | 233.08 | ULAZ | |
| PGW-09C | 59219.80 | 39191.00 | 154.79 | 251.60 | 249.55 | ULAZ | |
| PGW-10C | 64112.20 | 36660.10 | 147.745 | 227.16 | 226.98 | ULAZ | |
| PGW-11C | 69010.90 | 47630.80 | 153.635 | 228.52 | 230.46 | ULAZ | |
| PGW-12C | 71039.10 | 41280.20 | 157.185 | 224.85 | 224.14 | ULAZ | |
| RGW 7D | 62249.43 | 38738.68 | 170.45 | 245.58 | 241.05 | ULAZ | |
| RGW 9D | 56408.76 | 47441.31 | 156.69 | 240.65 | 235.63 | ULAZ | |

**Table B-1 (continued)**

| Well Name | SRS X (ft) | SRS Y (ft) | Mid Screen Elevation (ft msl) | Long Term Head (ft msl) | Computed Head (ft msl) | Unit | Comments |
|---|---|---|---|---|---|---|---|
| LSW 20C | 54002.06 | 45491.78 | 116.51 | 214.12 | 223.50 | LLAZ | |
| P 13C | 59999.99 | 35599.99 | 38.1 | 218.69 | 220.06 | LLAZ | |
| PGW014 B | 63253.30 | 44874.20 | 125.09 | 230.44 | 235.73 | LLAZ | |
| PGW016 B | 62341.30 | 44763.80 | 131.72 | 230.00 | 230.95 | LLAZ | |
| PGW017 B | 64037.40 | 44894.40 | 155.36 | 257.41 | 256.11 | LLAZ | |
| PGW018 B | 62947.80 | 43488.50 | 143.85 | 262.69 | 261.50 | LLAZ | |
| PGW-01B | 65328.10 | 46269.50 | 155.45 | 241.39 | 242.62 | LLAZ | |
| PGW020 B | 64473.50 | 43437.50 | 155.36 | 256.34 | 260.01 | LLAZ | |
| PGW-03B | 64204.90 | 42119.90 | 136.72 | 254.98 | 262.39 | LLAZ | |
| PGW-04B | 60977.30 | 44310.20 | 121.41 | 228.95 | 230.35 | LLAZ | |
| PGW-06B | 68193.90 | 42864.60 | 104.405 | 220.58 | 222.79 | LLAZ | |
| PGW-07B | 65564.90 | 45086.00 | 161.47 | 233.96 | 234.07 | LLAZ | |
| PGW-08B | 58714.70 | 42337.40 | 123.885 | 229.09 | 229.54 | LLAZ | |
| PGW-09B | 59205.30 | 39190.40 | 116.92 | 242.18 | 246.33 | LLAZ | |
| PGW-10B | 64129.81 | 36650.90 | 72.5 | 218.50 | 218.69 | LLAZ | |
| PGW-13C | 60552.00 | 47645.60 | 131.68 | 236.14 | 234.71 | LLAZ | |
| RGW 5C | 67896.06 | 47463.27 | 111.83 | 232.32 | 230.38 | LLAZ | |
| RGW 9C | 56408.67 | 47427.15 | 107.28 | 228.19 | 228.08 | LLAZ | |
| P 24B | 66572.99 | 43127.77 | 88.8 | 220.56 | 223.87 | UGA | |
| PGW-01A | 65337.70 | 46263.10 | 87.745 | 233.88 | 231.08 | UGA | |
| PGW024 A | 65720.90 | 43787.70 | 64.81 | 226.74 | 225.23 | UGA | |
| PGW-03A | 64196.21 | 42119.70 | 90.575 | 230.23 | 222.32 | UGA | |
| PGW-04A | 60968.00 | 44310.50 | 86.98 | 231.20 | 228.31 | UGA | |

**Table B-1 (continued)**

| Well Name | SRS X (ft) | SRS Y (ft) | Mid Screen Elevation (ft msl) | Long Term Head (ft msl) | Computed Head (ft msl) | Unit | Comments |
|---|---|---|---|---|---|---|---|
| PGW-06A | 68203.00 | 42869.70 | 63 | 221.25 | 222.98 | UGA | |
| PGW-07A | 65566.10 | 45094.90 | 111.51 | 229.31 | 228.15 | UGA | |
| PGW-08A | 58720.90 | 42344.20 | 65.01 | 228.84 | 226.16 | UGA | |
| LSW 20A | 54002.06 | 45491.78 | 55.665 | 181.41 | 182.44 | LGA | Move from UGA |
| P 13B | 59999.99 | 35599.99 | -2.1 | 178.91 | 176.57 | LGA | Move from UGA |
| P 24A | 66569.69 | 43142.20 | 3.5 | 193.92 | 196.44 | LGA | |
| PGW015 A | 63019.60 | 47171.30 | 26.7 | 190.51 | 190.82 | LGA | |
| PGW025 A | 64778.60 | 44340.00 | 38.11 | 194.39 | 196.59 | LGA | Move from MGA |
| PGW-02A | 57566.60 | 45311.70 | 35.085 | 185.45 | 184.80 | LGA | |
| PGW-05A | 68610.10 | 37479.10 | 4.78 | 185.57 | 186.30 | LGA | |
| PGW-11A | 68997.50 | 47643.40 | 19.335 | 199.12 | 200.68 | LGA | Move from MGA |
| PGW-12A | 71046.60 | 41285.20 | 36.195 | 195.19 | 193.57 | LGA | |
| PGW-13A | 60551.40 | 47636.70 | 62.915 | 188.88 | 188.25 | LGA | |
| P 13A | 59999.99 | 35599.99 | -62.35 | 173.51 | 176.32 | LGA-lower | |
| PGW014 A | 63246.40 | 44871.80 | -0.83 | 192.90 | 190.04 | LGA-lower | |
| PSB002AL | 63936.59 | 43619.59 | 2.56 | 193.54 | 190.65 | LGA-lower | |
| P13TC | 59999.99 | 35599.99 | -300 | 172.23 | 172.20 | CBAU | |
| P 24TD | 66554.90 | 43139.28 | -200 | 181.05 | 181.05 | CBAU | |

**Table B-2 Long-term Head Targets Removed from Model Calibration**

| Well Name | Unit | Removal Reason |
|---|---|---|
| PAC 1 | A/AA | Head >10ft higher than targets in area |
| PAC 4 | A/AA | Head >10ft higher than targets in area |
| PGW018 C | TCCZ | In TCCZ |
| PGW026DL | TCCZ | In TCCZ |
| PGW034DL | TCCZ | In TCCZ |
| PSB011C | TCCZ | In TCCZ |
| P 24C | ULAZ | Screened in TCCZ and ULAZ in log |
| PGW015 B | MC-LAZ | In MC LAZ |
| PGW019 B | MC-LAZ | In MC LAZ |
| PGW021 B | MC-LAZ | In MC LAZ |
| PGW022 B | MC-LAZ | In MC LAZ |
| PGW025 B | MC-LAZ | In MC LAZ |
| PGW026C | MC-LAZ | In MC LAZ |
| PGW027C | MC-LAZ | In MC LAZ |
| PGW-02C | MC-LAZ | In MC LAZ |
| PGW030BL | MC-LAZ | In MC LAZ |
| PGW031B | MC-LAZ | In MC LAZ |
| PGW-04C | MC-LAZ | In MC LAZ |
| PGW-13CU | MC-LAZ | In MC LAZ |
| PRB005C | MC-LAZ | In MC LAZ |
| PSB011B | MC-LAZ | In MC LAZ |
| RGW 4C | MC-LAZ | In MC LAZ |
| PGW033A | UGA | Well screened at very top of UGA, GCU head. |
| PGW-05B | UGA | Head matches MGA |
| PSB002AA | UGA | Well screened at very top of UGA, GCU head. |
| PGW-11B | UGA | Duplicate head of 11A and in the same unit |
| PGW-09A | LGA | Well screened at very top of LGAU, MGA head. |
| P13TD | CBCU | In CBCU |
| LSP1DU | A/AA | <11 measurements |
| LSP3DU | A/AA | <11 measurements |
| P002L | TZ/TCCZ | <11 measurements |
| P002U | AA | <11 measurements |
| P003L | TZ/TCCZ | <11 measurements |
| P003U | AA | <11 measurements |
| PAO002DL | UAZ | <11 measurements |
| PAO002DU | UAZ | <11 measurements |
| PAO003DU | UAZ | <11 measurements |
| PAS001C | LAZ | <11 measurements |
| PAS001D | UAZ | <11 measurements |
| PAS002D | UAZ | <11 measurements |
| PAS003D | UAZ | <11 measurements |
| PDB003C | ULAZ | <11 measurements |
| PGW016C | Unknown | <11 measurements |
| PGW026B | LLAZ | <11 measurements |
| PGW026C | LAZ | <11 measurements |
| PGW026DL | UAZ | <11 measurements |

**Table B-2 (continued)**

| Well Name | Unit | Removal Reason |
|---|---|---|
| PGW027C | ULAZ | <11 measurements |
| PGW027DL | LLAZ | <11 measurements |
| PGW027DU | UAZ | <11 measurements |
| PGW028C | ULAZ | <11 measurements |
| PGW028DU | UAZ | <11 measurements |
| PGW029C | ULAZ | <11 measurements |
| PGW029DL | UAZ | <11 measurements |
| PGW030B | LAZ | <11 measurements |
| PGW030BL | LLAZ | <11 measurements |
| PGW031B | LAZ | <11 measurements |
| PGW031C | ULAZ | <11 measurements |
| PMP001DL | UAZ | <11 measurements |
| PMP002DL | UAZ | <11 measurements |
| PMP003DL | UAZ | <11 measurements |
| PMP004DL | UAZ | <11 measurements |
| PMP005DL | UAZ | <11 measurements |
| PMP006DL | UAZ | <11 measurements |
| PMP007DL | UAZ | <11 measurements |
| PMP008DL | UAZ | <11 measurements |
| PMW002DL | UAZ | <11 measurements |
| PMW003DL | UAZ | <11 measurements |
| PMW004DL | UAZ | <11 measurements |
| PMW005DL | UAZ | <11 measurements |
| PRB001DU | UAZ | <11 measurements |
| PRB002DU | UAZ | <11 measurements |
| PRB003C | ULAZ | <11 measurements |
| PRB003DU | UAZ | <11 measurements |
| PRB004DU | UAZ | <11 measurements |
| PRB005C | ULAZ | <11 measurements |
| PRB005DU | UAZ | <11 measurements |
| PSB12 | Unknown | <11 measurements |
| PSB002B | LLAZ | <11 measurements |
| PSB002C | ULAZ | <11 measurements |
| PSB002DL | UAZ | <11 measurements |
| PSB003DL | UAZ | <11 measurements |
| PSB011A | UGA | <11 measurements |
| PSB011B | LLAZ | <11 measurements |
| PSB011C | ULAZ | <11 measurements |
| PSB011DL | UAZ | <11 measurements |
| RGW10CR | Unknown | <11 measurements |